Characterisation and modulation of the intracellular pro-inflammatory signalling pathways activated during surgery with cardiopulmonary bypass

Bao Anh Vu Nguyen

BSc(Hons) MB BS DIC MSc MRCS(Eng)

Heart Research UK Research Training Fellow

CID: 00235122

This thesis is submitted for the degree of
Doctor of Philosophy (PhD)
Imperial College, Faculty of Medicine and Life Sciences

2014

British Heart Foundation Cardiovascular Medicine Unit
National Heart and Lung Institute, Imperial College Faculty of Medicine
London, United Kingdom

&

Department of Cardiothoracic Surgery
Imperial College NHS Healthcare Trust, Hammersmith Hospital
London, United Kingdom

Xem việc biết người

Abstract

Surgery with cardiopulmonary bypass (CPB) is associated with post-operative complications due to systemic inflammation. However, the intracellular signalling pathways that promote inflammation in cardiac surgery with CPB are uncertain. The studies presented in this thesis were designed to illuminate these molecular mechanisms, thereby informing the development of novel anti-inflammatory strategies.

This was addressed through a clinical trial to determine the effects of CPB on inflammatory signalling in leukocytes (Chapter 4). In this study, the induction of reactive oxygen species (ROS) and the activation of NF-κB and p38 MAP kinase within leukocytes was compared in patients exposed to miniaturised CPB (mCPB; an optimised form of CPB designed to attenuate systemic inflammatory activation) or conventional CPB (cCPB). Twenty-six patients undergoing surgical revascularisation for advanced coronary artery disease were randomised to undergo surgery with either cCPB or mCPB. Blood samples were collected pre-operatively and at various times after the initiation of CPB and analysed by intracellular staining and flow cytometry for intracellular markers of activation. p38 MAP kinase phosphorylation in granulocytes was enhanced in patients receiving cCPB compared to mCPB ($p<0.05$). Levels of ROS in lymphocytes were elevated in cCPB compared to mCPB ($p<0.01$) whereas ROS levels in granulocytes and monocytes were similar between groups. NF-κB phosphorylation in leukocyte sub-sets, leukocyte tissue migration as well as conventional markers of inflammation were comparable between the investigative groups.

A porcine model was also established to study the signalling pathways that promote systemic inflammation in response to cardiac surgery with CPB under well-controlled experimental conditions. The influence of sulforaphane, an anti-inflammatory compound derived from green vegetables, on inflammation and injury in response to CPB was also studied. It was observed that pre-treatment of animals with sulforaphane reduced p38 MAP kinase ($p<0.05$)

and NF-κB ($p<0.05$) phosphorylation in leukocytes exposed to CPB and protected porcine kidneys from exhibiting histological features of early injury.

A small clinical study demonstrated biologically significant levels of sulforaphane could be determined in plasma, with lower levels of p38 MAP kinase ($p<0.01$) and attenuated ROS ($p<0.01$) in the early stages following consumption.

In conclusion, systemic inflammatory responses following CPB were associated with activation of p38 MAP kinase and NF-κB pathways in circulating leukocytes in both porcine and clinical studies. Inflammatory responses to CPB can be reduced by miniaturisation of the CPB circuit and pharmacologically using sulforaphane.

Table of contents

List of figures

List of tables

List of abbreviations

ABG	Arterial Blood gas
ACT	Activated clotting time
ALR	AIM2-like receptor
AF	Atrial Fibrillation
APC	Allophycocyanin
APF	Aminophenylfluroscein
ARDS	Acute respiratory distress syndrome
ARE	Antioxidant response element
ATP	Adenosine Triphosphate
CABG	Coronary artery bypass graft
CK-MB	Creatine Kinase MB isoenzyme
CPB	Cardiopulmonary Bypass
CRP	C-Reactive Protein
Cx	Connexin
Cox	Cyclooxygenase
DAMP	Damage associated molecular pattern
DCF	Carboxy-dihydroflurorescein
DMEM	Dulbecco's Modified Eagle's Medium
DMF	Dimethyl formamide
DMSO	Dimethyl sulphoxide
DTT	Dithiothreitol
EC	Endothelial cell
ECCO	Extra-corporeal Circulation Optimised
ECG	Electrocardiograph
ERK	Extracellular Regulated Protein
ESGL-1	E-Selectin glycoprotein ligand 1
FACS	Fluorescence-Activated Cell Sorting
FBS	Fetal Bovine Serum
FCS	Fetal Calf Serum
FGF	Fibroblast growth factor
FiO_2	Fraction of inspired oxygen
FITC	Fluorescein isothiocyanate
FPR	Formyl Peptide Receptor
G-CSF	Granulocyte colony stimulating factor
GPx	Glutathione peroxidase
H_2O_2	Hydrogen peroxide

HBSS	Hanks Balanced Salt Solution
HMGB1	High-mobility group protein B1
HO-1	Haemoxygenase 1
HOCl	Hypochlorus acid
HSP	Heat Shock Protein
HUVEC	Human umbilical vein endothelial cells
ICAM-1	Intercellular adhesion molecule 1
IFN	Interferon
IL	Interleukin
ISS	Injury Severity Score
ITU	Intensive Therapy Unit
JAM	Junctional adhesion molecule
JNK	c-Jun NH_2-Terminal Kinase
Keap1	Kelch-like ECH-associated protein 1
LC-MS	Liquid Chromatography – Mass spectroscopy
LPS	Lipopolysaccharide
LTB4	Leukotriene B4
MAP	Mitogen Activated Protein
MCP-1	Monocyte chemoattractant protein 1
MFI	Mean fluorescent Intensity
MOPS	3-(N-morpholino) propanesulfonic acid
mRNA	Messenger Ribose nuclei Acid
NADPH	Nicotinamide adenine dinucleotide phosphate
NF-κB	Nuclear Factor kappa B
NGAL	Neutrophil gelatinase-associated lipocalin
NLR	NOD-like receptor
NOS	Nitric Oxide sythetase
NQO1	NADPH dehydrogenase quinone 1
Nrf2	Nuclear Factor (erythroid-derived 2)-like 2
NSAID	Non steroidal anti-inflammatory drug
•OH	Hydroxyl radical
OPCAB	Off pump coronary artery bypass
PAEC	Porcine aortic endothelial cells
PAGE	Polyacrylamide gel electrophoresis
PAMP	Pathogen associated molecular pattern
PECAM-1	Platelet endothelial cell adhesion molecule
PBMC	Peripheral Blood Mononuclear Cells
PBS	Phosphate Buffered Saline

PCI	Percutaneous coronary intervention
PDGF	Platelet derived growth factor
PE	Phycoerythrin
PE-Cy7	Phycoerythrin Cyanide dye 7
PMA	Phorbol 12-myristate 13-acetate
PRR	Pattern recognition receptor
PSGL-1	P-Selectin glycoprotein ligand-1
PVDF	Polyvinyl difluoride
RAGE	Receptor for Advanced Glycation Endproducts
RLR	RIG-I-Like receptors
ROS	Reactive Oxygen Species
RT-PCR	Reverse Transcriptase - Polymerase Chain Reaction
SAP	Statistical analysis plan
SD	Standard deviation
SDS	Sodium dodecyl sulfate
SDF-1	Stromal cell derived factor 1
SEM	Standard error of the mean
SFN	Sulforaphane
SIRS	Systemic Inflammatory Response Syndrome
SOD	Superoxide dismutase
STEMI	ST-elevation myocardial infarction
TBST	Tris buffered saline and Tween 20
TGFβ	Transforming growth factor β
TLR	Toll-Like Receptor
TNFα	Tumour Necrosis Factor alpha
Trx	Thyoredoxin
VARD	Venous air removal device
XO	Xanthine Oxidase
ZO-1	Zona occludens protein 1

Acknowledgements

The beginning of knowledge is the discovery of something that we do not understand. I owe much gratitude to many individuals who have contributed to my scientific journey of discovery. Firstly, Professor Paul Evans has been an exemplary supervisor and the driving force behind this endeavour through his dedication, encouragement and scientific rigor. For their patient guidance and generosity throughout, I am grateful to Professor Dorian Haskard and Mr Jon Anderson as my project co-supervisors. Thank you for the opportunity to work on this thought-provoking project.

I am grateful to Mr Gentjan Jakaj, Dr Mark Vives, Dr Albert Busza, Mr Jonathan Finch, Mr Hatem Naase and Mr John Mulholland for their assistance with the large animal study and clinical perfusion services. Within the lab, I am indebted to Dr Le Luong, Miss Ellen McConnell, Dr Nicky Ambrose, Dr Dilip Patel, Dr John Krell and Mr Adam Frampton for their assistance in the development of the laboratory techniques and assays employed in generating the data for this thesis. Finally, I would like to thank everyone else in the Cardiovascular Sciences unit for providing an excellent and enjoyable environment to work in. It's been a rollercoaster.

With the most sincere of thanks, I acknowledge the generous financial support of Heart Research UK in contributing to the success of this project. Ultimately, it would not have been possible to achieve this work without the unwavering support of Yuki and the unfailing good company of Hugo, Leo, Alyssa and Thomas.

Declaration

This thesis including all the data, figures and illustrations contained within are the result of my own original investigations, except where indicated below. This work was conducted between January 2010 and September 2012 within the departments of Cardiovascular Medicine (at the National Heart and Lung Institute, London) and the department of Cardiothoracic Surgery (at Hammersmith Hospital, Imperial College NHS Healthcare Trust, London). This was completed under the supervision of Professor Paul Evans (University of Sheffield), Professor Dorian Haskard (Imperial College London) and Mr Jon Anderson (Imperial College NHS Trust).

Sulforaphane plasma concentrations were determined using LC-MS techniques with the assistance of Professor Sukneung Pyo in the porcine model (School of Pharmacy, Sungkyunkwan University, South Korea). Histological slides were produced with the help of Miss Lorraine Lawrence (Department of Histology, National Heart & Lung Institute, UK) and histological grading was performed by Dr Joseph Boyle (Department of Histopathology, Papworth Hospital, UK). Statistical considerations were provided by Dr Francesca Fiorentino and Professor Barney Reeves (Clinical Trials and Evaluation Unit, Hammersmith Hospital).

This thesis has not been submitted for a degree or diploma at any other university.

CHAPTER 1. INTRODUCTION

1.1 ATHEROSCLEROSIS AND ISCHAEMIC HEART DISEASE

Cardiovascular diseases are a significant health burden in the Western world[1-4]. Approximately 180,000 deaths occurred due to cardiovascular disease, accounting for a third of all deaths in the UK, in 2010[5]. *Coronary artery disease*, the most prevalent cardiovascular disease, resulted in over 94,000 deaths a year in the UK with an economic cost estimated at over £1.7 billion annually[2,6]. The British Heart Foundation reported the total prevalence of angina was over 140,000 cases in men and over 116,000 cases in women living in the UK in 2009, the principle symptom of ischaemic coronary artery disease[7].

The common drive for cardiovascular disease is atherosclerosis[1,8-10]. As a lipid-driven chronic inflammatory disease of medium and large arteries, the accumulation of macrophages, smooth muscle cells, lipids and extracellular matrix results in thickening of the blood vessel wall[8,10-12]. This can result in intraluminal plaque formation, reduction in blood flow and ischaemia[13]. Consequently, end-organ perfusion is compromised. Plaque material may become unstable and embolise causing tissue infarction or the presence of a fissure within a plaque can promote clot formation around the fissured defect resulting in a catastrophic rapid reduction in blood flow[14]. The deposition of plaque within a vessel wall can also compromise the wall integrity and pre-disposes to aneurysm formation, particularly in large calibre vessels[15,16].

The process of atherosclerosis typically progresses for many decades before clinical symptoms become apparent[17,18]. In advanced coronary artery disease, the usual presenting features can be exertional angina (chest pain) with or without dyspnoea (difficulty breathing) as a result of the impaired function of the myocardium. When there is sudden plaque rupture or rapid total occlusion of a vessel, myocardial infarction occurs with irreversible necrosis of tissue and loss of function[19]. Compromise to the left coronary system can impair myocardial contractility, reducing stroke volume and cardiac output with accompanying regional wall motion abnormalities and pulmonary oedema[20]. Disruption of the right coronary system may

interfere with the electrical conduction system of the heart causing dysrhythmias[21], loss of right-heart contractility with venous portal congestion[22]. Additional consequences of coronary artery disease are new valvular leak (arising from disturbance to the intra-cardiac valve apparatus)[23]; ventricular aneurysm formation[24]; ventricular septal defects[25] and myo-/peri- carditis[26]. Any disturbance of myocardial function leads to deleterious knock-on effects on all other organs of the systemic circulation.

With improvements in the understanding of the mechanisms responsible for atherosclerosis, adverse mortality rates have fallen[27,28]. Health benefits are achieved by the reduction in major risk factors such as smoking cessation, exercise, and improvements in preventative measures (e.g. enhanced blood pressure control; lipid lowering agents; long-term anti-platelet therapy and optimised blood glucose) in conjunction with healthy eating[29-33]. With advanced arterial disease, already under optimal medical treatment, the additional therapeutic options include; interventional percutaneous balloon angioplasty and intra-coronary artery stenting[34]; definitive surgical revascularisation in complex multi-vessel disease[35-37] or utilisation of an emerging combined hybrid approach of both surgery and stents[37-40].

1.1.1 Percutaneous coronary intervention

The coronary circulation can be accessed percutaneously, through the skin, via peripheral arteries. Radiological imaging guidance, the use of guide-wires and over-the-wire catheters can be employed for coronary artery interventions (PCI). The stenosed coronary vessel can be mechanically opened to enhance intra-luminal blood flow[41]. Implantation of intra-coronary stents (approximately 95% of current clinical practice[6]) can maintain vessel patency, with or without drug elution to prevent in-stent stenosis and neo-intimal hyperplasia.

There are 117 PCI centres within the United Kingdom[6]. In 2009, there were a total of 83,130 PCI procedures performed in the UK. The rate of primary PCI to treat acute ST-elevation

myocardial infarction (STEMI) in place of thrombolysis continues to rise. However, the overall mortality rate before discharge from hospital following PCI is gradually rising, perhaps from changing case mix. This is in contrast with the improving mortality rates observed with surgical treatments which show an improvement from 2.3% in 2001 to 1.5% in 2008 for isolated first time coronary artery surgery despite advanced age and co-morbidity[42]. However, the absolute risks from undergoing this procedure remain relatively low overall. Specifically, for stable elective patients, PCI carries a 0.15% mortality risk; for stable angina the risk is 0.6% and for STEMI patients, the risk is 4%[6].

1.1.2 Coronary artery bypass graft surgery

When coronary artery disease is extensive or disease anatomy is complex and unfavourable to PCI (e.g. with tight left main stem disease lesions), coronary artery bypass graft (CABG) surgery is employed for symptomatic and prognostic benefits[35,36,43]. This is the surgical process of placing a vascular conduit carrying oxygenated blood beyond a culprit coronary lesion directly onto a coronary artery. Placement of bypass grafts to the targeted mid coronary vessel protects whole zones of vulnerable myocardium and protects against the development of new proximal disease.

Alexis Carrel (1873-1944) performed aorto-coronary bypass grafts in canine models and recognised the link between coronary artery stenosis and angina pectoris[44] and was acknowledged with the Nobel prize in 1912 for his work on vascular techniques. One of the earliest surgical treatments for angina pectoris was total thyroidectomy, to reduce the sympathetic drive to the heart, described by Elliot Cutler (1888 - 1947)[45]. Arthur Vineberg (1903-1988), a Canadian surgeon, directly implanted the internal thoracic artery onto the myocardium in the 1940s as a means to improve blood flow with limited success[46]. The first direct coronary procedure was performed by William Longmire (1913-2003), without radiological angiographic planning, in 1958 after performing a coronary artery

endarterectomy to the right coronary artery during one of his procedures[47]. David Sabiston (1924-2009) of Duke University performed the first intentional saphenous vein graft to coronary vessel in 1962[48] and Vasilii Kolesov (1904-1992) performed the first internal thoracic artery anastomosis to the left anterior descending artery in 1964[49]. Alain Carpentier (1933-) was the first to champion the use of the radial artery as a conduit in 1973[50] with Rene Favaloro (1923-2000) championing the use of vein grafts[51].

The current technique of coronary artery bypass grafting uses a combination of either pedicled (internal mammary, right gastro-epiploic) or free arterial grafts (radial, inferior epigastric) or venous conduits (long saphenous, short saphenous) to anastomose distal to an atherosclerotic lesion in order to restore blood supply to the myocardium. The selection of conduit is dependent upon the surgeon and influenced by patient factors including age, co-morbidity and accessibility of grafts. The pedicled internal mammary artery is commonly regarded as the most optimal conduit in large cohort studies[52,53].

In the 5 year period between March 2003 and April 2008, there were 114,300 isolated CABG operations performed in the UK in 55 hospitals (6th National Adult Cardiac Surgical Database Report, 2008)[42]. The activity of surgery has plateaued at nearly 23,000 cases per annum. As a treatment modality in its 5th decade of clinical implementation, CABG remains the most intensively scrutinized surgical procedure in the history of medicine. Although commonly performed with the use of CPB, in the UK approximately 17-25% of all CABG operations are performed "off-pump"[42,54,55] without the need for extra-corporeal circulation support. The outcome for patients undergoing CABG surgery electively in the UK is excellent with the mortality rate for patients under the age of 70 years old less than 1%[42]. Medium-term survival is also favourable with a greater than 90% survival rate at 5 years post-surgery[42].

1.2 VALVULAR DISEASE AND SURGICAL DISEASES OF THE AORTA

The mainstay of cardiothoracic surgery worldwide is surgery on the coronary circulation for ischaemic heart disease. The remainder of adult surgical practice is directed towards replacement or repair of diseased intra-cardiac valves, surgery on the thoracic aorta and organ transplantation in specialist centres. All these procedures require the use of CPB systems for support. A brief outline of current UK surgical practice is given below but further detailed discussion is beyond the scope of this thesis.

The aortic valve functions as a one-way valve at the outlet of the left ventricle to the systemic circulation. The common pathologies of the aortic valve are stenosis (commonly due to calcific degeneration or congenital bicuspid abnormalities) or regurgitation (due to rheumatic heart disease or infective endocarditis)[56]. Currently, no effective medical (pharmacological) therapy exists for severe aortic stenosis or regurgitation other than valve replacement, or implantation[57]. Between April 2003 and March 2008, there were 30,127 recorded isolated aortic valve operations[42]. It is common to perform both aortic valve replacement and CABG at the same time as both disease pathologies commonly exist, so the workload is much more than indicated. Additionally, pathology in the thoracic aorta (such as aneurysm formation) can involve the aortic valve apparatus leading to the requirement for performing complex reconstructive procedures[58]. The aortic workload has increased by 50% between 2001 and 2008 with a 34% reduction in operative mortality, over 5 years reflecting improvements in patient care[42]. Transcatheter aortic valve implantation (TAVI) is an emerging option in the treatment of aortic valve disease, currently under evaluation in those patients considered unsuitable for operative management[59-62].

The mitral valve is a bicuspid valve acting as a one-way valve between the left atrium and left ventricular chambers and is the most complex of the 4 valves of the heart[63]. Surgery becomes necessary when there is stenosis of the valve (due to rheumatic disease) or regurgitation (commonly due again to rheumatic disease, ischaemic heart disease and infective

endocarditis)[64] . Between 2003 and 2008 there were 19,545 isolated mitral valve procedures performed in the UK[42]. In a similar profile to aortic valve surgery, there has been a doubling of the number of mitral valve repair procedures between 2001 and 2008. The mortality associated with valve repair is excellent (approximately 2% of all patients). The comparable risk that arises from mitral valve replacement is higher (at 6.1%), reflecting a much greater risk population[42].

The aorta is the largest calibre blood vessel in the body. It is the arterial blood conduit supplying the systemic circulation. The first branches of the aorta are the coronary arteries arising above the cusps of the aortic valve, within the left and right coronary ostia. The arch of the aorta gives rise to the head and neck blood vessels; upper limb circulation; supply blood to the thoracic structures and provides spinal blood flow. The descending aorta then becomes the abdominal aorta as it traverses the diaphragm, and thus enters the management domain of the vascular surgeons. Data is available for 5,245 cases of surgery on the thoracic aorta including thoracic aneurysms and aortic dissection. The mortality for patients undergoing urgent or emergency surgery (e.g. for rapidly expanding aneurysms, leaking aneurysms or acute dissections) was 23% for the UK[42].

1.3 CARDIOPULMONARY BYPASS

Since being introduced in the 1950s, cardiopulmonary bypass (CPB) has revolutionised cardiothoracic practice by facilitating surgery on and within the heart[65-67]. CPB circuits maintain the function of the heart and lung by achieving forward flow of blood, regulation of gas exchange and control of blood temperature[68]. Between 2003 and 2008, more than 145,000 cardiac surgical procedures were performed in the UK requiring the use of CPB[42]. The utility of CPB lies in its ability divert the circulation away from the heart to provide a *bloodless* operating field that is essential to the successful conduct of cardiac surgery. In addition, the use of K^+-containing cardioplegic solution to arrest the heart in diastole or, alternatively, using cross-clamp electrical myocardial fibrillation, renders the operating field *motionless*. CPB can also be utilised as an invasive re-warming technique in accidental deep hypothermia[69]; as a means of maintaining oxygenation where complex airway challenges exist[70,71] and as an adjunct in pulmonary embolectomy[72].

1.3.1 The Development of Cardiopulmonary Bypass

It has been 386 years since the first description of the flow and pulsatile nature of the vascular system. Before then, Galen (AD 129- c200) in *De Usu Partium Corporis Humani* had originally considered the liver - and not the heart - as the centre of the circulation[73]. His classical teachings influenced European medical instruction from the Roman era until the time of the Renaissance. This anatomical circulatory world view was finally widely challenged by William Harvey (1578-1657). Published in the city of Frankfurt in 1628, *De Motu Cordis* detailed the action of the heart and correctly postulated the direction of flow of blood within the circulation[74]. This was a postulation as Harvey was not directly able to visualise the capillary microcirculation that connected the arterial and venous systems. Marcello Malpighi (1628-1694) recorded observations four years after Harvey's death which confirmed Harvey's hypothetical assertions of a link between the two components of the circulation[75]. These studies described the *systemic* circulation but it was Michael Servetus

(1511-1553) who is credited with the first accurate description of the *pulmonary* circulation in his theological treatise *Christianismi Restitutio*[76,77]. However, unknown in the west until his writings were discovered in Berlin in 1924, the Syrian physician Avicenna (also known as Ibn Al Nafis, 1213-1288) had also rudimentarily described the pulmonary circulation, much before Servetus[78]. This informed the knowledge basis for the pulsatile pump nature of the heart and the importance of the pulmonary circulation for gas exchange.

It would be another 250 years before any advancements would be made on interventions on the human heart successfully. In the early phases of development of what would later be known as extracorporeal circulation technology, the first heart-lung machine that was capable of oxygenating blood was developed by Max von Frey (1852-1932) and Max Gruber (1853-1927) in Leipzig in their organ perfusion studies in 1885[79]. Building upon this foundation, the Russian scientist Sergei Brukhonenko (1890-1960) maintained the circulation of isolated dogs' heads using donor lungs for gas exchange and bellows-type pumps for circulating blood in 1929[80]. However, the individual who applied this technological concept successfully to humans was John Gibbon (1903-1973), at the Massachusetts General hospital in the USA. In 1931, he was monitoring the condition of a critically ill patient who had suffered from a pulmonary embolism. This patient subsequently died following an emergency pulmonary embolectomy procedure. Gibbon was convinced that an extracorporeal circuit could have saved the patient's life and realised the utility of this concept for all patients undergoing heart surgery. After 22 years of experimental animal work, Gibbon utilised cardiopulmonary bypass successfully for 26 minutes to repair an atrial septal defect in an 18 year old woman in May 1953[66]. His work made use of the discovery of heparin to anticoagulate the blood in 1916 by a medical student Jay McLean (1890-1957) and William Howell (1860-1945, of Howell-Jolly body fame)[81] at the John Hopkins medical school and the reversal of heparin with protamine in 1949, via the work of Friederich Mischer (1844-1895)[82]. These developments were facilitated by an improved understanding of circulatory physiology; the effects of hypothermia as well as a better understanding of bioengineering.

The early use of CPB met with limited success. Following his first success, the subsequent three other patients operated on by Gibbon using CPB did not survive and he abandoned all future surgery after these events. An alternative, limited, concept of 'controlled cross-circulation' was employed by Walton Lillehei (1915-1999) in the early 1950s. This involved connecting a child to the parent's circulation to provide both oxygenation and perfusion and a total of 45 such operations were performed[83]. John Kirklin (1917-2004) at the Mayo clinic performed the first series of operations using CPB in 1955[65] and the pioneers in Europe were led by Denis Melrose (1921-2007), William Cleland (1912-2005) and Hugh Bentall (1920-2012) in the UK in the mid-1950s at the Hammersmith Hospital in London[84]. Gibbon's heart-lung machine was adapted, refined and adopted for widespread use in the field of cardiothoracic surgery over the next fifty years throughout the world[67].

1.3.2 The conventional cardiopulmonary bypass circuit

Before being connected to a patient during surgery, the CPB tubing lines are looped in a single circuit. These lines are filled, in a process called "priming", with a variety of fluids - commonly Hartmann's solution with heparin before the lines are 'divided' into their respective arterial and venous components ready for connection to the patient. CPB is instituted following cannulation of the arterial circulation (typically the aorta, or femoral artery) and the venous circulation (typically the right atrium or the superior and inferior vena cavae or femoral vein). This permits the drainage of blood from the patient under gravity to the CPB apparatus where the blood gas content and temperature is regulated prior to being pumped back to the systemic circulation in the body to perfuse the organs (Figure 1.1). As a consequence of the gas regulation of the blood by the CPB circuit, both mechanical lung ventilation and oxygenation during CPB are no longer required.

Venous return within the reservoir is actively channelled using roller pumps through a membrane oxygenator to enable oxygen and carbon dioxide gaseous exchange. This blood is then passed through a heat exchanger which permits thermal control. Particulate material within the circuit is filtered before the blood is passed back into the circulation. The ascending aorta is cross-clamped proximally to the arterial cannulation site once cardiopulmonary bypass has been achieved to exclude it from the circulation (Figure 1.2). Thus the aortic cannula then directs blood flow away from the heart to the rest of the body. Cardioplegic arrest to reversibly stop the motion of the heart is achieved with a combination of topical myocardial cooling and infusion of potassium-rich solutions through the use of a cannula. The cardioplegia cannula can be placed either (a) proximal to the cross clamp within the aortic root thus facilitating 'antegrade' cardioplegic solution flow down the coronary vessels or (b) within the coronary sinus thus facilitating 'retrograde' cardioplegic solution flow. The result of this hyperkalaemic solution is arrest of cardiac tissue in diastole.

An alternative means of arresting the heart and maintaining the circulation is 'cross clamp fibrillation'. It is estimated that up to 15% of UK cardiac surgeons employ this technique during surgery[85]. When this form of arrest of the myocardium is employed, the heart is excluded from the circulation by the application of a cross-clamp, whilst rapid electrical impulses are delivered directly to the heart. This induces myocardial fibrillation and renders the tissues motionless.

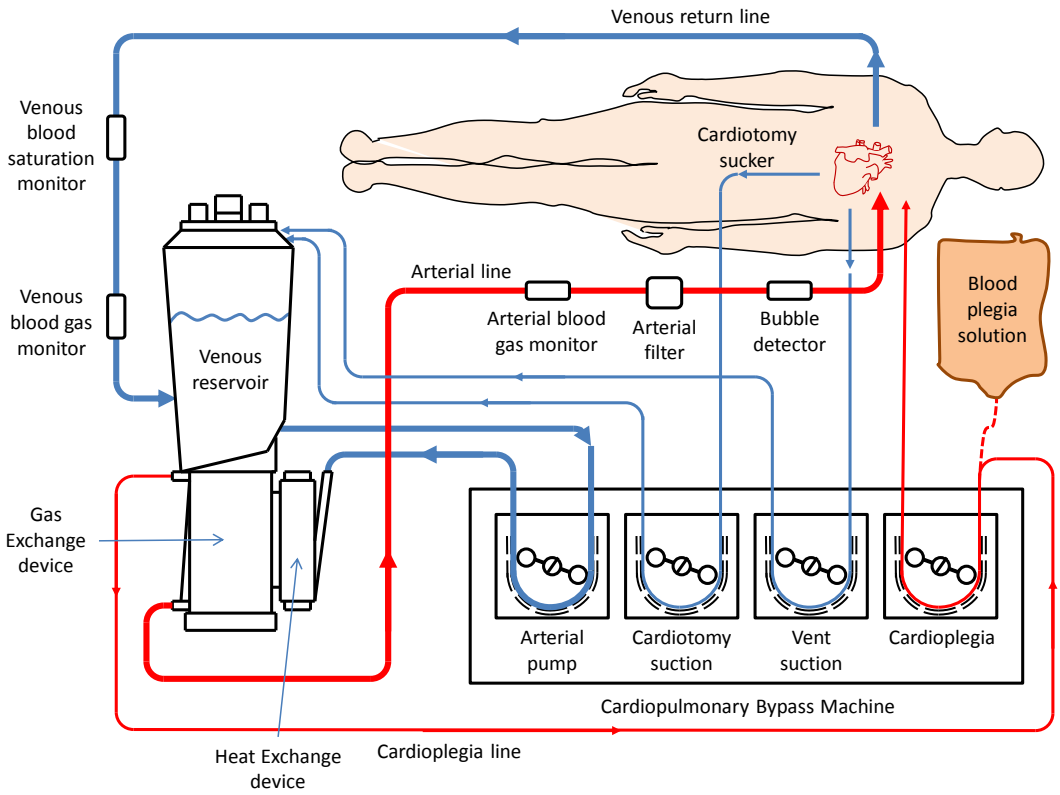

Figure 1.1 Conventional cardiopulmonary bypass circuit

Deoxygenated blood returning from the body is drained into the venous reservoir under gravitational forces via a cannula in the right atrium or central vein. This blood is then circulated using a conventional roller-pump to the heat-exchange device before moving the gas-exchange device for temperature and oxygen-carbon dioxide regulation. Oxygenated blood is then channelled into the systemic circulation via the arterial cannulation site, typically located within the arch of the aorta. Arterial and venous monitors in addition to filters provides a layer of safety within the circuit. Shed blood within the operative field can be recirculated via the cardiotomy sucker and intra-cardiac blood can be evacuated with the use of the vent. Cardioplegic solution can be delivered antegradely to the coronaries via an aortic cannula or retrogradely via a cannula in the coronary sinus.

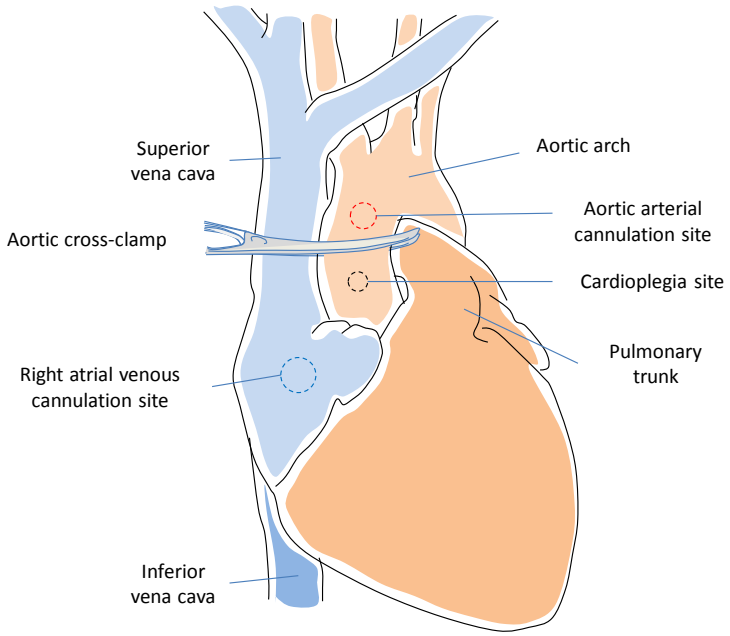

Figure 1.2 Cannulation of the heart with cross-clamp circulatory exclusion
The venous circuit is established via cannulation of the right atrium and the arterial circuit is completed via cannulation of the ascending aorta. Once secured in place, extracorporeal circulation can commence. The heart can be excluded from the circulation by application of an aortic cross-clamp placed proximal to the arterial cannulation site. Cardioplegia can then be given to arrest the myocardium.

1.3.3 Organ damage in association with surgery and cardiopulmonary bypass

Surgery on the heart may be associated with adverse changes in the function of organ systems which can be initiated at the time of surgery and persist into the post-operative period of recovery. The pathogenic mechanisms that lead to organ injury are multifactorial including haemodynamic, inflammatory and direct damage (e.g. embolic to the heart, brain and gut or nephrotoxic to the kidney). A brief overview of some of the clinical correlates and exposure to cardiopulmonary bypass are given below.

The lung is perhaps the organ most susceptible to injury following cardiac surgery with the use of CPB. The lung may be susceptible due to the inherently large vascular bed and the prolonged transit time of leukocytes[86]. It is uncertain if CPB itself is directly responsible for lung injury as post-operative lung dysfunction is similar in OPCAB CABG surgery[87,88]. The majority of patients manifest a subclinical picture of lung dysfunction and there is a relatively low incidence of acute respiratory distress syndrome (ARDS) occurring in less than 2% of patients[89,90]. However, the mortality rate of post-CPB ARDS can be >50%[90]. The mechanisms that drive lung dysfunction are numerous. The lungs are not ventilated during the conduct of CPB. This hypoventilation predisposes to atelectasis of lung units which becomes difficult to re-ventilate post-surgery due to the altered chest dynamics resulting from median sternotomy[91,92]. This is compounded by the alterations in the production of surfactant as a result of alveolar under-ventilation and also as a result of CPB induced inflammation[93]. Relative lung ischaemia occurs during CPB, and this may be an important factor in lung injury as the bronchial blood supply remains the only source of arterial blood during the conduct of bypass[94]. Conversely, improved respiratory parameters in CPB scenarios where perfusion is maintained (with the use of the Drew-Anderson technique) are associated with reduction in pro-inflammatory IL-6 and IL-8 levels in plasma[95]. Furthermore the interaction between putative lung ischaemia, a damaged endothelium and then reperfusion of this organ with the contributions of cytokine release leads to enhanced pulmonary capillary permeability[96]. At the end of surgery, broncheoalveolar lavage fluid in patients subject to

CPBs showed enhanced numbers of neutrophils, as well as increased concentrations of pro-inflammatory cytokines (IL-6, IL-8, TNFα) and neutrophil elastase[97]. Increases in cellular permeability and the additional fluid load of CPB leads to increased extravascular lung water and pulmonary oedema[98]. This scenario can be further exacerbated by blood transfusions and associated transfusion-associated lung injury in the post-operative period. The end result is the development of intrapulmonary shunts with mismatch between lung perfusion and alveolar ventilation as a consequence of hypoxic vasoconstriction. This results in a higher fraction of inspired oxygen (FiO_2) requirement in the post-operative period and prolonged stay in ITU. In addition to the respiratory function that are interrupted, the lungs are also responsible for the metabolism of noradrenaline[99] and sequestration of opioids[100]; both of which are perturbed by extracorporeal circulation, and complicate the clinical picture in recovery.

Kidney injury has a consensus definition according to the Risk-Injury-Failure-Loss-End stage (RIFLE) classification[101]. Up to 30% of cardiac surgery patients develop clinically evident kidney injury with 1% requiring dialysis[102]. Haemodynamic / ischaemia-reperfusion mechanisms are important in kidney injury as CPB can reduce renal perfusion by 30% (which may be beyond the normal auto-regulatory range of the kidney to maintain adequate function)[103]. Thus, experimentally, antagonists of endogenous vasoconstrictors ameliorate renal ischaemic injury in animal models[104]. Research also suggests that pulsatile perfusion (rather than conventional laminar flow) has as protective effect on the kidney during cardiopulmonary bypass[105]. From an inflammatory perspective, kidney parenchymal up-regulation of NF-κB was observed in rat models of renal ischaemia[106]. Following on from this, cardiopulmonary bypass exposure in a large animal model resulted in increases in urinary levels of IL-18 as well as vascular endothelial cell dysfunction and reduced nitric oxide tissue bio-availability[107]. Conventional blood markers of renal function such as creatinine are not elevated until >90% renal injury, and do not manifest clinically for a few days post-operatively. Newer biomarkers of injury have been studied. Neutrophil gelatinase-

associated lipocalin (NGAL) is released in renal tubular damage and is utilised as an early biomarker of kidney injury in cardiac surgery, having predictive value at 2 hours post-cardiopulmonary bypass[108].

Perioperative myocardial damage can be a significant problem. The incidence of post-operative myocardial infarction occurs in 2-3% of patients following cardiac surgery[109]. During cardiac surgery, the aorta is usually cross-clamped and the heart is rendered ischaemic. If the heart continues to beat, there is progressive consumption of high-energy phosphates from intracellular stores, with protection provided by cardioplegia or intermittent cross-clamp release [110]. Ischaemic myocardium during surgery results in microstructural and functional changes (previously discussed in 1.1, page 19). Cardio-specific proteins (CK-MB) and troponins are the mainstay markers of cellular damage[111]. Additionally, heart-type fatty-acid-binding protein hFABP is an emerging rapid marker of myocardial infarction[112]. There are consistently higher markers of myocardial injury in association with on-pump surgery compared to off-pump surgery[111,113]. This trend is also observed with optimised bypass systems, compared to conventional bypass systems[114-118].

Changes in regional blood flow and flow characteristics during cardiopulmonary bypass can be associated with hypoperfusion of the splanchnic circulation[119]. These can be compounded by the use of vasoconstrictor agents and by the embolization of material or atheroma from the aorta into the mesenteric circulation occluding blood flow. The gut circulation can be significantly reduced even when whole-body perfusion indices are 'normal' as the release of vasoactive substances (such as vasopressin and catecholamines) leads to the alterations in blood flow away from the gut in preference of other organ systems[120]. Gastrointestinal mucosal blood flow can be reduced with the use of CPB and can remain hypoperfused in the post-operative period[121]. These mechanisms combined with the inflammation from SIRS disrupt the barrier and absorptive functions of the gut[122]. Increased intestinal mucosal permeability may be a mechanism that allows the translocation of bacterial endotoxins into

the vasculature to propagate the inflammatory response and organ damage[123]. Approximately 2-4% of patients have a GI complication following surgery, with a particularly high mortality of 30%[124,125]. The complications are gastrointestinal bleeding, peritonitis or bowel obstruction.

The incidence rates of stroke are around 2-3% following cardiac surgery with increased risk in elderly patients[126]. The mechanisms for injury to the brain during cardiac surgery with cardiopulmonary bypass can occur via reduction in blood flow and embolism[127]. The effect of systemic inflammation is in dispute and the inflammatory response is not considered a primary driver of neurocognitive injury[128].

These deleterious events that occur in association with cardiopulmonary bypass are an important consideration for patients undergoing cardiac surgery. The key mechanistic aspects of the inflammatory response and its contribution to morbidity and mortality are discussed in the next part of this chapter.

1.4 THE INFLAMMATORY RESPONSE

Derived from the latin *inflammare* meaning literally 'to set alight', inflammation is a response of the body to harmful injury or infection. Activation of the inflammatory response involves the appropriate recognition of an adverse event. This is followed by the concerted co-ordinated release of pro-inflammatory molecules and immune-modulatory agents to protect against the deleterious stimuli. These molecules also direct the healing processes when inflammation resolves.

There are five classical signs of inflammation. Four of these were characterised by the Roman physician Aulus Cornelius Celsus (ca. 25 BC – 50 AD) in his treatise *De Medicina*[129]. These are *rubor* (redness), *calor* (heat), *dolor* (pain) and of *tumor* (swelling). The fifth sign of *functio laesa* (loss of function) was later contributed to by the Greek physician Galen (AD 129 - c200)[130] and also variously attributed to the German physician Rudolf Virchow (1821-1902)[131]. The classical features of inflammation occur due to increased blood flow into the area of injury from vasodilatation resulting in heat and redness. The movement of cells from the intravascular blood compartment into interstitial tissue compartment (occurring as a result of increased vascular permeability) results in tissue swelling and nerve compression causing pain with loss of function.

The inflammatory process can be broadly considered as either acute or chronic in nature. In the initial acute phase of the response, leukocytes migrate to the area of injury and neutralise the inflammatory stimulus. Once this process is complete and the responsible stimulus for leukocyte activation and migration has been removed, damaged tissues undergo repair. Following on from this, a return to basal homeostatic conditions occurs with the termination of the inflammatory response. In the situation where there is a persistence of the inflammatory stimulus, or the inflammatory response fails to resolve, chronic inflammation may occur[132]. The pathological state of chronic inflammation, and the molecular mechanisms

that underlie this status are important in a number of diseases including, inflammatory bowel disease[133-135], arthritis[136,137], vasculitis[138], cancer[139-141] and atherosclerosis[1,8-10].

1.4.1 Systemic inflammation following CPB

The benefits of CPB have also brought challenges in terms of its potentially deleterious effects on the immune system and the haematological manipulations necessary for safe conduct. As such, there is emerging research into techniques of coronary artery revascularisation avoiding the use of CPB, known as off-pump surgery, and movement towards the optimisation of CPB systems.

There is a systemic, generalised, inflammatory response associated with cardiac surgery and use of extracorporeal circulation[142-147]. This can result in both morbidity and mortality for the patient. In part, systemic inflammation occurs due to the exposure of circulating blood to artificial surfaces and un-physiological shear stresses during CPB[148]. Thus there is activation of the complement cascade following bypass[149-151] in a biphasic pattern both during and after CPB[152] which is compounded by the changes of ischaemia and reperfusion of the myocardium and other end organs. The consequence of conventional cardiopulmonary bypass is a disruption of coagulation, activation of leukocytes and complement and release of inflammatory and vasoactive substances into the circulation[144,145,153-156]. Microembolic particles composed of platelet aggregates and fibrin (with a combination of other particles introduced into the circulation) are produced which can obstruct the distal microcirculation[157,158]. The final outcome from this milieu is a disruption of haemodynamic homeostasis and organ failure at the most extreme end of injury.

The magnitude of the inflammatory response to CABG with CPB depends on a number of factors including: the biomaterials used in the components of the bypass circuit[159]; the rate and characteristics of blood flow[160,161]; oxygenator components[148]; biomaterial surface area in

direct contact with blood with benefits observed with heparin-coated circuits[162-164]. Patient factors such as (age, medical co-morbidities, surgical preparation[165]) and surgical factors (such as the duration of surgery[166], the type of surgery), administration of heparin-protamine, hypothermia[167-169] and lung ventilatory arrest[170] are also important elements. The effects of surgical access (incisions, sternotomy and electrocautery dissection) are important determinants of leukocyte activation as trauma (and other forms of physical injury) contribute to pro-inflammatory activation[171-174]. In addition, the immune-modulating effects of anaesthetic agents[175-177]; perioperative myocardial protection techniques[178,179]; and use of pharmacological cardiovascular support[180] all influence the characteristics and propagation of the immune response.

The process of acute inflammation predominates in the field of cardiothoracic surgery. This ranges from the minor local effects around a surgical incision site to the most severe manifestations of a body-wide 'systemic inflammatory response syndrome' (SIRS)[143,155,181]. Surgically relevant triggers of SIRS are physical trauma, infection, anaphylaxis, burns and the use of extracorporeal circulation[144,145,171,172]. SIRS can result in haemodynamic instability[146] and morbidity[182,183] contributing to an adverse clinical profile for patients. As a serious clinical entity, SIRS can drive multiple organ failure with disastrous consequences.

There are defined clinical criteria for the diagnosis of SIRS. These clinical features are (1) body temperature less than 36˚C or greater than 38˚C (2) heart rate greater than 90 beats per minute (3) tachnypnoea with a rate above 20 breaths per minute and (4) a leukocyte count of less than 4×10^9 cells/l or greater than 12×10^9 cells/l in a patient's whole blood [184,185]. SIRS is considered to be present when two or more of these explicit criteria are met[185].

In association with the use of cardiopulmonary bypass, activation of the circulating neutrophil pool can be demonstrated within 15 minutes of the bypass commencement by elevated expression of CD11b/CD18 integrin[186]. This cellular activation is driven by a host of pro-

inflammatory agents including: cytokines (including IL-1β, TNF-α, IL-8); arachidonic acid derivatives (leukotriene B4, thromboxane A2); contact proteins (kallikrein); the complement system molecules (C5a), heparin, histamine and DAMPs[149,187-190]. CPB also enhances neutrophil activity by inhibiting neutrophil apoptosis signals[191]. Periods of ischaemia and reperfusion associated with CPB enhances leukocyte transmigration due to altered blood flow enabling neutrophils to marginate. Ischaemia promotes endothelial cell activation leading to rapid expression of adhesion molecules, (e.g. P-selectin and ICAM-1)[192]. This facilitates the process of extravasation into tissues. Cells of the monocyte/macrophage lineage are activated between 2-24h post-bypass and at 24 hours post-bypass, elevated numbers of cells can be detected in broncheoalveolar lavage fluid[193,194]. When assessing the direct effect of cardiopulmonary bypass on leukocyte egress using the cantharidin technique, exposure to CPB triggered a 381% increase in leukocyte extravasation into skin blisters compared to reference blisters. In patients exposed to CPB for a mean of 76 minutes, the total leukocyte count increased from 4.84 to 24.48 × 10^5/blister; neutrophils increased from 2.79 to 14.37 × 10^5/blister; monocytes increased from 1.16 to 6.37 × 10^5/blister and lymphocyte count increased from 0.4 to 1.02 × 10^5/blister [195]. The regulatory mechanisms that lead to the activation, phenotypic changes and migratory capacity of leukocytes will be further explored in detail in later portions of this introduction.

Despite these inflammatory events, our clinical experience of cardiac surgery with short-term CPB exposure has shown that the use of extracorporeal circulation use is relatively safe. This may be a reflection of the body's ability to compensate for these effects and also in the parallel advance of post-operative recovery monitoring and intervention. However, the drive to optimise CPB is both crucial and necessary as the patient population undergoing cardiac surgery become more complex, possess greater co-morbidity and less physiological reserve in concert with requiring more advanced procedures and longer CPB runs.

1.4.2 Initiation of the inflammatory response

Cell death and tissue injury are triggers for inflammation. Of emerging importance is the release into the circulation of damage associated molecular patterns (DAMPs) which are generated following injury, in the context of cardiac surgery, from a variety of scenarios. These DAMPs function as the early promoters of the innate immune response[196].

The innate immune response is directed by a family of pattern recognition receptors (PRRs) [196-201,202-205,160,161]. These receptors are distributed on cell surfaces as well as being located within cells. PRRs detect highly conserved molecules known as pathogen-associated molecular patterns (PAMPs) which share characteristics with endogenous damage-associated molecular patterns (DAMPs) (Table 1.1). PAMPs are molecules associated with groups of pathogens, and their corresponding receptors are highly conserved throughout nature as a result of their intrinsic importance in survival. PAMP molecules include components such as bacterial cell wall glycoproteins, single and double stranded RNA fragments and bacterial flagellin which are clearly absent in the host. When detected, these components are able to provide clear unambiguous signals alerting the immune system to the presence of something pathogenic to direct a co-ordinated response[197]. Similarly, DAMPs are molecules / molecular substrates derived from host cells that can arise from injury in the absence of infection. They can be classified as protein (e.g. S100 proteins, heat shock proteins (HSP), HMGB1) or non-protein (e.g. ATP, uric acid, heparin sulphate, RNA, DNA, mitochondrial fragments) in origin[165,173,181,201,206-209].

PAMPs and DAMPs are recognised by several families of PRRs including the Toll-like receptors (TLRs)[210,211]; NOD-like receptors (NLRs)[212-214]; Formyl peptide receptors (FPRs)[202-205], RIG-I-like (RLRs) receptors, AIM2-like receptors (ALRs) and activation of the Receptor for Advanced Glycation Endproducts (RAGE) [196-200]. These receptors (receptor families) are found on circulating leukocytes, platelets, endothelial cells and mesenchymal cells, with emerging various subclasses of receptors being reported in the literature. Interactions

between DAMPs and PPRs regulate the induction of SIRS by CPB and a wide variety of DAMPs and associated signalling cascades are being identified as being directly relevant to the process of cardiothoracic surgery. The best characterised PPRs are the TLR family of proteins given their name due to the structural similarity they shared with the Toll gene in *Drosophila*. TLRs are highly conserved components of the immune system across species, and even in plants, with 11 classes of TLRs identified in humans thus far. TLR1, -2, -4, - and -6 are located on cell surfaces whereas TLR3, -7 and -9 are found intracellularly. They detect DAMPS including DNA, and mitochondrial DNA[207,210] nucleic acid fragments which are released following trauma and stress molecules such as heat shock proteins (HSP)[181], high-mobility group protein Box-1 (HMGB1)[209] generated following cellular stresses including haemorrhagic shock[215] and especially with ischaemia-reperfusion[216,217] with corresponding up regulation of TLR receptor expression on immune cells[218,219] and alveolar macrophages[220] with cardiac surgery or no effect on immune cell receptor expression[221].

Detection of DAMP/PAMP molecules by their respective receptors leads to the activation of intracellular signalling cascades which interface via secondary adaptor proteins and signalling molecules. When the DAMP/PAMP signals favour a pro-inflammatory response, the cascades ultimately converge on the activation of the AP-1 family of transcription factors (via activation of the mitogen-activated protein (MAP) kinases, NF-κB activation and are modulated by other redox-sensitive signalling molecules (see 1.5, page 56). These pathways regulate the activation and propagation of inflammatory cellular processes by enhancing leukocyte survival by inhibiting apoptosis signals[222-224], and also by activating vascular endothelial cells.

Access to the heart and great vessels within the chest is achieved surgically usually via a median sternotomy using a vibrating saw and electrocautery for dissection. This causes the release of cellular tissue fragments, bone components and fat globules to be released into the circulation, from localised electro-physical trauma. It is plausible that early release of

DAMPS during surgery results in the up-regulation of genes responsible for the release of TNFα and IL-1 pro-inflammatory cytokines from injured endothelial cells to create a chemokine gradient to attract cells of the immune system.

Receptor	PAMP	DAMP
TLR-1	Triacyl lipopeptides	
TLR-2	Lipoprotein, LPS, PGN, LTA, zymosan, trypanosmal phospholipids	HSP60, HSP70, defensins
TLR-3	dsRNA	mRNA
TLR-4	LPS, pseudomonas exoenzyme, RSV F protein, MMTV envelope protein, trepansomal lipids, taxol	HSP60, HSP70, HSP90, HMBB-1, hyaluronic acid, fibrinogen, fibronectin, fx1-defensin, heparin sulphate
TLR-5	Flagellin	
TLR-6	Diacyl lipopeptides	
TLR-7	ssRNA, imiquimod	
TLR-8	ssRNA, resquimod	
TLR-9	Bacterial/viral DNA, CpG DNA	Unmethylated CpG DNA, mitochondrial DNA
TLR-10	Unknown	
TLR-11	Ureobacteria, toxoplasma LPS	
NLRC1	Meso-DAP	
NLRC2	Muramyl dipeptide	
NLRP3	Muramyl dipeptide, CpG DNA, dsRNA	ATP, uric acid crystals
FPR	N-formyl peptides	

Table 1.1 Damage associated molecular pattern receptors with corresponding ligands

1.4.3 Regulation, circulating levels and phenotypic effects of DAMPS

The control and clearance of DAMPs depends on the context of their generation (i.e. single insult such as CPB or isolated traumatic injury, or conversely a chronic ongoing disease process) and on the mechanisms of their removal from the circulation. A suggestion from this thesis is that the release of DAMPS could be an initiating stimulus for CPB-associated activation in response to trauma or injury. However, there is a relative paucity of experimental human data that characterises the precise pharmacokinetics for many of the DAMPs in the circulation in the specific context of cardiac surgery. The studies reported in the literature give only glimpses at the mechanistic links and are described below.

Following major trauma, mitochondrial DNA fragments and formyl peptide fragments are released from injured tissues into the circulation[173,208]. These are known to activate leukocytes via TLR and FPR receptors[181,217,225]. Concentrations of mitochondrial DNA release also positively correlated with increased phosphorylation of p38 and ERK MAP kinases as well as IL-8[207], suggesting a mechanistic link in the leukocyte activation cascade[173]. Exposure to mitochondrial DNA enhances ICAM-1 and E-selectin on endothelial cells as well as CD18 and L-selectin on leukocytes to promote adhesion of leukocytes to vascular endothelium[226]. Mitochondrial DNA levels in trauma patients with high injury severity scores (ISS>25) were 2.7 ± 0.94 μg/mL (thousands of fold increase compared to healthy controls) and remained elevated at 24 hours post index injury event, in plasma[207]. This elevation of mitochondrial DNA was also evident in processed reamed bone fragments from femoral repair, in data from the same group. Circulating plasma cell-free DNA concentrations have also been shown to be significantly increased in severely injured patients in other studies (β-globin gene 80840 kilogenome-equivalents/L, ISS>25)[208]. These levels decrease within 2 hours (relative to the index injury) towards reference values with a second increase in plasma concentrations in the following days, coinciding with organ failure[208]. Correspondingly, elevated plasma cell-free DNA levels have been associated with worse clinical outcomes in severely injured patients[227]. The mechanisms for this increase of cell-free DNA in plasma

may be due to necrosis with direct tissue and cellular injury as the main precipitating source given plasma elevation changes are evident within 30 minutes of insult[228]; apoptosis as a secondary delayed phenomena[229], active release into the plasma[230] and impaired clearance from organ damage (given that fetal cell-free circulating DNA has a normal half-life of 16 minutes[231]). Circulating cell-free DNA in the plasma is mainly removed rapidly by the liver[232], with levels not being altered by chronic kidney disease or dialysis[233]. The release of mitochondrial DNA into the circulation has also been correlated with the development of SIRS[234]. Thus it is possible that elevated mitochondrial DNA may initiate inflammation following trauma. The plasma kinetic changes of mitochondrial DNA in the context of cardiopulmonary bypass has not yet been characterised although a study has demonstrated elevated levels of mitochondrial DNA transcripts in cardiomyocytes in aortic valve surgery using sevoflurane (compared to propofol) as a cardioprotective agent[235].

The DAMP High-mobility group protein B1 (HMGB1) is released from apoptotic, necrotic and activated immune cells in the context of ischaemia re-perfusion and binds to TLR-2, -4 and RAGE[197]. Plasma HMGB1 levels were elevated more than 30-fold above healthy controls within 1 hour of injury (median 57.8 ng/mL), peaking between 2-6 hours (median 526.2 ng/mL) following insult in ISS>15 populations. HMGB1 is released into the plasma in a variety of cardiac operations surgery with the use of CPB (valve replacements, septal closure, CABG), as well as in off-pump coronary revascularisation with peak levels after aortic-declamping or completion of anastomoses[209]. The peak levels were recorded at one hour following aortic declamping, in surgery with CPB (11.5±7.9 ng/mL) and at 30 minutes following revascularisation in OPCAB (8.4±3.9 ng/mL) remaining elevated at 1hour following admission to ITU in both groups, before returning to baseline at 24 hours[209]. Together, these studies suggest HMGB1 may be an integral part of the early inflammatory response to trauma and have a positive predictive effect for survival[236]. Release of HMGB1 has been shown to lead to activation of neutrophils and IL-8 and TNFα cytokine expression via both -p38 MAP kinase and -NF-κB pathways[237]. With the presumption that DAMPs are

derived from apoptotic and necrotic cells, enhancing the normal physiological clearance of these cells or prevention of their accumulation may provide a therapeutic window. For example impaired clearance of apoptotic cells is associated with elevated levels of HMGB1 in bone marrow of leukaemic patients[238].

Another DAMP, Heat Shock Protein 70 (HSP70), is induced in response to myocardial ischaemia and binds with PRRs. In patients undergoing CPB, levels of circulating HSP70, a ligand for TLR4, were enhanced at peak levels immediately after operative intervention in plasma (1809 pg/mL immediately after surgery; 1879 pg/mL 5 hours after surgery, returning to baseline at 19 hours post-surgery) with an up-regulation of monocyte TLR-2 and TLR-4 surface expression [181]. This was coupled with the observation of enhanced levels of IL-6 in plasma up until 2 days following surgery, following the HSP70 peak release[181]. Investigation of HSP70 release at earlier timepoints showed no release after heparin, before CPB nor enhancement at 30 minutes after CPB but only after protamine reversal with enhanced release into the plasma both in the context of off-pump (3700 pg/mL) and on-pump surgery (5100 pg/ml[239]. In the same paper, differential expression of intracellular HSP70 was observed in leukocytes suggesting a faster reaction of monocytes and granulocytes than lymphocytes to the effects of CPB[239]. The receptor for HSP70, TLR-4, has been demonstrated to influence the mediation myocardial injury via activation of downstream MAPK[225] and NF-κB[240] signalling pathways. Another member of this DAMP family, HSP72, is induced in patients with unstable angina undergoing CABG, and is additionally associated with up-regulation of NF-κB and AP-1 gene expression within the myocardium[241].

The S100 protein family are known to be expressed in cells of myeloid origin and are found in high concentrations in inflamed tissues, acting as DAMPs[242]. These family of proteins can signal via RAGE receptors to promote the inflammatory response[243]. The pro-inflammatory effects of S100 signalling can occur both via p38 MAP kinase[244] and NF-κB dependent systems[245]. Within endothelial cells, S100 enhances the expression of adhesion molecules

such as ICAM-1 and the expression of integrins such a Mac-1 on leukocytes[246]. S100 proteins are detected in higher concentrations following brain injury and stroke[247,248]. Consequently, the S100 proteins have been suggested as a biological marker of brain injury in cardiac surgery. S100 is detectable after 30 minutes post-CPB and becomes undetectable within 24 hours[249]. The highest levels of S100 in plasma were reported as 0.5g/L, dependent upon the duration of exposure to CPB[249]. It is suggested that there may be predictive value of this marker to identify hitherto undetected neurological injury.

In addition to the release of DAMPs, the complementary phenomena of up-regulation of expression of TLR receptors is seen following exposure to CPB in adults[162,163] and children[250] in leukocytes. Experimentally, genetic deletions of TLRs[251] or inhibition of TLR-MyD88[252] signalling or receptor blockade[253] has promise in the minimisation of warm hypoxic injury in the myocardium with reduction in infarct size and attenuated p38 MAP kinase and NF-κB activation in tissues.

Overall, these studies suggest that release of DAMPs may promote systemic inflammatory responses following surgery with signalling mediated via PPRs and secondary signalling cascades. These have different individual characteristics and further work to elucidate their mechanisms of release and biological characteristics is warranted in the field of cardiac surgery.

1.4.4 DAMPs and secondary messenger signalling cascades

DAMPs along with their corresponding receptors work in unison with intracellular signalling mechanisms to orchestrate the immune response (Figure 1.3). For example, TLRs signal via the adaptor protein myeloid differentiation factor 88 (MyD88) to control downstream regulation of signals that activate NF-κB[165]. Alternatively, TLR activation pathways (TLR3) leads to the recruitment of an adaptor protein known as TIR domain-containing-adaptor

which is capable of inducing IFNβ (TRIF). In turn, TRIF activates the kinases TBK1 and RIP1. The TBK1 kinase signals via IRF3 phosphorylation to induce IFN1. Activation of the RIP1 kinase leads to polyubiquitination and activation of TAK1, leading to activation of NF-κB via IKKβ[200]. The protein MyD88 alternatively phosphorylates TNF receptor-associated factor 6 (TRAF6) in a pathway which can lead to the activation of MAPKs also via the polyubiquitination of the protein TAK1[200]. The downstream effectors of FPR activation include the MAPKs ERK1/2, JNK and p38 via PI3K[204]. In addition, activation of NLR subclasses leads to RIP2 activation (via RIPK2) and enhances activation of MAPK and NF-κB pathways[214].

Their precise role of DAMPs and these pathways in cardiac surgery and their relative influence during cardiopulmonary bypass remain to be elucidated. These brief illustrative examples highlight the links between DAMPs/immune receptor signalling cascades to the phosphorylation of p38 MAP kinase and activation of NF-κB, of importance to this thesis. This evidence provides cohesion with the experimental plans described in later portions of this work.

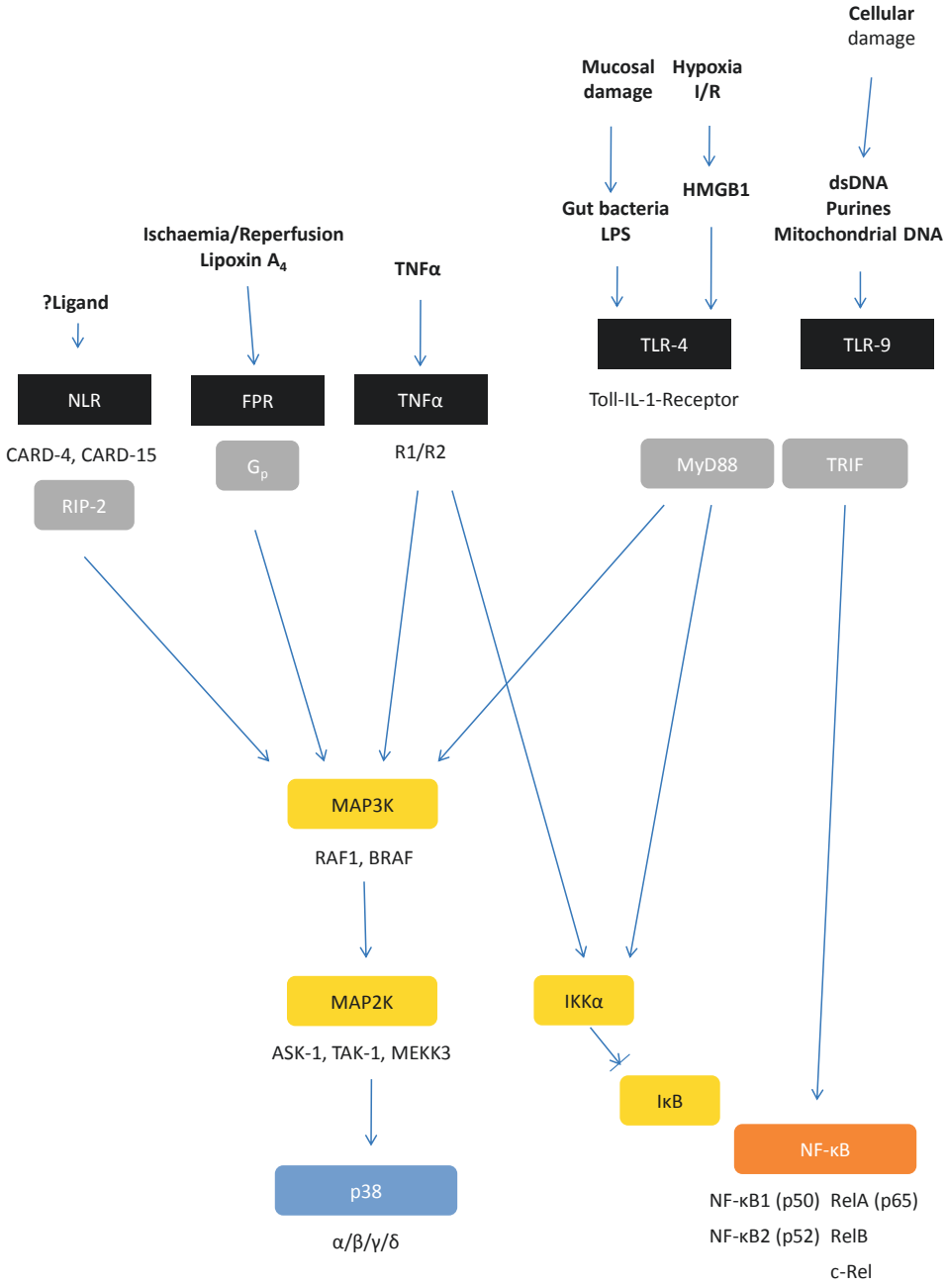

Figure 1.3 DAMP signalling relationships with inflammatory cell signalling pathways

1.4.5 Mechanisms of leukocyte activation

1.4.5.1 Cellular components of inflammation

The function of leukocytes in the acute phase of an inflammatory response is to neutralise and remove harmful agents such as microbes, antigens and cellular debris to limit the spread of injury and to pave the way for healing and resolution. Leukocytes are recruited locally (under chemokine/cytokine, DAMPs influence) from the circulation and also mobilised from the bone marrow (promoted under LTB_4, C5a, IL-8 influence, and controlled by stromal cell-derived factor-1, SDF-1, or granulocyte colony-stimulating factor, G-CSF)[189,190]. A schematic for these interactions is given in Figure 1.4.

The leukocyte population that responds early to injury are the neutrophils which are recruited to sites of inflammation within minutes. These polymorphonuclear cells comprise the most abundant subpopulation of leukocytes and have an approximate lifespan of 5 days[254]. They migrate under the influence of chemotactic mediators (such as C5a, IL-8, IFNγ and bacterial cell wall components) and marginate and migrate to the site of injury via selectin-dependent capture and integrin-dependent adhesion[255]. Recognition of an inflammatory stimulus occurs through opsonisation, with immunoglobulins or complement, thus leading to phagocytosis[256]. This process results in the formation of a phagocytic vacuole which internalises cellular debris and foreign particles which are then exposed to lysosomal enzymes (elastase, myeloperoxidase, lactoferrin) ensuring their destruction. Neutrophils are also capable of generating reactive oxygen species and utilise a "respiratory burst" (involving NADPH oxidase generating superoxide) to kill infected or damaged cells[257]. After performing their function, neutrophils undergo programmed cell death leading to the down regulation of the inflammatory cellular response.

Derived from bone marrow monoblasts, monocytes comprise approximately 8% of the total leukocyte population and, on leaving the circulation, differentiate into macrophages in tissue.

Monocytes can migrate to the site of inflammation within 8-12 hours of injury to produce cytokines, to present antigens and to perform phagocytic functions. They are important in the pro-inflammatory response and also in the resolution of inflammation by clearing cellular debris and apoptotic neutrophils (under the influence of TGFβ, PGE2 and PAF)[258]. They function to clear cellular debris via phagocytosis and regulate fibroblasts, smooth muscle and endothelial cells via tissue growth factors (FGF, PDGF) for the production and organisation of the extracellular matrix with the aim of complete resolution. This results in scar formation characterised by the deposition of large amounts of fibrin which cannot be easily removed.

All lymphocytes are derived from a common lymphoid progenitor in the bone marrow. Lymphocytes are broadly divided into B- and T-cell subtypes. The B-cell subset matures in the bone marrow whereas T-cells mature and undergo selection within the thymus gland. Once established, lymphocytes are found in the circulation in small numbers and peripheral lymphoid organs – namely the spleen and lymph nodes. They play an essential role in adaptive immunity by releasing antibodies (B-cells); direct cellular cytotoxicity (cytoxic T-cells, NK cells) or by signalling to other cells of the immune system (helper T-cells). In contrast to other leukocytes, lymphocytes can persist for a whole lifetime and are important in the regulation of the immune response, self-tolerance to tissue specific antigens and in the development of 'immunity' to pathogens.

Platelets are cellular fragments of the precursor megakaryocyte within the bone marrow with a life span of 5-9 days and possess important haemostatic and inflammatory functions where their predominant role is to respond to damaged endothelium[259]. They outnumber all other leukocytes by a factor of 10. Considering their immune functions, platelets can bind to leukocytes (e.g. via P-selectin) and lead to pro-inflammatory rolling and activation[260]. Activated platelets release a wide variety of pro-inflammatory (e.g. IL-1β, IL-8), anti-inflammatory (e.g. C1-inhibitor, alpha 1-antitrypsin), mitogenic factors (e.g. platelet derived growth factor, transforming growth factor β) and angiogenic factors (e.g. vascular endothelial

growth factor) into the circulation when stimulated[261]. These megakaryocyte fragments also possess TLR-4, important in platelet-neutrophil pro-inflammatory interactions and responses to DAMPs and other molecular triggers[262].

1.4.5.2 Leukocyte interactions with the vascular endothelium

The vascular endothelial cells (EC) form a semi-permeable barrier that regulates the transport of macromolecules and fluids across the vascular wall. This endothelial barrier is maintained by intercellular junctions – the gap junctions which allow passage of small molecular weight solutes between cells (formed by connex*ins* (Cx) i.e. Cx43, Cx40, Cx37 – organised as connex*ions* acting as channels for molecular movements); the adherens junctions which play an important role in contact inhibition and EC growth (zonula adherens, which are composed of transmembrane proteins of the cadherin family, VE-cadherin, N-cadherin and PECAM-1) and the tight junctions which maintain paracellular permeability (zonula occludens, which are composed of Occludin-1, Claudins-1/-2, junctional adhesion molecule (JAM)-A/B components)[263].

Activation of the inflammatory response leads to recruitment of leukocytes at sites of local injury or infection via the release of cytokines and chemokines or other activating signal (e.g. TNFα, IL-1, IL-8, DAMPs, leukotrienes, complement components) from sentinel cells (e.g. dendritic cells, endothelial cells, mast cells) into the plasma to initiate the leukocyte recruitment cascade and also the vascular endothelium facilitating leukocyte extravasation to the site of injury[255]. The vascular endothelium exhibits increased permeability during periods of acute and chronic inflammation, with the site of the post-capillary venule being the main site of inducibility and leukocyte interactions. Up-regulation of adhesion molecules such as P-selectin and E-selectin in endothelial cells transiently bind to up-regulated ligands on leukocytes, including P-selectin glycoprotein ligand-1 (PSGL-1) and E-selectin glycoprotein ligand-1 (ESL-1), resulting in tethering and rolling of inflammatory cells on the vascular

endothelium[264,265]. Guided by the chemokine/cytokine inflammatory gradient, interactions of integrins (e.g. LFA-1, VLA-1, Mac-1) on leukocytes with their corresponding ligands on endothelium (e.g. ICAM-1, ICAM-2, VCAM-1) results in arrest and transmigration into tissues[266,267]. Endothelial membrane protein including PECAM-1, ESAM-1 aid leukocyte movement across membranes, with reverse migration prevented by endothelial JAM-C[255,268]. There can be considerable overlap between the stages of leukocyte extravasation with close co-ordination between adhesion molecules and ligands[269].

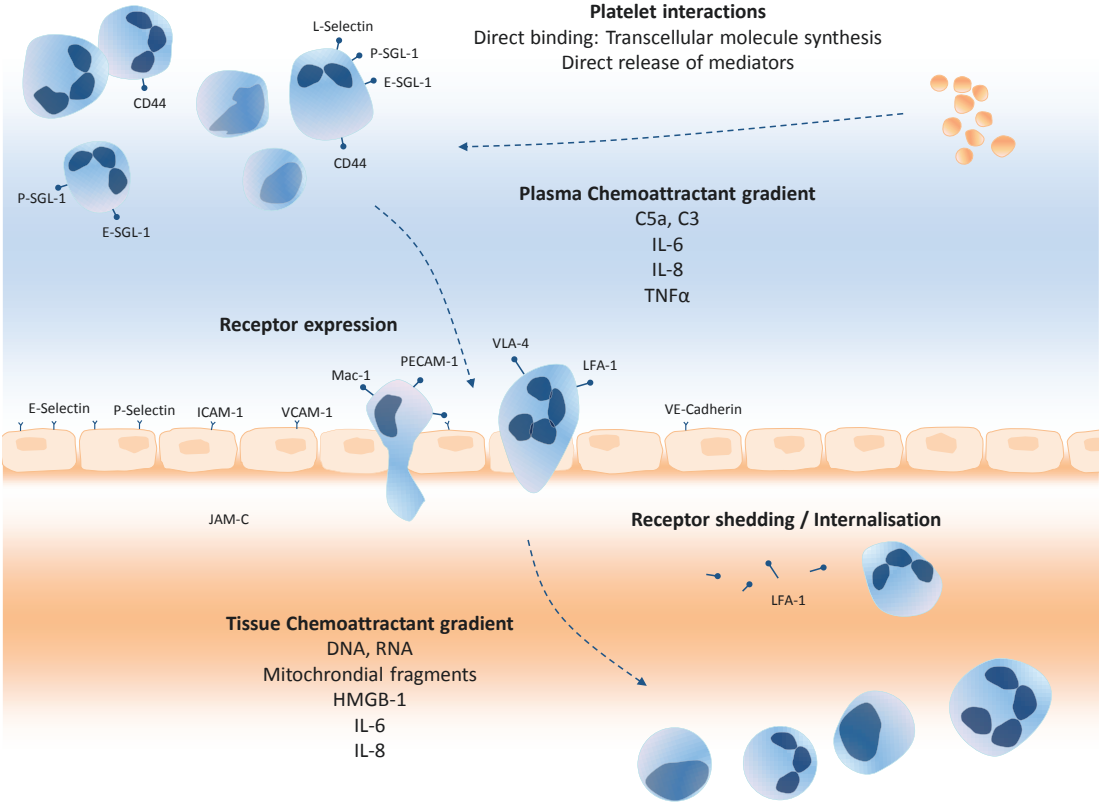

Figure 1.4 Overview of cellular interactions in inflammation

The molecular mediators that regulate the adherence of endothelial cells to circulating leukocytes is complex and multi-step. The selectins (E- and P- selectin) initiate the capture and rolling of circulating leukocytes. The integrin ligands (ICAM-1 and VCAM-1) enable the arrest of rolling leukocytes. The expression of these molecules by endothelial cells in vitro is regulated by inflammatory factors such as IL-1 and TNFα. Additionally, the sheer-stress profile of flowing blood alters endothelial cell activation and the ultimate transmigration of arrested leukocytes between (paracellular) or through (transcellular) the endothelial barrier.

1.4.6 Assessment of leukocyte migration

Human in-vivo models of leukocyte migration have been studied using the skin. Other experimental animal (e.g. peritonitis[270], cremasteric vessels[271], air pouch[272]) models do not possess a favourable translation profile for adaption into human subjects. The human skin is an innate barrier to protect against the environment. This organ is composed of distinct layers: namely the superficial epidermis with the basement membrane above the dermis. The epidermis is composed of an impermeable layer of dead cells on the surface, the stratum corneum. The remainder of the epidermis is relatively avascular with blood coming from dermal capillaries.

Historically, a "skin window" model was used to assess leukocyte migration; in removing the outer epidermal layer from skin, leukocyte egression could be studied into this particular tissue compartment. Early studies utilised a scalpel to remove the stratum corneum layer of skin with lesions being covered with glass coverslips with subsequent assessment of adherence of leukocytes onto the glass[273]. Alternative techniques used include skin abrasions using a drill[274,275] and tape-stripping to cause superficial lesions[276]. However, these techniques were difficult to standardise in terms of reproducibility of size and depth of lesions created, as well as complications of bleeding. An alternative means of assessment of leukocyte movement into skin is to use a 'skin blister' model using mechanical or pharmacological means to induce the separation of the epidermis from the dermis. The technique of applying a negative-pressure suction device onto the skin allows for the harvesting of blister fluid, but this can be traumatic and yields small volumes[277].

Pharmacologically, reproducible and effective volumes of blister fluid can be developed using the topical blistering agent cantharidin[278]. Cantharidin is a protein phosphatase 1 and 2 inhibitor found in the hemolymph of blister beetles (*Meloidae coleoptera*)[279]. When applied to the skin, it causes separation of the superficial layer of cells (acantholysis) and blister formation. Cantharidin is an odourless and colourless agent that has been used medically to

remove warts[280,281] and unwanted tattoos[282] with more than one million prescriptions having been dispensed without serious adverse effects[283].

Experimentally, cantharidin can be used in humans to study leukocyte emigration and cytokine production in the skin[195,278,284,285]. The cantharidin technique has been previously validated by our group as a tool for analysing the inflammatory response to standard CPB and anti-inflammatory interventions by comparing blisters in patients receiving aprotinin with those receiving saline[195] as well as defining changes in cell surface receptor expression changes[285]. The approach lends itself well to the investigation, development and validation of alternative anti-inflammatory strategies related to surgery.

1.5 PRO-INFLAMMATORY INTRACELLULAR SIGNALLING PATHWAYS

In the earlier parts of this chapter, the initiating events of DAMPs generation was considered and how these pathways were connected illustrated in the context of leukocyte activation, relating to cardiac surgery. Inflammation is controlled by key intracellular signalling cascades regulating the AP-1 superfamily and NF-κB family members. Importantly, the relative influence of particular signalling intermediates/pathways varies according to cellular and environmental context. In the following section, this thesis will focus on delineation of the MAP kinases and NF-κB, and the relative influence of ROS on leukocyte activation, as a mechanism to explain the injury that can occur following cardiac surgery with the use of cardiopulmonary bypass. A descriptive overview of the generation, physiological importance and regulation/modulation of ROS, p38 MAP kinase and NF-κB in inflammation is given below.

1.5.1 Reactive oxygen species

Oxygen is an essential molecule for all aerobic organisms facilitating the production of energy via the oxidative phosphorylation pathway. Derivatives of oxygen known as reactive oxygen species (ROS) are generated by all cell types as a by-product of this process and are important early signalling mediators for cellular pathways including transcriptional regulation, proliferation and differentiation and apoptosis[286-288]. These species are becoming increasingly important in clinical fields of heart failure[289] and cardioprotection[290]. ROS are acknowledged to be important in inflammatory signalling but the precise roles/mechanism and kinetics of influence are not fully understood. ROS can be deleterious at high concentrations leading to protein oxidation and damage DNA[291]. At lower concentrations, ROS can function as signalling molecules[292].

ROS can exist broadly in two forms as free radicals with unpaired electrons or as non-radical forms. The sources of intracellular ROS differ under physiological and pathophysiological

conditions. Within mitochondria, the superoxide radical ($\cdot O_2^-$) is generated via the leakage of electrons from the electron transport chain or alternatively by catalysis via NADPH or xanthine oxidase. The superoxide radical can be converted by dismutation, enhanced by superoxide dismuates enzymes, to hydrogen peroxide (H_2O_2) which can in turn be converted into highly reactive hydroxyl radicals ($\cdot OH$)[292]. Other sources of ROS include, peroxisomes, the plasma membrane, cytosol and endoplasmic reticulum. Within these systems, ROS are formed via the action of the cytochrome P450, NADPH oxidases and enzymes important in arachidonic acid metabolism[286].

The half-lifes of ROS are extremely short - the superoxide radical ($\cdot O_2^-$) is 1 μs[292]; hydrogen peroxide (H_2O_2) is 1 ms[293] and the hydroxyl radical ($\cdot OH$) 1 ns[293]. Due to their reactivity and short half-lives, ROS have a limited range (distance) of influence within cells. However mechanisms exist to facilitate the movement of certain ROS species. For example, H_2O_2 can be transported across biological membranes via aquaporin channels giving a potential for transference between cells in direct contact[294]. Voltage-dependent anion channels in mitochondrial membranes regulates the release of superoxide into the cytosol[295].

The production of ROS is important in the inflammatory response. ROS are generated by cells of the immune system leading to oxidation of signalling molecules as well as in the process of phagocytosis. At sites of inflammation where neutrophils are abundant, H_2O_2 with chloride is converted by the enzyme myeloperoxidase into hypochlorus acid (HOCl) important in the respiratory burst[296]. Superoxide radical generation is important in the killing of microbial organisms of the phagolysosomes of macrophages in humans, as part of the repertoire of ROS responses. Consistent with this, mutations in the genes for NADPH oxidases, ordinarily responsible for the generation of superoxide radicals, has been associated with chronic granulomatous disease associated with greater susceptibility to fungal and bacterial infections.[297]. Experimentally, phorbol esters (PMA)[298], TNFα[298] and LPS[299] mechanistically are known to induce the phosphorylation of the NADPH oxidase complexes,

and thus enhance ROS. This induction of phosphorylation occurs via many mechanisms including p38 MAP kinase[300].

Oxidative stress and ROS signalling regulates the expression of cell adhesion molecules by direct activation (e.g. direct release of P-Selectin from Weibel-Palade bodies) and by transcription-dependent mechanisms. For example, HUVEC treated with H_2O_2 for 1 hour showed enhanced P-selectin expression and increased PMN adhesion[301]. Similarly, H_2O_2 treatment of HUVEC enhanced transcription of ICAM-1[302]. ROS are known to enhance NF-κB activation and up-regulate expression of ICAM-1, VCAM-1 and E-Selectin to promote leukocyte binding[286]. Enhanced ROS activity following TNFα stimulation of PMNs was associated with up-regulation of leukocyte cell surface adhesion molecule CD11b/Mac-1[303]. Enhanced ROS generation also influence endothelial permeability by increasing tyrosine kinase activity (e.g. c-Src, PYK2) leading to VE-cadherin phosphorylation and destabilisation of adherens junctions, as interaction of β-catenin and p120 catenin are prevented[292]. Treatment of endothelial cells with hydrogen peroxide enhanced endothelial cell permeability by disruption of occludin on the cell surface and dissociation from ZO-1 protein, via MAP kinase dependent mechanism, altering tight junctions[304]. Taken together, these studies highlight some potential mechanism for ROS to enhance leukocyte adhesion to endothelial cells and migration into tissues.

Antioxidant defence mechanisms that modulate the activity of ROS have been linked to inflammatory responses. For example, superoxide dismutase (SOD) dismutates superoxide to hydrogen peroxide; the enzymes catalase and glutathione peroxidase are responsible for conversion of hydrogen peroxide to water whereas additional ROS scavenging can be facilitated by peroxiredoxins[305]. SOD has tissue specific distribution, with the highest levels in lung with knock-out animals exhibiting enhanced susceptibility to lung injury[306]. Catalase is highly expressed in liver and erythrocytes[307]. However, the congenital absence of catalase is reportedly a benign condition[292]. The family of glutathione peroxidases (GPx) deals with

hydrogen peroxide by oxidising glutathione into dimeric glutathione disulphide, which is then converted back by glutathione reductase. The depletion of glutathione is associated with enhanced immune airways responses[308,309]. The peroxiredoxins convert hydrogen peroxide to water and are found particularly expressed in lung tissues[310]. In animal peroxiredoxin knockout studies, there was enhanced susceptibility to hyper-oxic injury[311,312]. The thyorexodin (Trx) system is an important defence mechanism against oxidative stress via its disulphide reductase activity and provides electrns to the thiol-dependent peroxidases to remove ROS[313] The absence of thyoredoxin is associated with oxidative stress in dopaminergic cells, of importance in neurogenerative diseases such as Parkinson's disease[314]. The induction of the genes for these cytoprotective mechanisms is regulated by the transcription factor NF-E2-related factor 2 (Nrf2)[315-322], which is discussed in further detail in section 1.6.4 (page 85). This illustrates the multiple systems that exist to regulate and modulate the activities of ROS in biological systems and their importance in inflammation.

Ischaemia-reperfusion occurring from cardiac surgery, is recognised as a key event in ROS-mediated injury[323,324]. ROS levels, and plasma markers of ROS-mediated injury, are elevated following CPB[178,325-327]. This has been particularly associated with the historical use of bubble oxygenators/gas exchange devices[328]. In the scenario of off-pump surgery, there is less oxidative stress illustrating the relative ROS-generating effect of CPB exposure[329]. In parallel with these enhanced levels of ROS, studies have shown an association with reduction/depletion of radical scavenging molecules post-operatively[330]. These perturbations in ROS following CPB influence inflammatory processes since clinical studies with N-acetylcysteine, an anti-oxidant and glutathione precursor, have been shown to attenuate myocardial ROS[331] and apoptosis markers[332] following CPB.

1.5.2 MAP Kinases

MAP kinases regulate multiple diverse physiological processes. Aberrant MAP kinase signalling is implicated in cancer biology, inflammatory disorders[333,334] neurological diseases[335,336] as well as altered development and function of the heart[337,338]. The MAP kinase signalling cascade is illustrated in Figure 1.5. Three major families have been identified: the extracellular signal-related kinases (ERK); c-Jun NH_2-terminal protein kinases (JNK – also known as stress-activated protein kinase, SAPK) and the p38 kinases. p38 MAP kinase was identified as a 38-kDa protein that shared approximately 49% homology with ERK. There are four members of the p38 MAP kinase family: p38α (MAPK14), p38β (MAPK11), p38γ (MAPK12) and p38δ (MAPK13). These are all activated by dual phosphorylation on threonine (T) and tyrosine (Y) within the motif Thr-Gly-Tyr within the kinase subdomain VIII. p38 MAP kinase regulates the activity of multiple transcription factors by phosphorylation (e.g. ATF-2, Elk-1 and CHOP) which induce the expression of many genes, including pro-inflammatory response genes (e.g. VCAM-1, IL-6[339], IL-8[340]). The p38 MAP kinases are expressed in multiple cell types including vascular endothelium, smooth muscle cells, cardiomyocytes and leukocytes. p38 MAP kinase can be activated by a variety of stimuli including physiological stresses (e.g. ROS, mechanical forces), microbial products (e.g. LPS), cytokines (e.g. TNFα, IL-1) and other molecules[336,341-343]. Pro-inflammatory p38 MAP kinase signalling can be mediated via phosphorylation of MAP kinase kinases 3 and 6 (MKK 3/6). These are themselves activated by MAP kinase kinase kinases (e.g. TAK1, ASK1, MEKK3). The MAP kinase phosphatases are negative regulators of these molecules[344,345] by the simultaneous de-phosphorylation of both phospho-threonine and phospho-tyrosine residues as a mechanism for control.

The activation of p38 MAP kinases is in the order of minutes for phosphorylation to occur, dependent on the stimulus agent and duration of treatment. For example, stimulation of macrophages with LPS (1μg/ml) demonstrated p38 phosphorylation after 1 minute and peak activation at 30 minutes[346]. Human neutrophils exhibited p38 phosphorylation after 5 minutes

treatment with TNFα (25ng/ml) or with PMA (20ng/ml)[347]. Polymorphonuclear cells treated for 10 minutes were maximally activated with TNFα at 5ng/ml concentrations[348].

Previous studies suggest that MAP kinases may be activated by cardiac surgery in a variety of tissue compartments. Ischaemia-reperfusion, use of cardiopulmonary bypass and heart-lung transplantation increase phosphorylated forms of the ERK1/2 and p38 MAP kinases in myocardium[349] and lung tissue[350-352]. The effects on phosphorylation in right atrial tissue following cardiopulmonary bypass appear to occur irrespective of the administration of methylprednisolone pre-surgery[353]. There appears to be a genetic variation in p38 MAP kinase activation in monocytes 24hs following CPB, particularly prominent in South Asians, compared to Caucasians (and corresponding up-regulation of TLR4 expression)[354]. In adult surgery, the termination of CPB was associated with an attenuation of p38 MAP kinase signalling in leukocytes by western blotting, a phenomenon preserved in Off-pump patients[355]. There are no other reports in the literature regarding neither leukocyte p38 MAP kinase activity, nor a detailed kinetic analysis in the context of cardiac surgery with the use of cardiopulmonary bypass.

Within other compartments, following cardioplegic arrest, p38 MAP kinase activation regulates myocardial function through immunomodulatory heat shock proteins[356] with p38 MAP kinase suppression associated with improved myocardial contractile function[349]. In congenital paediatric surgery with the use of CPB, ex-vivo leukocytes subject to LPS-induced stress showed attenuated levels of p38 MAP kinase (as well as down regulation of TLR2/4)[357] and an attenuated inflammatory response, after CPB. In paediatric tetralogy surgery, remote ischaemic pre-conditioning using a blood pressure cuff on the lower limb did not alter p38 MAP kinase activity post-surgery in sampled myocardial tissue, with a finding that these proteins were already in a predominantly phosphorylated form at a basal level[358].

Despite these insights, the function of MAP kinases in the response to cardiac surgery is uncertain and critical appraisal of data needs to be made especially in consideration to the duration of exposure to CPB and the timing of tissue / cellular sampling as well as the tissue compartment, as these appear to have markedly differing characteristics. Although MAP kinases are known to be activated in cardiac and other tissues during cardiac surgery, their regulation and function in leukocytes is uncertain and is an important subject for this thesis.

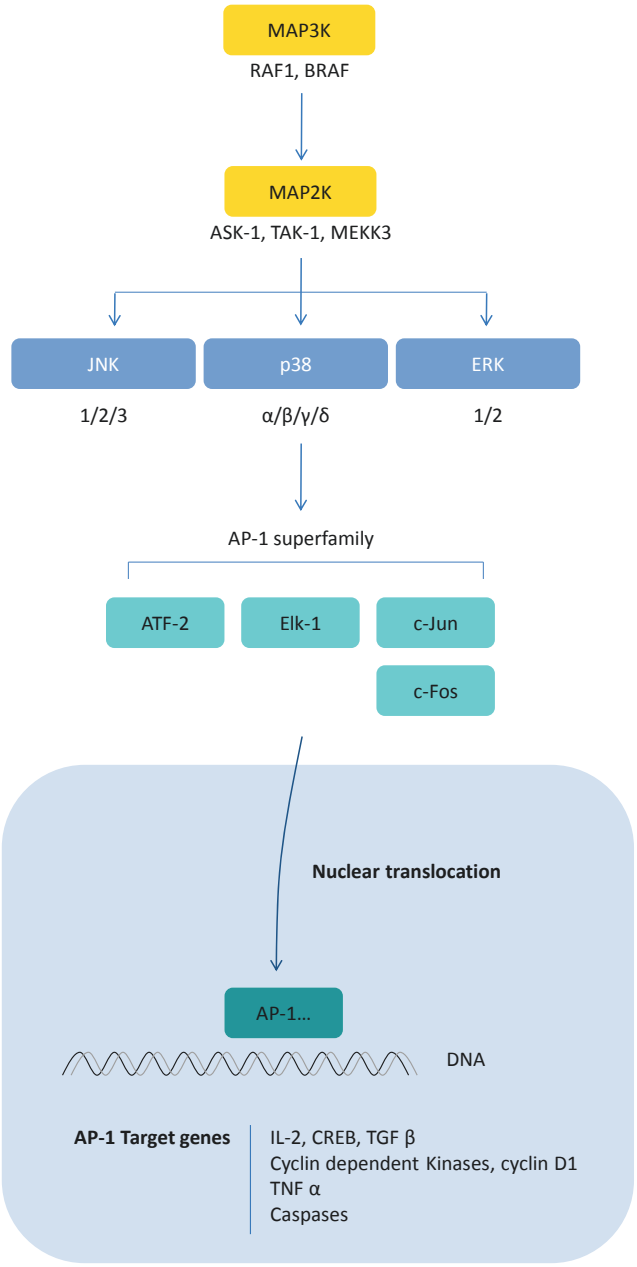

Figure 1.5 The MAP kinase signalling cascade

1.5.3 Nuclear Factor-κB

Nuclear factor-κB (NF-κB) is a central regulator of expression of inflammation, cellular proliferation, programmed cell death and other processes[359,360]. NF-κB activation, recruitment to target genes and post transcriptional events are tightly regulated[361]. The signalling cascades for NF-κB are illustrated in Figure 1.6. In mammals, the NF-κB family contains five proteins: RelA (p65), RelB, c-Rel, NF-κB1 (p50/p105) and NF-κB2 (p52/p100)[362]. Each of these proteins is characterized by a Rel homology domain (RHD) which is involved in homo- and hetero-dimerisation; interactions with regulatory molecules, nuclear localisation and DNA binding[363]. In addition to this, RelA, RelB and c-Rel all contain a transcriptional activation domain (TAD) on the C-terminus which is important in transcriptional activation. In basal conditions, the NF-κB complex is located within the cytoplasm. This state is maintained via associations with specific inhibitory molecules known as the inhibitors of NF-*κ*B (IκB). This family consists of: IκBα, IκBβ, IκBγ, IκBε, IκBζ, Bcl-3, p100, p105. Functionally, these molecules mask the nuclear localisation sequence of NF-κB binding via ankryn repeats retaining it in cytoplasm[364].

The kinetics of activation of NF-κB varies according to the stimulus. For example, leukocytes treated with TNFα (10pM) for 30 minutes or hydrogen peroxide (250μM) for 2 hours exhibited phosphorylation[365]. At 0.5nM TNFα concentrations, NF-κB activation was observed as early as 15 minutes before declining at 4 hours of stimulation in leukocytes[365].

A variety of stimuli can activate NF-κB by triggering its release from IκB and subsequent cytoplasmic to nuclear translocation[364]. Two major pathways in the activation of NF-*κ*B have been described – the canonical (classical) and non-canonical (alternative) pathways. In the canonical pathway (triggered by physiological stressors, pro-inflammatory cytokines, microbial molecules, reactive oxygen species intermediates[366], hypoxia and mechanical forces[367]), activation of p50/RelA and p50/c-Rel occurs via IKKβ. This kinase modifies IκBα

via phosphorylation at Ser-32 and Ser-36. The resultant phosphorylation promotes the ubiquitination of the IκB proteins at lysine residues 21 and 22 resulting in proteosomal degradation via the 26S proteosome. This exposes the nuclear localisation signals on the p50-p65 heterodimer to promote nuclear translocation. In the non-canonical pathway, activation of p52/RelB is dependent on NF-κB-inducing kinase (NIK) which functions together with a downstream kinase, IKKα[368]. Transcriptional activation of NF-κB relies on several post-translational modifications including phosphorylation and acetylation which promote DNA binding and recruitment of co-activators of transcription. NF-κB is negatively regulated at multiple levels by molecules such as A20 and Cezanne[369].

NF-κB activation and its effects on transcription are complex and can be both pro- and anti-inflammatory in nature[359,370]. NF-κB enhances the expression of adhesion molecules on endothelial cell surfaces by promoting E-selectin, VCAM-1 and ICAM-1 gene expression during acute inflammation in association with leukocyte sequestration[371]. The synthesis of pro-inflammatory cytokines such as TNFα, IL-1β, IL-6 and IL-8 are also regulated by NF-κB[372]. NF-κB can be both pro- and anti-apoptotic depending on the cell type and interactions, and is implicated in a range of diseases including atherosclerosis, rheumatoid arthritis, multiple sclerosis, asthma, inflammatory bowel disease[372]. However, there are no reports in the literature regarding leukocyte NF-κB activity during cardiac surgery, nor a detailed kinetic analysis in the context of cardiac surgery with the use of cardiopulmonary bypass.

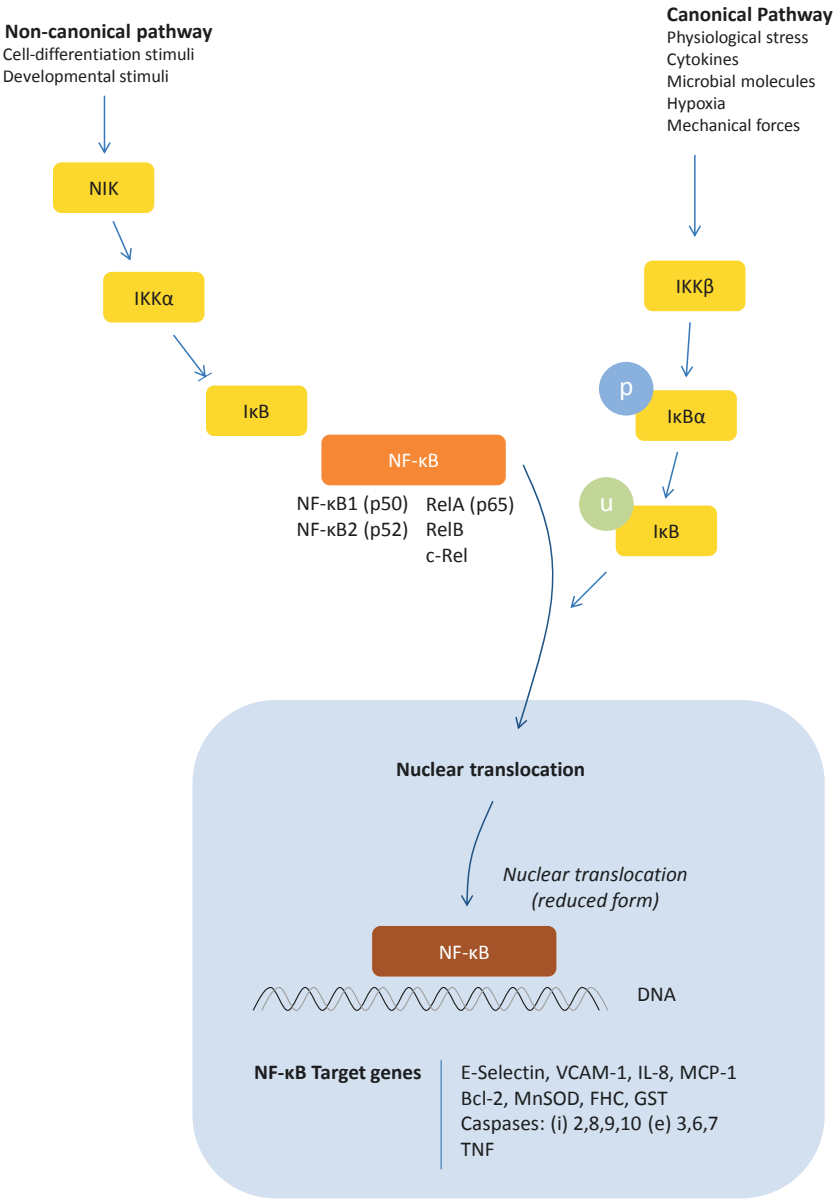

Figure 1.6 The NF-κB signalling cascade

1.5.4 Cross-talk between signalling pathways

The inflammatory signalling pathways are complex with functional overlap and regulation. For example, ROS enhances the activation of NF-κB, p38 MAP kinase and by regulating inhibitory MKP signalling pathways[286,373-375]. Neutrophil survival is enhanced by p38 MAP kinase through reciprocal NF-κB attenuation[376] and propagates injury in tissues including lung[377]. ROS signalling occurs following ischaemia/reperfusion with both protective[290] and damaging effects[378] depending on the circumstances and ROS species involved. The release of DAMPs from surgical trauma[196,199,216] whilst signalling via TLR pathways can also interface with various oxidative stress pathways[379]. ROS can enhance MAP kinase induction via the inhibition of MAP kinase phosphatases (MKP) which negatively regulates p38 MAP kinase activity[373,380]. ROS can also enhance NF-κB activation directly via IκBα phosphorylation[20,365]. Functional NF-κB transcription activity can be activated by p38 MAP kinase through RelA phosphorylation[381]. Alternatively, NF-κB induces MKP-1, GADD45β and XIAP which regulate p38 and JNK MAP kinases[286]. Within leukocytes, these changes promote the expression of cellular adhesion molecules as well as cellular release of cytokines into the plasma that promote the inflammatory response, and tissue migration. Interactions are highlighted in Figure 1.3.

1.5.5 Leukocyte priming

The focus of this thesis is on the activation of early pro-inflammatory signalling events within leukocytes by the process of surgery and CPB exposure. Leukocytes can be primed so that they mount an enhanced response to subsequent stimuli. Primed populations of leukocytes have been reported in patients with acute bacterial infection with enhanced responsiveness to hydrogen peroxide stress[382]. This phenomenon has also been reported in the context of sepsis[383], ARDS[384], term/preterm labour[385] and significant traumatic injury[386]. The mediators that are implicated in this process include TNFα, IL-8, IL-1β and growth factors such as GM-CSF[387] as well as activated endothelium[388]. These are an important considerations in the

context of surgical access, cardiopulmonary bypass, ischaemia-reperfusion and post-surgical recovery in the context of cardiothoracic practice as these are inflammatory events.

Priming may exist to modulate the chemotactic potential of leukocytes to promote recruitment to an inflamed focus. A "two-hit" hypothesis of an enhanced immune response following significant injury has been proposed[389]. This hypothesis suggests that once primed, immune cells can produce enhanced levels of cytokines and signalling mediators which can be both beneficial and harmful. For example, mice that were burn-injured demonstrated improved resistance to microbial infections[390] whereas those subject to a polymicrobial challenge exhibited a higher mortality rate[391].

Phenotypically, primed neutrophils exhibit an enhanced respiratory burst[388,392]. Functionally, priming alters leukocyte behaviour characteristics and expression of cellular surface markers. For example, PAF and TNFα had concentration-dependent effects on neutrophil adhesion - at low priming concentrations TNFα and PAF enhanced neutrophil binding where this was not observed at higher concentrations[393]. By varying hypoxic cellular stressors neutrophils were primed to exhibit differing cell surface Mac-1 expression[303]. Moreover, PMA-treated or fMLP-treated primed leukocytes exhibited L-selectin shedding and reduced leukocyte recruitment under flow-stress conditions[394]. Primed neutrophils have altered shape and reduced cellular deformability[395]. Priming may require transcriptional mechanisms since messenger RNA of pro-inflammatory transcripts of IL-1β, IL-8, MCP-1 and TLR-2 are enhanced with leukocyte priming[385] in vivo in pre-term labour. Primed leukocytes also exhibit a reduced apoptotic index following traumatic injury[396].

Given the large vascular bed and the prolonged transit time of leukocytes in lungs[86], this organ may be a site for physiological 'neutrophil de-priming'[387]. Clinically, patients with lung injury exhibit a greater transpulmonary hydrogen peroxide ROS gradient in systemic

arterial blood:pulmonary blood compared to reference control patients[397]. This suggests a failure of the de-priming mechanism in lungs in disease. This may represent a novel consideration in lung pathology that whilst severe lung injury is associated with primed leukocytes, the critically ill patient with functional pulmonary vasculature will conversely not manifest with a clinically severe picture[398]. This is an important consideration for cardiac surgical patients. The mortality rate from cardiac surgery with the use of cardiopulmonary bypass is low[42]. This is in part due to improvements in intensive care medicine, end-organ support and accurate diagnostic investigations which are key in the assessment and management of all patients following surgery. When inflammatory activation, and therefore by implication, pre-activation, is excessive, clinically patients may manifest a SIRS, in particular with ARDS[90,145,156,384]. However, when the response is appropriate and balanced inflammation is more likely a proportionate response which assists in fighting infection, wound healing and return to a normal physiological state. Thus, what is important is the targeted modulation of the response to favour healing and resolution, rather than inappropriate amplification and propagation when the physiological state does not warrant this.

From a clinical standpoint, in-vivo priming of leukocytes was evidenced by higher ROS generation post cardiac surgery to an ex-vivo PMA stimulus[399]. This priming effect was further enhanced by ex-vivo priming with PAF followed by PMA treatment, suggesting a synergistic effect and these findings that correlated with increased plasma levels of IL-6 and IL-8[399]. Significant leukocyte priming was observed up till 12 hours following CPB with enhanced ROS activity and elastase release[400]. This observation suggests that a vulnerable window post-surgery exists where patients may be at increased risk of developing adverse effects should a second event (e.g. chest re-opening, bleeding or sepsis) can tip the balance of recovery into organ failure. The process of priming is complex and the responsiveness of cells is not precisely delineated. It is unclear what the exact priming or activating stimuli are but potential candidates have been reviewed in earlier sections of this thesis (DAMPs, cytokines, oxidative stress), as known molecular triggers of inflammation. It would, therefore,

be of paramount importance to prevent a secondary hit phenomenon, and to be able to identify patients at risk.

1.6 STRATEGIES TO ATTENUATE THE INFLAMMATORY RESPONSE IN CARDIAC SURGERY

Given the mechanistic cascade of pro-inflammatory activation discussed in the earlier parts of this chapter, there are 4 broad points during the scenario of surgery with the use of cardiopulmonary bypass that can be targets for modulating and attenuating the immune response. Firstly, there is the aim in reducing DAMP generation – achieved by *better* surgery, small access incisions, optimised cardiopulmonary bypass technology or avoiding surgery altogether, if possible through percutaneous interventions. Secondly, there is targeting of DAMP receptor signalling, for example in the form of TLR receptor antagonists and targeting FPRs. Thirdly are targets of intracellular signalling cascades prior to the final intervention step of modulating the migration of leukocytes (Table 1.2).

The work in this thesis examines stage 1 and 3. A brief overview is given below, focusing on miniaturisation of cardiopulmonary bypass and the agent sulforaphane, of particular relevance to this thesis.

Target	Therapeutic intervention
Reduction in DAMP generation	Miniaturised CPB[114,401-405, 298,299] Off pump surgery[306,307] Active lung ventilation[91,170,406-408] Active lung perfusion[95] IABP counterpulsation / pulsatile flow[409,410] Hypothermia[167,168]
Targeting DAMP receptor signalling	TLR antagonists FPR targeting
Modulating intracellular signalling	Sulforaphane[263,411,412,312-315,318-320] Glutathione[331,332] Aspirin[413] Statins[414-416] ACE-inhibitors[415] Steroids[417,418] Aprotinin[419-422] p38 MAP kinase inhibitors[416,423-429] NF-κB modulation[369,413,417,418,430]
Modulating leukocyte migration	Adhesion molecule targeting Leukocyte depleting filters

Table 1.2 Anti-inflammatory interventions in cardiac surgery
The four steps of intervention in the leukocyte activating cascade are shown. Some illustrative examples are highlighted.

1.6.1 Minimising organ injury and DAMPs generation

The concept of minimising tissue injury has been a key aim in the development of surgery. Shorter durations of inpatient stay, reduced pain and a more rapid return of function are all achievable with limited access coronary surgery, minimally invasive surgery and robot-assisted surgery. Each is progressively less invasive but has an increasing cost and learning curve. The most readily and easily changed component of cardiac surgery is the cardiopulmonary bypass circuit. Essential for intra-cardiac work, cardiopulmonary bypass can be completely avoided in off-pump coronary revascularisation, or optimised for all other clinical applications.

1.6.1.1 Off pump beating heart surgery

Coronary revascularisation can be performed without the use of CPB in what is known as "off pump" coronary artery bypass (OPCAB) [42,54,55], a technique which dates back to the late 1980s[431]. This technique avoids the potentially deleterious effects of CPB, although randomised trial data shows little difference between on and off pump surgery for morbidity and mortality as well as criticism for inadequate revascularisation[432,433]. Performed via a traditional median sternotomy, conduits are harvested as for conventional CABG and formation of the anastomoses are facilitated by the use of stabilisation devices (Figure 1.7). As no extracorporeal circuit is involved, there is approximately 1/3 of the dosing requirement for anticoagulation. Coronary flow is maintained by the use of shunts and the operating field is kept clear with sparing use of a CO_2 blower, to minimise damage to the coronary endothelium and gas embolization. The success of OPCAB is critical on surgical and anaesthetic teamwork especially when the heart is placed in unfavourable haemodynamic positions.

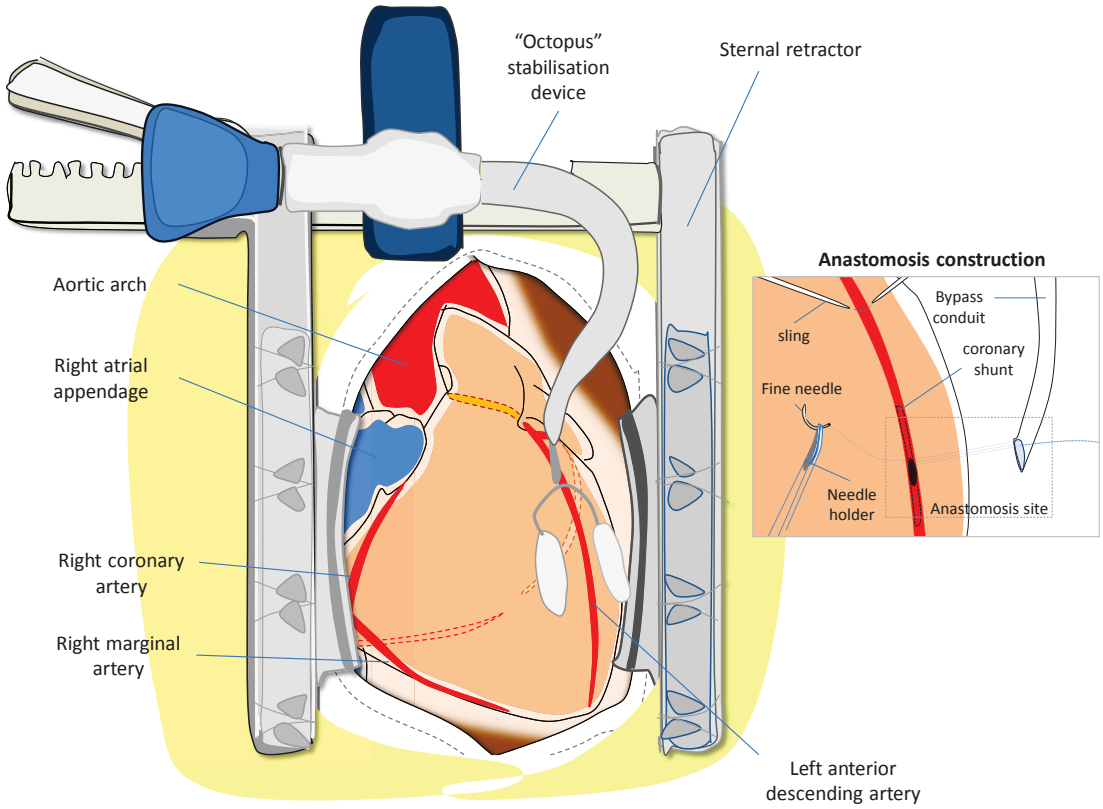

Figure 1.7 Beating heart surgery is facilitated by stabilisation devices
Off pump surgery is performed with the aid of stabilisation apparatus, such as the octopus (illustrated) or starfish (not illustrated) device, to ensure that the target area, in this case the left anterior descending artery, is immobilised during the construction of anastomoses. The most difficult vessels to operate upon are those on the inferior and posterior surfaces of the heart as careful positioning of these vessels is paramount in maintaining cardiac output and haemodynamic stability. Myocardial blood flow can be controlled by the use of vascular slings to kink the coronary arteries whilst the maintenance of distal flow is achieved with intra-coronary shunts during the fashioning of anastomoses (inset).

1.6.1.2 Other interventions to minimise physical injury

Lung injury that occurs following cardiopulmonary bypass varies from minor aberrations through to fulminant adult respiratory distress syndrome (ARDS). This carries a significant mortality association[90]. How the generalised inflammatory response translates into specific lung injury is uncertain. The absence of ventilation and relative pulmonary tissue ischaemia with the use of conventional CPB may be significant aetiological factors in addition to the trauma of opening of the pleura during mammary artery harvest and cold cardioplegia may have contributing effects compounded with lung collapse and atelectasis occurring in under-ventilated lung units. There has been a concerted drive to elucidate the optimal strategy for the management of the non-functioning lung through a number of clinical trials[170]. These have included repeated vital capacity manoeuvres to improve alveolar recruitment at the end of bypass[91]; intermittent ventilation and continuous positive pressure airway pressure (CPAP) during bypass[434]. The Drew-Anderson cannulation technique has been employed to maintain perfusion of the lungs so that they can act as a physiological oxygenator and has been shown to be associated with a reduction in pro-inflammatory cytokine release[95]. Continuously ventilated patients exhibit enhanced preservation of postoperative dynamic lung compliance[406] and reduction in the extravascular water index[407]. The maintenance of continuous pulsatile blood flow throughout the process of cardiopulmonary bypass with the use of a mechanical intra-aortic balloon pump has also been shown to attenuate the inflammatory response[409,410]. The precise mechanism for this is uncertain although we understand that flow stress and shear dynamics are important in modulating the behaviour of endothelial cells in blood vessels. In large animal models of conventional CPB followed by reperfusion, active pulsatile perfusion within the lung resulted in attenuation of both AP-1 and NF-κB within pulmonary tissues[408].

1.6.2 Miniaturised cardiopulmonary bypass

Miniaturised bypass is an advanced concept applied to the conduct of extracorporeal circulation (Figure 1.8). Miniaturised cardiopulmonary bypass circuits come in a number of different forms from a variety of manufacturers. This technology is central to experiments presented in this thesis and an overview of the range of technologies involved is given in the following section. A summary of some of the different miniaturised cardiopulmonary bypass systems reported in the literature is given in Table 1.3.

The concept of the miniaturised CPB circuit features:

1. An improved efficiency gas-exchange device which reduces the surface area that interfaces with blood, compared to that of a conventional oxygenator[435,436].
2. Smaller diameter tubing (3/8' tubing compared to ½ inch tubing)[435] and other circuit length optimisations[437] leading to the reduction of fluid priming volumes within the circuit and thus decreasing blood haemodilution from approximately 1.5 litres in conventional systems to 500mls, or less.
3. Biocompatible coatings (e.g. phosphorylcholine or bonded-heparin) that are designed to attenuate blood contact activation[438,439].
4. No blood-air contact interface that is inherent in the design of the conventional bypass circuit is negated as the venous reservoir is removed from the system. This has the additional effect of removing size and additional volume from the circuit.
5. Centrifugal pump mechanisms that are designed to minimise mechanical trauma of blood cells are employed in contrast to occlusive roller pump mechanisms in miniaturised circuits[437].
6. Incorporated safety features (arterial filters, bubble traps, venous air removal devices) to reduce the risk of clot and air embolization (Figure 1.6).
7. Parallel autologous blood salvage system which recovers erythrocytes from operative shed blood (removing leukocytes and vasoactive substances) prior to re-transfusion into the patient. This is in keeping with the concept of a closed system without a blood-air

interface. Re-transfusion of blood from the operative field has been shown to be a contributor to the inflammatory process[440,441].

In parallel with the benefits of the use of miniature cardiopulmonary bypass, there are secondary considerations relating to safety and potential disadvantages with its use. The miniaturised CPB circuit is a 'closed' system, as the venous blood reservoir component (ordinarily presenting direct blood exposure to air) has been removed. Therefore, care in avoiding the introduction of air in to the system is paramount in conducting safe surgery. The absence of a venous reservoir also means that blood is not readily available to infuse into the patient should the situation arise during a surgical procedure when rapid volume transfusion would be beneficial. Blood that is lost in the operating field may not be directly re-circulated in miniaturised cardiopulmonary bypass circuits that do not feature 'sump suction', alternatively using blood salvage devices, and therefore greater care is necessary to avoid bleeding at the time of surgery.

The Hammersmith Hospital Cardiothoracic unit has particular expertise with the use of extracorporeal circulation optimized (ECCO) miniaturised CPB from the Sorin Group utilised during this research project[404,405,435,436,442]. This system features low prime volumes, low heat generation, reduced index of haemolysis with low blood transit time. The reported learning curve for the introduction of miniaturised bypass was optimally achieved after 50 cases in reports from the practice at Hammersmith[404]. The conduct of surgery does not appear to be influenced by the use of miniaturised bypass with similar cross clamp and bypass times in miniaturised and comparative bypass groups for both coronary revascularisation[115-117,402,437,443-448] and aortic valve surgery[116,402,445,449,450]. In the following section, a review of all clinical experimental evidence related to the use of miniaturised bypass systems is presented.

In terms of adverse outcomes, there was no increase in peri-operative mortality associated with the use of miniaturised cardiopulmonary bypass systems[115,402,437,443,446,450]. The

cumulative overall mortality associated with mini CPB is 1.1% vs 2.2% in conventional CPB with an OR of 0.58 (95% CI 0.23 to 1.47, p=0.25) in a meta-analysis of thirteen randomised trials by Biancari in 2009[451]. Immer reported the length of ITU stay was 22.6±6.3 hours with mCPB compared to 30.9±35.2 hours in cCPB and a total hospital stay of 7.5±2.1 days in mCPB compared to 8.8±3.8 days in cCPB groups[114]. In keeping with these observations, shorter durations of ventilation have also been reported with the use of mCPB (11.8±7.3h mCPB vs 17.4±26.8h CPB)[114].

Miniaturised CPB has been consistently shown to be associated with reduced perioperative blood loss with fewer red-cell and platelet transfusion requirements post-operatively[116,402,443,445,449,452]. This may be due to the benefits in reduction of blood priming volumes in these circuits with cost savings and removing the risk from blood transfusions[453] and of benefit in Jehovah's Witnesses[454].

The degree of myocardial injury has been reported to be lower with the use of mCPB as evidenced by lower troponin within the first 6 hours following surgery (7.9±6.1 vs 18.8±21.9 ng/L)[114], 12 hours and 24 hours[116,445] . Similarly, CK-MB trends following surgery with CPB are lower at 1 hour (9.7±7.5 vs 11.9±3.6 U/L)[115], 6 and 12 hours[116] as well as peak CK-MB in mCPB groups[117]. This corresponds with a lower incidence of peri-operative myocardial infarction in mCPB groups reported in the literature (1.9% vs 3.3%)[118]. However, other groups have reported no difference in troponin, but their published data indicate trends towards favouring mCPB[117,403]. The mechanisms of myocardial injury following cardiac surgery is likely to occur from a variety of factors and may in part occur due to inadequacy of cardioprotection resulting in metabolic myocardial stress[455] and ischaemia-reperfusion[456]. The differences in markers of cardiac injury observed may be also attributed to the absence of re-transfusion of blood from the operative field, as a driver for inflammation[440,441]. As a consequence of myocardial injury, low cardiac output states (with reduced measured cardiac index) are more frequently observed in cCPB compared to mCPB groups[118,403] with increases

in serum lactate[118] as a marker of metabolic stress. Correspondingly, perioperative inotropic requirements are higher in patients undergoing surgery with cCPB systems when compared to mCPB[114,443]. Additionally, cardiac rhythm disturbances may be more frequently observed in the context of myocardial injury. Peri-operative atrial fibrillation (AF) was reported to be higher in CABG patients cCPB[114,118,443] whereas no difference in the incidence of AF was reported by Remadi in patients undergoing valve replacement[450].

A lower incidence of urinary haemofiltration[443] and better preservation of renal function[443] was reported with the use of mCPB.

Cerebral blood oxygenation measured by near-infrared spectroscopy was shown to be reduced during cardiac surgery, but this was better preserved with mCPB with fewer micro-emboli counts[457]. In the early phase following CPB, cCPB circuits exhibited higher numbers of plasmin-antiplasmin complexes, prothrombin fragments and higher d-dimer levels[458]. Some groups have reported lower incidence of peri-operative stroke with the use of mCPB[118,443] whereas no stroke difference were reported by other groups[114]. Meta-analysis suggests that mCPB may be associated with an overall reduced risk of stroke[451].

In terms of alterations in the inflammatory process, lower peak plasma SC5b-9 complement levels are detected following mCPB[114,115]. Furthermore, lower levels of IL-6[444,459,460], IL-8[402], TNFα[444], MCP-1[459], neutrophil elastase are detected following weaning off CPB[402,444] suggesting less activation of the immune system with mCPB. A mechanistic link for this may be due to reduced generation of DAMPS. To exemplify this, the DAMP molecule S100 is found in higher concentrations in cCPB compared to mCPB[115,444]. In addition to this, levels of oxidative stress and ROS activity, indicated by elevated malondialdehyde levels, were lower in mCPB patients[461]. To complement the observations of altered pro-inflammatory cytokine release, attenuated DAMP generation and reduced pro-inflammatory signalling, reduced conventional clinical markers of inflammation have been demonstrated. For instance,

Huybregts reported lower post-operative white cell counts in blood[445]. CRP levels were reported to be lower, up till 48 hours following surgery, with mCPB compared to cCPB by Remadi[443]. Levels of urinary IL-6, thromboxane B2, N-acetyl-glucosaminidase were attenuated in patients undergoing surgery with mCPB compared to cCPB[445]. However, in contrast, other researchers reported no differences in white count nor CRP between CPB systems[403,437,443,444]. In association with immune system changes, and perhaps a better preservation of immune function in mCPB patients, a lower incidence of respiratory infection (0.8% vs 3.1%) reported by Wiesenack[118].

It should be noted that there are significant differences between miniaturised systems. This heterogeneity in technology can make direct comparisons difficult. In the studies conducted, surgery and scientific evaluation have only been performed in low-risk patients, whereas it may be posited that studies of high-risk patients and prolonged CPB times may be of more scientific merit. In addition, no long-term data from the trials have been reported and therefore the later benefits (or detrimental effects) of miniaturised bypass have not been assessed.

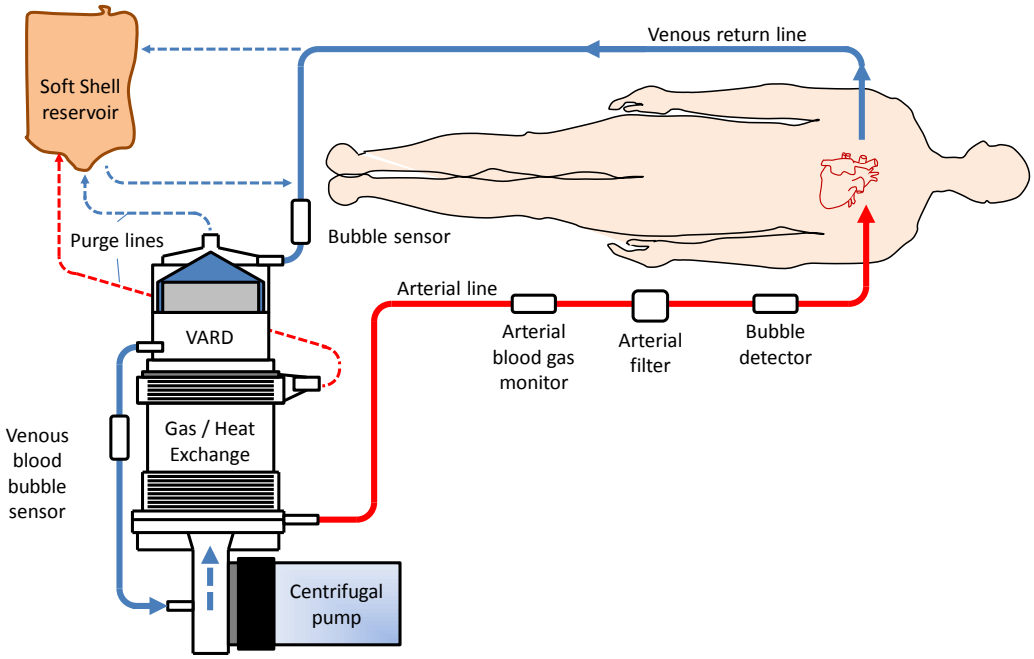

Figure 1.8 Miniaturised optimised extracorporeal cardiopulmonary bypass circuit
Blood is drained from the atrium or great venous vessel directly into the miniaturised circuit via the venous air removal device (VARD). If any air is entrained in the circuit, the VARD is activated and this blood is purged into a soft shell reservoir. Otherwise, venous blood is actively circulated using a centrifugal pump into the gas- and heat- exchange device to regulate blood oxygen content and temperature. Oxygenated blood is then fed into the systemic circulation via the arterial cannulation site usually via the arch of the aorta. Blood from the operative field is removed to a cell-salvage device in parallel to the CPB circuit (not shown) with recovery and re-transfusion of the isolated erythrocyte component.

System	Oxygenator	Pump	Tube coating	Prime volume	Total surface area
ECCO (Sorin)[279,280,313-315462]	Eos oxygenator 1.1m^2	Revolution centrifugal pump	Phosphorylcholine	380mls	-
Synergy (Sorin)[445,463]	Synergy integrated oxygenator	Revolution integrated centrifugal pump	Phosphorylcholine	680mls	2.0m^2
Resting Heart (Medtronic)[446,447,459]	Carmeda Affinity NT oxygenator	Affinity pump	Carmeda attached heparin	990mls	2.5m^2
MECC (Maquet/Jostra)[116,117, 443,444,449,464,465]	Quadrox-I Adult oxygenator 1.8m^2	Rotaflow 32mls 0.19m^2	Bioline (polypeptide and heparin)	550mls	-
COR*x* (CardioVention)[115,448, 458]	Integrated oxygenator system <1.2m^2	Integrated impeller-designed centrifugal pump	Conventional 3/8' polyvinylchloride tubing. Uncoated	820mls	1.4m^2
ROCSafe Hybrid Perfusion System (Terumo)[402]	Capiox RX15 1.5m^2	SARNS™ with XCoating™	Polymer-based Xcoating™ (Poly 2-methoxyethylacrylate)	665mls	1.9m^2

Table 1.3 Overview of miniaturised bypass systems

Optimised extracorporeal circulatory support systems reported in the literature are shown. Relative surface areas of individual components of the support systems are shown along with total surface areas for the entire circuits, where published.

1.6.3 Modulating intracellular signalling

Given that ROS, p38 MAP kinase and NF-κB pathways are activated by experimental stress, surgery and cardiopulmonary bypass, they can be targeted for modulation of systemic inflammation. A review of some classes of immunomodulatory agents with particular focus on sulforaphane is given in the following section.

1.6.3.1 Antioxidants

Epidemiological evidence supports the use of anti-oxidants in the treatment and prevention of cardiovascular disease[466] with divergent results from *clinical* trial evidence, in part due to population selection[467]. Clinical trials with large numbers of participants have not yet revealed benefits in antioxidant use and improved mortality or adverse event profiles in individuals at risk of cardiovascular disease[468]. In CABG, surgery is associated with a consumptive decrease in homocysteine an important component of glutathione anti-oxidant protection[330]. The use of *N*-acetylcysteine as a ROS scavenger reduced tissue oxidative stress[331] and attenuated pro-apoptotic pathways in myocardium[332]. In addition, short-term treatments with statins have been shown to improve the redox-status of saphenous vein grafts in patients requiring coronary artery bypass surgery[414]. There may also be a beneficial synergistic effect of statin therapy when combined with angiotensin converting enzyme (ACE) inhibition[415].

1.6.3.2 Signalling cascade molecular inhibitors

Small molecular inhibitors of p38 MAP kinase target the ATP binding site in a competitive fashion[423]. However, non-specific off-target inhibition of other molecular kinases has been reported[424]. With p38 MAP kinase inhibitors, there is the additional challenge of targeting individual isoforms which possess differential effects within specific tissues[337]. Clinical trials of p38 MAP kinase inhibitors have been promising but have been stopped due to adverse side

effects (occurring due to the non-selective inhibition, or due to the inherent multi-signalling importance of p38 MAP kinase)[425]. Additionally, p38 MAP kinase suppression has been observed to escape from prolonged inhibition[426]. Despite these considerations, a specific p38α/β inhibitor (SB-681323) has been used to target the inflammatory cascade activation seen after percutaneous coronary intervention with reduction in high sensitivity C-reactive protein post-procedure, with a modulatory effect additionally observed with pre-treatment[416]. No selective p38 MAP kinase inhibitor has yet reached clinical trials in the context of cardiac surgery.

Experimentally, steroids suppress p38 MAP kinase activation by enhancing the activity of MKP-1[417]. Targeting of p38 MAP kinase activation using specific blockers, following ischaemia-reperfusion, afforded protection from apoptosis and reduced infarct tissue size in an animal model of MI[429]. Inhibition of p38 MAP kinase activation during CPB with SB203580 affected the contractile response of the mesenteric microcirculation in porcine models resulting in relative vasodilation[428] and attenuated pro-inflammatory cytokine expression in rat lung tissues[469]. Experimental use of NF-κB decoy peptides has shown promise in reducing macrophage migration into vein grafts[430]. However, *in vivo* applications requires far more precision of delivery and targeted specificity to avoid enhancing the potentially deleterious effects of NF-κB activity[286].

1.6.3.3 Signalling effects of common drugs used in cardiothoracic surgery

Aprotinin is a naturally-occurring proteolytic enzyme isolated from bovine lung and pancreatic tissue[470]. Mechanistically as a broad-spectrum serine protease inhibitor, aprotinin can inhibit trypsin, chymotrypsin, plasmin and kallikrein[144], a component of the contact activation system and limits fibrinolysis. Aprotinin can decrease neutrophil and macrophage activation and chemotaxis and reduces oxidative stress. Following CPB, aprotinin preserves cellular junctions and attenuates oedema in myocardial tissues in association with a

suppression of p38 MAP kinase in porcine experimental models[419]. Aprotinin has been shown to suppress the induction of MAP kinases via the induction of HO-1 and a ROS-protective effect in smooth muscle cells from rat aortae[420]. In human broncho-alveolar fluid from patients undergoing surgery with conventional CPB, levels of IL-8 and neutrophil accumulation are attenuated[421] along with suppression of nitric oxide[422] in with aprotinin dosing.

In contrast to specific molecular inhibitors described, salicylates/NSAIDs[413] and glucocorticoids[418] have been used as anti-inflammatory agents clinically, modulating NF-κB signalling but also suffering from the same off target non-specificity. Aspirin is known to enhance the phosphorylation of p38 MAP kinase to regulate COX-2 expression[471]. Aspirin also regulates the thrombotic function of platelets via a p38 MAP kinase mediated pathway[472]. Immune-modulatory effects have also been reported in statins[473], ACE inhibitors[474], anti-diabetic medication[475], analgesics[476] and a comprehensive review is beyond the scope of this thesis. Given this, any study in patients has the added dimension of the effects of polypharmacy as well as whatever intervention is undertaken on the patient.

1.6.4 Sulforaphane

Sulforaphane (1-isothiocyanato-4-methylsulhinylbutane) is an organosulfur compound which has been associated with a variety of protective biological effects. These include anti-microbial and anti-cancer properties in addition to anti-inflammatory effects, which are the focus of this thesis. An outline of the biological relevance of sulforaphane to cardiac surgery is given below.

1.6.4.1 Biochemical properties

Sulforaphane is found naturally in cruciferous vegetables belonging to the Brassicaceae family. These vegetables include broccoli, cauliflower, bok choy and cabbage. Sulforaphane

is produced during dietary consumption of the precursor glucoraphanin which is particularly abundant in broccoli sprouts[411,412]. Chemically derived from glucose and amino acids, sulforaphane belongs to a class of organic compounds known as the glucosinolates. It has the molecular formula $C_6H_{11}NOS_2$ and has a molar mass of 177.29g.

The enzyme myrosinase (thioglucoside glucohydrolase) is responsible for the conversion of the precursor glucoraphanin into the active form of sulforaphane. Myrosinase is inherently present within plants and also present in the bacterial flora of the human intestine[477]. This enzyme is found in the highest quantities in Daikon (Japanese white radish). Myrosinase belongs to a family of plant defence enzymes against herbivores - some glucosinolate hydrolysed metabolites can be toxic[478]. The chewing action whilst eating food enhances the release of myrosinase (Figure 1.9).

The primary site of absorption of sulforaphane occurs within the jejunum[479]. Due to sulforaphane's lipophilic profile and small molecular size, it is passively absorbed via enterocytes in the liver from the entero-portal system[480]. Sulforaphane is conjugated in the liver with glutathione by the action of glutathione-s-transferase and excreted in the urine[481]. Investigators have reported that high cellular accumulation of sulforaphane occurs in mammalian cells noting cellular concentrations of 4.4-13.3mM following 30 minutes incubation with 0.028-0.28mM sulforaphane, suggesting a plasma-tissue difference of 47-145 fold accumulation[482]. When fed to rats, sulforaphane is detected in all tissues with concentrations highest in gut, prostate, kidney and lung[317].

1.6.4.2 Experimental studies using sulforaphane

Sulforaphane modulates phase I metabolism via the inhibition of the cytochrome P450 enzyme system, or via the regulation of the mRNA expression of these enzymes[483]. Sulforaphane also modulates phase II drug metabolism enzymes and antioxidant enzyme

systems via the antioxidant response element (ARE)-mediated gene expression. The mechanism of sulforaphane mediated regulation of the ARE-mediated genes is via the transcription factor nuclear factor E2-related factor 2 (Nrf2)[318,322,374,484-486]. In the resting unstimulated state, kelch-like ECH-associated protein 1 (Keap1) suppresses Nrf2 by targeting it for ubiquitination within the cytosol of the cell[487]. The keap1-Nrf2 interactions can be disrupted by a variety of stimuli including dietary antioxidants (e.g. sulforaphane) and shear stress[374]. Sulforaphane reacts with the thiol groups of the Keap1 protein and enhances the dissociation of Nrf2 from this complex. This then results in the stabilisation of Nrf2 and its translocation into the nucleus of the cell to manifest its effects. Following nuclear translocation, Nrf2 forms a heterodimer with Maf proteins[487]. This leads to enhancement of binding of the Nrf2/Maf complex to the ARE-enhancer in the promoter region of the protective phase II / antioxidant genes. A number of antioxidant defence genes can be activated following Nrf2 nuclear translocation; these include haem-oxygenase 1 (HO-1), NADPH, GPx and Trx[488]. The importance of this on ROS regulation and inflammatory activation has been discussed in 1.5.1 (page 56). These have the effect of reducing activation of p38 MAP kinase[320,321,489-491] as well as on NF-κB[286].

Pre-clinical studies from our group and others have demonstrated that sulforaphane suppresses inflammation by inhibiting activation of p38 MAP kinase and NF-κB[374,486,492-496]. Genetic polymorphisms in Nrf2 has been reported to be associated with increased risk of developing acute lung injury following trauma, in patients[497]. Pre-treatment of endothelial cells with sulforaphane at 1μmol/L for 4 hours elevated Nrf2 expression at protein level but not enhance Nrf2 transcripts with suppression of VCAM-1 expression via a p38 mechanism[374]. This effect occurs at two levels; by targeting MKP-1 to reduce MKK3/6 signalling and thus attenuate p38 phosphorylation and also by altering redox status of cells and upstream MAP kinase kinase kinases (ASK1) are inhibited by Nrf2-inducible thioredoxin[498].

A potential alternative mechanism includes the removal of activated cells from injured tissues via cell cycle arrest and apoptosis. Overexpression of Bax, down-regulation of Bcl-2 along with modified caspase signalling are reported with sulforaphane-induced apoptosis in colon cancer cells[499]. Sulforaphane can induce cell-cycle arrest in the G_2/M phase with decrease in cyclin B1 and accumulation of cyclin dependent kinases[500]. Thus it is feasible that sulforaphane may also target leukocytes for apoptosis but this has not yet been tested.

It can take hours before alterations in gene expression become functionally evident at the protein level. In this regard, the kinetics of the biological effects of sulforaphane may be different to the kinetics of sulforaphane bioavailability. In the literature, early pre- and co-treatment with sulforaphane appears to have relatively fast biological effects within 1-2 hours. For example, following iv administration of 25mg/kg sulforaphane into wild-type male Sprague-Dawley rats, maximal induction of NQO1 mRNA expression in lymphocytes was observed at 1.6 hours; GPx at 0.72 hours; and HO-1 at 0.56 hours[501]. One-hour pretreatment of aortic endothelial cells with sulforaphane (1-4 μM) suppressed TNFα-indued MCP-1 and VCAM-1 pro-inflammatory gene transcription as well as protein levels with suppression of p38 MAP kinase phosphorylation but no effect on NF-κB[493]. Co-treatment of raw macrophages with Sulforaphane (5 μM) and LPS (500 ng/ml) revealed down-regulation of inducible iNOS and Cox-2 within 2 hours[494]. Similarly, Sulforaphane (10-20 μM) pre-treatment for 45 minutes in macrophages exhibited reduced NF-κB activation following LPS stress[494]. Together, these observations suggest that Nrf2 is a fast-acting transcription factor (not requiring synthesis but moreover, stabilisation and nuclear translocation) or that the anti-inflammatory effects observed with short/early treatments occur independently of genes activated via the Nrf2/ARE pathway. Further studies are required to distinguish between these possibilities.

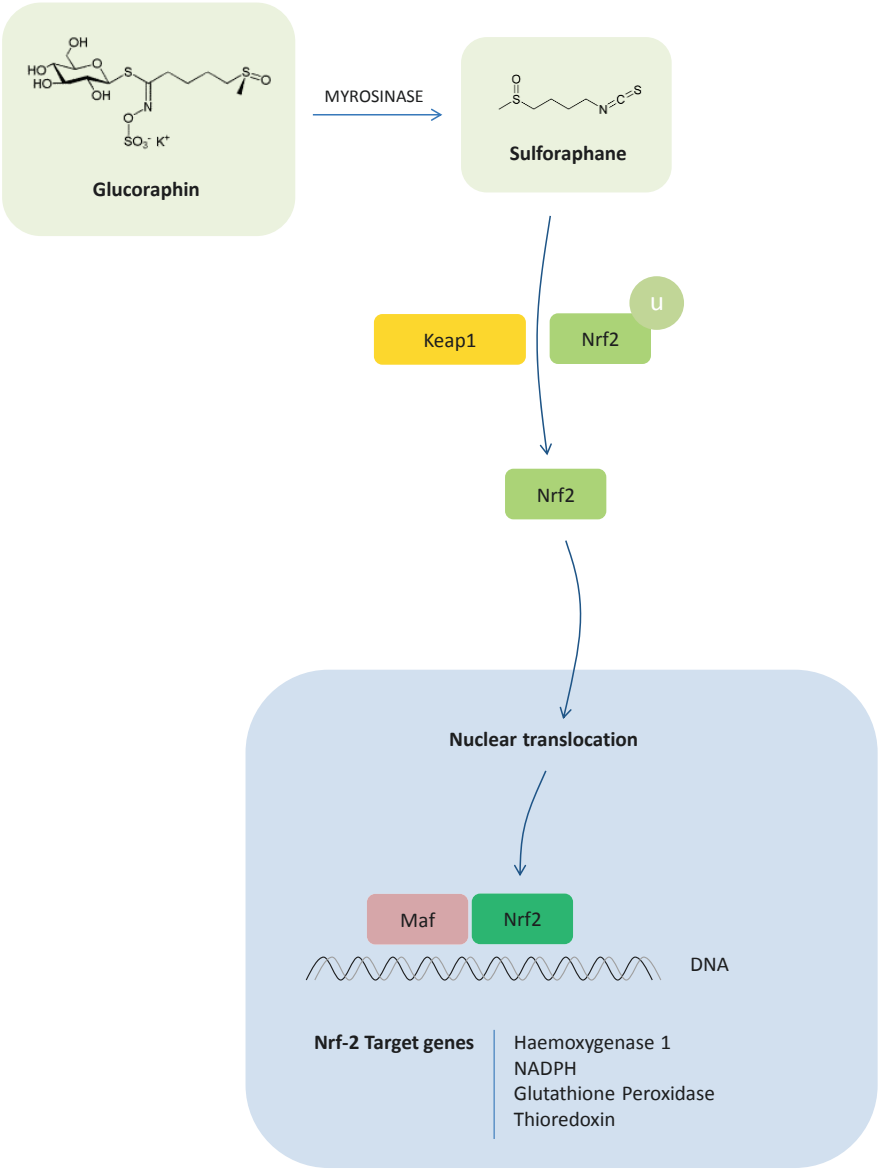

Figure 1.9 The biochemical conversion and interactions of sulforaphane

1.6.4.3 Clinical Studies

Epidemiological evidence revealed that consumption of broccoli and related vegetables is associated with reduced risk of coronary heart disease mortality[502-504]. In humans, consumption of a single portion of broccoli sprouts generated sulforaphane concentrations in plasma that reached a peak value at 1-1.5 hours after feeding and declined with first-order kinetics[411,412,505]. A single portion of broccoli cress generated sulforaphane concentrations in plasma that reached approximately 1μM at 1 hour after feeding and were sufficient to dampen inflammatory responses[411,412,505]. Although sulforaphane is rapidly cleared from plasma, consumption of broccoli can induce antioxidant enzymes for at least 24h in leukocytes of healthy volunteers[505]. Oral consumption of broccoli sprout homogenates containing sulforaphane have shown increased levels of antioxidant enzymes in human upper airways from nasal lavage[505]. There are numerous studies currently open to recruitment utilising sulforaphane for the treatment of breast cancer, prostate cancer, asthma, schizophrenia and cystic fibrosis[506]. The studies presented in chapter 5 (page 199); explores the effect of sulforaphane pre-treatment on leukocyte pro-inflammatory activation in the context of a large-animal model of cardiopulmonary bypass and in human volunteers.

1.7 HYPOTHESES

The inflammatory response following cardiopulmonary bypass is well characterised as are the deleterious consequences. Despite this, the precise molecular signalling mechanisms regulating this process are uncertain. In this thesis, the following hypotheses were addressed:

i. Cardiopulmonary bypass leads to the rapid induction of reactive oxygen species in leukocytes which is associated with early activation of pro-inflammatory signalling (e.g. p38 MAP kinase and NF-κB activation) associated with leukocyte transmigration.

ii. Both miniaturised cardiopulmonary bypass are associated with reduced reactive oxygen species / pro-inflammatory activation in leukocytes and attenuated systemic inflammation compared to conventional cardiopulmonary bypass.

iii. Pre-treatment with sulforaphane may attenuate intracellular pro-inflammatory signalling in response to surgery with cardiopulmonary bypass.

1.8 AIMS OF THE PROJECT

This project was conducted in the following stages:

i. A preliminary phase of technical development and validation of assays for ROS, p38 MAP kinase activation and NF-κB activation in leukocytes was completed.

ii. These assays and the cantharidin blister assay were then used to determine the influence of cardiac surgery on inflammatory signalling in leukocytes and to compare the effects of miniaturised cardiopulmonary bypass with conventional cardiopulmonary bypass systems.

iii. Finally, studies of cultured cells, animal models and humans were undertaken to determine whether sulforaphane attenuated the pro-inflammatory signalling responses following exposure to cardiopulmonary bypass.

A flow chart detailing the overall sequence of the various components studied is given in Figure 1.10. The precise details of experiments are covered in the respective sections of this thesis.

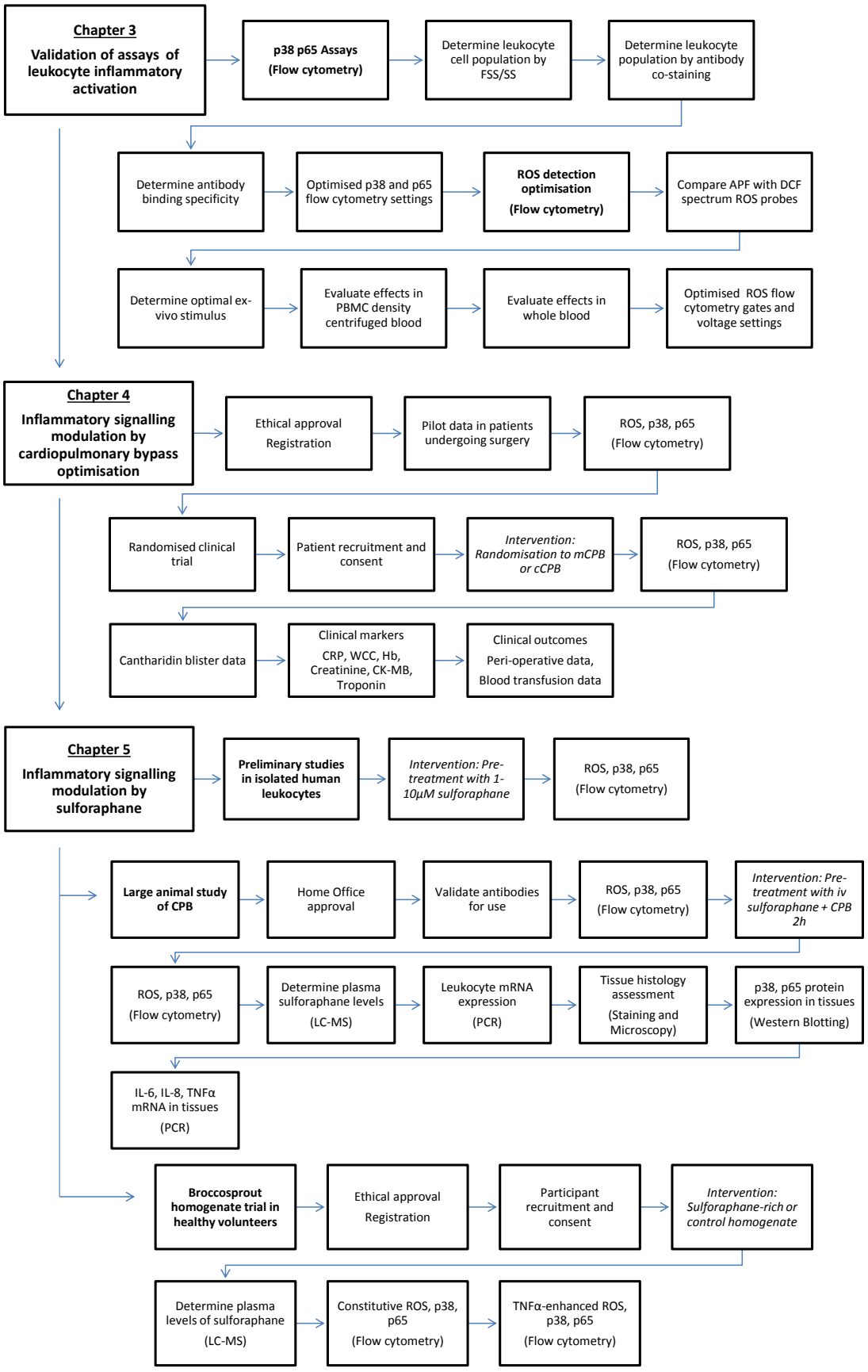

Figure 1.10 Flow-chart schematic of experimental approaches considered in this thesis

CHAPTER 2. MATERIALS AND METHODS

2.1 MATERIALS

2.1.1 Reagents

Buffers for intracellular staining were obtained from BD Biosciences. The ROS-sensitive probe 3'-(p-aminophenyl) fluorescein (APF) and 2'7'-di-chlorodihydrofluorescein diacetate (DCF) were obtained from Molecular Probes. Cantharidin (Cantharone™) was obtained from Dormer Laboratories Inc (Rexdale, Ontario, Canada). p38 MAP kinase blocking peptide was obtained from Cell Signalling. p65 blocking peptide was obtained from SAB Signalway. D,L-Sulforaphane was obtained from Toronto Research Chemicals Inc. All other reagents were obtained from Sigma-Aldrich unless otherwise indicated.

2.1.2 Antibodies

Specific primary conjugated and secondary conjugated antibodies were purchased or obtained as gifts and are listed in Table 2.1.

2.1.3 Gel Electrophoresis and Western Immunoblotting

TBS-T (10× stock solution) was prepared by dissolving 24.2g Trizma® base with 80.0g sodium chloride and 5ml Tween-20 made up to 1L with de-ionised water with adjustment of pH to 7.0 by the addition of hydrochloric acid. Transfer buffer was prepared by dissolving 50ml NuPAGE transfer buffer (20×) (Invitrogen) with 200ml methanol (Fisher Scientific) and 750ml de-ionised water and 1ml NuPAGE antioxidant (Invitrogen). Stripping buffer was prepared by dissolving 15g glycine with 1g SDS and 10ml Tween 20 adjusted to a pH of 2.2 with hydrochloric acid made up to 1L with ultrapure water.

2.1.4 PCR primer sequences

Primer sequences are given in Table 2.2 and were purchased from Sigma-Aldrich.

Target Antigen	Target	Host	Conjugated Fluorophore	Isotype	Source	Storage	Applications
CD32	Human	Mouse	FITC	IgG1	Serotec	-20˚C	Flow cytometry
CD14	Human	Mouse	Pacific Blue	IgG2a	Caltag Medsystems	4˚C	Flow cytometry
CD3	Human	Mouse	PE-Cy7	IgG1	Beckman Coulter	4˚C	Flow cytometry
CD14	Human	Mouse	Pacific Blue	IgG2a, κ	BioLegend	4˚C	Flow cytometry
CD3	Human	Mouse	APC	IgG1, κ	BioLegend	4˚C	Flow cytometry
Phospho-p38 MAPK (pT180/pY182)	Human	Mouse	PE-Cy7	IgG1, κ	BD Biosciences	4˚C	Flow cytometry
Phospho-NF-κB p65 (pS529)	Human	Mouse	PE	IgG2b, κ	BD Biosciences	4˚C	Flow cytometry
IgG1 Isotype control	Human	Mouse	PE-Cy7	IgG1, κ	BioLegend	4˚C	Flow cytometry
IgG2b Isotype control	Human	Mouse	PE	IgG2b, κ	BioLegend	4˚C	Flow cytometry
Phospho-p38 MAPK (pT180/pY182)	Human	Mouse	-		New England Biolabs	-20 ˚C	Western Blotting
p38 MAPK	Human	Rabbit	-		New England Biolabs	-20 ˚C	Western Blotting
Phospho-NF-κB p65 (pS536)	Human	Rabbit	-		New England Biolabs	-20 ˚C	Western Blotting
NF-κB p65 (C-20)	Human, pig	Rabbit	-	IgG	New England Biolabs	-20 ˚C	Western Blotting
α-Tubulin	Human, Pig	Mouse	-	IgG1	Sigma-Aldrich	-20 ˚C	Western Blotting
Anti-rabbit IgG HRP	Rabbit	Goat	-		Dako	4˚C	Western Blotting
Anti-mouse IgG HRP	Mouse	Goat	-		Dako	4˚C	Western Blotting

Table 2.1 Antibodies used

Target gene	Species	Sequence
IL-6 (F)	Pig	5’-GCTTCCAATCTGGGTTCAAT
IL-6 (R)	Pig	5’-CTAATCTGCACAGCCTCGAC
IL-8 (F)	Pig	5’-GACCAGAGCCAGGAAGAGAC
IL-8 (R)	Pig	5’-ACAGAGAGCTGCAGAAAGCA
TNFα (F)	Pig	5’-GACAGATGGGCTGTACCTCA
TNFα (R)	Pig	5’-GAGGTTGACCTTGGTCTGGT
Cyclophilin (F)	Pig	5’-ATTTGATGATGAGAATTTTATC
Cyclophilin (R)	Pig	5’-ATGCCCTCTTTCACTTTG

Table 2.2 Primer sequences utilised

2.2 METHODS

2.2.1 Isolation of peripheral blood mononuclear cells

Heparinised blood was gently layered onto histopaque at an approximate ratio of 2:1 or less, prior to centrifugation at 300g for 30 minutes (Figure 2.1). Following centrifugation, the peripheral blood mononuclear cell (PBMC) layer was carefully transferred into a clean 15ml tube and gently mixed with isotonic PBS. These cells were then washed twice by centrifugation and re-suspension in PBS (as above), re-suspended in PBS and counted using a haemocytometer, prior to experimentation at a concentration of 1×10^6/ml.

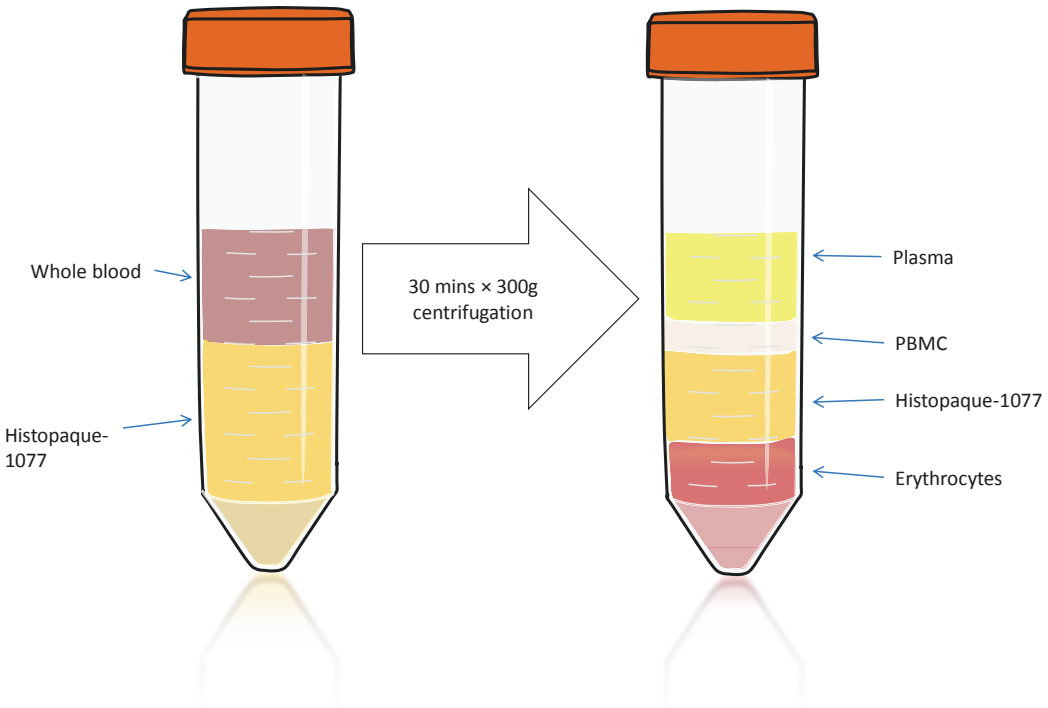

Figure 2.1 Isolation of blood leukocyte populations via density-gradient centrifugation
After careful layering of whole blood onto Histopaque-1077 (left panel) and centrifugation at 300 × g for 30 minutes at room temperature, erythrocytes and granulocytes relocated to the bottom of the tube (right panel). PBMCs were located at the interface between Histopaque-1077 and the plasma (right panel).

2.2.2 Cantharidin skin blister assay to study leucocyte extravasation

Cantharidin was pre-diluted 1:6 with acetone and (25µL) carefully applied on to 10mm radius discs of filter paper on the non-dominant forearm to achieve a working concentration of 0.1% (Figure 2.2). This was covered with a 20mm × 20mm square of paraffin paper and protected with mefix and mepore dressings to provide a protective and waterproof covering. At desired time points following typical blister formation the epithelial surfaces of the vesicles were breeched and fluid gently aspirated using siliconised tips.

Following aspiration of the vesicle, 10µl of neat blister fluid was diluted 1/25 in 240µl PBS and gently mixed. The diluted blister fluid was then loaded into a cytospin apparatus (Figure 2.3) and centrifuged at 300 × g for 5 minutes onto a glass slide. The preparation was allowed to air-dry prior to staining using the Diff-Quick kit consisting of a fixative (triarylmethane), an eosinophilic stain (xanthine dye) and a basophilic stain (thiazine dye) to facilitate leukocyte subpopulation determination. A glass cover slip was applied prior to bright-field imaging.

The microscopic appearance of a blister is shown in Figure 2.4A, and an example of histological data from blister fluid is shown in .Figure 2.4B.

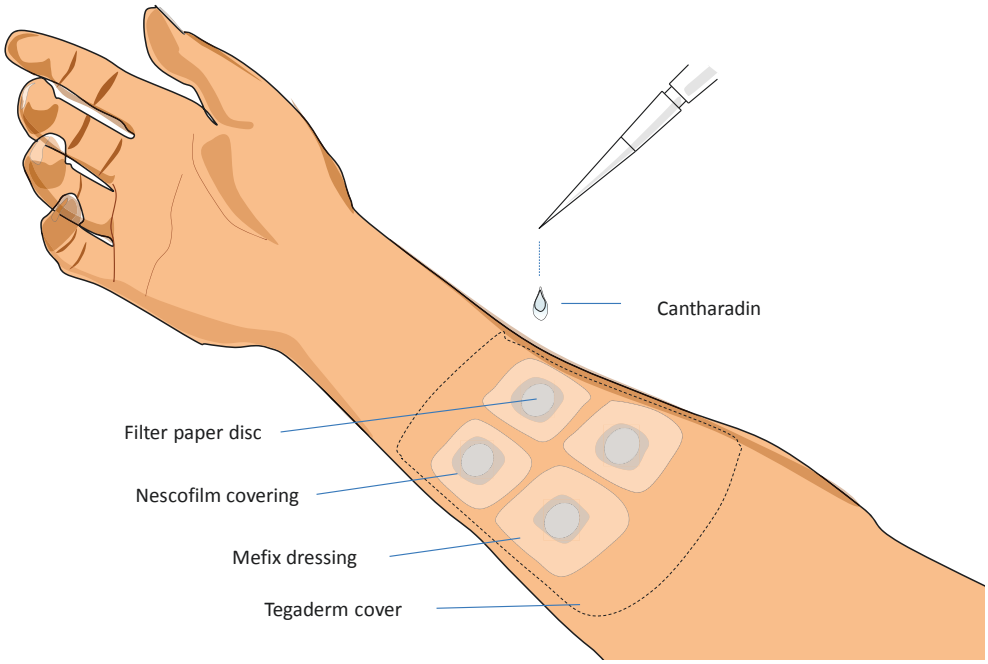

Figure 2.2 Creation of Cantharidin skin blisters on the volar aspect of the forearm
Cantharidin was applied directly onto 8mm filter paper discs applied directly onto the skin. These discs were then covered by nescofilm. Mefix dressings were applied above these to secure both the disc and nescofilm. Tegaderm was applied as the top-most layer to provide water-proofing.

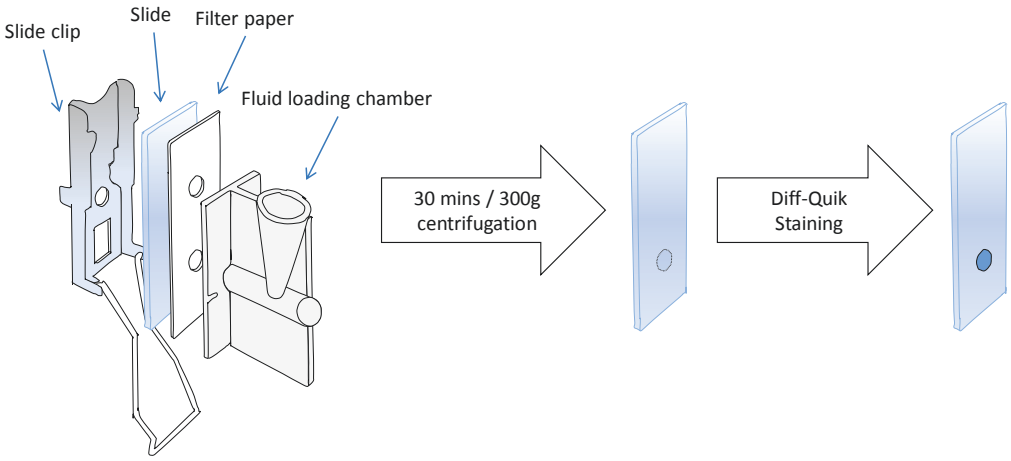

Figure 2.3 Analysis of leukocytes in blister fluid by centrifugation and staining
Slides were assembled onto a clip, covered by filter paper and a fluid loading chamber and secured (left panel). Blister fluid was then introduced into the chamber. The assembly was then centrifuged for 5 minutes at 300g. Slides were then carefully removed from the assembly and air-dried (centre panel). Once dry, the slides were then stained using the Diff-Quik kit for leukocyte identification, prior to protection with a coverslip and analysis by light microscopy (right panel).

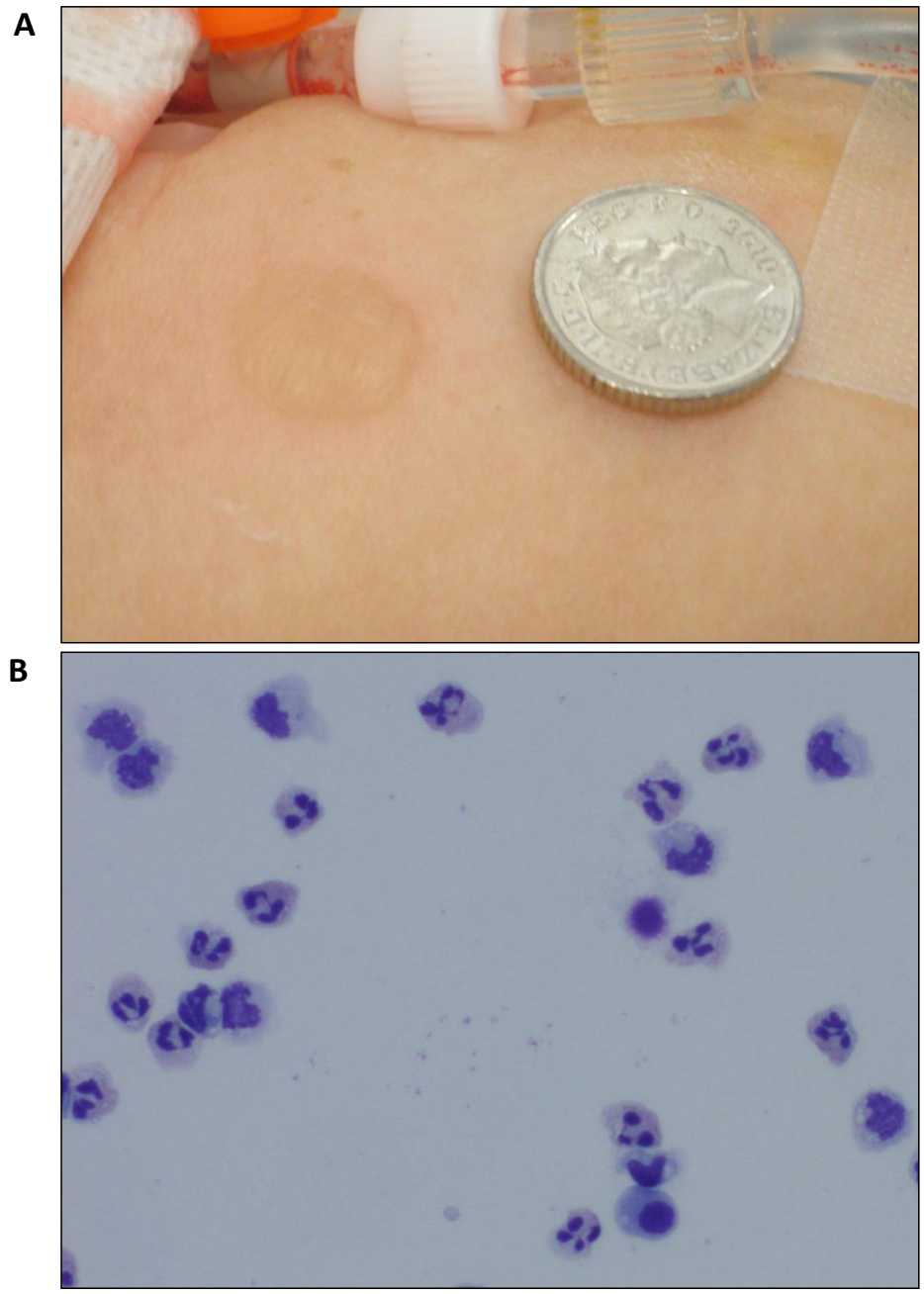

Figure 2.4 Typical macro and microscopic appearance of cantharidin blisters
Skin blister formation occurs within the area of direct skin application of cantharidin here shown with a 5 pence coin for size comparison (**A**). Following centrifugation of blister fluid onto a glass slide, and Diff-Quick staining (**B**), neutrophils are characterised by blue nuclei, pink cytoplasm and violet granules; eosinophils are characterised by blue nuclei, blue cytoplasm and red granules; basophils are characterised by purple/dark blue nuclei and violet granules and monocytes possessing a characteristic violet nucleus and light blue cytoplasm. A representative image is shown from a healthy individual.

2.2.3 Detection of reactive oxygen species (ROS)

Intracellular ROS levels were measured using the redox-sensitive fluorescent dyes APF and DCF (Figure 2.5). These dyes are activated by distinct albeit overlapping sets of ROS species (Table 2.3). To load cells with APF or DCF, 500µl of suspended PBMC or (1:10) diluted blood were combined with each dye (final concentration of 10µM) and incubated for 30 minutes at 37˚C prior to quantification of fluorescence by flow cytometry (see below).

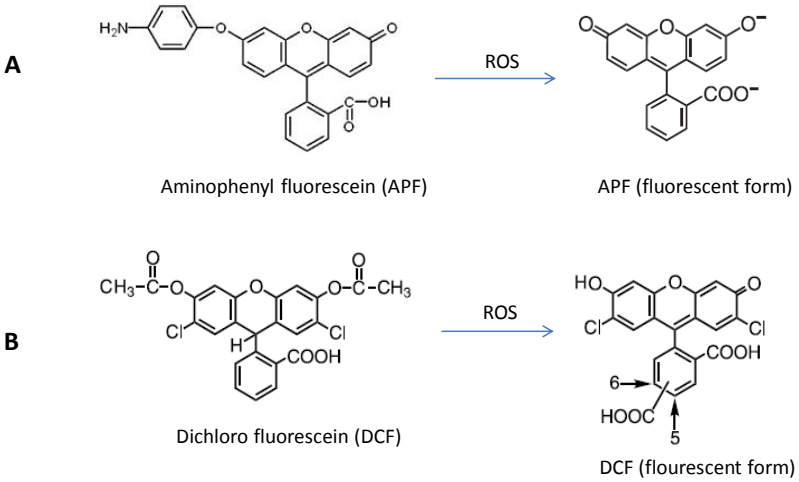

Figure 2.5 Chemical basis for ROS detection assays

(A) APF is non-fluorescent until it reacts with the hydroxyl radical, peroxynitrite anion or hypochlorite anion. Upon oxidation, the ROS dyes exhibit bright green fluorescence detectable by flow cytometry. (B) DCF is non-fluorescent until the acetate groups are removed by intracellular esterases and oxidation occurs within a cell driven by a wide variety of ROS including peroxyl and hydroxyl radicals and the peroxynitrite anion.

		ROS detection Method	
	ROS	APF	DCF
Species	•OH	1200	7400
	$ONOO^-$	560	6600
	^-OCl	3600	86
	$^1O_2$	9	26
	$•O_2^-$	6	67
	H_2O_2	<1	190
	NO	<1	150
	ROO•	2	710
	Auto-oxidation	<1	2000

Table 2.3 Specificity of APF and DCF activation by various reactive oxygen species

APF and DCF have distinct but overlapping specificities towards ROS. ROS were generated experimentally and fluorescence was measured using excitation/emission wavelengths of 490/515nm for APF and 500/520nm for DCF. Average fluorescence values are shown for various ROS species. APF resists auto-oxidation with a greater sensitivity for neutrophil/granulocyte ROS signalling. These data were generated and published by an external laboratory[507].

2.2.4 Intracellular staining for phosphorylated p38 MAP kinase and NF-κB

Whole blood was sampled into a vacutainer containing anticoagulant (citrate). 500µl of this blood was combined with pre-warmed (1:5 de-ionised water) BD Lyse/Fix Buffer (containing phosphatase inhibitors) and incubated in a water bath for 10 minutes at 37˚C. Leukocytes were purified by centrifugation (300 g for 5 minutes) and washed once with PBS. Cells were re-suspended in 0.5 ml BD Perm Buffer III pre-chilled (to -20˚C), vortexed, and incubated on ice for 30 minutes. Following this, cells were then washed twice with PBS and re-suspended in 0.5ml BD Stain Buffer (FBS) prior to incubation for 30 minutes (at room temperature) with PE-Cy7- or PE- conjugated antibodies that recognised either Ser529 phosphorylated RelA (p65; NF-κB) or Thr180/Tyr182 phosphorylated p38 MAP kinase or isotype-matched controls, with subsequent washing and analysis by flow cytometry (Figure 2.6).

2.2.5 Flow cytometric data collection and analysis

Samples were analysed using a CyanADP flow cytometer (Beckton Dickinson). Fluorescence of APF, DCF or fluorophore-conjugated antibodies to p38 MAP kinase, p65 NF-κB, anti-CD32, anti-CD14 and anti-CD3 was excited using a 488nm laser. Prior to analysis on the Cyan ADP flow cytometer, the laser was allowed at least 15 minutes to warm up and stabilise. Chroma-beads were used to check the laser's alignment (Figure 2.7). At least 10,000 cells were studied in each sample. Data files were then analysed using *Summit 4.3* software to determine the fluorescent intensities of individual cells within the sample (Figure 2.6).

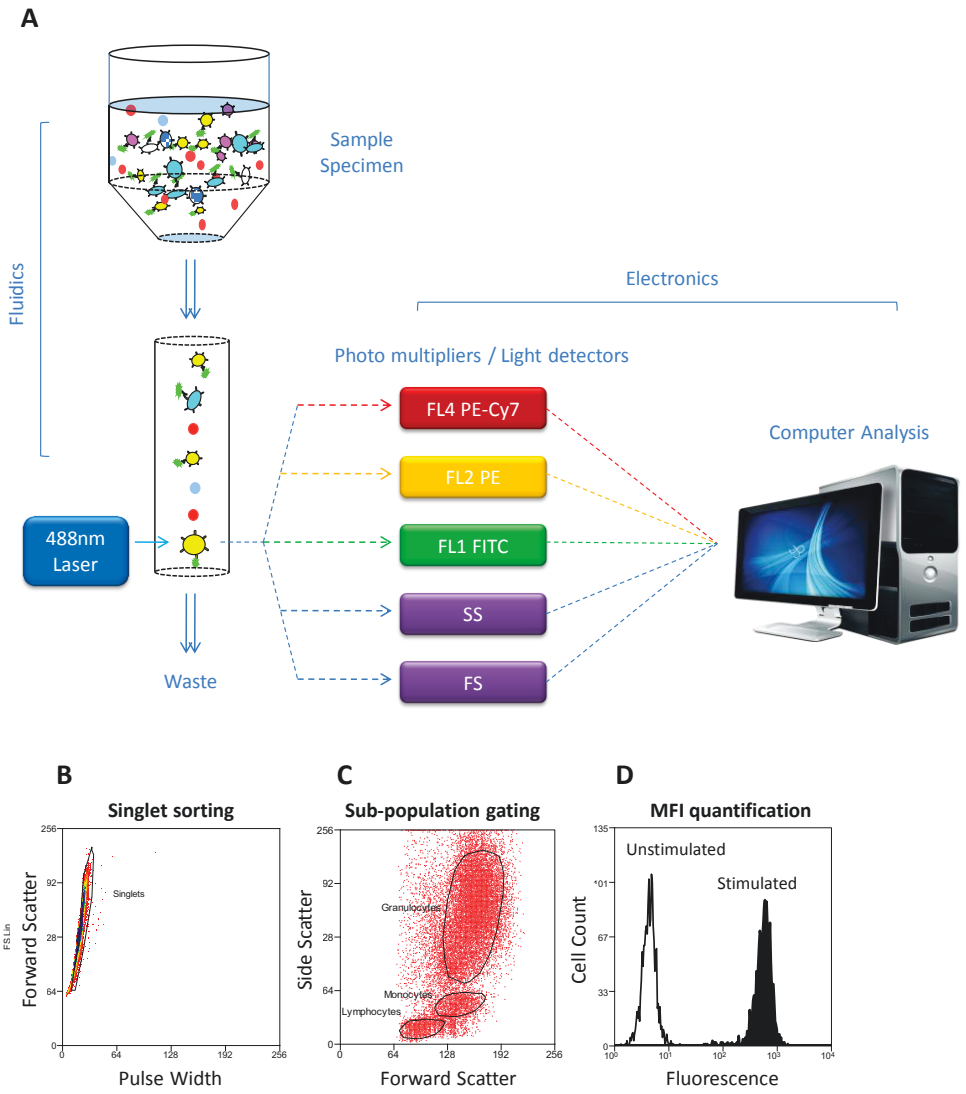

Figure 2.6 Flow cytometry measurement and channels utilised in intracellular detection assays

Leukocytes were either loaded with a ROS-sensitive fluorescent dye (APF or DCF) or permeabilised and stained with a directly conjugated fluorescent antibody (or the relevant matched isotype controls for the target molecule). Samples were then re-suspended in PBS for analysis. (**A**) The fluidics of the flow cytometer channels a column of cells into single file prior to excitation with a blue 488nm laser. As they pass through the beam the light deflection gives values of forward (FS) and side scatter (SS) indicating cell size and intracellular granularity. ROS induction was evaluated within the FITC (FL1 filter) channel with phospho-p38 and phospho-p65 induction being detected in the PE-Cy7 (FL4 filter) and PE (FL2 filter) channels respectively. Following data acquisition, samples were (**B**) sorted by forward scatter and pulse width profiles to select out singlets, eliminating clumped cells. The remaining cells were (**C**) analysed using forward and side scatter to differentiate between granulocyte, monocyte and lymphocyte cell subpopulations. Quantification of fluorescence was then determined for each subpopulation and (**D**) recorded as the mean fluorescent intensity between un-stimulated and stimulated specimens. In some experiments, cells were co-stained with specific markers to allow gating of specific populations.

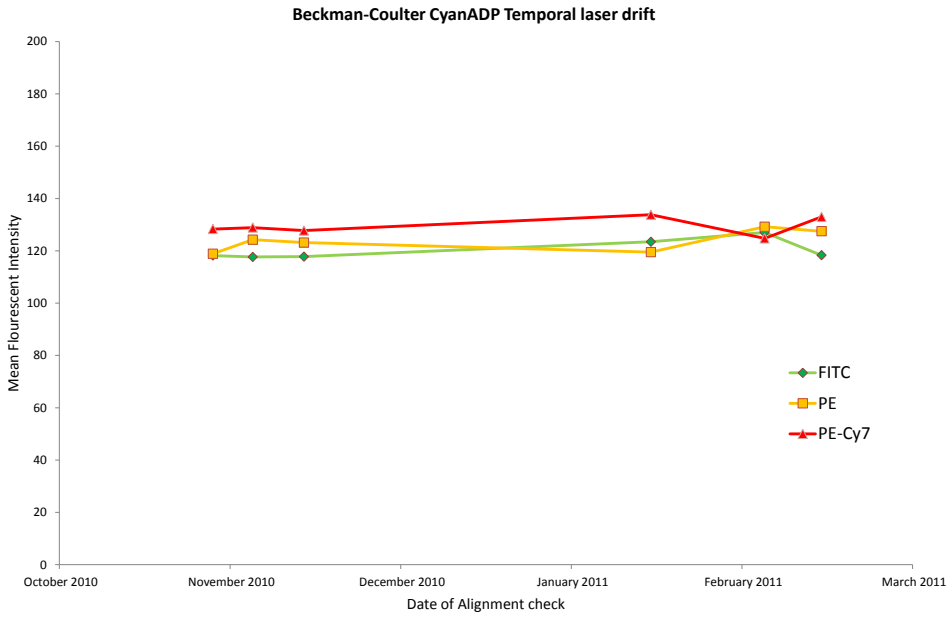

Figure 2.7 Temporal stability of the 488nm blue laser

Multi-coloured fluorescent beads were run through the flow cytometer prior to sample analysis and at interim intervals to determine the temporal variability in laser intensity and/or detection sensitivity. There was less than 5% drift.

2.2.6 Culture of porcine aortic endothelial cells

Pig aortic endothelial cells (PAEC) were obtained by collagenase digestion of pig aortas (Landrace Cross; 4-6 months old; approximately 80 kg weight) and then cultured in M199 (Sigma-Aldrich) supplemented with 10% foetal calf serum, 5 mM L-Glutamine, 5 μg/ml endothelial cell growth factor, 100 U/ml penicillin, 100 μg/ml streptomycin, 50 μg/ml gentamycin and 2.5 μg/ml amphotericin. Cells were cultured using gelatin-coated flasks/6-well plates and used at passage 2-3.

2.2.7 RNA extraction from leukocytes

RNA was extracted from blood using the RNA blood mini Kit (Qiagen®) according to manufacturer's instructions. Blood cells were lysed in two separate procedures: erythrocyte lysis and leukocyte lysis. Erythrocytes are more susceptible to hypotonic shock than leukocytes. Thus in the presence of a hypotonic buffer, erythrocytes were lysed. Intact leukocytes were then recovered using centrifugation and lysed under highly denaturing conditions which immediately inactivate RNAases, allowing for isolation of intact RNA.

2.2.8 RNA extraction from tissues

Tissues (1-2g) were disrupted/shredded in an eppendorf tube containing 1ml TRIZOL reagent (a mono-phasic solution of phenol and guanidine isothiocyante) to isolate total RNA. This was performed at room temperature with precautions taken to minimise the risk of RNAase contamination. The integrity of RNA was maintained during the process of sample homogenisation/disruption by TRIZOL reagent which additionally disrupts cells and dissolves cell components. Chloroform (0.2ml) was added to each sample-containing microfuge tube to allow for the separation of the solution into an aqueous phase (containing RNA) and an organic phase/interphase (containing DNA and proteins), once subject to centrifugation at 12,000g for 15 minutes at 2-8°C. The aqueous phase was isolated and transferred to a fresh microfuge tube. RNA was precipitated with the addition of 0.5mL

isopropyl alcohol. This formed a gel-like pellet on the side and bottom of the tube. The pellet was washed with 75% ethanol before allowing the pellet to air dry. The RNA pellet was then re-dissolved in molecular grade RNAase-free water followed by quantification by spectrophotometry and subsequent analysis.

2.2.9 Reverse Transcription PCR

Following RNA extraction from tissues, yields were quantified using spectrophometric / nano-drop assays. Purity was determined by the ratio of absorbance at 260nm and 280nm ($A_{260/280}$) ultraviolet light wavelengths. For each reaction, 0.5µg RNA template was used to generate cDNA. RNA template was added to a mixture containing Quanta Biosciences qScript™ cDNA SuperMix (a reaction buffer containing $MgCl_2$, dNTPs, recombinant RNase inhibitor protein, primers - random and oligoDTs - and qScript reverse transcriptase). Mixtures were then incubated as follows: 5 min at 25°C (annealing); 30 min at 42°C (extension); 5 min at 85°C (inactivation of reverse transcriptase). After completion of cDNA synthesis, samples were stored at -20°C, prior to amplification.

2.2.10 Quantitative Real-Time PCR

Following reverse transcription of extracted RNA, cDNA at 1:5 dilution was used for PCR amplification of target genes; and 1:20 dilution for housekeeping genes (e.g. cyclophilin-D). Reaction mixtures were set up on ice. Forward and reverse primers specific for the target genes were diluted to 10µM in RNase/DNase-free dH_2O. A reaction mastermix for each primer set was prepared containing the following reagents; 12.5 µl PerfectA SuperMix; 0.5 µl forward primer; 0.5 µl reverse primer and 6.5 µl RNase/DNase-free dH_2O per reaction. All samples were analysed in triplicate, in addition to a 'no-template' control. Samples were then analysed on the CFX96 Real-Time PCR detection system (BioRad Hercules, CA) using the following protocol: 95°C for 2-3 minutes (initial denaturation); 35-40 cycles of 95°C for 10-

15 seconds (denaturation); 55-65°C for 30-45 seconds (annealing); 68-72°C for 30 seconds (extension).

2.2.11 Protein extraction

Total protein extracts were obtained using the commercially available kits (Active Motif). Tissue samples were disrupted in ice-cold Complete Lysis Buffer (containing DTT, lysis buffer and protease inhibitor cocktail as per the manufacturer's recommendations) and incubated for 30 minutes on ice. Specimens were then centrifuged at 10,000 × *g* for 10 minutes at 4°C to obtain the supernatant containing the whole-cell lysate. Specimens were then aliquoted and stored at -80°C prior to analysis.

2.2.12 Immunoblotting

Protein samples were quantified by spectrophotometric methods prior to analysis. NuPAGE LDS loading buffer (Invitrogen) was added to samples containing equivalent amounts of protein which were then denatured by incubation at 98°C for 5 minutes. Samples were then loaded onto NuPAGE Novex 4-12% Bis-Tris gels (Invitrogen) at 10ug/well concentrations alongside a pre-stained standard (Spectra™ Broad Range Protein ladder, Thermo scientific) and electrophoresed for approximately 60 minutes at 150 volts in NuPAGE MOPS SDS running buffer (Invitrogen). Separated proteins were then transferred to a Polyvinyl Difluoride (PVDF) membrane (Millipore) using transfer buffer and applying a potential difference of 30 volts for 90 minutes. Once transfer was completed, membranes were incubated in 25ml of blocking buffer for 60 minutes at room temperature on a rocking platform followed by washing three times for 5 minutes using TBS-T. Membranes were then incubated in the antibody of interest (1:1000) diluted in 25ml of a suitable blocking buffer, placed on a rocking platform for 1 hour at room temperature. After three consecutive washes with TBS-T, membranes were incubated in 25ml of diluted secondary antibody (1:30,000) for 60 minutes and then washed a further three times with TBS-T. Proteins were then detected

using Western Lightening Enhanced Chemi-luminescence Substrate (ECL) (Perkin Elmer) for 1 minute and exposing the membranes to autographic films (Kodak). Films were then developed using the Compact X4 automatic X-ray film developer (X-ograph).

2.2.13 Plasma sulforaphane assay

Sulforaphane levels were measured in plasma samples by liquid chromatography mass spectrometry (LC-MS). HPLC was performed with a Water 2690 Separation Module system (Milford, MA, USA) equipped with a phenomenex Gemini 3µ C18 110A column (150 × 2 mm) using a isocratic elution (acetonitrile / 0.1% formic acid in water = 50:50). The flow rate of the mobile phase and the column oven temperature were set at 0.2 ml/min and 30˚C, respectively. The HPLC system was coupled to an API 2000 triple-quadrupole mass spectrometer equipped with a turbo ion spray ionization source (AB MDS Sciex, Toronto, Canada). The MS-MS detection was achieved using a positive ion multiple reaction monitoring (MRM) mode with an m/z transitions of 177.9 → 114.0 for sulforaphane, and 256.1 → 167.0 for diphenhydramine.

2.2.14 Histological processing

Formalin-preserved tissues were carefully trimmed using, double edged razor blades, and placed into embedding cassettes. The embedding schedule involved : 70% ethanol (two changes, 1 hour each); 80% ethanol (one change, 1 hour); 95% ethanol (one change, 1 hour); 100% ethanol (three changes, 1 hour each); xylene (three changes, 1.5 hours each); paraffin wax (58-60°C, two changes, 2 hours each) followed by embedding of tissues into paraffin blocks. The paraffin blocks were then cut at 5 µm sections and mounted onto slides.

2.2.15 Haematoxylin and Eosin staining

Tissue specimens were de-paraffinised and rehydrated in xylene (3 changes, 3 minutes each), 100% ethanol (3 changes, 3 minutes each), 95% ethanol (3 minutes), 80% ethanol (3 minutes) and deionized water. Excess water was then blotted prior to haematoxylin staining for 8 minutes. Specimens were then washed in running tap water for 5 minutes and allowed to differentiate in 1% acid alcohol for 30 seconds. Specimens were then washed in tap water for 1 minute prior to bluing in 0.2% ammonia and then washed again. Following a rinse in 95% ethanol, the eosin counterstain was applied for 30 seconds. Specimens were then rinsed in 95% ethanol (3 changes, 5 minutes each), 100% ethanol (3 changes, 5 minutes each) and xylene (3 changes, 15 minutes each). Results were then mounted with a xylene based medium.

2.2.16 Conduct of large animal study

Female Landrace pigs, mean 53.6kg (range 49.6 - 61.2kg) were purchased from a farm supplier and acclimatised for 3 days within the animal facility. Animals were identified by tattoo markings and ear notchings and weighed on the day of transfer to the facility. They were managed on a low-calorie, cruciferous vegetable-free diet for the preceding 1 week on the farm. All animals were housed under specific-pathogen free conditions and studied according to UK Home Office regulations and after appropriate local ethical review. Animals alternately received control or sulforaphane injections in pairs. The study was part-blinded. I performed the surgery with an assistant who was blinded to the allocation. The perfusion team were blinded to treatment allocation. The study involved live (ROS) assays and assays of p38 MAP kinase and p65 NF-κB phosphorylation that could be processed at the end of the study. An assistant researcher (blinded to treatment allocation) performed the live ROS assays. I performed the p38 MAP and NF-κB kinase assays at the end of the surgical procedure as well as the protein blots and genetic transcription analysis. The histological

analysis was undertaken by an expert experimental histopathologist who was blinded to treatment allocation.

2.2.16.1 Statistical considerations

Given the considerations of sulforaphane activity in-vitro and in-vivo and based on the assumption of being able to detect a 50% difference between sulforaphane-pretreated and control test groups, using an alpha value (p value) of 0.05 and a power of 0.85, a minimum of 5.344 pigs per group were required for the study.

2.2.16.2 Anaesthesia and surgical preparation

On the day before surgery, animals were fasted for 12 hours prior to the use of general anaesthesia. They were allowed access to water without restriction during this time. Animals were then allowed out of the farm pen and manually restrained in the holding pen by technical support staff. An intramuscular sedative was given using a combination of Ketamine (20mg/kg) / Xylazine (2mg/kg). Adequately sedated animals were then loaded into a transport trolley and moved to the surgical facility. Facemask induction was performed with 5% isoflurane gas to induce anaesthesia and oxygen flow rates of between 8-10 litres/min. Pigs were then transferred to the operating table, positioned prone followed by the insertion of indwelling venous cannulae into an accessible ear vein, secured with tape. A basal blood sample was taken for analysis. An extension line was connected before injection of 10ml of saline or 2mg/kg sulforaphane in 10ml of saline into the animal. Topical anaesthetic (lignocaine) was sprayed onto the hypopharynx prior to intubation using animal size 8-10 endotracheal tubes. Adequacy of intubation was confirmed by the presence of ventilatory sounds in the lungs; the absence of air in the stomach and end-tidal CO_2 capnography. Animals were then connected to the ventilator with FiO_2 adjustments that achieve an oxygen saturation tension of >90% and tidal volumes of 5-10ml/kg/minute. Anaesthesia was maintained with an isoflurane/O_2 mixture driven by medical air. Animals were then

repositioned supine with attachment of diathermy, rectal temperature probe, ECG electrodes with continuous monitoring and connection to the defibrillator using external paddles. All areas outside of the anaesthetic and surgical field were blanketed to maintain temperature homeostasis; with the assistance of a heated operating table.

2.2.16.3 Surgical access

Surgery was performed using strict aseptic technique. The operative field was cleaned with hibiscrub wash and waterproof drapes applied, exposing the neck and the sternum. The CPB circuit was primed with Hartmann's solution (2000ml) and heparin (5000IU). Lines were divided and clamped in preparation for extracorporeal circulation. Continuous arterial blood pressure monitoring was instituted via an indwelling arterial line in the external carotid artery following surgical neck dissection. The first arterial blood aspirate was used to determine the basal arterial blood gas (ABG). Central venous monitoring was instituted via an indwelling jugular vein line. The first venous blood aspirate was used to determine the basal activated clotting time (ACT). A skin incision from the supra-sternal notch to xiphisternum was created using a 10-blade scalpel. Dissection down to the sternum was performed using hand-held diathermy at 50J with release of the supra-sternal ligament, with close attention to haemostasis throughout. Retro-sternal adhesions were released with a finger sweep prior to division of the sternum using a pair of heavy Mayo's scissors (in some cases sternotomy was completed using a Gigli saw). Intravenous heparin was given following the completion of sternotomy (300IU/kg). The aorta and right atrium were then dissected and exposed using hand-held diathermy at 50J. The aortic cannulation site was prepared using 2/O ethibond double purse-string sutures (1 × 1 cm) with two snuggers on opposing sides secured with Dunhill clips. Aortic cannulation was performed when the ACT >400 seconds. The aortic pipe was inserted into the aorta, with the direction of flow orientated towards the arch and descending aorta. The right atrium was cannulated using a two-stage venous cannula,

directing the distal end towards the inferior vena cava. Cardiopulmonary bypass was subsequently maintained for two hours. Lung ventilation was discontinued during this period.

2.2.16.4 Details of Cardiopulmonary bypass

Normothermic (porcine 38-39˚C) non-pulsatile CPB was maintained using a Stöckert multiflow roller pump (Sorin Group GmbH, Munich, Germany) generating forward flow of between 2-4l/min with line pressures <300mmHg. Gas exchange was achieved via hollow fibre-membrane oxygenator apparatus (Dideco). Mean arterial pressures between 50-65mmHg were achieved with incremental doses of metaraminol, as required. The adequacy of cardiopulmonary bypass was checked by blood gas analysis at 30 minute intervals. Animals remained on cardiopulmonary bypass for 2 hours.

2.2.16.5 Termination of study and organ procurement

Tissues (kidney, lung, heart in order) were harvested prior to termination, under anaesthesia. Firstly, the abdomen was incised using a 10-blade scalpel from the lower portion of the median sternotomy incision to above the pubic symphysis. Cutaneous bleeding was controlled with handheld diathermy at 50J and incision through the linea alba was made to expose the parietal peritoneum. This was carefully opened between a pair of Dunhill clips ensuring the bowel contents were not breached. The omentum along with the small and large bowel were eviscerated en-masse and displaced laterally to expose the left kidney. Gerota's fascia was opened over the surface of the kidney and the hilum was carefully dissected to expose the ureter and vascular structures. The renal hilum was then clamped between two pairs of Roberts forceps and cleanly divided with a 10-blade scalpel. The superior pole of the kidney was then detached (approximately 3cm), and divided in half. One half was placed into a sterile 50ml falcon tube and snap frozen in liquid nitrogen and stored at -80°C until required for protein and RNA extraction (as described above). Alternatively, the other half of tissue was placed into a 50ml falcon tube containing 10% neutral buffered formalin and stored at

4°C for histological processing (as described below). Next, the anterior edge of visible the middle lobe of the right lung was gently grasped with a Duvall clip and an approximate 5 × 5 cm wedge of tissue was carefully excised using a 10-blade scalpel. This was then cut in half and prepared in the same way as previously for protein/RNA extraction and histological processing. Finally, the apex of the heart was gently grasped using a Debakey clamp and the ventricular apex (approximately 3cm of tissue) was cleanly divided using a 10-blade scalpel. This was then divided in half and processed as above. Once completed, the experiment was terminated using a schedule 1 method (>150mg/kg iv phenobarbital delivered either through the CPB machine or central access site). Death was confirmed via absence of brainstem reflexes – e.g. absence of response to corneal reflex.

2.2.17 Conduct of human broccoli consumption clinical trial

Prior to commencing the study, a favourable ethical opinion was obtained locally (REC reference 11/H0707/10). Six healthy individuals were studied on two separate occasions, in random order. Leukocyte activity in study participants was measured following the consumption of 200g of homogenized broccosprouts (from Discover Fresh, the Netherlands - a patented variety containing a precisely known amount of sulforaphane; 1200μmol/200g) or following the consumption of 200g alfalfa sprouts (from Sky Sprouts, Totnes, UK - non-sulforaphane containing control diet). The dose of 200g broccosprouts was chosen because it was tolerated well in humans and led to maximal induction of antioxidant enzymes (in previous studies)[505].

We know that sulforaphane reaches peak plasma levels 1.5 hours after oral ingestion[412], has a plasma half-life of approximately 1.77 hours[411] and is cleared from the plasma via urinary excretion in 24 hours. A generous wash-out period of two weeks between each arm of the study was included in the trial design. During the study, participants were asked to refrain from eating green vegetables, spices and condiments for 72h prior to study on both occasions.

Blood was sampled prior to consumption of Broccosprout homogenate (BSH) or Alfalfa sprout homogenate (ASH), and then repeated at varying times (1 to 24h afterwards). The resistance of leukocytes to inflammatory activation was assessed by treating blood samples with TNFα, ex-vivo, and measuring the activity of NF-κB and p38 MAP kinase by intracellular staining and flow cytometry. Alternatively, the resistance of leukocytes to ROS-associated inflammatory activation was assessed by treated blood samples with PMA 200ng/ml ex-vivo and flow cytometry.

2.2.17.1 Preparation of broccoli or alfalfa sprout homogenates

Broccoli sprouts from a single production lot were used three days following germination (Discover Fresh, the Netherlands). Sprouts were processed in a designated food product preparation area immediately upon arrival and prior to the expiration date. Proper hand-washing procedures and vinyl gloves were used to prevent contamination during processing. Sprouts were combined with sterile water in 1:1.2, w:w proportions. This mixture was then homogenized in 1l aliquots in a clean blender to eliminate the variable of chewing by subjects. The aliquots of homogenate were then pooled and mixed with daikon sprouts. This was accomplished by adding 2% daikon (compared to broccoli sprout mixture based on fresh weight) and homogenizing the preparation in the blender once again. The daikon/broccoli sprout mixture was then incubated at 37°C for 2 h. This process adds excess myrosinase to maximally convert the free glucosinolates of the broccoli sprouts to sulforaphane, the biologically active compound. After incubation, the isothiocyanate mixture was aliquoted into 50 ml sterile Falcon tubes (equivalent to 70g dry weight per aliquot – single dose) and stored at −20°C using dedicated freezer storage space. The broccoli sprout homogenates were thawed at 4°C 12–24 h prior to dosing and were not administered if thawed for greater than 24 h. Alfalfa sprout homogenates were prepared using the same procedures, substituting locally purchased organic alfalfa sprouts (Sky Sprouts, Totnes, Devon) for Broccosprouts, as above.

2.2.17.2 Inclusion/Exclusion criteria

Participants were considered eligible for the trial if they met the following inclusion criteria: age 18+ years; male or female and able to commit for the duration of the trial. Participants were considered ineligible if any of the following circumstances applied: pregnancy; practising vegetarian; history of allergy; current smoker or smoking cessation within the last 3 months; current use of inhaled, topical or systemic corticosteroids or within the last 2 weeks; current use of non-steroidal anti-inflammatory use or within the last 1 week; current use of nutritional or multivitamin supplements or current participation in any other randomised controlled trial.

2.2.17.3 Participant allocation and sample size determination

Participants were randomised by trials unit personnel not otherwise involved in the study. Randomisation was blocked (one block of six volunteers) and, because the preparations were concealed, the study personnel were blind to the allocations until the end of the study. Based on the following assumptions, a sample size of 6 was required to detect a difference of 1 standard deviation in reactive oxygen species (ROS) between broccoli and alfalfa conditions at a 5% significance level (2-sided) with 90% power. The assumptions were: cross-over trial design, i.e. one sample inference test; 1 baseline measurement of the outcome ROS; 5 post-intervention measurements of the outcome ROS; correlation between baseline and post-intervention ROS measurements = 0.50; correlation between post-intervention ROS measurements = 0.70.

2.2.17.4 Statistical Analysis

Outcome measurements were analysed in a mixed regression model to take into account the repeated measurements over time. The baseline measurements were fitted as a covariate. The sample size calculation was powered to detect a main effect difference between broccoli and alfalfa conditions but the interaction of condition and time of measurement were also

estimated and retained in the model if found to be statistically significant at the level of $p<0.05$.

CHAPTER 3. VALIDATION OF ASSAYS OF LEUKOCYTE INFLAMMATORY ACTIVATION

3.1 INTRODUCTION

The induction of ROS and phosphorylation of p38 MAP kinase and NF-κB are important processes in inflammatory activation of leukocytes. A key aim of this thesis was to determine the kinetics of activation of these signalling pathways in response to cardiac surgery with the use of CPB. This was achieved by serial sampling of peripheral blood from patients undergoing CABG with CPB (Chapter 4) or from pigs exposed to experimental CPB (Chapter 5). Thus the work relied on accurate quantitation of ROS and active forms of p38 MAP kinase or NF-κB (RelA) in specific leukocyte populations from whole blood samples.

Specifically, the following assays were developed using commercially-available staining kits and measurement of fluorescence by flow cytometry:

1. Quantitation of ROS levels in leukocytes using fluorescent ROS-sensitive dyes (DCF or APF).
2. Quantitation of levels of Thr180/Tyr182 phosphorylated p38 MAP kinase by intracellular staining using antibodies directly conjugated to PE-Cy7.
3. Quantitation of levels of Ser529 phosphorylated NF-κB (RelA) by intracellular staining using antibodies directly conjugated to PE.

In this chapter, a series of studies to validate these assays prior to their use in clinical or animal studies was undertaken. The intention was to measure these species in specific leukocyte populations, namely lymphocytes, monocytes and granulocytes. Previous studies have achieved this by co-staining leukocyte sub-populations using antibodies that recognise specific markers. For example, staining of CD3, CD14 and CD32 can discriminate between lymphocytes (CD3+, CD14-, CD32-), monocytes (CD3-, CD14+, CD32+) and granulocytes (CD3-, CD14-, CD32+). The identity of leukocyte sub-populations can also be inferred by flow cytometry via their distinctive profiles of forward scatter (FSC; proportional to size) and side scatter (SSC; proportional to granularity).

3.2 HYPOTHESIS AND AIMS

The hypotheses tested in the following chapter were:

i. Intracellular staining using specific antibodies can be used to measure the levels of phosphorylated p38 MAP kinase or phosphorylated NF-κB (RelA) in leukocyte populations from whole blood samples
ii. DCF and APF can be used to measure levels of ROS in leukocyte populations from whole blood samples.

The aims of the studies presented in this chapter were to:

i. Examine whether FSC and SSC profiles can be used to identify lymphocytes, monocytes and granulocyte populations in whole blood samples
ii. Assess the specificity of intracellular staining for phosphorylated p38 MAP kinase or NF-κB (RelA) using isotype-matched control antibodies and blocking peptides,
iii. Determine whether DCF or APF can be activated by experimental conditions that are known to induce ROS.

3.3 RESULTS

3.3.1 Identification of leukocyte sub-populations using FSC and SSC profiles

A key aim of this study was to measure inflammatory signalling in specific leukocyte populations in multiple blood samples (generated via clinical trials and animal studies). Although leukocyte population identity can be achieved by co-staining using specific antibodies (e.g. CD3, CD14, CD32), this approach was judged unsuitable for the analysis of large numbers of samples because it is time consuming and expensive. Because of these constraints, the possibility of identifying leukocyte sub-populations based on their size and granularity was considered, an approach that does not require additional staining procedures.

To validate this approach, leukocytes were stained for cell surface markers (CD3, CD14 or CD32) and expression was assessed by flow cytometry (Fig 3.1 A-C). Back-gating of fluorescence data onto FSC and SSC profiles revealed three populations that possessed distinct size and granularity (Figure 3.1D). The population that stained CD3+ (CD14-, CD32-) was nominated lymphocytes (Figure 3.1B, D), while the population that stained CD14+, CD32+ (CD3-) was nominated monocytes (Figure 3.1A, C, D). A highly granular population stained positive for CD32 (but negative for CD3 and CD14) and was nominated granulocytes (Figure 3.1C, D).

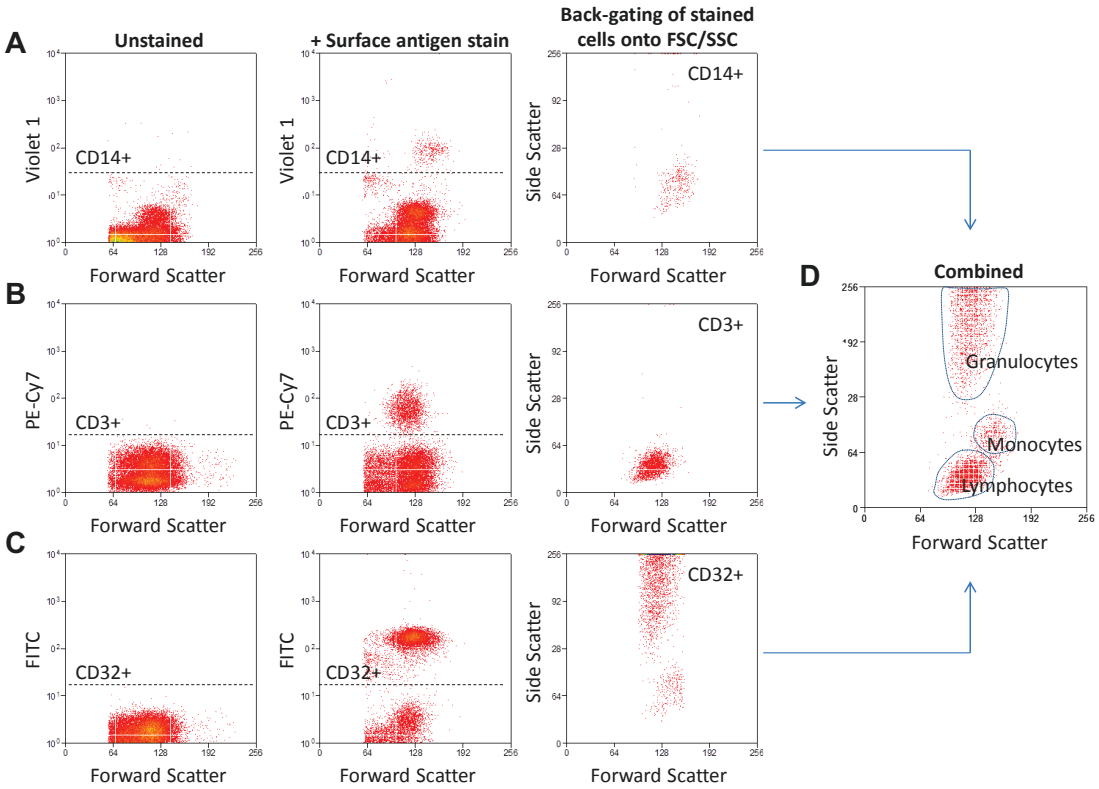

Figure 3.1 Leukocyte subpopulations identified via forward and side scatter profiles
Freshly-isolated peripheral blood samples were incubated with either (A) Pacific blue-conjugated anti-CD14, (B) PE-Cy7 conjugated anti-CD3 or (C) FITC-conjugated anti-CD32 antibodies (middle panel). Alternatively, they were left unstained (left panel). Fluorescence of cells was measured by flow cytometry. Dots plots are presented to compare fluorescence with forward scatter. Positively-stained cells exhibited higher fluorescence than that obtained in the absence of staining (observed above the dotted line in centre panels). Positive cells were back-gated into forward and side scatter (FSC/SSC) profiles to assess their size and granularity (right panels). (D) Forward and side scatter profiles were combined for lymphocytes, monocytes and granulocytes (indicated).

To measure p38 MAP kinase and NF-κB phosphorylation by intracellular staining, whole blood samples were treated with a buffer that simultaneously lysed the red blood cells and permeabilised the leukocytes (see Methods 2.2.4). Interestingly, the application of this buffer (BD Perm III buffer) to whole blood samples for 15 min significantly altered the FSC and SSC profiles of human leukocytes (Figure 3.2A). Specifically, although populations corresponding to lymphocytes and granulocytes could be observed, monocytes could not be distinguished by FSC/SSC profiles (Figure 3.2A, compare unpermeabilised with permeabilised).

Staining of fixed/permeabilised cells using anti-CD3 antibodies and back-gating confirmed the FSC and SSC profile of the lymphocyte population (Figure 3.2B, left panel). However, parallel studies revealed that the FSC/SSC profile of CD14-positive permeabilised cells overlapped with the profile for granulocytes (Figure 3.2B, right panel). Indeed, the process of fixation and permeabilisation led to increased SSC in CD14-positive cells (Figure 3.1A with Figure 3.2B). In conclusion, we could not discriminate between monocytes and lymphocytes in fixed/permeabilised cells.

These data informed the gating strategy and interpretation of future experiments using clinical and porcine samples. Specifically, we analysed three populations of cells (lymphocytes, monocytes and granulocytes) for studies of ROS using APF or DCF dyes which were conducted using non-fixed, non-permeabilised cells (Figure 3.2A, left panel). By contrast, we analysed two populations (mononuclear cells and granulocytes) for studies of p38 MAP kinase and NF-κB phosphorylation which were carried out using fixed, permeabilised cells (Figure 3.2A, right panels).

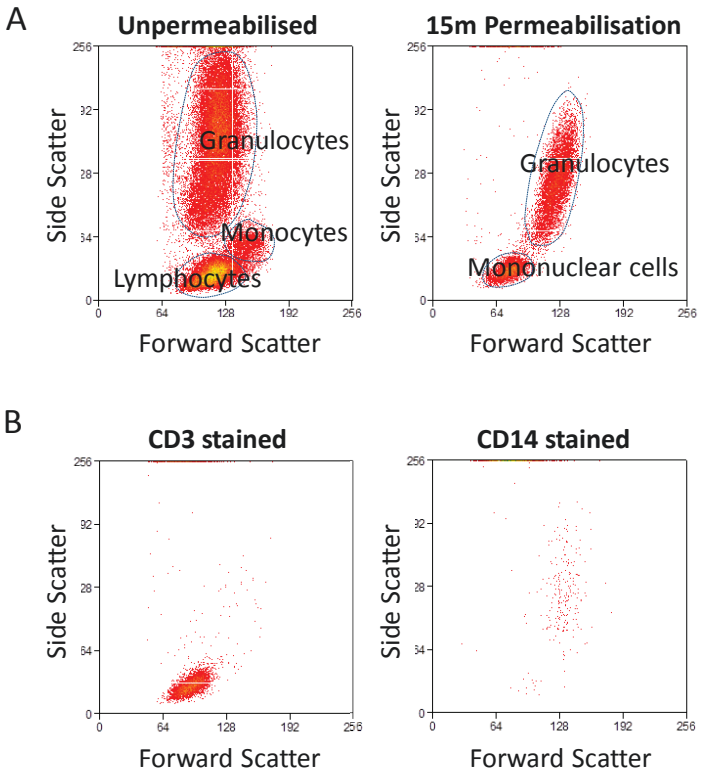

Figure 3.2 Permeabilisation of leukocytes alters scatter profiles

Whole blood was treated with BD Perm III buffer on ice for 15 min (fixed and permeabilised) or remained untreated (freshly isolated). Samples were then analysed by flow cytometry with assessment of the forward and side scatter flow characteristics, after sorting for singlets. Dot plots are presented to compare forward scatter and side scatter profiles. The identity of particular cell populations is indicated (A). Whole blood treated with BD Perm III buffer on ice for 15 min were incubated with either PE-Cy7 conjugated anti-CD3 (left panel) or with Pacific blue-conjugated anti-CD14 (right panel) antibodies. Fluorescence was measured by flow cytometry after gating out red blood cells and debris. Positive cells were back-gated into forward and side scatter (FSC/SSC) profiles to assess size and granularity and dot plots are presented (B).

3.3.2 Determining specificity of intracellular staining

The specificity of antibody binding was confirmed using blocking peptides and by using isotype-matched control antibodies. Blood samples were analysed at the basal state or following treatment with TNFα or LPS because these stimuli are known to activate NF-κB and p38 MAP kinase in multiple cells types.

In the first instance, binding of PE-Cy7-conjugated antibodies that were raised against either a peptide corresponding to phosphorylated p38 MAP kinase or against an irrelevant peptide (control) was compared. This comparison is valuable because fluorescence generated with control antibodies reflects autofluorescence and/or non-specific binding of antibodies per se (e.g. via the Fc portion). Samples were treated with LPS or remained untreated as a control prior to staining. Analysis of granulocytes (identified by FSC/SSC profiles) revealed that fluorescence generated by anti-phosphorylated p38 MAP kinase antibodies was higher than fluorescence from isotype-matched control antibodies in LPS-treated cells but not in untreated cells (Figure 3.3A, left and centre panels). These data demonstrate that the anti-phosphorylated p38 MAP kinase antibodies bind to a molecule that is induced by LPS in granulocytes. We concluded that this molecule corresponds to phosphorylated p38 MAP kinase, because a specific blocking peptide for phosphorylated p38 MAP kinase significantly reduced binding of anti-phosphorylated p38 MAP kinase antibodies (Figure 3.3B, compare sample 1 and sample 2) whereas control peptides had little effect (Figure 3.3B, compare samples 1-2 with samples 3-4) and MFI measured with control peptides was similar to that measured in the absence of any peptide or negative irrelevant controls (Figure 3.3, compare samples 1-2 with samples 5-6). The antibody is highly specific, as complete blockade of detectable fluorescence occurred with the blocking peptides; the PE-Cy7 MFI in Figure 3.3B sample 1 represent the arbitrary lower limit of fluorescence set by the flow cytometry protocols, and no inducible signal was observed with LPS stimulation shown in Figure 3.3B sample 2. In the absence of a specific p38-blocking peptide, constitutive levels of p38 MAP

kinase are indicated in Figure 3.3B sample 3 and sample 5, and inducible levels are shown in Figure 3.3B sample 4 and sample 6.

Parallel studies demonstrated that binding of anti-phosphorylated NF-κB to permeabilised mononuclear cells was enhanced by treatment of leukocytes with TNFα (Figure 3.3C, compare samples 13 and 14). In the presence of varying concentration of specific blocking peptides (0-100 μg/μl) for phosphorylated NF-κB, antibody binding was reduced whereas control peptides had little effect (Figure 3.3C, compare samples 1-6 with samples 7-12). Collectively, these data suggest that anti-phosphorylated p38 MAP kinase or anti-phosphorylated NF-κB antibodies react specifically with their respective targets.

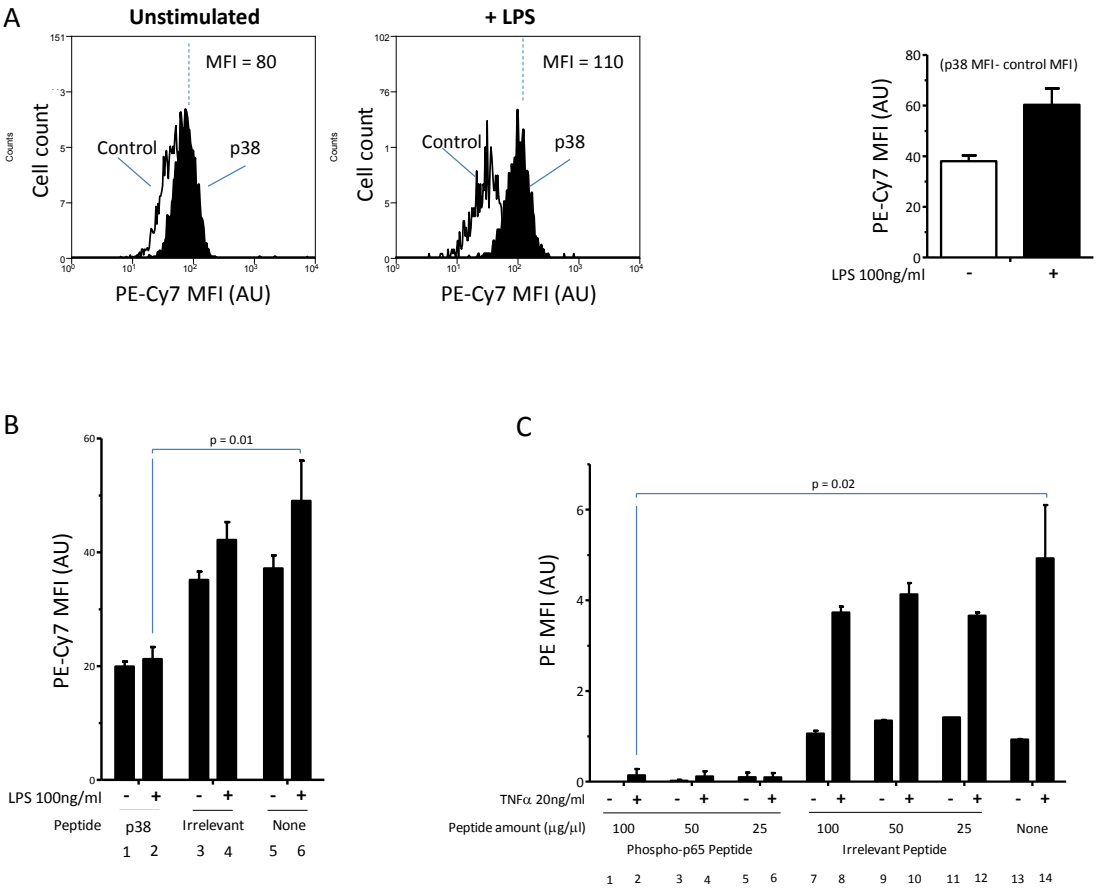

Figure 3.3 Confirmation of antibody binding specificity

Peripheral blood samples were incubated with LPS (100ng/ml for 30min; centre panel) or remained untreated as a control (**A**, left panel). They were then treated with BD Perm III buffer on ice for 15 minutes to fix and permeabilise leukocytes prior to incubation with PE-Cy7-conjugated antibodies that were raised against phosphorylated p38 MAP kinase (p38) or an irrelevant antigen (Control). Fluorescence of samples was quantified by flow cytometry and histograms are presented. The mean fluorescence intensities (PE-Cy7 MFI) of cells incubated with anti-phosphorylated p38 MAP kinase antibodies are presented (**A**, inset). The level of p38 MAP kinase phosphorylation was calculated by subtracting fluorescence generated using control antibodies from fluorescence generated using anti-phosphorylated p38 MAP kinase antibodies (**A**, right panel) in granulocytes. Statistical calculations indicated are Student's t-test.

Anti-phosphorylated p38 MAP kinase antibodies were pre-incubated with a specific p38 MAP kinase blocking peptide or a non-specific irrelevant peptide for 1 hour on ice (or remained untreated)(**B**). Anti-phosphorylated NF-κB antibodies were pre-incubated with a specific NF-κB blocking peptide or a non-specific irrelevant peptide at varying concentrations for 1 hour on ice (or remained untreated)(**C**). These preparations were used for intracellular staining of leukocytes exposed to LPS (**B**) or TNFα (**C**) for 30 min. Fluorescence of samples was quantified by flow cytometry and mean values generated from multiple cells for p38 MAP kinase phosphorylation (PE-Cy7 MFI) (**B**) or NF-κB phosphorylation (PE MFI) (**C**) in mononuclear cells. Statistical calculations indicated are Student's t-test.

3.3.3 p38 MAP kinase and NF-κB were phosphorylated in peripheral blood leukocytes by inflammatory stimuli

The following experiments examined whether the anti-phosphorylated p38 MAP kinase or anti-phosphorylated NF-κB antibodies could be used to monitor activation in leukocytes exposed to a variety of stress stimuli. Intracellular staining followed by flow cytometry revealed that phosphorylation of p38 MAP kinase and NF-κB were elevated by incubation of samples at room temperature with arsenite in mononuclear cells (Figure 3.4A and B, lower panels). By contrast, PMA enhanced p38 MAP kinase phosphorylation in granulocytes and mononuclear cells but did not influence NF-κB phosphorylation whereas TNFα stimulation induced NF-κB and not p38 MAP kinase in both granulocytes and mononuclear cell populations (Figure 3.4B, compare A and B). Taken together, these data suggest that intracellular staining followed by flow cytometry can be used to monitor the activity of p38 MAP kinase and NF-κB in leukocytes in whole blood samples.

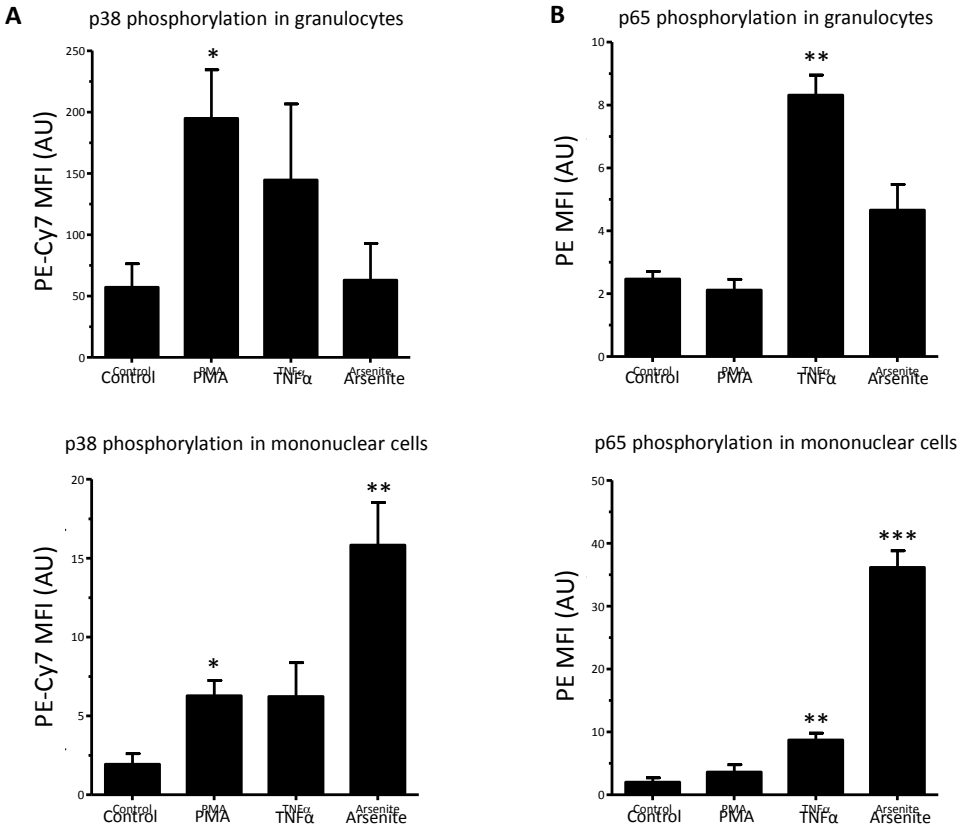

Figure 3.4 p38 MAP kinase and NF-κB phosphorylation was induced with experimental stress in mononuclear cells

Whole blood from healthy volunteers was treated with 200ng/ml PMA, 250μM sodium arsenite, 20ng/ml TNFα for 30 minutes (or remained unstimulated). Levels of phosphorylated p38 MAP kinase (A) or NF-κB (B) were assessed by intracellular staining followed by flow cytometry. Mean fluorescence values generated from multiple cells are presented for granulocytes and mononuclear cells (identified by their FSC/SSC profiles). The level of p38 MAP kinase or NF-κB phosphorylation was calculated by subtracting fluorescence generated using control antibodies from fluorescence generated using anti-phosphorylated p38 MAP kinase or anti-phosphorylated NF-κB antibodies. Mean MFI values were calculated from 6 independent experiments and are presented with standard error of the mean. (*p<0.05; **p<0.01; ***p<0.005 Student's t-test, compared to control).

3.3.4 ROS were induced in peripheral blood leukocytes by inflammatory stimuli

To validate the ROS assays, preliminary experiments were conducted using whole blood or purified peripheral blood mononuclear cells (PBMC) from healthy volunteers. Samples were loaded with APF or DCF and fluorescence was quantified by flow cytometry. Basal ROS levels were measured in mononuclear cells that were either purified from peripheral blood or remained unpurified (whole blood) prior to labelling. They were greatly enhanced in purified PBMC compared to whole blood (Figure 3.5, compare left and right panels and note the different scales used on the y-axes). It is plausible that prolonged incubation at room temperature or mechanical stimulation during PBMC purification led to enhanced ROS levels. Regardless of the mechanism, whole blood samples were selected for use in all future experiments in order to minimise activation during sample preparation which could potentially mask biological effects.

Furthermore, an evaluation of whether APF or DCF could be used to monitor ROS induction in granulocytes, monocytes or lymphocytes exposed to a stress stimulus was undertaken. Treatment with PMA enhanced the fluorescence of both DCF and APF in granulocytes and monocytes (Figure 3.5B) and the most significant changes were observed using APF (compare left and right panels). APF was therefore selected to measure basal and inducible ROS in leukocytes in subsequent experiments.

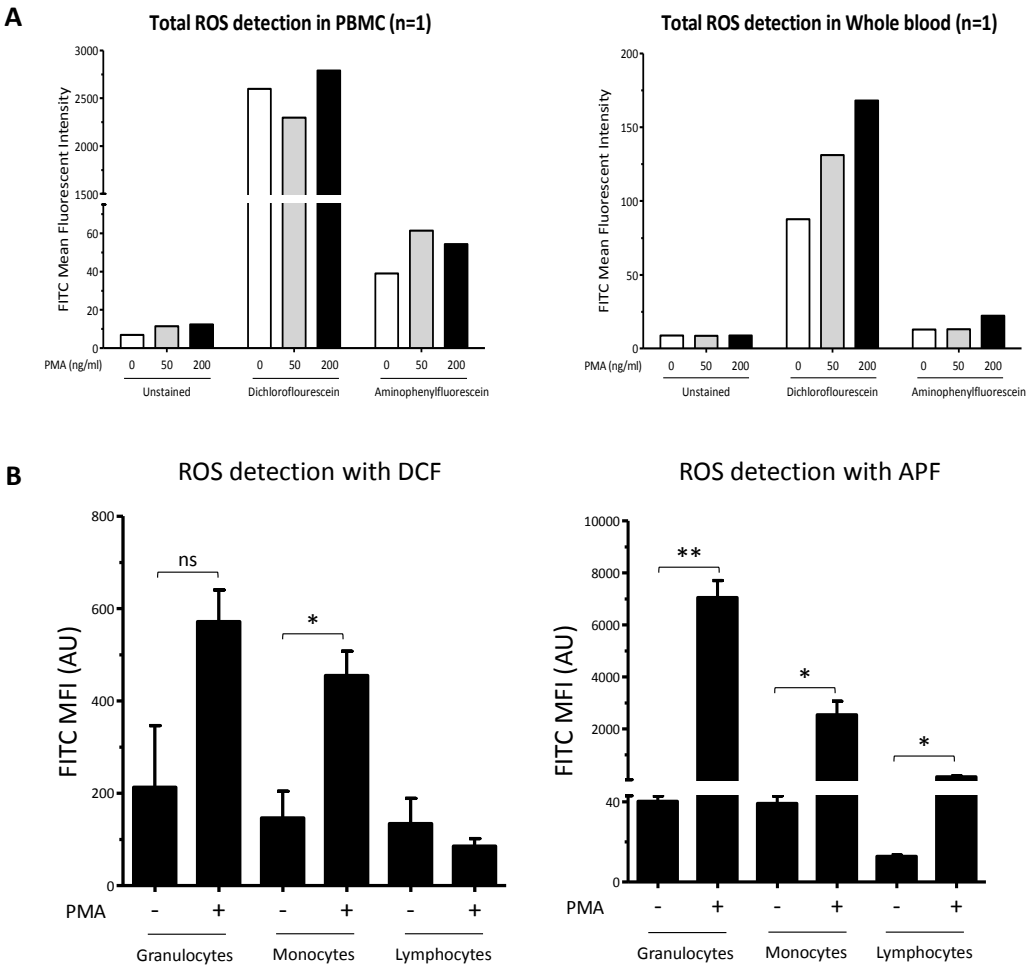

Figure 3.5 PMA induced ROS in peripheral blood leukocytes from healthy volunteers

Whole blood samples (right panel) or isolated PBMC (**A**, left panel) from healthy volunteers were loaded with APF or DCF (or remained untreated as a control). Samples were then either stimulated with PMA (50ng/ml or 200ng/ml) or remained unstimulated as a control. Fluorescence of mononuclear cells was quantified by flow cytometry after gating using FSC/SSC data and mean values generated from multiple cells are presented. Whole blood samples from healthy volunteers were loaded with DCF (**B**, left panel) or APF (**B**, right panel). Samples were then either stimulated with PMA (200ng/ml) or remained unstimulated as a control. Mean fluorescence intensity (MFI) values generated from multiple cells are presented for granulocytes, monocytes and lymphocytes (identified by their FSC/SSC profiles). Mean MFI values were pooled from studies of 4 individuals and are presented together with individual MFI data. (*p<0.05; **p<0.01 Student's t-test)

3.4 CONCLUSIONS

1. FSC and SSC profiles could be utilised to distinguish lymphocytes, monocytes and granulocytes in freshly-isolated peripheral blood samples in flow-cytometric analyses.

2. Fixation and permeabilization of leukocytes alters the FSC/SSC profile of monocytes, thus causing partial overlap with the profile of granulocyte population.

3. Nevertheless, granulocytes and mononuclear cells can be distinguished by their FSC/SSC profiles in fixed and permeabilised peripheral blood samples.

4. Isotype-matched irrelevant antibodies and blocking peptides confirmed the specificity of antibodies against phosphorylated p38 MAP kinase or phosphorylated p65-NF-κB.

5. Intracellular staining and flow cytometry detected enhanced p38 MAP kinase and NF-κB phosphorylation in whole blood samples exposed to stressful stimuli.

6. DCF and APF dyes and flow cytometry detected enhanced ROS in whole blood samples exposed to stressful stimuli.

3.5 DISCUSSION

Although the ROS-sensitive dyes and intracellular staining antibodies used in this study have been tested extensively in previous studies, it was felt that they should be validated in our hands prior to their use in clinical and animal studies. This exercise was useful since we observed an unexpected interaction between sample preparation and the identification of leukocyte sub-populations using FSC and SSC profiles. Specifically, fixation and/or permeabilization enhanced the apparent granularity of monocytes. The consequence is that only two populations could be discriminated by FSC/SSC profiling of cells following intracellular staining, namely mononuclear cells and granulocytes. This is important because it influenced the interpretation of our data which could not be used to interrogate monocytes following intracellular staining. By contrast, ROS levels could be measured in monocytes, lymphocytes and granulocytes because this assay did not require cell fixation and permeabilisation.

The earliest experiments conducted utilised PBMCs. However, it was concluded that purified PBMCs were unsuitable for monitoring of ROS and p38 MAP kinase or NF-κB phosphorylation for the following reasons; (1) for the detection of ROS, elevated levels of intracellular ROS were detected in isolated PBMCs by comparison to whole blood, indicating that PBMC analysis may overestimate ROS levels in vivo. (2) Although phosphorylation of MAP kinases and phosphorylation of NF-κB were not determined in PBMCs, altered phosphorylation states are expected since MAP kinases are exquisitely sensitive to mechanical force[343,508,509]. (3) The inherent time constraints of handling and processing were unsuitable because a rapid assay was required for the planned studies. (4) PBMC isolation requires approximately 50mls of blood to yield a sufficient number of cells for experimental work. This may be reasonable for pilot studies in healthy volunteers but it is difficult to justify this volume of blood, at multiple time points (as per the anticipated design of the cardiopulmonary bypass study), in patients who have undergone major surgery that is

inherently associated with bleeding. The flow cytometric assays requiring <5mls of whole blood were adopted for this reason.

TNFα, LPS, PMA and arsenite were selected for study as these stimuli are known to be strong activators of leukocytes. The pathways and signalling molecules downstream from these stimuli have previously been described in 1.5.1, 1.5.2 and 1.5.3. The purpose of these studies was not to elucidate the mechanisms and inflammatory cascades limited to these particular stimuli but to establish the assays as a reliable tool for detection of our markers of interest. Thus we used several stimuli in parallel to test the suitability of the assays for analysis of whole blood samples. It should be stressed that the experimental set up was not designed to look at kinetics of activation nor the relative influence of ROS on p38 MAP kinase and NF-κB (and their cross-talk). These questions cannot be answered on the basis of the experimental data generated in this chapter. What the data do show, is that different kinetics of activation of ROS, p38 MAP kinase and NF-κB are associated with PMA treatment, and that LPS, TNFα and arsenite have different effects on the signalling p38 MAP kinase and NF-κB cascades.

A limitation of the assays used is that they do not generate absolute quantitate data on levels of p38 MAP kinase nor NF-κB phosphorylated forms or ROS. Instead, they can provide information on the relative abundance of these molecules in cells exposed to different conditions. Because of this limitation, it was not possible to determine the sensitivity of the assay at a formal level. Thus the ability of these assays to detect activation of p38 MAP kinase, NF-κB or ROS induction in samples from patients or large animals undergoing bypass was determined empirically (see chapters 4 and 5).

The technical validation work presented in this chapter were important because they led to the development of tools and protocols to analyse ROS induction and p38 MAP kinase and NF-

κB activation in leukocytes from patients (Chapter 4) and health human volunteers, or pigs exposed to CPB (Chapter 5).

CHAPTER 4. INFLAMMATORY SIGNALLING MODULATION BY CARDIOPULMONARY BYPASS OPTIMISATION

4.1 INTRODUCTION

Coronary artery bypass graft surgery, for ischaemic heart disease, performed with the use of conventional CPB systems can lead to the generation of molecular triggers that promote inflammation. These signals orchestrate the inflammatory response to surgery by influencing pro-inflammatory signalling within and between blood and tissue cellular compartments. Therefore, from a therapeutic perspective, the optimisation of CPB (in the form of the currently available miniaturised CPB system) may result in attenuated pro-inflammatory leukocyte signalling. This reduction in pro-inflammatory signalling, in turn, may lead to a reduction in the margination of activated leukocytes into organs after cardiac surgery, and consequently a lower incidence organ dysfunction with corresponding improvements in clinical outcome measures.

Although it is well recognised that CPB can induce systemic inflammation as discussed in 1.4.1 (page 36), the regulatory signalling pathways that are activated by CPB have not been precisely defined. Moreover, the mechanism underlying the inflammatory effects of CPB miniaturisation has not been characterised at a molecular level.

In the work presented in this chapter, preliminary studies of ROS, p38 MAP kinase and p65 NF-κB activation were conducted prior to their full assessment within a randomised clinical study.

4.2 HYPOTHESIS

The hypotheses tested in this chapter were:

i. Cardiopulmonary bypass leads to the rapid induction of reactive oxygen species in leukocytes which is associated with early activation of pro-inflammatory signalling (e.g. p38 MAP kinase and NF-κB activation) associated with leukocyte transmigration.

ii. Miniaturised cardiopulmonary bypass leads to reduced pro-inflammatory activation in leukocytes and an attenuated systemic inflammatory response compared to conventional cardiopulmonary bypass.

4.3 RESULTS: PRELIMINARY STUDIES

4.3.1 The effect of cardiopulmonary bypass on reactive oxygen species induction

Preliminary pilot studies were performed to determine whether surgery with CPB activates pro-inflammatory intracellular signalling pathways. Initially, ROS levels in leukocytes were studied in three patients undergoing heart surgery (CABG, aortic valve replacement, aortic root replacement) with conventional CPB support. Given that these are rapid signalling molecules with short half-lives (discussed in 1.5.1, page 56) and that CPB was considered the initiating event in pro-inflammatory activation, blood was sampled at baseline (on the morning of surgery); then at the start of CPB support followed by further blood sampling at 30 minutes, 1 hour, 5 hour and 24 hour timepoints relative to the initiation of CPB. Two different ROS sensitive probes were utilised (APF and DCF) to assess the induction of ROS. Ex-vivo phorbol ester (PMA 200ng/ml for 30 minutes) was also applied to leukocytes within this experimental setting. As these were preliminary sets of experiments, it was uncertain if changes in ROS were detectable in leukocytes from patients and this element of ex-vivo stress was included in the study to amplify and enhance the intrinsic ROS response within the cells of interest to us. This approach also allowed for the assessment of the leukocyte priming phenomenon post exposure to CPB.

Firstly, the DCF redox-sensitive dye was used to determine broad ROS changes in leukocytes with analysis by flow cytometry. The two-way analysis of variance in the granulocyte fraction identified via flow cytometry (Figure 4.1A) revealed the main effect of CPB exposure was significant, $F(5,20) = 3.442$, $p<0.05$; as was the effect of ex-vivo PMA stimulus $F(1,4) = 8.369$, $p<0.05$. Post-hoc evaluation performed with the *Dunnett* multiple comparisons test to compare differing time points to baseline controls. These statistical evaluations indicated that there was a significant increase in mean PMA-enhanced ROS levels at the start of CPB (mean 3684 ± 2110 FITC MFI units, $p<0.01$) and at 30 minutes (mean 3150 ± 1998 FITC MFI units, $p<0.05$), compared to baseline (mean 1104 ± 463 FITC MFI units). By contrast, in PMA-unstimulated leukocytes subject to CPB, the change of means

from baseline (333 ± 235 FITC MFI units) to the start of CPB (1215 ± 617 FITC MFI units) was not statistically significant. There was a trend towards ROS levels returning to baseline levels at 5 hours (PMA-unstimulated, 471 ± 178 FITC MFI units) from the start of CPB in the granulocyte fraction.

Two-way analysis of variance in the monocyte fraction (Figure 4.1B) revealed no effect from CPB exposure nor an effect from PMA-stimulation at the 0.05 alpha level. The trends in PMA-unenhanced ROS were similar to those seen in granulocytes: baseline mean 378 ± 489 FITC MFI units vs start of CPB mean 1875 ± 1867 FITC MFI units vs 5 hours post CPB mean 409 ± 80 FITC MFI units.

In the lymphocyte fraction determined by flow cytometry (Figure 4.1C) two-way analysis of variance in fluorescence revealed the main effect of CPB exposure was significant, $F(5,20) = 2.797$, $p<0.05$; but the effect of ex-vivo PMA stimulus was not significant; $F(1,4) = 0.2006$, $p<0.67$. This is evident in the graph when we compare the scale of fluorescent intensity in unstimulated and stimulated leukocytes throughout the duration of surgery and into the post-operative recovery period. PMA-enhanced ROS levels increased significantly at the start of CPB (mean 1023 ± 1157 FITC MFI units, $p<0.05$) and persisting up till 30 minutes (mean 1109 ± 796 FITC MFI units, $p<0.05$) of CPB exposure, compared to baseline levels (mean 287 ± 356 FITC MFI units).

In keeping with the patterns observed in the granulocyte and monocyte fraction data, the changes between baseline (mean 253 ± 294 FITC MFI units) and the start of CPB (mean 922 ± 680 FITC MFI units) and at 5 hours post-CPB (mean 380 ± 105 FITC MFI units) in untreated cells were not statistically significantly different.

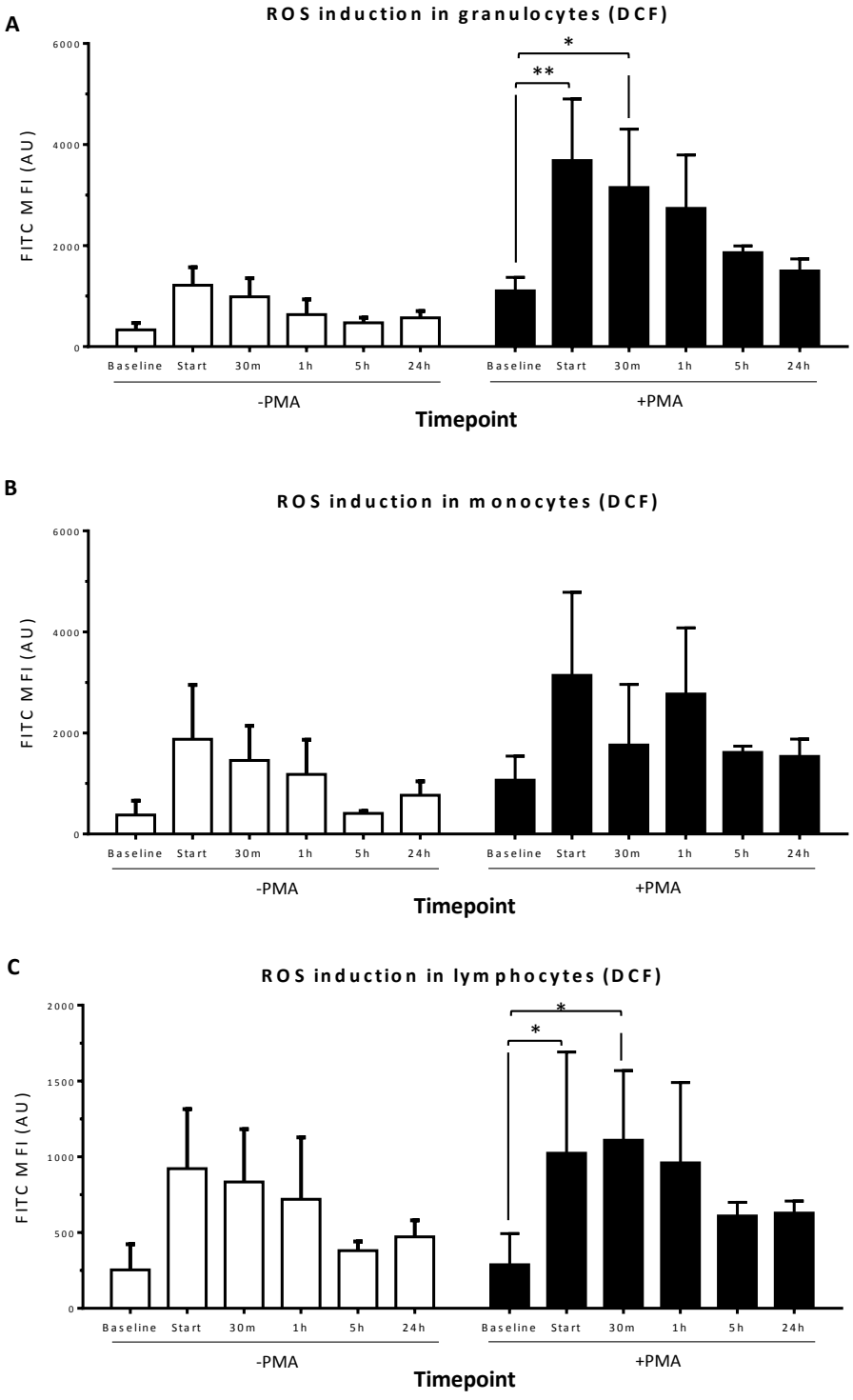

Figure 4.1 DCF-spectrum ROS activation during cardiac surgery

Surgery with conventional cardiopulmonary bypass was studied. Blood was sampled prior to surgery on the morning of the operation (baseline), at the start of CPB and 30 minutes, 1 hour, 5 hours and 24 hours post initiation of CPB. Samples were loaded with the DCF ROS-sensitive probe and treated with PMA (200ng/ml) for 30 minutes (or remained untreated as controls) prior to analysis by flow cytometry. Fluorescence was assessed by flow cytometry for (A) granulocyte (B) monocyte and (C) lymphocyte subpopulations by forward and side scatter profiles. Fluorescence values were pooled from data generated using 3 patients and mean values ± SEM are shown. (* $p<0.05$; ** $p<0.01$; two-way ANOVA with Dunnett's post-hoc multiple comparisons test post-hoc multiple comparisons test).

In parallel, the APF ROS-sensitive probe was used to evaluate leukocyte changes in the context of cardiac surgery with cardiopulmonary bypass. Two-way analysis of variance in fluorescence in the granulocyte fraction (Figure 4.2A) revealed the main effect of PMA-stimulus was highly significant, $F(1,4) = 192.9$, $p<0.0005$; whereas the main effect of CPB exposure was not; $F(5,20) = 0.1653$, $p<0.97$. Post-hoc evaluation using the Bonferroni multiple comparisons test between groups showed highly significant PMA-inducible ROS activation at all timepoints (e.g. baseline comparison PMA-unstimulated 36.4±16.1 vs PMA-enhanced 7708 ± 1994 FITC MFI units, $p<0.0001$). In unstimulated cells, APF-detectable ROS at the start of CPB (mean 54.1 ± 33.8 FITC MFI units) were not statistically different from baseline levels (mean 36.2 ± 16.1 FITC MFI units) nor at 5 hours (mean 56.3 ± 17.3 FITC MFI units) in the granulocyte fraction. Mean fluorescence levels were similar for all granulocyte samples treated with PMA, irrespective of CPB time (Figure 4.2). This could be because PMA-enhanced levels of ROS approach the maximum detection threshold of the flow cytometry settings (Figure 4.2A, compare scales of -PMA and +PMA; note the maximum threshold for flow cytometry is arbitrarily set at 10,000 MFI units).

Two-way analysis of variance in fluorescence in the monocyte fraction (Figure 4.2B) revealed the main effect of PMA-stimulus was significant, $F(1,4) = 15.43$, $p<0.05$; as was the effect of CPB exposure $F(5,20) = 22.17$, $p<0.0001$. Highly significant PMA-enhanced ROS activation was detected at 1 hour (mean 1617 ± 1169 FITC MFI units, $p<0.01$), 5 hours (mean 4092 ± 1221 FITC MFI units, $p<0.0001$) persisting up to 24 hours (mean 4494 ± 757 FITC MFI units, $p<0.0001$) post-CPB compared to baseline levels (mean 1514 ± 1169 FITC MFI units). Levels of ROS at the start of CPB (mean 59.4 ± 38.8 FITC MFI units), 1 hour (69.1 ± 41.2 FITC MFI units) and 5 hours (mean 69.3 ± 14.2 FITC MFI units) were not statistically significantly different compared to baseline (mean 47.1 ± 42.8 FITC MFI units) in unstimulated specimens.

In the lymphocyte fraction determined by flow cytometry (Figure 4.2C), two-way analysis of variance revealed a significant effect with PMA-stimulus, $F(1,4) = 130.5$, $p<0.0005$; as was the effect of CPB exposure $F(5,20) = 7.615$, $p<0.0005$. PMA-enhanced ROS activation was enhanced at 5 hours (mean 622.5 ± 187.3 FITC MFI units, $p<0.005$) and at 24 hours (mean 716.1 ± 304.5 FITC MFI units, $p<0.001$), compared to baseline (mean 88.2 ± 56.8 FITC MFI units).. However, there were no significant changes in ROS levels in unstimulated lymphocytes over time

Taken together, these data suggest that PMA-enhanced ROS increased following anaesthesia, sternotomy, surgical access, heparinsation, cannulation - all before the initiation of CPB - and remained elevated for between 1-5 hours. The pattern of PMA-unenhanced ROS mirrors that of PMA-enhanced values at early timepoints (up to 1 hour) relative to the use of CPB. The ROS data suggests that following CPB, leukocytes may be primed towards exhibiting an enhanced ROS response to an external PMA stimulus at late timepoints (5 hours and 24 hours, most evident in Figure 4.2B and C).

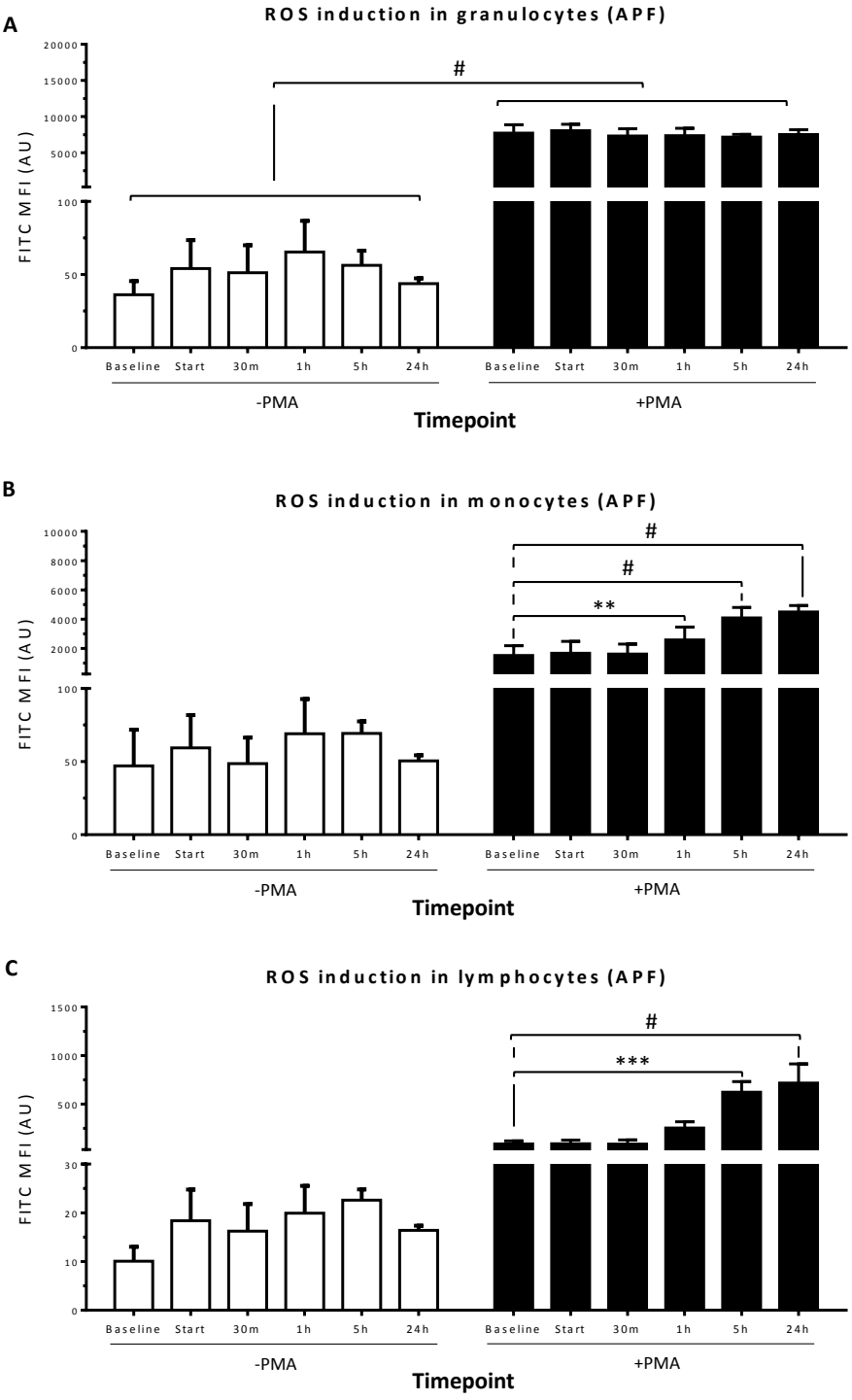

Figure 4.2 APF-spectrum ROS activation during cardiac surgery

Surgery with conventional cardiopulmonary bypass was studied. Blood was sampled prior to surgery on the morning of the operation (baseline), at the start of CPB and 30 minutes, 1 hour, 5 hours and 24 hours post initiation of CPB. Samples were loaded with the APF ROS-sensitive probe and treated with PMA (200ng/ml) for 30 minutes (or remained untreated as controls) prior to analysis by flow cytometry. Fluorescence was assessed by flow cytometry for (A) granulocyte (B) monocyte and (C) lymphocyte subpopulations by forward and side scatter profiles. Fluorescence values were pooled from data generated using 3 patients and mean values ± SEM are shown. (** $p<0.01$; ***$p<0.005$; # $p<0.001$; two-way ANOVA with (A) Bonferroni multiple comparisons test between goups or (B and C) Dunnett post-hoc multiple comparisons test within groups).

4.3.2 Cardiopulmonary bypass alters p38 MAP kinase and NF-κB signalling in circulating leukocytes

Further pilot experiments were conducted in three patients undergoing surgery (aortic valve, mitral valve surgery, combined valve surgery) to assess the influence of CPB on p38 MAP kinase and p65 NF-κB phosphorylation in leukocytes. These assays were performed on fixed/permeabilised cells (in contrast to the live ROS assays) and afforded the opportunity to perform tests at shorter time intervals between sampling (i.e. 15 minutes rather than 30 minutes in the ROS experiments). Given the observation of enhanced ROS between baseline and the start of CPB, an extra blood sampling time point was taken at the post-anaesthetic induction stage. The rationale for this was to provide a window for evaluation of the changes from anaesthesia / monitoring and the surgical process that follows, prior to the initiation of CPB. Blood specimens for these experiments were therefore taken at baseline (on the morning of surgery); post anaesthesia; at the start of CPB and then at 15 minutes, 30 minutes, 45 minutes, 60 minutes and 1 hour and 6 hours post-CPB. CPB was considered the main driving event for inflammation and the timings of the experiments were designed around this index 'stimulus event'. Given the kinetics of activation of p38 MAP kinase as discussed in 1.5.2 (page 60) and NF-κB 1.5.3 (page 64), the majority of blood sampling timings occurred within the first hour, relative to CPB exposure. Whole blood specimens were not subject to an ex-vivo stress, as the assay did not rely on 'loading' of a detecting probe (whose effect may or may not need amplifying), but instead detected the intrinsic phosphorylation levels of p38 MAP kinase and NF-κB within leukocytes.

To begin, levels of p38 MAP kinase activity in granulocytes were detected by flow cytometry (Figure 4.3A). A one-way ANOVA was conducted to compare the effect of CPB exposure on p38 MAP kinase phosphorylation at multiple timepoints. There was a significant effect of CPB exposure over time with p38 MAP kinase phosphorylation levels, $F(6,12) = 4.376$, $p<0.01$. Post-hoc analysis showed post induction p38 MAP kinase phosphorylation (mean 384.6 ± 162.3 PE-Cy7 MFI units) was not different compared to baseline (mean 347.7 ±

171.7 PE-Cy7 MFI units). These correspond to anaesthesia and monitoring events in the surgical process. Statistically significant peak levels of p38 MAP kinase were measured at the start of CPB (mean 557.8 ± 221.2 PE-Cy7 MFI units, $p<0.05$), corresponding to surgical access/trauma and these levels declined and reached a sub-baseline level at 2 hours post-CPB (mean 102.7 ± 9.0 PE-Cy7 MFI units, $p<0.05$), compared to baseline. In mononuclear cells, these trends were repeated between baseline (mean 14.2 ± 3.4 PE-Cy7 MFI units), peaking at the start of CPB (mean 30.13 ± 24.4 PE-Cy7 MFI units) and reaching sub-baseline trough levels 2 hours (mean 4.7 ± 2.5 PE-Cy7 MFI units) post-CPB but these differences were not statistically significant (Figure 4.3B).

There was a significant effect of CPB exposure over time with levels of phosphorylated p65 NF-κB levels in granulocytes, $F(6,12) = 8.092$, $p<0.005$. In contrast to p38 MAP kinase, levels of phosphorylated p65 NF-κB were maximally induced at 2 hours following CPB (mean 10.28 ± 2.88 PE MFI units, $p<0.05$) compared to baseline (mean 4.41 ± 2.37 PE MFI units). These levels then subsequently declined to sub-baseline levels at 6h (mean 1.60 ± 1.31 PE MFI units, $p<0.01$) post-CPB (Figure 4.3C). During the period of exposure to CPB, there was a downward trend for levels of phosphorylated p65 NF-κB but these data did not reach statistical significance compared to baseline.

When considering the mononuclear cell fraction, there was a significant effect of CPB exposure over time with levels of phosphorylated p65 NF-κB levels, $F(6,12) = 7.244$, $p<0.005$. Peak activation occurred at 2 hours (mean 3.70 ± 1.47 PE MFI units, $p<0.05$) followed by a decline of p65 NF-κB at 6 hours (0.62 ± 0.43 PE MFI units, $p<0.01$) with reference to baseline levels (mean 1.14 ± 0.43 PE MFI units). This is in keeping with the patterns observed in the granulocyte fraction.

Thus we concluded that surgery with CPB was associated with activation of p38 MAP kinase and NF-κB in leukocytes with differing kinetic profiles.

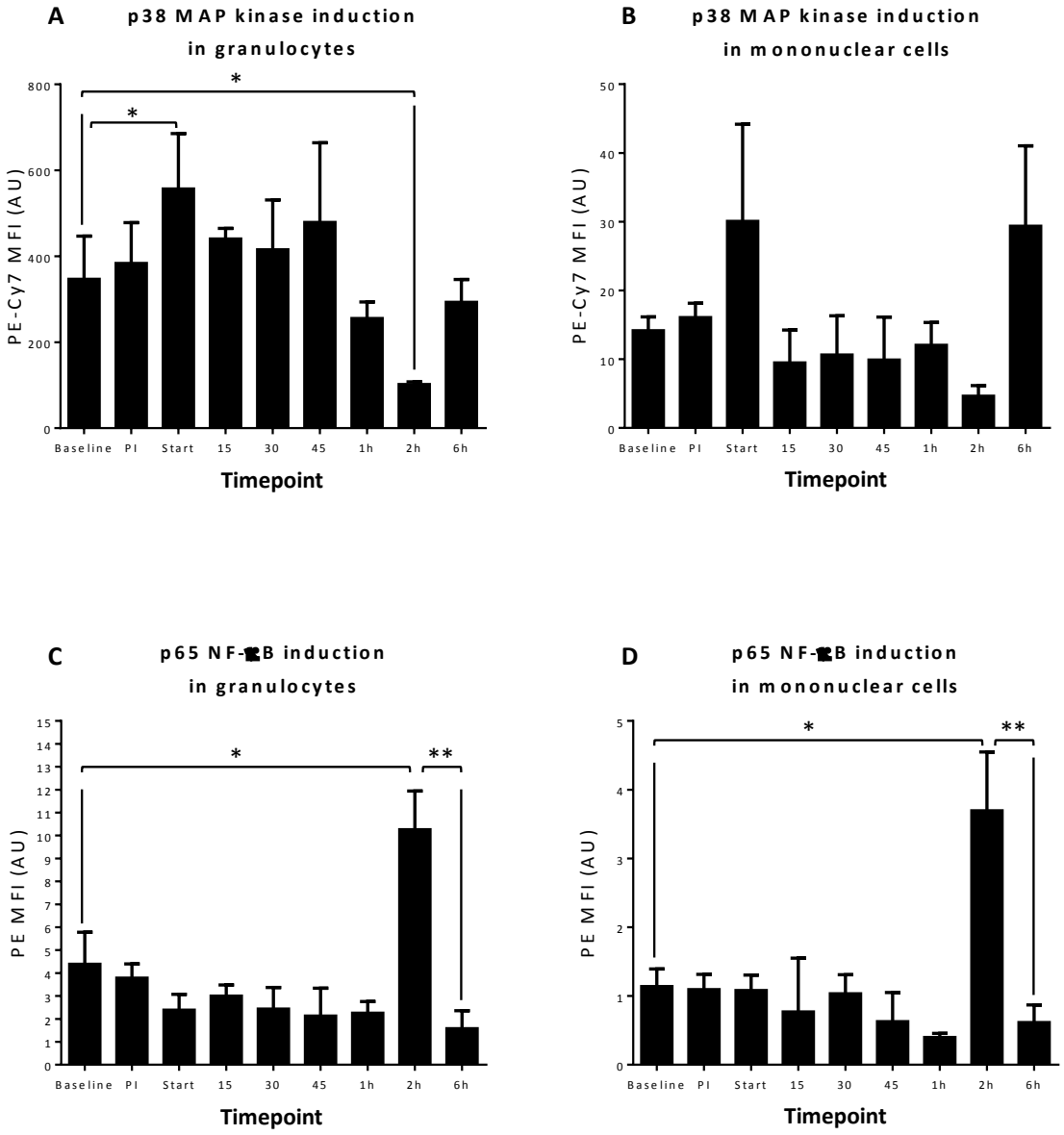

Figure 4.3 p38 MAP kinase and NF-κB induction with cardiac surgery

Surgery with conventional cardiopulmonary bypass was studied. Blood was sampled prior to surgery on the morning of the operation (baseline), post anaesthetic induction (PI) at the start of CPB and 15 minutes, 30 minutes, 45 minutes, 60 minutes and 6 hours post initiation of CPB. Leukocytes were immediately fixed and permeabilised prior to staining with anti-phospho Thr180/Tyr182 p38 MAP kinase (**A**) granulocytes**,** (**B**) mononuclear cells or anti-phospho Ser529 NF-κB antibodies (C) granulocytes (**D)** mononuclear cells. Fluorescence was assessed by flow cytometry and adjusted by subtracting values generated using fluorescent isotype-matched antibodies. Fluorescence values were pooled from data generated using 3 patients and mean values ± SEM are shown. (* $p<0.05$; ** $p<0.01$; repeat measures one-way ANOVA with Bonferroni's post-hoc multiple comparisons test).

4.4 RESULTS: CLINICAL STUDY

Although other studies have shown that CPB can induce systemic inflammation, the pro-inflammatory signalling pathways that are activated by CPB have not been defined. Moreover, the mechanism underlying the anti-inflammatory effects of CPB miniaturisation has not been characterised at a molecular level. To address the question of whether optimising cardiopulmonary bypass systems can attenuate pro-inflammatory signalling in human leukocytes, a randomised clinical trial was performed using the Sorin ECCO miniaturised bypass system.

Building on the earlier work in this chapter, pro-inflammatory signalling pathways in leukocytes were assessed at multiple time points relative to the initiation of CPB. Primary outcome measures were defined as activation of p38 MAP kinase (which is known to promote inflammation by activating downstream AP-1 superfamily transcription factors and by stabilising inflammatory transcripts), and activation of p65 Rel A sub-unit NF-κB transcription factor (which activates multiple inflammatory genes). In addition, the effects of ROS signalling, (which is known to modulate both p38 MAP kinase and NF-κB activities), was evaluated. Secondary outcome measures included assessment of the number of leukocytes within cantharidin skin blisters (as a marker of leukocyte margination), circulating white cell counts, serum C-reactive protein levels (as secondary markers of inflammation) and serum troponin and creatinine levels (as markers of myocardial injury and of renal dysfunction).

This study was conducted in patients undergoing surgical revascularisation for coronary artery disease, which is frequently carried out at the Hammersmith institution. In order to determine the kinetics of inflammatory signalling pathway activation with cardiopulmonary bypass, this study compared conventional CPB (cCPB) and miniaturised CPB (mCPB) in a clinical setting.

4.4.1 Study design and settings

A single centre, open, parallel-group RCT was performed (ISRCTN30610605). A favourable local ethics opinion was obtained prior to commencement of the clinical trial (REC reference 08/H0708/67). The study took place within the Department of Cardiothoracic surgery of the Hammersmith Hospital, Imperial College NHS Healthcare Trust in London, UK. The randomised patients were enrolled between August 2010 and January 2012. Informed written consent was obtained from the research participants.

4.4.1.1 Participants

Patients referred for primary isolated, non-emergent CABG to a single surgeon with extensive experience with the use of both cCPB and mCPB systems were considered for inclusion. Excluded were patients under 18 years of age; emergency surgery requiring an operation within 24h; combined valve replacement procedures in addition to CABG; repeat surgery requiring re-sternotomy; poor left ventricular function with an ejection fraction of <30% on echocardiogram; recent cerebro-vascular accident within 3 months preoperatively or more than 75% carotid artery obstruction on ultrasound; pre-existing renal impairment with serum creatinine in excess of 177 μmol/L; pre-existing coagulopathy; pre-existing liver dysfunction or the recent (within 5 days) use of antiplatelet agents (aspirin/clopidogrel).

4.4.1.2 Intervention and comparator

Anaesthetic technique was standardized for all patients. Thiopentone (1–3 mg/kg) was used for induction with 3–5 mg/kg fentanyl, and volatile agents were delivered in 50% air–O_2 mixture for maintenance. Propofol (3mg/kg/h) was given as an infusion during CPB and neuromuscular blockade was achieved by 0.1–0.15 mg/kg pancuronium. Initial anticoagulation was accomplished with 3 mg/kg body weight of intravenous heparin and was supplemented as required in order to maintain an active clotting time of 480 s or above. All operations were performed using cCPB or mCPB with ascending aortic cannulation, two

stage venous cannulation, and moderate systemic hypothermia (32°C) with parallel blood cell salvage (Electa, Sorin group, Milan, Italy). Coronary artery anastomoses were constructed using intermittent cross-clamp fibrillation (ICCF) in the randomised CPB groups. ICCF was introduced after cross clamping of the aorta in order to perform coronary grafting. This was followed by de-clamping the aorta and reperfusion of the heart. The same procedure was then repeated for each of the subsequent grafts. No cardioplegia was utilised.

mCPB was conducted using the Sorin Dideco Extracorporeal Circulation Optimized (ECCO) system as described previously[435]. During the use of mCPB, the patients' systemic vascular resistance was used to perform a retrograde autologous prime of the arterial line and the arterial line filter. In this way, the patient's own arterial blood pressure was used to displace the circulating prime into the soft-shell reservoir. This displaced prime was then removed via suction to the cell salvage device. An autologous antegrade prime was then carried out by kinetically draining blood from the right atrium and displacing the prime volume into the soft shell reservoir. mCPB was then initiated with a flow of 1.7-2.4/min/m^2. The cCPB circuit utilised a Stockert roller pump, membrane oxygenator, venous reservoir and non-heparin bonded circuit with cardiotomy suction. The details of these two systems are summarised in Table 4.1.

	cCPB system	mCPB system
Target ACT	>400s	>400s
Venous cannula	34 Fr 2 stage (Medtronic) 1/2 inch tubing	29Fr Optiflow (Sorin) 3/8 inch tubing
Reservoir	Sorin Evo	Soft Shell reservoir
Pump	Roller pump (Stockert, Germany)	Centrifugal pump (Stockert, Germany)
Heat exchanger / Oxygenator	Avant (Sorin)	Eos (Sorin)
Flows (target cardiac index)	1.8-2.4L/min/m^2 cooled to 32°C	1.8-2.4L/min/m^2 cooled to 32°C
Prime volume	1400mls Hartmann's	300mls Hartmann's with retrograde autologous prime
Safety features		Venous air removal device (VARD)
Operative field blood	Cardiotomy suction	Cell salvage

Table 4.1 Characteristics of Cardiopulmonary bypass systems

4.4.1.3 Timing of measurements

Sampling times are summarised in Figure 4.4. Participants underwent baseline blister formation on the day before surgery. Baseline blood samples and blister fluid were harvested on the following day, the morning of the operation. Patients received high-flow oxygen prior to anaesthetic induction and endotracheal intubation. Central venous cannulation of the right internal jugular vein and arterial access from the right radial artery was performed and a second 'post-induction' (PI) blood specimen was subsequently taken. Blood was then sampled on commencement of CPB (0 h time point) and then at 30 min, 1h, 2h and a final 5h specimen relative to the initiation of CPB. Blister fluid was harvested 5h following the start of CPB.

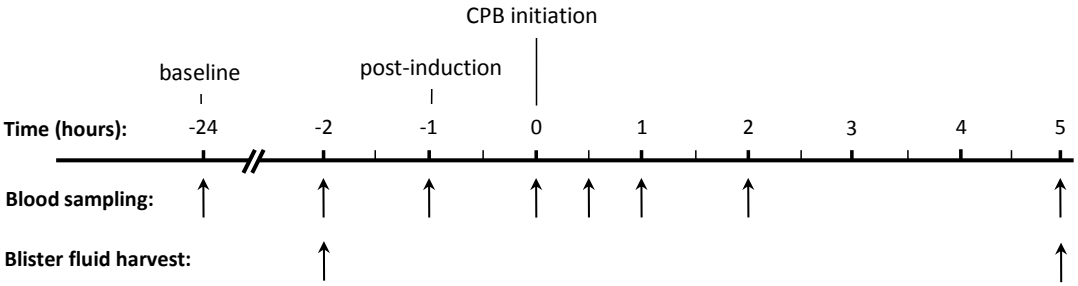

Figure 4.4 Summary of blood and blister fluid sampling times

Blood and cantharidin-induced skin blister fluid were sampled in patients exposed to cCPB or mCPB. Blister fluid was harvested pre-operatively and on the day of surgery. Blood was sampled before surgery and at multiple time points after CPB. A time-line is presented to summarise sampling times (calculated relative to the time of CPB induction which is indicated as t=0h).

4.4.1.4 Outcome measures

Primary outcome measures were blood parameters of cellular stress, specifically reactive oxygen species levels and phosphorylation of p38 MAP kinase and NF-κB (RelA). Secondary outcomes included leukocyte counts in cantharidin-induced skin blisters, circulating white cell counts, serum C-reactive protein levels (secondary markers of inflammation) and serum troponin and creatinine levels.

4.4.1.5 Randomisation

Participants were randomised using the Clinical Trials Evaluation Unit (CTEU) portal system established by staff not otherwise involved in the study. Random allocations were blocked and generated in advance of the study by computer. The random allocations were concealed at the time of recruitment. Randomisation was carried out by one of the investigators after the patient's eligibility had been checked and written informed consent had been obtained. No member of the clinical or research team was blinded to the treatment allocation. Participants were blinded to the allocation.

4.4.1.6 Statistical determinants and analysis

We chose to study 13 patients per group. Based on the data from a previous study[195], a sample size of 13 in each group would have 99% power to detect a difference in means of 1448×10^5 cells between any two groups assuming that the common standard deviation is 1×10^5 using the Wilcoxon (Mann-Whitney) rank-sum test analysis with a 0.05 two-sided significance level. Statistical advice was provided by Joseph Eliahoo, Statistical Advisory Service, Imperial College London.

Statistical analyses of the data were carried out according to a pre-specified statistical analysis plan (SAP) after all subjects had completed the study and after the database had been locked. Continuously scaled outcomes are described as means and SD for each treatment group, at all

time points if measured more than once. A natural logarithm transformation was applied before analysis if outcome data were positively skewed, in which case findings are reported on the natural logarithm scale.

The effects of mCPB compared to cCPB were estimated by fitting mixed regression models (using STATA v.11.2) to take into account the repeated measurements. The following predictors were included: main effect of time, fitted categorically, and main effect of the intervention (mCPB vs. cCPB). Interactions between treatment group and time were also fitted and, if statistically significant at the 5% level, differences between groups with 95% confidence intervals (CI) are described for each time point separately; otherwise an overall treatment difference (with 95% CI) is reported. All data analyses were performed on an intention-to-treat basis irrespective of the final actual treatment modality received. The statistical analysis with regression models was conducted by the trial statisticians Dr Francesca Fiorentino and Professor Barnaby Reeves of the local clinical trials unit.

4.4.2 Patient recruitment

A total of 50 patients were considered for inclusion into the study. Of these, 7 declined to take part in the study and a further 17 were not enrolled due to them meeting one, or more, of the exclusion criteria. The commonest reason for exclusion was pre-existing renal impairment, as defined by a creatinine of >177μmol/l (n=8), followed by concomitant anti-platelet therapy with aspirin or clopidogrel (n=5). The remaining 26 were randomised by computer allocation, using the clinical trials evaluation unit electronic portal, to undergo surgery with either mCPB (n=13) or cCPB (n=13).

4.4.3 Protocol violations

All patients allocated to cCPB had surgery performed as allocated with the use of cCPB circuits as described previously. Of the participants allocated to undergo surgery using

mCPB, one participant underwent surgery with the use of cCPB (because the perfusionist available was not fully-trained in the running of mCPB). The remaining 12 mCPB allocations underwent surgery with the allocated CPB circuit as planned. The sequence of allocations to the study are outlined in the CONSORT diagram illustrated in Figure 4.5.

Figure 2

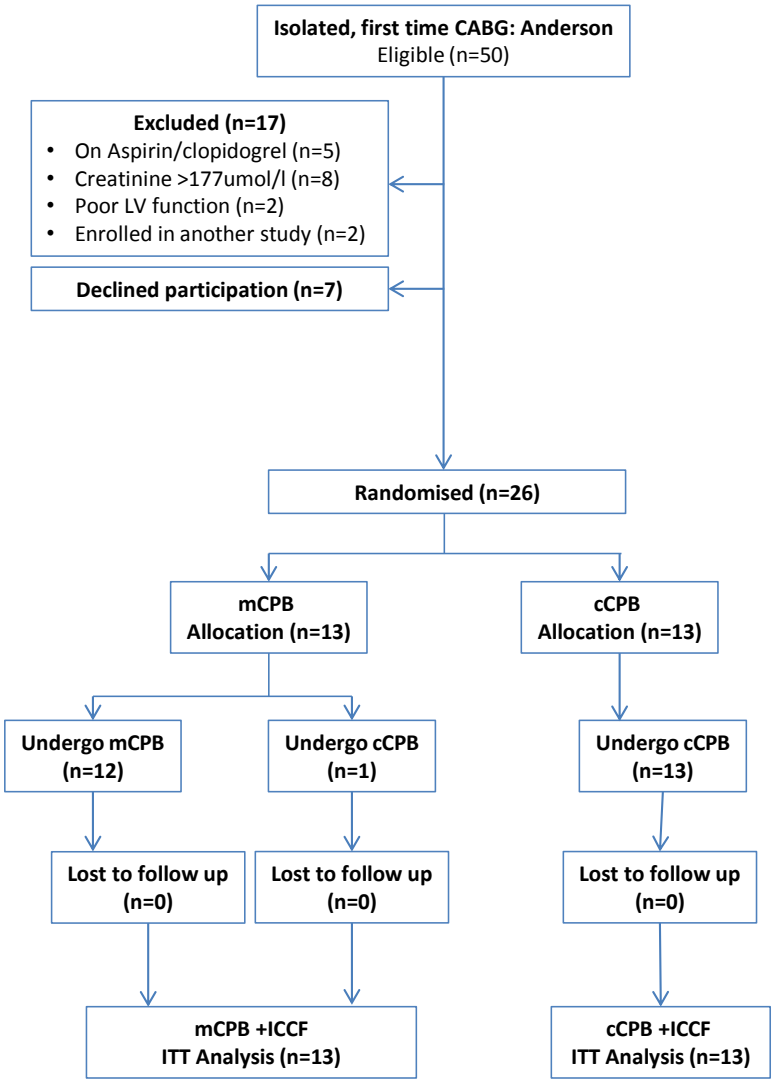

Figure 4.5 Overview of participant selection

Trial participants were recruited and then assessed for various exclusion criteria (indicated). Of those included in the study, computer randomisation allocated participants to either mCPB (investigative group) or cCPB (control group) with coronary surgery performed with intermittent cross-clamp fibrillation (ICCF). One patient in the mCPB group received cCPB as indicated. Statistical analysis was based on intention to treat (ITT).

4.4.4 Baseline characteristics and peri-operative details

Patient characteristics are summarised in Table 4.2. Statistical comparisons of baseline group characteristics are not presented in keeping with CONSORT recommendations. Participant ages were comparable between cCPB (mean 66.3 ± 8.1 years) and mCPB (mean 68.4 ± 6.8 years) groups. The male:female ratio was higher in the cCPB (10:3) than the mCPB (8:5) group. The mean body mass index was similar for both groups 29.7 ± 4.5 kg/m^2 for the mCPB group and 29.3 ± 4.1 kg/m^2 for the cCPB group. The mean logistic EuroSCORE for mCPB and cCPB was 3.35 ± 2.36% and 3.74 ± 3.14% respectively. There tended to be more diabetic patients in the cCPB group (38 % type I, 15% type II) compared to the mCPB group (8 % type I, 8% type II). All other parameters in terms of previous myocardial infarction, left ventricular function, smoking status, hypertension, renal disease, lung disease, extracardiac arterial pathology and neurological dysfunction were comparable between groups.

Peri- and post- operative data are given in Table 4.3. The median duration of CPB was 71 min (IQR 62 – 84) in the mCPB group and 74 min (IQR 67 – 91) in the cCPB group. Median aortic cross-clamp times were 30 min (IQR 24-33) and 34 min (IQR 29-38) in the mCPB and cCPB groups respectively. The mean number of coronary artery bypass grafts performed in the randomised group was 3.2 for both mCPB and cCPB groups. The mean number of red cells transfused was 1.07 ± 1.38 units in the mCPB group and 1.15 ± 1.57 units in the cCPB group in the first 24 hours following surgery. Mean platelet transfusions were 0.15 ± 0.37 pools in the mCPB group and 0.38 ± 0.51 pools in the cCPB group. FFP requirements were 0.54 ± 1.05 pools in the mCPB group and 0.46 ± 1.13 pools in the cCPB group in the early post-operative period. The median hospital stay was 8 days for both the mCPB and the cCPB group (IQR [5,11] for the mCPB group and IQR[7,13] for the cCPB group). There were no perioperative incidences of gross neurological dysfunction nor return to theatre for bleeding in any patient groups. The cCPB group had 3 instances of surgical site wound infections and 1 instance of the requirement for renal support therapy post-operatively.

Variable	mCPB (n=13)	cCPB (n=13)
Female (n)	5 (38.4%)	3 (23.1%)
Age (years)	68.4 ± 6.8	66.3 ± 8.1
Body Mass Index (kg/m2)	29.74 ± 4.53	29.31 ± 4.11
Logistic euroSCORE (%)	3.35 ± 2.36	3.74 ± 3.14
Coronary vessel disease		
Single vessel disease	0	1 (8%)
Two vessel disease	1 (8%)	1 (8%)
Three vessel disease	12 (92%)	11 (84%)
Angina Status		
Asymptomatic	1 (8%)	1 (8%)
CCSI	0	0
CCS II	10 (77%)	7 (54%)
CCS III	1 (8%)	3 (23%)
CCS IV	1 (8%)	2 (15%)
Previous MI	3 (23%)	4 (31%)
Ejection fraction		
Good >50%	11 (85%)	12 (92%)
Fair 30-50%	2 (15%)	1 (8%)
Poor <30%	0	0
Diabetes		
Not diabetic	11 (85%)	6 (46%)
Diet controlled	0	0
Oral Therapy	1 (8%)	5 (38%)
Insulin	1 (8%)	2 (15%)
Smoking status		
Never smoked	6 (46%)	6 (46%)
Current smoker	1 (8%)	0
Ex-smoker	6 (46%)	7 (54%)
Hypertension		
Treated for BP>140/90	12 (92%)	12 (92%)
Chronic lung disease		
No	11 (85%)	12 (92%)
Yes	2 (15%)	1 (8%)
Extracardiac arteriopathy		
No	12 (92%)	12 (92%)
Yes	1 (8%)	1 (8%)
Pre-operative cardiac rhythm		
Sinus rhythm	11 (84%)	12 (92%)
Atrial fibrillation/flutter	1 (8%)	1 (8%)

Table 4.2 Pre-operative patient characteristics
Values are expressed as mean with standard deviation or number with percentage in parentheses as indicated.

Variable	mCPB (n=13)	cCPB (n=13)
Cardiopulmonary bypass time (min)	71 (IQR 62-84)	74 (IQR 67-91)
Total cross clamp time (min)	30 (IQR 24-33)	34 (IQR 29-38)
Number of coronary artery grafts	3.23 ± 0.62	3.23 ± 0.93
Time in ITU (days)	0.86 (IQR 0.80-1.33)	1.00 (IQR 0.80-1.10)
Hospital stay (days)	8 (IQR 5-11)	8 (IQR 7-13)
Transfusions in first 24 hours		
Packed red cells (units)	1.07 ± 1.38	1.15 ± 1.57
Platelets (pools)	0.15 ± 0.37	0.38 ± 0.51
Fresh frozen plasma (pools)	0.54 ± 1.05	0.46 ± 1.13
Post-operative neurological dysfunction		
No	13 (100%)	13 (100%)
Haemofiltration post-operatively		
No	13 (100%)	12 (92%)
Infective complications		
None	13 (100%)	10 (77%)
Harvest site infection	0	1 (8%)
Sternal wound infection	0	2 (15%)
Return to theatre		
No re-operation	13 (100%)	13 (100%)
Return for bleeding	0	0

Table 4.3 Operative and post-operative patient parameters
Values are expressed as medians with inter-quartile range (IQR) or means with standard deviation or number with percentage in parentheses, as indicated.

4.4.5 Primary outcome: leukocyte pro-inflammatory activation profiles

In the 26 patients studied, given the number of observations, data distributions from flow cytometry measures of ROS, p38 and p65 in leukocytes from whole blood samples were found to be positively skewed. The data were transformed into natural logarithms to (statistically) improve the nornality of the data distribution. This normalised data was then evaluated using mixed-effects regression statistical models and presented in Table 4.4 for between-group comparisons.

There were 6/546 missing data points for ROS; 2/364 for p38 MAP kinase and 2/364 for p65 NF-κB over the duration of the study (due to technical failure of the flow cytometer). Consequently, ANOVA could not be performed and multiple assessments could not be made on the basis of conventional post-hoc tests. Instead, focused pair-wise tests were applied to the data (using the *Wilcoxon rank* test, given the non-Gaussian distribution of the data) between timepoints of interest and presented for within-group comparisons. The mixed effects statistical analytical models were selected because of their advantage in dealing with missing values and have particular applicability over longitudinal studies such as the one presented here.

	Endpoint	Difference between mCPB and cCPB (log units)	95% Confidence Interval	p value
Primary	ROS in granulocytes[a]	-0.0531	-0.2740 to 0.1678	0.638
	ROS in monocytes[a]	0.0102	-0.3251 to 0.3456	0.9520
	ROS in lymphocytes[a] 30 mins post-CPB induction 60 mins post-CPB induction 120 mins post-CPB induction 300 mins post-CPB induction	 0.3192 -0.0122 -0.0428 0.1460	 0.1114 to 0.5270 -0.2200 to 0.1957 -0.2506 to 0.1650 -0.0618 to 0.3538	 0.003 0.909 0.686 0.168
	p38 in granulocytes[b]	-0.4688	-0.8923, -0.0453	0.03
	p38 in mononuclear cells[b]	0.4932	-0.4004, 1.3868	0.279
	p65 in granulocytes[c]	0.0517	-0.2426, 0.3459	0.731
	p65 in mononuclear cells[c]	0.1712	-0.2885, 0.6308	0.465
Secondary	Cantharidin blister polymorphonuclear cell count[d]	0.6998	-0.3449, 1.7445	0.173
	Cantharidin blister mononuclear cell count[d]	0.3294	-0.3926, 1.0514	0.342

Table 4.4 Treatment effects of mCPB vs cCPB for primary and secondary endpoints
[a]FITC Mean Fluorescent Intensity (MFL) / arbitrary units (AU); [b]PE-Cy7 MFI/AU; [c]PE MFI/AU; [d]cell counts per blister ($\times 10^5$). Other units otherwise indicated.

4.4.5.1 Cardiopulmonary bypass and the induction of ROS

APF-spectrum ROS induction was first evaluated in patients undergoing surgery. Compared to baseline, ROS were induced maximally at 30 minutes after CPB induction in the cCPB group (mean 12.88 ± 4.619 FITC MFI units vs 17.20 ± 7.68 FITC MFI units, p=0.052). In the mCPB group, peak levels were recorded at the 30 minute post-CPB time point (mean 17.97 ± 20.06 FITC MFI units), but these were not significantly different to baseline. The data from the mCPB group exhibited a higher level of variation and multi-effects regression modelling revealed no difference between either cCPB or mCPB for ROS induction in granulocytes; mean difference -0.0531 log units, 95% CI (-0.2740 to 0.1678), p = 0.638 (Table 4.4, Figure 4.6A).

There were no differences between either cCPB or mCPB groups for their pattern of induction of ROS in monocytes; mean difference 0.0102 log units, CI (-0.3251 to 0.3456), p = 0.9520. In this leukocyte subpopulation, peak levels of ROS were observed at 30 minutes post-CPB for both cCPB (mean 15.51 ± 9.86 FITC MFI units) and mCPB (mean 16.68 ± 23.15 FITC MFI units) groups, although the changes were not statistically significant compared with baseline levels (Table 4.4, Figure 4.6B).

In lymphocytes, ROS levels were significantly higher, between groups, in patients exposed to cCPB (mean 5.78 ± 3.44 FITC MFI units) compared to mCPB (mean 3.74 ± 1.81 FITC MFI units) at 30 min; mean difference= 0.32 log units, 95% CI (0.1114, 0.5270), p=0.003. This is exemplified by the change in ROS in the cCPB group between baseline and 30 minutes (mean 3.38 ± 0.91 vs 3.74 ± 1.81 FITC MFI units, $p<0.05$) that does not occur in the mCPB group (Table 4.4, Figure 4.6C).

Taken together, these data suggest that ROS pro-inflammatory signalling is induced maximally at 30 minutes of CPB and that mCPB differentially alters this induction in the lymphocyte population.

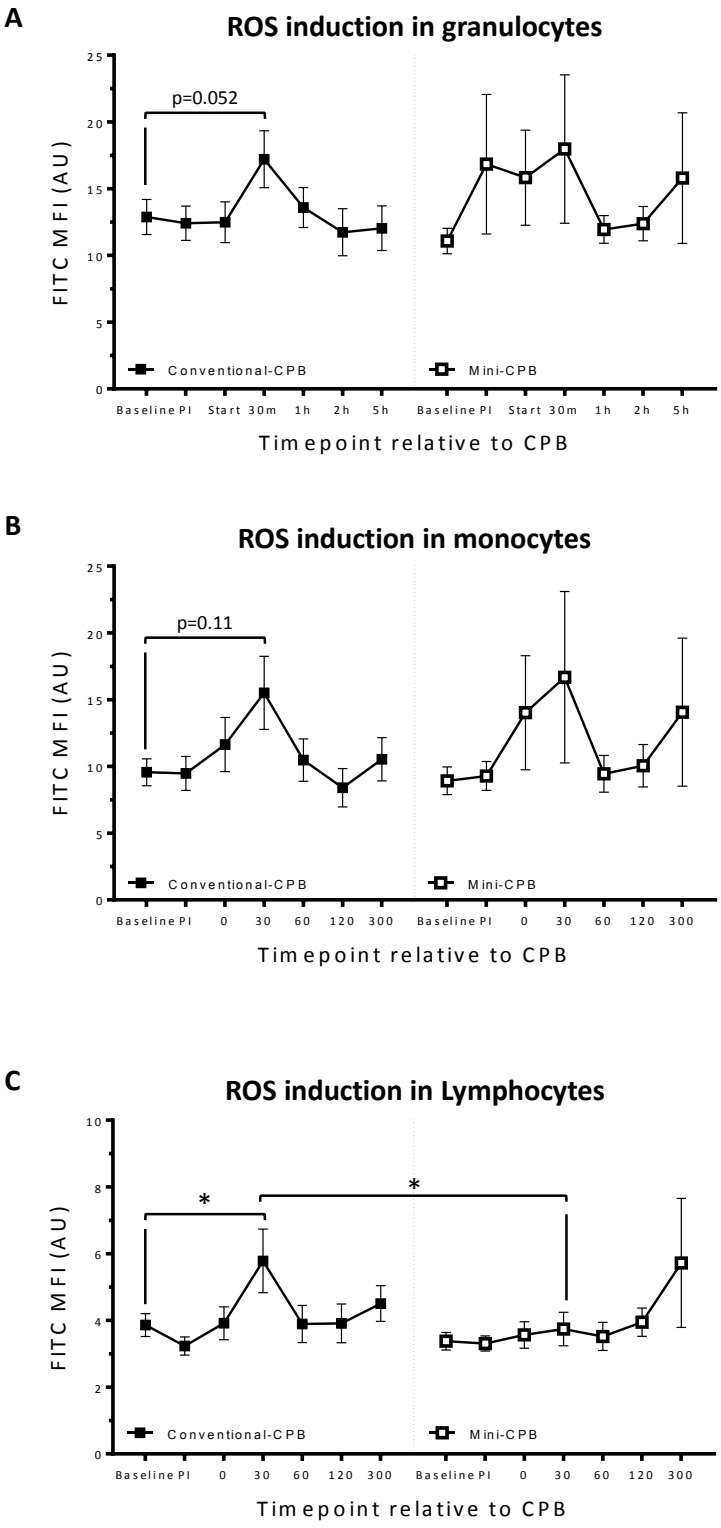

Figure 4.6 Effects of CPB on ROS induction in leukocytes

CABG was performed with cCPB or mCPB. Peripheral blood samples were collected prior to surgery, post-induction, immediately prior to CPB (0 h) and at varying times following CPB initiation. Samples were incubated with a ROS-sensitive dye, APF, prior to analysis by flow cytometry to quantify fluorescence in granulocytes or mononuclear cells (after gating of cells by size and granularity). Fluorescence levels were pooled and mean values ± SEM are shown. (* $p<0.05$ Wilcoxon matched-pairs signed rank test within-group, or statistical result from mixed-effect regression modelling are indicated between-groups).

4.4.5.2 Influence of optimisation of cardiopulmonary bypass on p38 MAP kinase phosphorylation

Intracellular staining and flow cytometry revealed that phosphorylated p38 MAP kinase levels in the cCPB group at baseline (mean 118.44 ± 77.26 PE-Cy7 MFI units) reached a maximal level at the start of CPB (mean 135.98 ± 78.55 PE-Cy7 MFI units). These changes did not reach statistical significance. In keeping with the pilot data shown in the earlier part of this chapter, maximal levels of phosphorylated p38 MAP kinase significantly declined over the duration of CPB exposure to sub-baseline levels at 2 hours (mean 97.88 ± 74.58 PE-Cy7 MFI units, $p<0.05$). In the mCPB group, p38 MAP kinase phosphorylation between baseline (mean 101.89 ± 74.19 PE-Cy7 MFI units) and the start of CPB (mean 122.05 ± 113.79 PE-Cy7 MFI units) were not significantly different. The decline in phosphorylated levelsof p38 MAP kinase were more pronounced with mCPB exposure at 2 hours, significantly falling to sub-baseline levels (mean 60.55 ± 52.67 PE-Cy7 MFI units, $p<0.005$). In comparing between the two CPB groups, at all timepoints from the start of CPB support to 2 hours, phosphorylated forms of p38 MAP kinase were lower in the mCPB group. These were significant differences on assessment by mixed-effects regression modelling; mean difference= 0.47 log units, 95% CI (0.89 to -0.05), p=0.03 (Table 4.4, Figure 4.7A).

In mononuclear cells, the phosphorylated forms of p38 MAP kinase were not significantly different within groups nor between groups; mean difference 0.4932 log units, 95% CI (-0.4004, 1.3868), p = 0.279 (Table 4.4, Figure 4.7B).

Together, these data suggest that mCPB differentially alters pro-inflammatory p38 MAP kinase activation over time favouring earlier attenuation of this response preferentially within the granulocyte cell population.

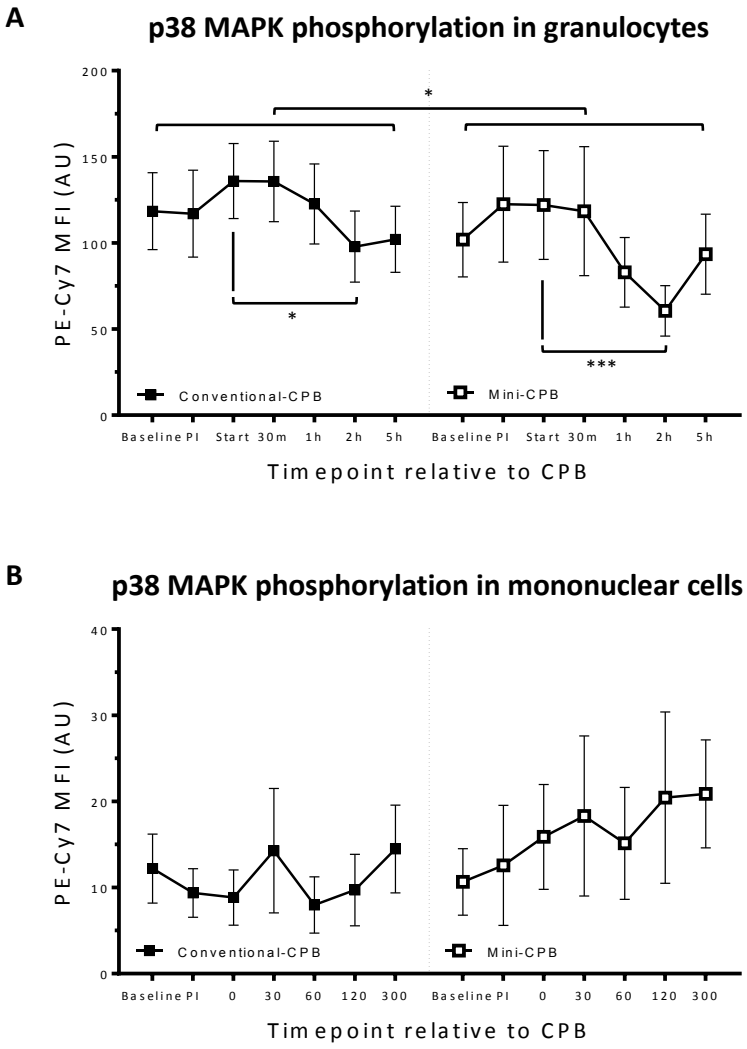

Figure 4.7 Effects of CPB on p38 MAP kinase activation in leukocytes

CABG was performed with cCPB or mCPB. Peripheral blood samples were collected prior to surgery, post-induction, immediately prior to CPB (0h) and at varying times following CPB initiation. Leukocytes were fixed and permeabilised prior to intracellular staining using PE-Cy7-conjugated antibodies that recognise Thr180/Tyr182 phosphorylated p38 MAP kinase or with isotype-matched irrelevant antibodies as a control. Fluorescence of (A) granulocytes or (B) mononuclear cells was quantified by flow cytometry (after gating of cells by size and granularity). Fluorescence levels, calculated after subtracting values from isotype-control antibodies, were pooled and mean values ± SEM are shown. (* $p<0.05$; ***$p<0.001$ Wilcoxon matched-pairs signed rank test within-group, or statistical result from mixed-effect regression modelling are indicated between-groups).

4.4.5.3 Influence of optimisation of cardiopulmonary bypass on NF-κB phosphorylation

Phosphorylation of NF-κB p65 subunits in granulocytes did not significantly differ between groups; mean difference 0.0517 log units, 95% CI (-0.2426, 0.3459), p = 0.731 (Table 4.4, Figure 4.8A). Similarly, phosphorylated forms of NF-κB p65 subunits in mononuclear cells also did not significantly differ between CPB groups; mean difference 0.1712 log units, 95% CI (-0.2885, 0.6308), p = 0.465 (Table 4.4, Figure 4.8B).

However, within groups, there was significant attenuation in phosphorylated levels of granulocyte fraction p65 NF-κB between baseline and 5 hours for both cCPB (mean 3.21 ± 1.98 PE MFI units vs mean 1.71 ± 1.73 PE MFI units, $p<0.005$) and mCPB (mean 3.00 ± 1.09 PE MFI units vs mean 2.08 ± 1.22 PE MFI units, $p<0.05$) groups (Figure 4.7A).

Within groups, there was significant attenuation in phosphorylated levels p65 NF-κB in the mononuclear cell fraction between baseline and 5 hours also for both cCPB (mean 1.57 ± 1.53 PE MFI units vs mean 0.55 ± 0.47 PE MFI units, $p<0.005$) and mCPB (mean 1.10 ± 0.73 PE MFI units vs mean 0.52 ± 0.68 PE MFI units, $p<0.005$) groups (Figure 4.7B).

These data suggest that altering the components of the cardiopulmonary bypass circuit does not alter the inflammatory activation profile of phosphorylated forms of p65 NF-κB in the context of cardiac surgery. A consistent message that does emerge is phosphorylated forms of p65 NF-κB declines over the passage of time, following anaesthesia, surgical trauma and cardiopulmonary bypass.

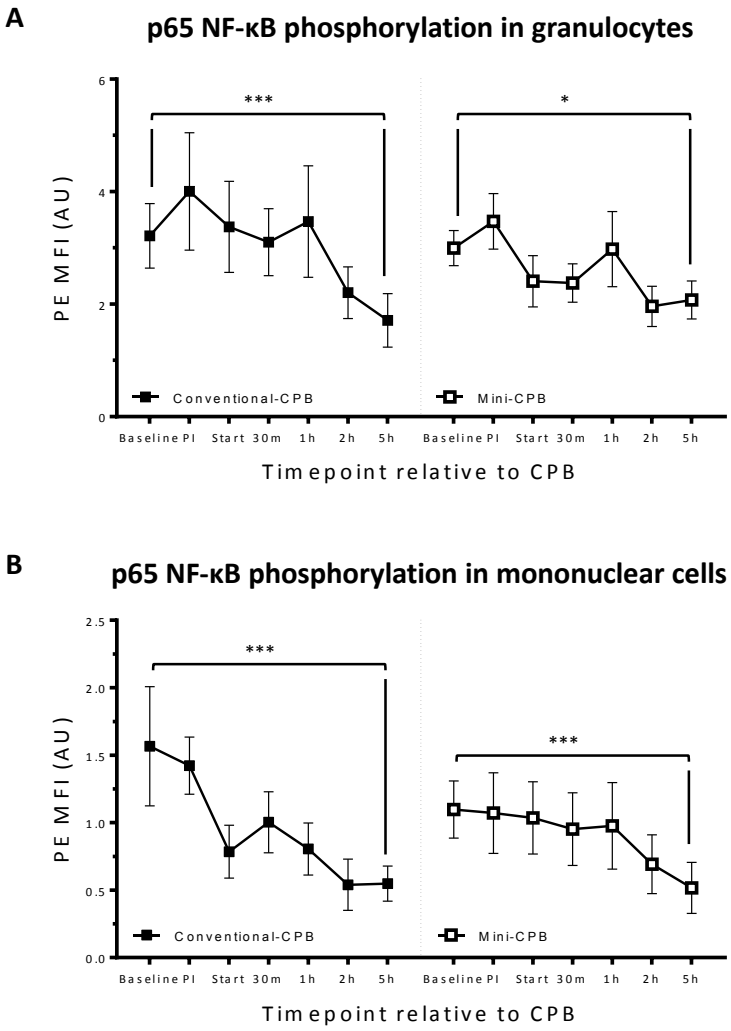

Figure 4.8 Effects of CPB on leukocyte NF-κB phosphorylation

CABG was performed with cCPB or mCPB. Peripheral blood samples were collected prior to surgery, post-induction, immediately prior to CPB (0h) and at varying times following CPB initiation. Leukocytes were fixed and permeabilised prior to intracellular staining using PE-conjugated antibodies that recognise Ser529 phosphorylated RelA or with isotype-matched irrelevant antibodies as a control. Fluorescence of (A) granulocytes or (B) mononuclear cells was quantified by flow cytometry (after gating of cells by size and granularity). Fluorescence levels, calculated after subtracting values from isotype-control antibodies, were pooled and mean values ± SEM are shown. (*p<0.05; *** p<0.005 Wilcoxon matched-pairs signed rank test within-group).

4.4.6 Secondary outcomes

4.4.6.1 Leukocyte migration into skin blisters

Leukocyte migration into cantharidin-induced blisters was assessed by studying blister fluid which was sampled pre-operatively and at 5 h post-operatively. Representative images of blister fluid under light microscopy are shown in Figure 4.9 Cardiac surgery with CPB promoted leukocyte migration into skin blisters. An additional representative image from off-pump surgery without CPB is presented to set the context for coronary surgery in the absence of CPB support.

A 15 fold increase in PMN margination into blisters was observed post operatively in the mCPB group (mean 4.41 ± 4.28 × 10^5 cells/blister vs mean 65.50 ± 62.40 × 10^5 cells/blister, $p<0.05$ *Wilcoxon matched-pairs signed rank* test) and a 6 fold increase (mean 6.63 ± 6.87 × 10^5 cells/blister vs mean 41.33 ± 37.85 × 10^5 cells/blister, $p<0.005$ *Wilcoxon* test) in patients exposed to cCPB (Figure 4.9). There was no difference between groups on mixed regression analysis modelling: mean difference 0.6998 log units, 95% CI (-0.3449, 1.7445), $p = 0.173$ (Table 4.4). Mononuclear cell accumulation in blister fluid was also enhanced following surgery with CPB. The cCPB group there was 7 fold increase in mononuclear cell margination into tissues (mean 2.77 ± 2.29 × 10^5 cells/blister vs mean 19.38 ± 12.74 × 10^5 cells/blister, $p<0.005$ *Wilcoxon* test). In the mCPB a 13 fold increase in tissue margination was observed (mean 1.84 ± 0.76 × 10^5 cells/blister vs mean 23.61 ± 9.61 × 10^5 cells/blister, $p<0.05$ *Wilcoxon* test). However, there were no significant differences in leukocyte migration between the cCPB or mCPB groups. In keeping with the granulocyte margination data, there was no difference between groups on mixed regression analysis modelling: mean difference 0.3294 log units, 95% CI (-0.3926, 1.0514), $p = 0.342$ (Table 4.4).

These data demonstrate that surgery leads to leukocyte activation and tissue extravasation. However, this test did not discriminate between cCPB or mCPB technologies.

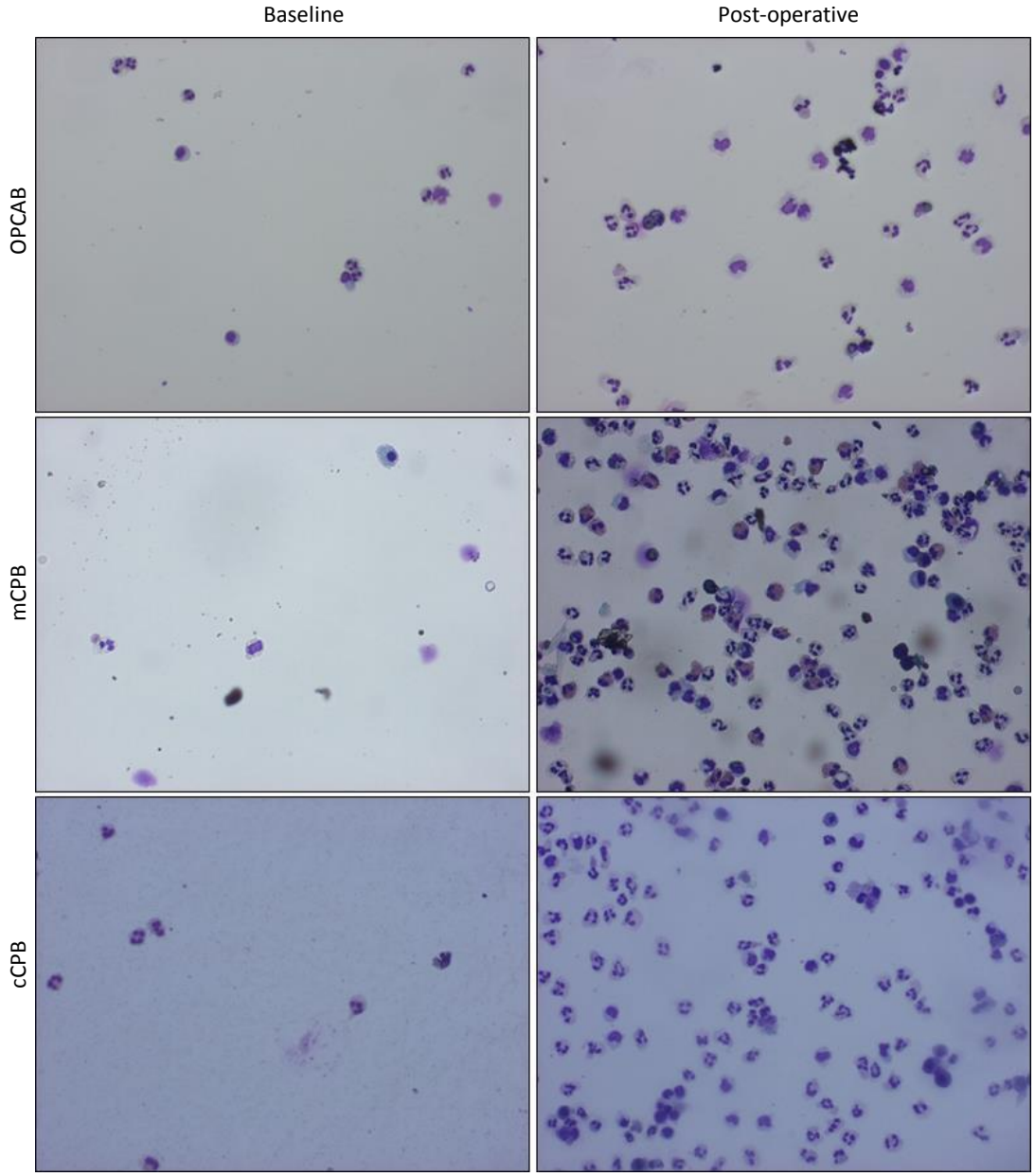

Figure 4.9 Cardiac surgery with CPB promoted leukocyte migration into skin blisters
CABG was performed with cCPB or mCPB. An additional Off-pump coronary revascularisation (OPCAB) patient was studied, independently of the randomised trial, to highlight the effect of coronary surgery, but without CPB support. Blister fluid samples were collected prior to surgery (Baseline) and at 5 h following CPB initiation (Post-CPB). Cells were collected, stained using Diffquick and visualised by microscopy. Representative images are shown.

4.4.6.2 Conventional clinical markers of inflammation

White cell counts and CRP were measured in all patients in peripheral blood. Two-way analysis of variance of peri-operative white cell counts revealed that the main effect of timing of measurements between baseline and on days 1 and 4 was significant, $F(2,48) = 12.04$, $p<0.0001$; but the modality of CPB use (whether conventional or miniaturised) did not account for any differences observed $F(1,24) = 0.0002$, $p = 0.99$. Post-hoc evaluation using the *Dunnett* multiple comparisons test showed a significant rise in white cell counts between baseline and day 1 (mean 7.5 ± 2.4 $\times 10^9$/L vs 10.2 ± 2.0 $\times 10^9$/L, $p<0.005$) returning to baseline levels on day 4, in the mCPB group. Similarly, in the cCPB group, surgery with CPB exposure resulted in significant rises in white cell counts from baseline to day 1 (mean 8.0 ± 1.7 $\times 10^9$/L vs 9.5 ± 2.4 $\times 10^9$/L, $p<0.05$), normalising by day 4 (Table 4.5).

When considering the influence of surgery and CPB on CRP levels, two-way analysis of variance revealed the main effect of timing of measurements between baseline and on days 1 and 4 was highly significant as expected, $F(2,48) = 72.66$, $p<0.0001$. However, the modality of CPB use (whether conventional or miniaturised) did not account for any differences observed between the mCPB and cCPB groups: $F(1,24) = 1.469$, $p = 0.24$. Post-hoc evaluation using the *Dunnett* multiple comparisons test showed rises in CRP between baseline and day 1 were not significant (mean 2.38 ± 2.28 mg/mL vs 48.39 ± 30.35 mg/mL, $p = 0.07$) but significant changes appeared on day 4 (baseline vs mean 162.44 ± 87.37 mg/mL, $p<0.0001$), in the mCPB group. Similarly, in the cCPB group, surgery with CPB exposure resulted in significant rises in CRP from baseline to day 1 (mean 3.00 ± 2.53 $\times 10^9$/L vs 55.52 ± 32.94 $\times 10^9$/L, $p<0.05$), and even more pronounced on day 4 (baseline vs mean 195.44 ± 84.12 $\times 10^9$/L, $p<0.0001$)(Table 4.5).

Together these data highlight the inflammatory nature of cardiac surgery with the use of CPB support but have little sensitivity in discriminating between mCPB or cCPB systems,

Time	White cell counts ($\times 10^9$/L)		CRP (mg/mL)	
	mCPB	cCPB	mCPB	cCPB
Baseline	7.5 ± 2.4	8.0 ± 1.7	2.38 ± 2.27	2.97 ± 2.54
Day 1	10.2 ± 2.0	9.5 ± 2.4	48.39 ± 30.35	55.52 ± 32.93
Day 4	8.9 ± 2.4	9.2 ± 2.2	162.44 ± 87.37	195.44 ± 84.12

Table 4.5 White cell counts and CRP are enhanced by surgery with CPB

CABG was performed with cCPB or mCPB. Peripheral blood samples were collected prior to surgery (Baseline) and at 1 or 4 days post-surgery. Samples were tested for numbers of white cells or CRP. Mean values ± SD are shown.

4.4.6.3 Plasma markers of organ dysfunction

In this study, we also monitored markers of renal dysfunction, cardiac injury and end-markers of blood loss. There were no significant changes in serum creatinine levels between pre- and post- operative time points in the mCPB group. A significant decline in measured creatinine levels occurred in the cCPB group between day 1 and day 4 post-CPB (mean 84.00 ± 28.78 μmol/L vs mean 118.31 ± 76.09 μmol/L, $p<0.05$, *Bonferroni* multiple comparisons test following two-way analysis of variance). Serum creatinine levels were significantly lower in the mCPB compared to the cCPB group (mean 75.62 ± 29.90 μmol/L vs mean 118.31 ± 76.09 μmol/L, $p<0.05$) on the 4th post-operative day (Table 4.6).

We also monitored markers of cardiac injury in the early phases (0 and 30 minutes) after the commencement of CPB. In view of the known reports suggesting that different markers appear at different time points during reperfusion, we measured two markers of injury; cardiac Troponin T (cTnT) and Creatine Kinase isoenzyme MB (CK-MB). cTnT is a cardio-specific and highly sensitive marker for myocardial damage. In studies using intermittent cross clamp fibrillation during CABG, it was shown that this biomarker peaks at 5-6 hours post-operatively[178,510]. CK-MB mass is used to determine cardiac injury post infarction. Significantly elevated levels of markers of myocardial injury were observed in blood within 30 min after institution of CPB (this period is likely to be associated with at least 2 grafts and two sessions of ischemia and reperfusion) irrespective of whether the biomarker was CK-MB or cTnT (Figure 4.104). Whilst total CK-MB levels were similar for both interventions (mean 3.5 ± 0.3 μg/ml vs. mean 3.3 ± 0.3μg/ml) total cTnT release was significantly lower in the mCPB group (mean 95.9 ± 14.4 μg/L vs. mean 58.8±7.6 μg/L, $p=0.02$). Area under the curve to estimate total protein for cTnT and CK-MB release during CPB was calculated using the trapezium rule. These findings are in keeping with the published literature on optimised bypass systems discussed in 1.6.2, page 76.

Blood transfusion requirement data are summarised in Table 4.3 and already discussed in section 4.4.4, page 162. To complement these data, levels of haemoglobin pre-operatively and on the 1st and 4th post-operative days are presented in Table 4.6. Two-way analysis of variance revealed the main effect of timing of measurements between baseline and on post-operative days to be significant, $F(2,48) = 64.72$, $p<0.0001$. The modality of CPB used during surgery in this parameter did not account for any differences observed: $F(1,24) = 0.4016$, $p = 0.53$. Post-hoc evaluation using the *Dunnett* multiple comparisons test showed falls in haemoglobin between baseline and day 1 (mean 13.4 ± 1.3 g/dL vs mean 9.6 ± 0.9 g/dL, $p<0.0001$) and day 4 (baseline vs 10.1 ± mean 0.9 g/dL, $p<0.0001$) were significant. Similarly, in the cCPB group, surgery with CPB exposure resulted in significant falls in haemoglobin count from baseline to day 1 (mean 13.3 ± 1.8 g/dL vs mean 10.1 ± 1.1 g/dL, $p<0.0001$) and day 4 (baseline vs mean 10.4 ± 1.6 g/dL, $p<0.0001$).

Together, these data support the conclusion that cardiac surgery results in significant blood loss, myocardial injury and derangement in serum markers of kidney function. Optimisation of cardiopulmonary bypass appears to confer a protective effect on biochemical markers of kidney function and is associated with a reduction in biochemical markers of myocardial injury.

Time	Haemoglobin (g/dL)		Creatinine (µmol/L)	
	mCPB	cCPB	mCPB	cCPB
Baseline	13.4 ± 1.3	13.3 ± 1.8	88.69 ± 22.58	97.39 ± 28.75
Day 1	9.6 ± 0.9	10.1 ± 1.1	70.39 ± 31.04	84.00 ± 28.78
Day 4	10.1 ± 0.9	10.4 ± 1.6	75.66 ± 29.90	118.31 ± 76.09

Table 4.6 Changes in haemoglobin and serum creatinine levels with CPB

CABG was performed with cCPB or mCPB. Peripheral blood samples were collected prior to surgery (Baseline) and at 1 or 4 days post-surgery. Samples were tested for haemoglobin count or serum creatinine levels. Mean values ± SD are shown.

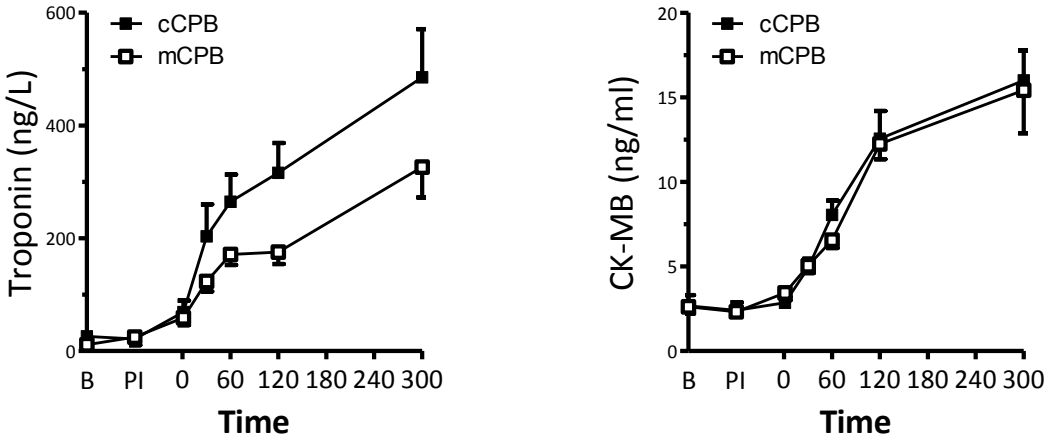

Figure 4.10 Myocardial injury markers are elevated with the use of CPB
Blood collections were made before surgery (on the morning of surgery and post intubation following anaesthesia) and immediately after starting CPB and then at 30, 60, 120 and 300 min after the initiation of CPB. Immunoassay for the in-vitro quantitative determination of both proteins was used (Roche Diagnostics GmbH).

4.4.6.4 Flow cytometry profiles during cardiopulmonary bypass

Representative flow cytometry histogram profiles from experiments are shown in Figure 4.11 of cells for ROS, p38 MAP kinase and p65 NF-κB analysis. There was a shift in the entire population for each leukocyte subset of interest at different timepoints in the surgical process.

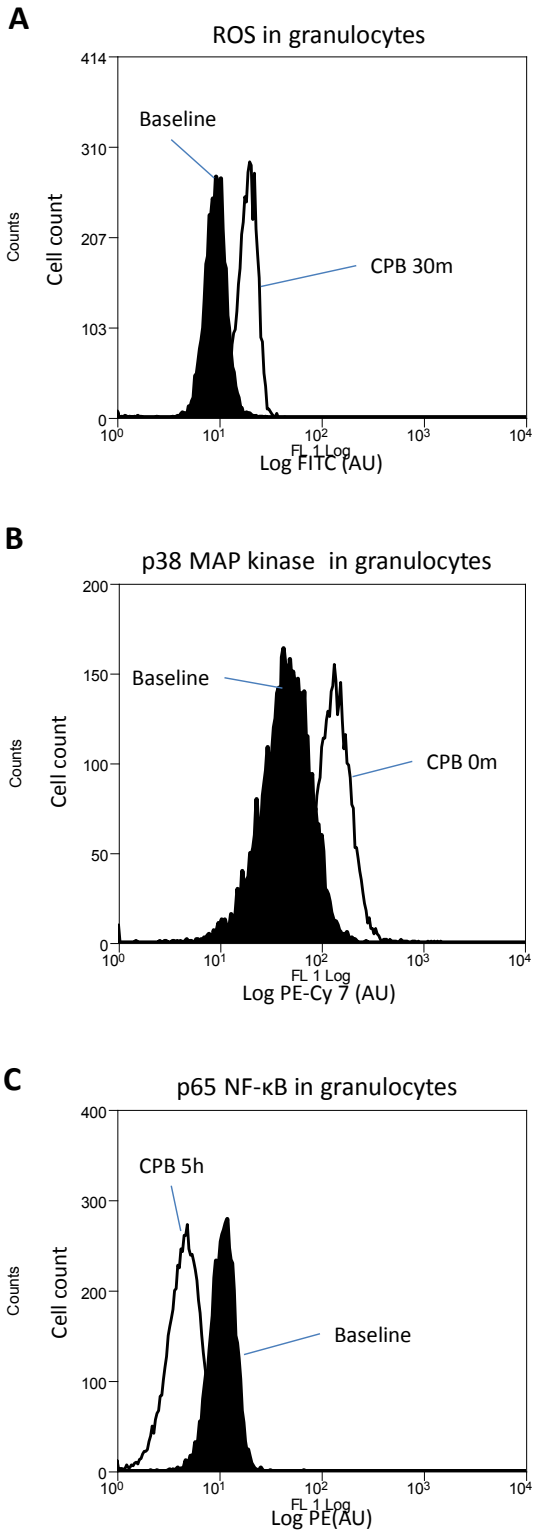

Figure 4.11 Representative flow cytometry profiles for ROS, p38 MAP kinase and p65 NF-κB

Blood was sampled at various timepoints (indicated) in patients undergoing coronary surgery with CPB. Samples were (A) loaded with APF to detect ROS or alternatively fixed and permeabilised prior to staining with antibodies for (B) p38 MAP kinase or (C) p65 NF-κB phosphorylation, followed by analysis by flow cytometry.

4.4.7 Adverse events

No adverse events occurred as a direct result of exposure to CPB. One patient in the mCPB group developed a pulmonary embolus in the post-operative period, requiring admission to the intensive care unit and prolonged ventilatory support until eventual recovery and successful discharge from hospital. Three patients in the cCPB group developed post-operative wound-related infections and were treated with long-term antibiotics. There were no clinically evident wound-related infections in the mCPB group. One patient in the cCPB group required renal support therapy in the post-operative period. No patients required return to theatre for adverse peri-operative events. All participants in the study were ultimately discharged home.

4.5 CONCLUSIONS

Comparison of inflammatory signalling between cCPB and mCPB groups revealed the following differences:

1. ROS induction occurred following surgical trauma prior to the initiation of CPB and peaked at approximately 30 minutes into the CPB run. ROS-signalling events were similar in the mCPB and cCPB groups for granulocytes, the predominant cell populations involved in the early phases of inflammation. In the lymphocyte cell fraction, ROS activation was significantly higher in the cCPB group at the 30 minute time point following the initiation of CPB, compared to mCPB.

2. Activation by phosphorylation of p38 MAP kinase occurred following surgical access and initiation of CPB. Levels of p38 MAP kinase activity were significantly higher in the cCPB group compared to the mCPB group following the end of the bypass run. Attenuation of p38 MAP kinase levels was more pronounced in the mCPB group.

3. NF-κB phosphorylation did not appear to be significantly influenced by surgery or CPB, with attenuation of levels of phosphorylation of p65 at the later time points in the study in both groups.

4. Surgery and exposure to CPB was associated with accumulation of leukocytes in tissue. However, despite the different characteristics of p38 MAP kinase and ROS activation, there were no statistically significant differences in leukocyte migration into cantharidin blisters between either the two groups.

5. Correspondingly, there were similar rises in inflammatory markers (CRP, WCC) at late timepoints in keeping with the intensely inflammatory nature of surgery.

6. Serum creatinine was significantly higher in the cCPB group than compared to the mCPB group on the 4th post-operative day following surgery.

7. Troponin release was reduced in the mCPB group compared to the cCPB group

Together, these data show for the first time that surgical access and CPB *per se* influences inflammatory signalling pathways.

4.6 DISCUSSION

4.6.1 Molecular mechanisms and surgical factors influencing the systemic inflammatory response

This study has assessed the intracellular signalling pathways that promote systemic inflammation in patients undergoing CABG with CPB. Specifically, cardiac surgery leads to the activation by phosphorylation of p38 MAP kinase, in circulating leukocytes and induction of ROS. In addition, induction of ROS and activation of p38 MAP kinase occurred *prior to* the commencement of CPB. This is an important observation because it suggests that factors associated with early surgical procedures (i.e. up to the point of cannulation of the great vessels) are sufficient to trigger pro-inflammatory pathways within leukocytes in patients undergoing cardiac surgery for coronary revascularisation. This process is likely to involve the release of DAMPs into the circulation[207,511]. Further work is required to define the specific DAMPs that promote systemic inflammation in response to cardiac surgery. Although cardiac surgery with cCPB induced ROS and activated p38 MAP kinase in leukocytes, this process did not activate NF-κB via phosphorylation at Ser 529. It is plausible that cardiac surgery activates NF-κB through other mechanisms, or at other phosphorylation sites, and further studies should be carried out to assess this. Alternatively, systemic inflammatory responses following cardiac surgery with CPB may be governed primarily by p38 MAP kinase signalling in the absence of NF-κB activation, at least in circulating leukocytes prior to their migration into tissues. The corollary is that p38 MAP kinase activation in granulocytes may be an important initiator of systemic inflammation and end-organ damage in patients exposed to cCPB. This has obvious implications for the development of therapeutic strategies to target pro-inflammatory signalling pathways in patients undergoing cardiac surgery with CPB.

4.6.2 Timing of blood sampling in clinical studies

The precise timing of sampling of blood during the clinical study was considered with great care. Firstly, the over-arching aim of the study was to define the precise effects of CPB *distinct* from surgery and other aspects of the surgical process (such as weaning off support, protamine reversal etc.). Therefore, all timings were conducted with reference to the initiation of CPB as our starting hypothesis was that CPB is the index initiating event of pro-inflammatory activation.

This central consideration informed the basis for the timings in the original preliminary ROS experiments. In these early ROS experiments, a relatively late (24 hour) time point was studied. This was of interest to determine if there are late ROS signalling events, and afforded the opportunity to evaluate the potential phenomenon of leukocyte priming. However, it is important to also consider the effect of other interventions and events that occur at the 24 hour time point that are inherently different to those of earlier periods. Namely, the patient has usually been recovered on ITU: mechanical ventilatory support has been weaned; the patient has been recovered from anaesthesia and been extubated. During this period, there are varying levels of inotropic drugs used for support as well as a variable amount of blood transfusion. Patients will have gone from a physiological state of starvation and stress and potential catabolism, in preparation for surgery, to the limited re-introduction of food whilst recovering. Additionally, the introduction of some drugs (routinely aspirin, diuretics, b-blockers, laxatives) will have commenced. Together, these events and interventions complicate the interpretation of the results, particularly those of a marker considered to be rapidly changing and short-lived. It appears that a priming phenomenon may occur in the data presented. However, an alternative interpretation of the data is that these post-operative events (of drugs, transfusion, recovery) actually trigger the enhanced ROS response to ex-vivo stress and no such priming actually is taking place. For these confounding reasons, the later time point of 24 hours post CPB was not evaluated in patients

in the clinical trial. It is also difficult to relate the changes observed at late timepoints back to the earlier period of CPB exposure and be confident about causality.

In the subsequent experiments, a 5 hour time point was selected as this coincided with the blister assays. This facilitated comparisons between ROS, p38 MAP kinase and p65 NF-κB changes within leukocytes in the circulation, and numbers of marginated (and therefore presumably activated) leukocytes within the tissue compartments.

Shorter intervals between blood sampling were also considered, and indeed sampling was carried out at 15 minute intervals in the preliminary p38 MAP kinase and p65 NF-κB experiments in patient pilot studies. This afforded the generation of valuable detailed information regarding the kinetics of activation. However, the data did not reveal more meaningful changes than the 30 minute intervals settled upon in the final randomised clinical study. An additional point to note is that having shorter (15 minute) intervals between blood sampling was not compatible with shorter interval ROS assays that were planned to run in parallel. There is a very practical reason for this as sampling patient blood and performing the assays occurs by the bedside. However, the specimens need to be transported back to the lab, and processed in time to return for the next assay. The shortest practical interval to achieve this was 30 minutes.

Consideration was given to timing of blood sampling to occur after the termination of bypass or after protamine reversal. However, these proposed timepoints are variable and cannot be precisely controlled in these experiments (because experimentally we have no control over the duration of the operation). The number of coronary artery grafts determines the duration of the cross clamp time which in turn determines the duration of CPB. The inherent variation in these aspects of the operation makes interpretation of data difficult, particularly in trying to understand the kinetic profiles of activation, as the design of these experiments was targeted to address. Re-analysis of the existing data in this context with respect to the pro-

inflammatory markers is not meaningful given the timing of measurements have no relation to CPB duration or cross clamp time. In an alternative experimental design, measuring the levels of ROS, p38 MAP kinase and NF-κB *at the end of CPB* (or alternative timepoints) could yield some mechanistic insight. However, the activation profile that emerges from the studies presented here suggests that CPB is not the initiating event but instead a modulatory phenomenon in the inflammatory cascade. This is exemplified by the fact that OPCAB surgery can result in SIRS manifestations, despite there being no cardiopulmonary bypass at all[174,512].

4.6.3 Molecular probe selection in the detection of ROS

The ROS dyes presented in these studies have a differing spectrum of sensitivity and specificity for particular subtypes of ROS. A summary of experimental data of ROS-spectrum reactivity for the molecular probes is indicated in Table 2.3 (page 106). The DCF dye is particularly sensitive at detecting •OH and ONOO- ROS species whereas the APF dye is highly sensitive for –OCl species as well as •OH events. The differences observed in the pilot studies in patients may be reflective of this difference in ROS-spectrum sensitivity. As well as this, the induction of ROS in the presence of the same phorbol ester stimulus was far greater in the APF group, nearing the detection thresholds of flow cytometry. Importantly, the level of auto-oxidation of APF is significantly less than the level of auto-oxidation in DCF, and this may account for the apparently higher levels basal ROS seen with DCF in unstimulated conditions (mean 333 ± 235 FITC MFI units in DCF compared to 36.4 ± 16.1 FITC MFI units in APF studies). For the reasons of neutrophil hypochlorite radical specificity, of importance in inflammation, inducible-ROS sensitivity, negligible auto-oxidation and technical ease of handling, APF was selected as the ROS probe of choice in the randomised clinical trial (and the large animal study presented in Chapter 5).

4.6.4 Comparisons within and between experimental data

Selected summary data for ROS, p38 MAP kinase and p65 NF-κB levels are presented in Table 4.7, to facilitate comparison between the studies presented in this chapter and those presented in Chapter 3. No formal statistical inferences were made between these data as this was not the purpose or design of the original experiments.

The lowest levels of basal APF-spectrum, constitutive, ROS were observed in the patients in the randomised trial, even lower than those of healthy volunteers, with the highest levels in the pilot data group. This pattern is also observed for the DCF-spectrum ROS (not measured in the randomised trial) that shows higher levels in clinical pilot data compared to controls. This may be a function of the differences in medical treatment between the three groups being considered. The common cardiovascular preventative medications (aspirin[513-515], statins[414,516], ACE-inhibition[517], beta receptor blockade[518]) for ischaemic heart disease all possess anti-oxidant properties. Therefore, the implication of long term treatment with these medications (in the run up to surgery) will alter the basal levels of ROS. The nature of coronary artery disease for the randomised trial and other heart diseases (in the case of patients in the pilot clinical study, valvular pathology) is different with variation in pharmacological management. These differences may therefore be an important consideration for the variation observed between the clinical pilot data and the formal trial data. In addition to the basal levels observed, the pilot clinical data demonstrates an enhanced effect of CPB on both DCF-spectrum and APF-spectrum ROS. In particular, the effects are more enhanced in the monocyte and lymphocyte fractions, as a proportion, implying a redox-sensitive mechanism for leukocyte priming and activation, where the effects are most marked at later timepoints after CPB exposure. This may also reflect a priming effect of CPB in the context of an already enhanced basal level of ROS.

Considering the profiles for phosphorylated p38 MAP kinase between experiments, this marker was lowest in samples from healthy volunteers and progressively increases with the

population of patients undergoing CABG in the randomised trial to a peak in the pilot series of patients who underwent more complex surgery (valve, combined surgery). This concurs with the assertion of enhanced basal levels of pro-inflammatory markers with increased disease complexity and morbidity described in the literature[349,416,426]. The pilot data is in agreement with the randomised trial in demonstrating that p38 MAP kinase is induced with surgery, but also *prior* to CPB exposure, and the pattern of attenuation also occurs at 2 hours. These observations imply some other additional molecular trigger (which includes DAMPs) may be the driver for the inflammatory response and CPB has a differentially modulatory effect. The size of the p38 MAP kinase signalling changes are greatest with the pilot study group whereas the randomised data and volunteer data share similar degrees of response to stimuli / changes. This implies that experimental models for p38 MAP kinase activation may replicate the stress conditions for coronary surgery, whereas more potent stimuli are required to reproduce the stress conditions for valve, or more complex surgery conditions in future studies.

Levels of phosphorylated forms of NF-κB activity tended to be higher in both the pilot and the randomised clinical studies compared to those in the blood from healthy volunteers. It is possible that activated forms of p65 NF-κB are already 'high' at the basal time point in patients, prior to surgery, because of existing co-morbidities and physiological stress. For example, as angina and heart failure are known to enhance NF-κB in myocardium and leukocytes[241,519-521] whereas basal NF-κB is 'low' in healthy volunteers. Alternatively, age is an important factor influencing these manifestations as the disease process for atherosclerosis is one of chronic inflammation, NF-κB is at the hub of inflammatory ageing networks[522]. Blood in the clinical trials came from patients who were in their late 60s whereas the blood from volunteers was obtained from young adults in their mid-20s - early 30s. Another contrasting observation is the reactivity of leukocytes between groups. Both the pilot clinical data and the data from the randomised trial show an overall downtrend in the levels of phosphorylated forms of p65 NF-κB. However, experimentally, we have seen that TNFα

phosphorylation of p65 NF-κB, in healthy volunteer blood to levels that far exceed those seen in the randomised trial. One explanation is that chronic NF-κB activation in leukocytes of patients with cardiovascular diseases could lead to induction of negative regulations (e.g. IκBα, A20) that dampen subsequent NF-κB responses to inflammatory stimuli.

	Validation data in Chapter 3 (healthy controls)	Pilot Clinical data (patients)	Randomised Clinical trial data (patients)
ROS	DCF Basal G: 213.2 ± 266.6 M: 146.5 ± 115.8 L: 134.5 ± 109.1 DCF Peak G: 572.0 ± 136,6 (+PMA) M: 455.0 ± 105.5 (+PMA) L: 134.5.0 ± 109.1 (+PMA) APF Basal G: 40.31 ± 5.27 M: 39.23 ± 7.50 L: 12.79 ± 1.35 APF Peak G: 7056 ± 1301 (+PMA) M: 2542 ± 1045 (+PMA) L: 156 ± 68 (+PMA)	DCF Basal G: 333 ± 235 M: 378 ± 489 L: 253 ± 294 DCF Peak G: 3683 ± 2110 (CPB 0 + PMA) M: 3139 ± 2851 (CPB 0 +PMA) L: 1108 ± 797 (CPB 30 + PMA) APF Basal G: 54.1 ± 33.8 M: 47.1 ± 42.8 L: 10.07 ± 5.12 APF Peak G: 8041 ± 1550 (CPB 0 + PMA) M: 4494 ± 757 (CPB 24 + PMA) L: 716 ± 340 (CPB 24 + PMA)	DCF Basal (no data) APF Basal G: 12.88 ± 4.69 M: 9.56 ± 3.50 L: 3.86 ± 1.18 APF Peak G: 17.20 ± 7.68 (CPB 30m) M: 15.51 ± 9.86 (CPB 30m) L: 5.78 ± 3.44 (CPB 30m)
p38 MAP kinase	Basal G: 57.2 ± 33.1 M: 1.9 ± 1.2 Peak G: 194.9 ± 79.25 (PMA) M:15.83 ± 5.40 (Arsenite)	Basal G: 347.7 ± 171.1 M: 14.2 ± 3.4 Peak G: 557.9 ± 221.2 (Start CPB) M: 30.13 ± 24.4 (Start of CPB)	Basal G: 118. 4 ± 77.3 M: 12.2 ± 13.9 Peak G: 135.984 (Start of CPB) M: 14.48 (CPB 300)
p65 NF-κB	Basal G: 2.46 ± 0.35 M: 2.01 ± 1.23 Peak G: 8.32 ± 1.11 (Arsenite) M: 36.15 ± 3.76 (Arsenite)	Basal G: 4.41 ± 2.37 M: 1.14 ± 0.43 Peak G: 10.28 ± 2.88 (CPB 2h) M: 3.70 ± 1.47 (CPB 2h)	Basal G: 2.99 ± 1.09 M: 1.57 ± 1.53 Peak B: 3.47 ± 1.78 (PI) M: 1.57 ± 1.53 (Baseline)

Table 4.7 Comparative levels of ROS, p38 MAP kinase an NF-κB between experiments
Summary data was extracted from previous experiments and populated into this table. Data for granulocytes (G), monocytes (M) or lymphocytes (L) is presented for ROS. Data for granulocytes (G) and mononuclear cells (M) is presented for human studies of p38 MAP kinase or p65 NF-κB. Selected peak and basal levels are presented, in the respective MFI arbitrary units ± SD.

4.6.5 The effects of CPB miniaturisation on leukocyte activation and inflammation

A majority of the studies investigating mCPB have used the early generation Minimized Extracorporeal Circulation (MECC) system manufactured by Jostra (Hirrlingen, Germany). The Hammersmith Unit has developed significant experience with the latest generation of mCPB systems, the ECCO circuit, which has proven to be safe and standardized[404,405,435]. Over 3 years, more than 600 patients have safely undergone cardiac surgery using the mCPB technique without any CPB-related adverse events. In a small retrospective study, blood transfusion requirements fell by 56% compared to cCPB[523]. The ECCO mCPB system is a significant advance over previous technology because it includes a venous air removal device, whereas earlier mCPB systems carried the risk of air entering the circuit and air embolism. The ECCO circuit also requires significantly less priming volume and, therefore, would be expected to further reduce local haemodilution and reduce blood/non-endothelial surface contact. In addition, the ECCO system also has a tip to tip biocompatible coating using phosphorylcholine, which may attenuate the inflammatory response.

Previous studies demonstrated that mCPB reduces blood loss and transfusion requirements[443,452] and attenuates renal, myocardial and intestinal injury compared to cCPB. The beneficial effects of mCPB have been attributed to reduced inflammation since miniaturization of CPB lessens cytokine release and neutrophil activation in patients undergoing cardiac surgery[114,402,403]. Here the effects of cCPB and mCPB on ROS, p38 MAP kinase and NF-κB signalling molecules were compared. p38 MAP kinase activation in granulocytes was significantly reduced in patients exposed to mCPB compared to cCPB. By contrast, p38 MAP kinase activation in mononuclear cells, ROS induction and NF-κB activity in both granulocytes and mononuclear cells was similar between both groups. These data support the conclusion that miniaturisation of CPB had a highly specific inhibitory effect on p38 MAP kinase activation in granulocytes. The observation that surgery with CPB promoted migration of leukocytes into cantharidin blisters confirms a previous finding[195]. Of

note, mCPB and cCPB were associated with comparable numbers of leukocytes migrating into blisters and equivalent numbers of circulating white blood cells. Collectively, these studies suggests that the activation status of granulocytes (assessed by measuring p38 MAP kinase phosphorylation) correlates more tightly with systemic inflammation and renal injury than measures of leukocyte numbers. Thus, measuring p38 MAP kinase activation status in granulocytes could provide a useful clinical diagnostic for the prediction of systemic inflammation and tissue injury in patients undergoing cardiac surgery.

4.6.6 Limitations and considerations

This RCT was conducted to assess the pro-inflammatory signalling profile in the leukocytes of patients exposed to CPB extracorporeal circulation circuits. Participants were randomly allocated to either mCPB or cCPB and were not aware of their allocation. The operating staff were not blinded to allocations which, in theory, may have introduced unconscious performance bias. However, aortic cross-clamp and total CPB exposure times for both cCPB and mCPB were equivalent suggesting that surgical performance was similar in both randomised groups. Moreover, the randomised trial was designed around the operative practices of a single surgeon to eliminate variation in practice between different surgeons. Observers were not blinded as sampling was done undertaken directly from the patient during surgery.

Another limitation is that we studied only a few of the myriad of factors that are activated in leukocytes in response to inflammatory signals. For example, measuring TLR-receptor up-regulation for the detection of DAMPs events; evaluating up-regulation of adhesion molecules cell surface markers; determining the activation of protective cellular pathways would give weight to the mechanistic insights required to understand the precise effects of CPB on inflammation. Although these have been undertaken in isolated forms, there has not yet been one single unifying study with all of these considerations. One approach to capture

some of this information at a broad level would be to assess leukocyte transcriptomes (e.g. using RNA sequencing) in patients undergoing surgery. The studies presented also only consider leukocyte activation in isolation. We understand the importance of endothelial cell activation, platelet activation and leukocyte-leukocyte interactions. However, this is particularly difficult to study in vivo, particularly in humans.

This trial was powered on leukocyte activation endpoints and the sample size was relatively small. The study was underpowered for clinical observations, thus conclusions could not be drawn on the relative effects of cCPB or mCPB on end organ injury. Consequently, no formal assessment of organ dysfunction was made. With hindsight, it may have been less than optimal to base the target sample size on cell counts rather than the primary outcomes, in particular choosing such a large target difference (1.5 standard deviations, even though this was based on pilot data). Using the relevant correlations observed in the trial, we can now know that the trial was only able to detect a relatively large standardised difference in ROS levels in granulocytes (about 0.85 standard deviations) with 90% power and a 2-tailed significance level of 0.05.

Miniaturised bypass is designed to attenuate the post-operative inflammatory response in patients undergoing cardiac surgery. Studies, including this one, have been targeted at patients without significant co-morbidities and an ethical consideration always needs to be made when new technology is involved. A criticism is that the patients are low-risk and may not be the best population to benefit from the protective effects of miniaturised bypass. There is no literature on the use of miniaturised cardiopulmonary in complex surgical scenarios and prolonged bypass, and these groups of patients may be considered for future research.

Although the current study has generated useful information, it is complicated by variation in patient demographics, pathophysiology of the primary disease, medical co-morbidities and inherent polypharmacy. Variation also arose operatively in the total duration of surgery and

exposure to CPB, reflecting primarily the number of coronary artery targets that required revascularisation. To minimize these sources of variation, a large animal model of CPB was established in which healthy adult female pigs of, similar age, were exposed to CPB for a uniform duration. This study allowed assessment of the kinetics of leukocyte activation in response to CPB under well-controlled experimental conditions, presented in the next chapter.

CHAPTER 5. INFLAMMATORY SIGNALLING MODULATION BY SULFORAPHANE

5.1 INTRODUCTION

In the preceding chapter, modulation of the inflammatory response to surgery was investigated. Technological optimisations of cardiopulmonary bypass systems were evaluated using the Sorin ECCO system in the context of coronary artery revascularisation. With this approach, alterations in ROS induction and p38 MAP kinase activation were observed in leukocytes from patients. Given that inflammation in response to cardiac surgery with CPB can be induced by a predictable and controlled stimulus (ie. the surgical access and cardiopulmonary bypass organ support itself), it may be possible to prevent or reduce inflammation by pretreatment with an anti-inflammatory compound. Here the potential anti-inflammatory effects of sulforaphane were investigated. The work that is described in this chapter deals with the use of sulforaphane, in a number of differing forms and modalities of delivery, as a means to influence the inflammatory signalling events within leukocytes.

In the preliminary studies, detailed in the first parts of this chapter, ex-vivo experiments using whole blood sampled from healthy human volunteers with the use of purified sulforaphane were conducted. This was done to evaluate the effects on leukocyte activation in the context of a variety of experimental chemical stressors. Next, the hypothesis of whether pre-treatment using sulforaphane would reduce inflammation and tissue injury in response to CPB was investigated. Using a large animal model of conventional CPB, the influence of sulforaphane on leukocyte activity after exposure to the effects of extracorporeal circulation was determined. Finally, the hypothesis of whether dietary consumption of sulforaphane-rich preparations would lead to suppressed leukocyte activity was examined in healthy human volunteers.

5.2 HYPOTHESIS

The hypotheses tested in this chapter were:

1. Sulforaphane pre-treatment leads to attenuation of intracellular ROS induction, phosphorylated p38 MAP kinase or phosphorylated NF-κB in leukocyte populations following experimental stress.

2. Cardiopulmonary bypass leads to the rapid induction of reactive oxygen species in porcine leukocytes in association with early activation of pro-inflammatory signalling (e.g. p38 MAP kinase and NF-κB activation) and up-regulation of pro-inflammatory transcripts in tissues leading to end-organ injury.

3. Intravenous administration of sulforaphane 1h prior to cardiopulmonary bypass leads to biologically significant levels of sulforaphane in the plasma during the entire period of exposure to extracorporeal circulation in large animals.

4. Pre-treatment of large animals prior to exposure to cardiopulmonary bypass protects against pro-inflammatory signalling and attenuation of tissue injury.

5. Administration of the pre-cursor dietary form of sulforaphane attenuates leukocyte activation in human subjects.

5.3 RESULTS

5.3.1 Influence of sulforaphane pre-treatment on ROS signalling in leukocytes

The influence of sulforaphane on leukocyte activation was initially studied using peripheral blood samples from healthy human volunteers. ROS activation was studied using the APF dye due to its relative selectivity for neutrophil-related ROS events (as show in previous chapters) and relative affinity for hypochlorite events. Firstly, blood samples were pre-treated with purified sulforaphane (1μM or 10μM) or DMSO vehicle control for 1 hour. Samples were then loaded with the APF dye for 30 minutes prior to the application of TNFα (20μg/ml) or PMA (200ng/ml) for 30 minutes. Flow cytometry of cells loaded with APF revealed that ROS were induced by PMA treatment in granulocytes (baseline mean 53.0 ± 31.52 FITC MFI units vs mean 4133 ± 984 FITC MFI units, $p<0.0001$), monocytes (baseline mean 84.3 ± 38.9 FITC MFI units vs mean 673 ± 286 FITC MFI units, $p = 0.15$) and lymphocytes (baseline mean 4.1 ± 0.30 FITC MFI units vs 17.1 ± 7.5 FITC MFI units, $p<0.001$)(Figure 5.15A-C, compare 7-9 with 1-3). By contrast, TNFα did not enhance ROS levels in granulocytes (baseline mean 53.0 ± 31.5 FITC MFI units vs 329.1 ± 130 FITC MFI units), monocytes or lymphocyte subpopulations significantly (Figure 5.15A-C; compare 4-6 with 1-3). Pre-treatment of human leukocytes using sulforaphane suppressed the induction of ROS by PMA predominantly in the lymphocyte population at both 1μM (mean 11.8 FITC MFI units, $p<0.05$) and 10μM (mean 9.4 FITC MFI units, $p<0.01$) concentrations (Figure 5.15C; compare 8,9 with 7). Similar trends are observed in both the granulocyte and monocyte groups but these differences were not significant. However, there were no effects with sulforaphane pre-treatment in the TNFα-treated leukocytes. Statistical inference was undertaken using two-way analysis of variance considering the effect of stimulus and the effect of sulforaphane pre-treatment. Comparisons were performed using Bonferroni correction for multiple tests when effects were shown to be significant.

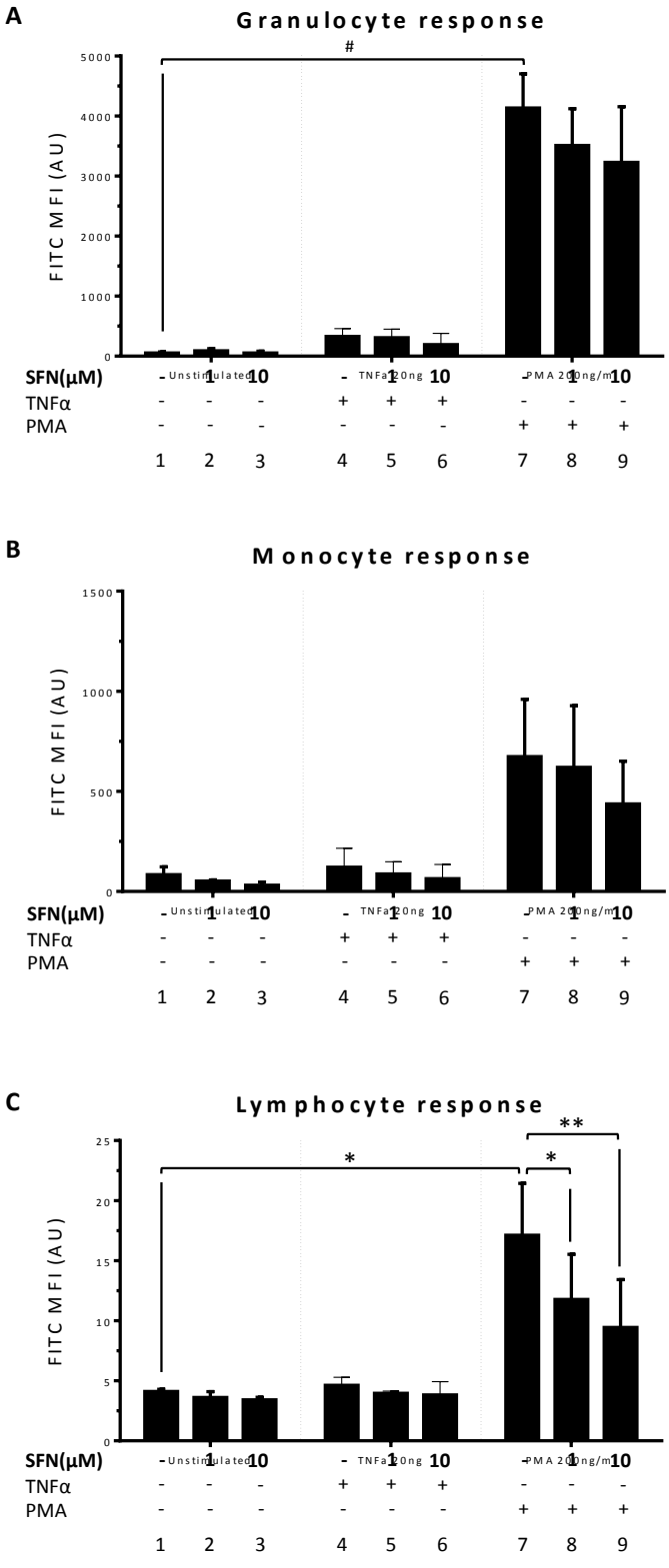

Figure 5.1 ROS induction in human leukocytes was attenuated by sulforaphane
Whole blood from healthy volunteers (n=3) was pre-incubated with sulforaphane for 1 hour and then loaded with APF ROS probe for 30 minutes prior to treatment with PMA (200ng/ml) or TNFα (20μg/ml) for 30 minutes. Samples were then processed and ROS levels were assessed by flow cytometry. Data were pooled and presented as means ± SEM (*p<0.05; **p<0.01; #p<0.0001, Bonferroni multi comparisons test).

5.3.2 Effect of sulforaphane pre-treatment on p38 MAP kinase and NF-κB phosphorylation in leukocytes

Given the effects of sulforaphane on ROS, we proceeded to evaluate the effects on the other pro-inflammatory markers. The effects of sulforaphane pre-treatment on p38 MAP kinase and NF-κB activation were determined by intracellular staining for phosphorylated forms of these molecules followed by flow cytometry, with human blood pre-incubated with sulforaphane at 1-5μM concentrations of sulforaphane (or DMSO control) prior to TNFα (20ng/ml) for 30 minutes.

Basal levels of phosphorylated in p38 MAP kinase in granulocytes were measured at 13.42 ± 14.52 PE-Cy7 MFI units. Following stimulation with TNFα, levels were measured at 33.38 ± 34.59 PE-Cy7 MFI units and with sulforaphane pre-treatment at 5μM were measured as 19.92 ± 12.74 PE-Cy7 MFI units. On an individual basis, the stimulus and pre-treatment effect appear clear, but on combined group statistical analysis, the data do not reach significance at the 0.05 α level, given the degree of variation, as evidenced by the standard deviations (Figure 5.2A). The trends are similar in the mononuclear cell fraction, but no statistically significant biological effect from stimulation nor pre-treatment is evident (Figure 5.2B). In assessing the effect of sulforaphane on NF-κB signalling, two-way analysis of variance showed a significant effect of pre-treatment; $F(2,12) = 8.266$, $p<0.01$, but not of stimulus. At baseline, phosphorylated p65 NF-κB levels were 5.26 ± 4.24 PE MFI units. The levels following TNFα stress (mean 8.53 ± 4.70 PE MFI units) were significantly reduced with sulforaphane pre-treatment at 1μM (mean 5.29 ± 2.99 PE MFI units, $p<0.01$) and 5μM (mean 5.75 ± 2.76 PE MFI units, $p<0.05$) concentrations (Figure 5.2C). The effects in mononuclear cells follow a similar trend but did not reach statistical significance (Figure 5.2D).

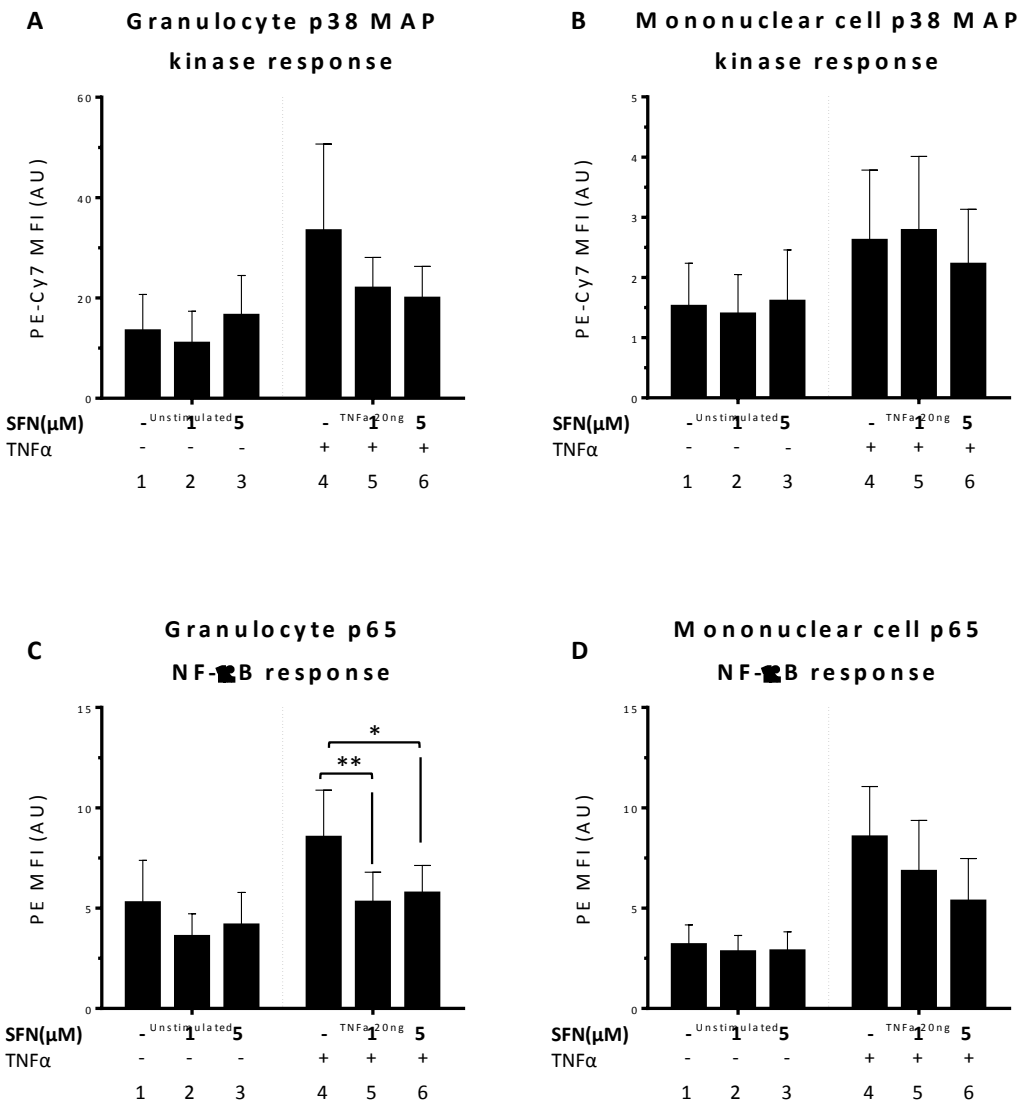

Figure 5.2 Sulforaphane pre-treatment suppressed NF-κB activation in response to TNFα
Whole blood from healthy volunteers (n=4) was pre-incubated with varying concentrations of sulforaphane for 1 hour prior to experimental stress with TNFα for 30 minutes. Samples were then fixed and permeabilised prior to intracellular staining for phosphorylated p38 MAP kinase (A and B) or p65/RelA (C and D) followed by flow cytometry. Mean fluorescence intensity values were pooled and presented as means ± SEM. (*p<0.05; **p<0.01, Bonferroni multi-comparisons test).

5.3.3 Antibody validation in porcine leukocytes

Prior to in vivo studies using pigs, antibodies that target phosphorylated p38 MAP kinase or phosphorylated NF-κB (RelA/p65 subunit) in human cells were validated for use in porcine tissues. Comparison of porcine and human protein sequences demonstrated a high degree of homology in protein sequences for p38 MAP kinase (Figure 5.3) and for p65/RelA NF-κB subunits with conservation at the phospho- acceptor sites of interest. This is particularly important because peptides corresponding to these regions were used to generate antibodies that recognise phosphorylated p38 MAP kinase or phosphorylated p65 NF-κB. Sequential analysis demonstrated 96% similarity between the human and porcine p38 MAP kinase protein sequence. Similarly, p65 protein sequences showed 93% similarity between species. Moreover, staining of porcine leukocytes obtained from animals under sedation using anti phospho p38 MAP kinase antibodies was elevated by TNFα treatment (101.2 ± 25.3 PE-Cy7 MFI units vs 172.3 ± 15.0 PE-Cy7 MFI units in granulocytes and 4.1 ± 8.7 PE-Cy7 MFI units vs 8.7 ± 1.9 PE-Cy7 MFI units in mononuclear cells)(Figure 5.5A). Similarly, staining of leukocytes with anti phospho-p65 antibodies was elevated by TNFα treatment (1.01 ± 0.1 PE MFI units vs 5.6 ± 0.6 PE MFI units in granulocytes and 1.22 ± 0.2 PE MFI units vs 7.0 ± 1.5 PE MFI units in the mononuclear cell fraction)(Figure 5.5B). These data suggest these antibodies recognise modified p38 MAP kinase and NF-κB in porcine cells. Representative forward and side scatter profiles from flow cytometry corresponding to porcine leukocyte size and granularity are shown in Figure 5.5C and D. Unlike in humans, there was no discernible monocyte middle cell population in normal unpermeabilised cells (Figure 5.5C). Permeabilisation appeared to have affected forward and side scatter profiles in porcine leukocytes in keeping with observations seen in human cells (Figure 5.5D). For experimental purposes, the cell population with enhanced side scatter were labelled as granulocytes, and the low-granular side scatter population were by default labelled as mononuclear cells.

```
Porcine         1 MSQERPTFYRQELNKTIWEVPERYQNLSPVGSGAYGSVCSAFDTKTGLRVAVKKLSRPFQ
Human           1 MSQERPTFYRQELNKTIWEVPERYQNLSPVGSGAYGSVCAAFDTKTGLRVAVKKLSRPFQ
                  ************************************ ********************

Porcine        61 SIIHAKRTYRELRLLKHMKHENVIGLLDVFTPARSLEEFSDVYLVTHLMGADLNNIVKCQ
Human          61 SIIHAKRTYRELRLLKHMKHENVIGLLDVFTPARSLEEFNDVYLVTHLMGADLNNIVKCQ
                  ************************************ ********************

Porcine       121 KLTDDHVQFLIYQILRGLKYIHSADIIHRDLKPSNLAVNEDCELKILDFGLARHTDDEMT
Human         121 KLTDDHVQFLIYQILRGLKYIHSADIIHRDLKPSNLAVNEDCELKILDFGLARHTDDEMT
                  ************************************************************

Porcine       181 GYVATRWYRAPEIMLNWMHYNQTVDIWSVGCIMAELLTGRTLFPGTDHINQLQQIMRLTG
Human         181 GYVATRWYRAPEIMLNWMHYNQTVDIWSVGCIMAELLTGRTLFPGTDHIDQLKLILRLVG
                  ********************************************** **  * ** *

Porcine       241 TPPAYLINRMPSHEARNYIQSLTQMPKMNFANVFIGANPLAVDLLEKMLVLDSDKRITAA
Human         241 TPGAELLKKISSESARNYIQSLTQMPKMNFANVFIGANPLAVDLLEKMLVLDSDKRITAA
                  ** * *     *  ******************************************

Porcine       301 QALAHAYFAQYHDPDDEPVADPYDQSFESRDLLIDEWKSLTYDEVISFVPPPLDQEEMES
Human         301 QALAHAYFAQYHDPDDEPVADPYDQSFESRDLLIDEWKSLTYDEVISFVPPPLDQEEMES
                  ************************************************************
```

Figure 5.3 Protein sequence homology between porcine and human p38 MAP kinase
Protein sequences for porcine (accession number XP_003356663) and human (accession number CAG38743) p38 MAP kinase were obtained from the National Centre for Biotechnology Information database portal. Sequence homology between species was determined using the Sequence Analyser tool from the Swiss Institute of bioinformatics. *denotes matching protein sequences. Thr180 and Tyr182 phosphorylation sites of interest are highlighted in yellow.

```
Porcine        1 MDDLFPLIFPSEPAPASGPYVEIIEQPKQRGMRFRYKCEGRSAGSIPGERSTDTTKTHPT
Human          1 MDELFPLIFPAEPAQASGPYVEIIEQPKQRGMRFRYKCEGRSAGSIPGERSTDTTKTHPT
                 ** ******* *** ****************************************

Porcine       61 IKINGYTGPGTVRISLVTKDPPHRPHPHELVGKDCRDGFYEAELCPDRCIHSFQNLGIQC
Human         61 IKINGYTGPGTVRISLVTKDPPHRPHPHELVGKDCRDGFYEAELCPDRCIHSFQNLGIQC
                 ************************************************************

Porcine      121 VKKRDLEQAINQRIQTNNNPFQVPIEEQRGDYDLNAVRLCFQVTVRDPAGRPLRLPPVLS
Human        121 VKKRDLEQAISQRIQTNNNPFQVPIEEQRGDYDLNAVRLCFQVTVRDPSGRPLRLPPVLS
                 ********** ********************************** ***********

Porcine      181 HPIFDNRAPNTAELKICRVNRNSGSCLGGDEIFLLCDKVQKEDIEVYFTGPGWEARGSFS
Human        181 HPIFDNRAPNTAELKICRVNRNSGSCLGGDEIFLLCDKVQKEDIEVYFTGPGWEARGSFS
                 ************************************************************

Porcine      241 QADVHRQVAIVFRTPPYADPSLQAPVRVSMQLRRPSDRELSEPMEFQYLPDTDDRHRIEE
Human        241 QADVHRQVAIVFRTPPYADPSLQAPVRVSMQLRRPSDRELSEPMEFQYLPDTDDRHRIEE
                 ************************************************************

Porcine      301 KRKRTYETFKSIMKKSPFNGPTDPRPATRRIAVPSRSSASVPKPAPQPYPFTPSLSTINF
Human        301 KRKRTYETFKSIMKKSPFSGPTDPRPPPRRIAVPSRSSASVPKPAPQPYPFTSSLSTINY
                 ****************** *******  ************************ ******

Porcine      361 DEFTPMAFASGQIPGQTSALAPAPAPVLVQAPAPAPAPAMASALAQAPAPVPVLAPGLAQ
Human        361 DEFPTMVFPSGQI-SQASALAPAPPQVLPQAPAPAPAPAMVSALAQAPAPVPVLAPGPPQ
                 ***  * * ****  * *******  ** *********** ****************  *

Porcine      421 AVAPPAPKTNQAGEGTLTEALLQLQFDTDEDLGALLGNNTDPTVFTDLASVDNSEFQQLL
Human        420 AVAPPAPKPTQAGEGTLSEALLQLQFD-DEDLGALLGNSTDPAVFTDLASVDNSEFQQLL
                 ********  ******* ********* ********** *** *****************

Porcine      481 NQGVSMPPHTAEPMLMEYPEAITRLVTGSQRPPDPAPTPLGASGLTNGLLSGDEDFSSIA
Human        479 NQGIPVAPHTTEPMLMEYPEAITRLVTGAQRPPDPAPAPLGAPGLPNGLLSGDEDFSSIA
                 ***    *** ***************** ******** **** ** **************

Porcine      541 DMDFSALLSQISS
Human        539 DMDFSALLSQISS
                 *************
```

Figure 5.4 Protein sequence homology between porcine and human p65 NF-κB

Protein sequences for porcine (accession number NP_001107753) and human (accession number NP_068810) p65 obtained from the National Centre for Biotechnology Information database portal. Sequence homology between species was determined using the Sequence Analyser tool from the Swiss Institute of bioinformatics. *denotes matching protein sequences. Ser529 and Ser536 phosphorylation sites of interest are highlighted in yellow.

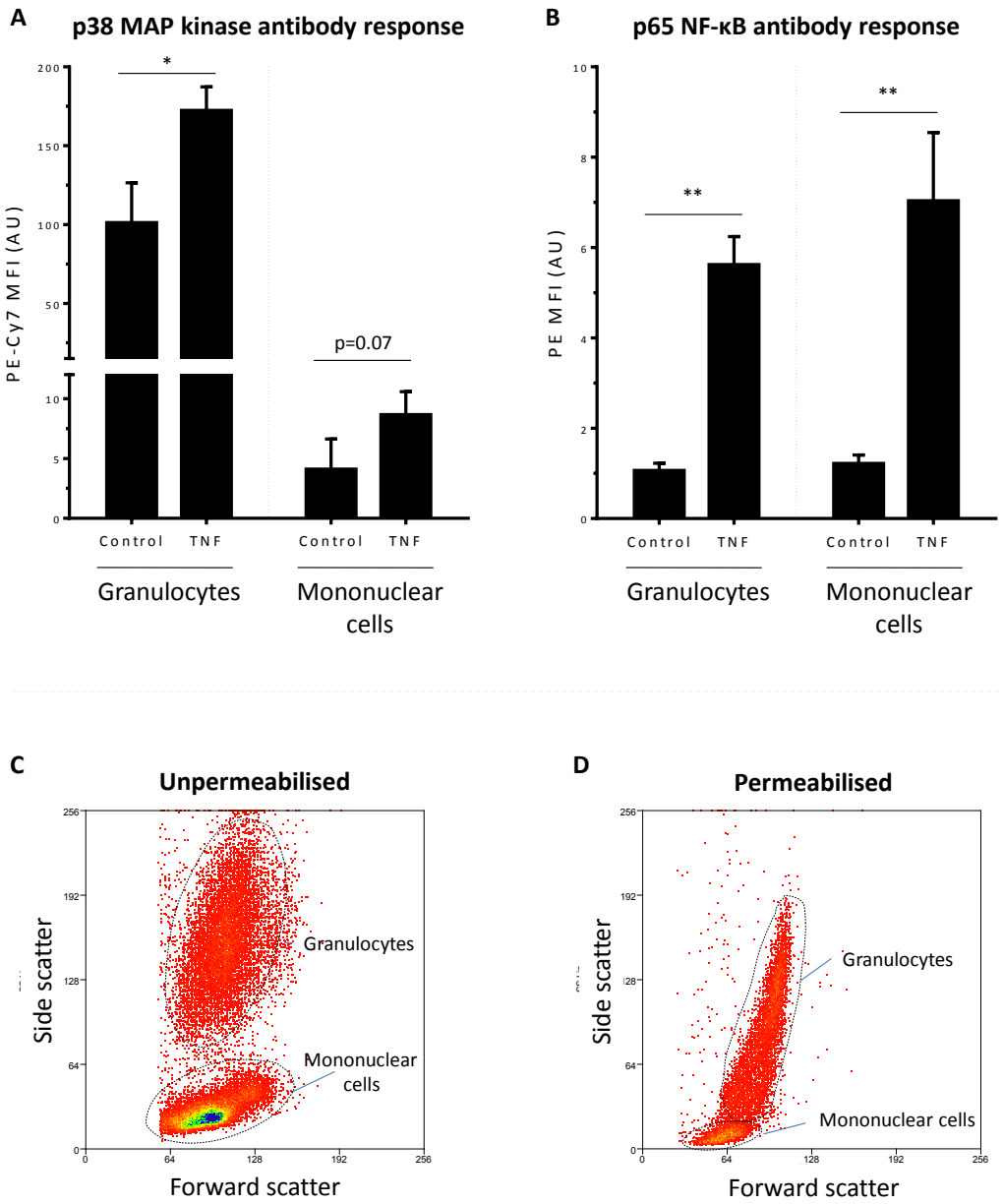

Figure 5.5 Validation of anti-phospho-p38 and anti-phospho-p65 antibody staining using porcine cells by flow cytometric analysis

Porcine blood samples were incubated with TNFα (10ng/µl for 30 minutes) or remained untreated as a control. Leukocytes were fixed, permeabilised and stained using anti-phospho p38 antibodies (A) or anti-phospho p65 antibodies (B). Fluorescence in distinct populations (identified by gating on forward and side scatter profiles) was measured by flow cytometry. Representative images of unpermeabilised cells (C) and permeabilised cells (D) are shown for reference. Mean values ± standard deviations were generated from data pooled from 3 independent experiments. *p<0.05; **p<0.01, Student's t-test.

5.3.4 Effect of sulforaphane pre-treatment in a large animal model of cardiopulmonary bypass

The influence of sulforaphane on physiological responses to CPB was studied under well-controlled experimental conditions by pre-treating pigs either with purified sulforaphane (i.v. 2 mg/kg) or with saline as a control. Animals were treated in accordance with the protocols described in 2.2.16, page 114. In brief, adult female landrace pigs were prepared on a cruciferous vegetable-free diet for the preceding week. Animals were anaesthetised and underwent sternotomy, cannulation and exposure to full cardiopulmonary bypass using a 'conventional' cardiopulmonary bypass circuit described in 2.2.16.4 (page 117) conducted under porcine normothermia. Blood was taken immediately after sedation (before surgical access, sternotomy etc.); at the initiation of cardiopulmonary bypass support and then at 1 and 2 hours after the start of CPB. Control or purified sulforaphane intervention injections were given immediately after the first blood specimen was taken. Tissues were harvested as described in 2.2.16.5 (page 117). Specimens were snap frozen and stored in -80°C conditions until the completion of all experiments and then studied *en masse*. Animals were treated in according with Home Office regulations.

The mean time from injection until the initiation of CPB was 106 ± 12 minutes in the control group and 107 ± 24 minutes in the sulforaphane intervention group. In the first instance, plasma levels of sulforaphane were measured by LC-MS (Figure 5.6). This demonstrated that plasma sulforaphane levels were significantly elevated immediately prior to the commencement of CPB (mean 353.25 ± 61.51 ng/ml)(CPB Start) and persisted for at least 2 h (mean 187.5 ± 40.73 ng/ml) in animals that were pre-treated with sulforaphane. Sulforaphane was not detected in saline-treated animals, indicating that endogenous levels of this compound were negligible (Figure 5.7).

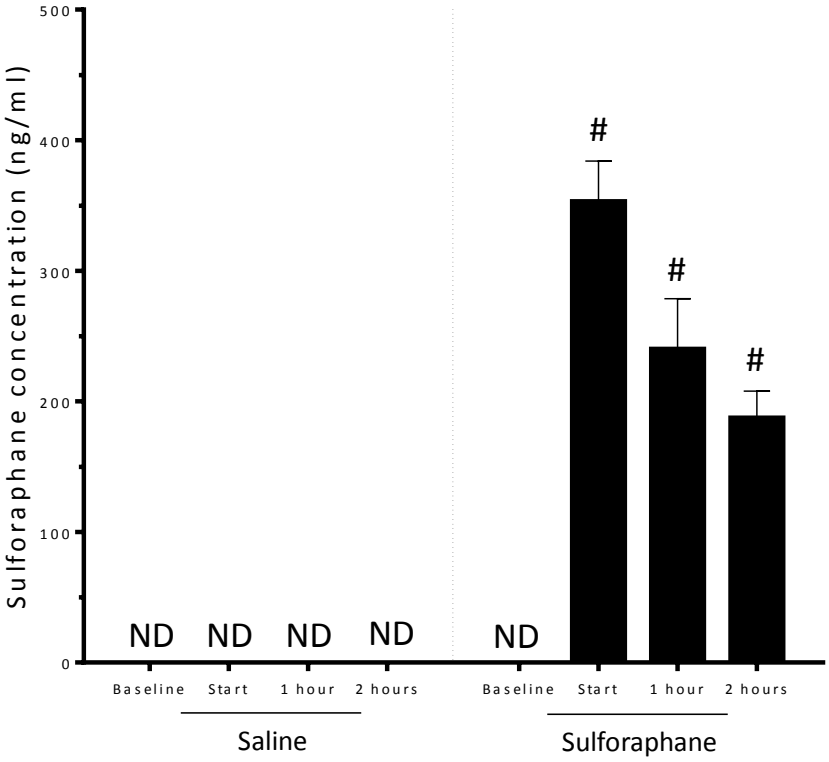

Figure 5.6 Plasma sulforaphane levels in experimental groups
Animals were treated with sulforaphane or with vehicle alone as a control and were then subjected to CPB for 2 h. Plasma samples were collected prior to sulforaphane or control injection (baseline), immediately prior to CPB (cannulation) and at varying times following CPB initiation. Sulforaphane levels were determined by LC-MS (ND, not detected). Data were pooled from five animals and mean levels and standard error. #$p<0.0001$, ANOVA followed by Dunnett's test, compared to baseline.

5.3.4.1 Sulforaphane effects on intracellular pro-inflammatory pathways in leukocytes during cardiopulmonary bypass

The kinetics of leukocyte activation in response to CPB were determined by measuring p38 MAP kinase phosphorylation, NF-κB phosphorylation and ROS induction in leukocytes in pigs. Blood samples were collected pre-operatively (baseline), following cannulation of the aorta and right atrium prior to the initiation of CPB (CPB start) and at 1-2 h following initiation of CPB. Intracellular staining and flow cytometry demonstrated that CPB did not significantly induce phosphorylation of p38 MAP kinase in granulocytes (baseline 241.88 ± 79.29 PE-Cy7 MFI units vs mean 210.26 ± 121.69 PE-Cy7 MFI units) at the start of CPB. In keeping with the human data, levels of p38 MAP kinase were sub-baseline at 2 hours (mean 187.08 ± 88.94 PE-Cy7 MFI units) but these changes were also not statistically significant (Figure 5.7A). In mononuclear cells, the maximal levels of p38 MAP kinase were achieved at 1 hour post-CPB (baseline mean 4.96 ± 3.56 PE-Cy7 MFI units vs mean 11.55 ± 13.4 PE-Cy7 MFI units), but this did not reach statistical significance. Sulforaphane pre-treatment initiated approximately 2 hours before the commencement of CPB showed a reduction in levels of p38 MAP kinase at 1 hour (control mean 11.55 ± 13.4 PE-Cy7 MFI units vs sulforaphane mean 1.40 ± 0.96 PE-Cy7 MFI units, $p<0.05$) between groups; and at 2 hours (control mean 9.51 ± 12.36 PE-Cy7 MFI units vs sulforaphane mean 0.77 ± 0.83 PE-Cy7 MFI units, $p<0.052$)(Figure 5.7B).

Compared to baseline (mean 2.46 ± 1.18 PE MFI units), the maximal levels of phosphorylated p65 NF-κB were measured at 1 hour post CPB (mean 3.46 ± 0.68 PE MFI units) in granulocytes. This induction was not statistically significant. The same pattern was observed in the mononuclear cell fraction (baseline mean 2.18 ± 0.72 PE MFI units vs mean 3.171 ± 0.58 PE MFI units at CPB 1 hour). Following pre-treatment with sulforaphane, granulocytes exhibited significantly lower levels of phosphorylated NF-κB RelA at 1 hour (mean 3.46 ± 0.69 PE MFI units in controls vs 0.72 ± 0.25 PE MFI units, $p <0.01$) and 2 hour

time points (mean 3.03 ± 1.54 PE MFI units in controls vs 0.84 ± 0.46 PE MFI units, $p < 0.05$) (Figure 5.7C). In porcine mononuclear cells, baseline levels of p65 NF-κB were 2.16 ± 0.72 PE MFI units. The peak levels were recorded at 1 h following CPB (3.17 ± 0.58 PE MFI units), with this trend in elevation up until 2 hours of CPB. Sulforaphane pre-treated animals exhibited significantly reduced levels of p65 at 1 hour post-CPB (mean 1.55 ± 0.29 PE MFI units, $p<0.05$) and 2 hours post-CPB timepoints (control means 2.96 ± 2.04 PE MFI units vs 1.32 ± 0.31 PE MFI units, $p<0.05$)(Figure 5.7D).

When considering ROS, compared to baseline (mean 9.92 ± 4.55 FITC MFI units), peak levels of ROS in granulocytes was recorded at 2 hours (12.25 ± 7.37 FITC MFI units) post-CPB (Figure 5.8A). The changes are small in magnitude and are not statistically significant. This is also seen in the mononuclear cell fraction, where induction changes are small (baseline mean 4.90 ± 5.98 FITC MFI units vs 6.41 ± 9.50 FITC MFI units at 2 hours post CPB) (Figure 5.8B). There are no effects on ROS in sulforaphane treated animals.

Together, these data show the signalling response to CPB in animals is distinct from that observed in the clinical CPB trial because p38 MAP kinase and NF-κB phosphorylation were not enhanced by surgery with CPB. Despite this, sulforaphane appears to exert a biological effect at 1 and 2 hours following CPB by reducing p38 MAP kinase and NF-κB phosphorylation; having been delivered approximately 2 hours before the exposure to CPB.

Levels of mRNA for TNFα, IL-6 and IL-8 were studied by quantitative SYBR-green PCR using gene specific primers as described (Table 2.2, page 97). RNA was extracted using commercially-available kits and reverse transcribed using dedicated pipettes and reagents to avoid potential RNAase contamination. Accurate quantification and quality assessment of the starting RNA sample was conducted by optical density assessment and samples used only if $A_{260/280}$ approaching 2.0. A water negative control was included in each run to exclude the possibility that fluorescent signal may arise from amplification of contaminating sequences.

Data were inspected after each run and it was ensured that amplification was logarithmic and a single PCR product with high temperature denaturing characteristics was produced (and low-temperature denaturing primer-dimers were absent).

Analysis of mRNA levels of TNFα showed a significant increase from basal levels at 1 hour (mean 3.2 fold increase, $p<0.001$) and 2 hours (mean 2.2 fold increase, $p<0.05$) post-CPB exposure. Sulforaphane pre-treatment significantly attenuated the level of mRNA transcripts at both timepoints 1 hour (mean 1.2 fold relative expression, $p<0.01$) and 2 hour (mean 0.94 relative expression, $p<0.05$)(Figure 5.9A). IL-8 transcripts were enhanced following CPB for 1h (2.2 fold relative expression, $p<0.01$) and subsequently declined at 2 h post-CPB. This induction was attenuated in the sulforaphane-treated group (1.1 relative expression, $p<0.005$) at the same 1 hour time point (Figure 5.9C). Interestingly, IL-6 mRNA levels in leukocytes were enhanced in pigs that were prepared for CPB (prior to the commencement of CPB; Figure 5.95B, compare 'Baseline' with 'CPB Start'), indicating that this cytokine was induced by surgical procedures per se.

Taken together, these data suggest that CPB exerts a pro-inflammatory effect on gene transcripts for TNFα and IL-8 in response to CPB. Up-regulation of IL-6 transcripts appears before CPB and may represent the effects of other molecular triggers of inflammation independent of extracorporeal support. The use of sulforaphane is associated attenuation of these gene transcripts in the large animal model.

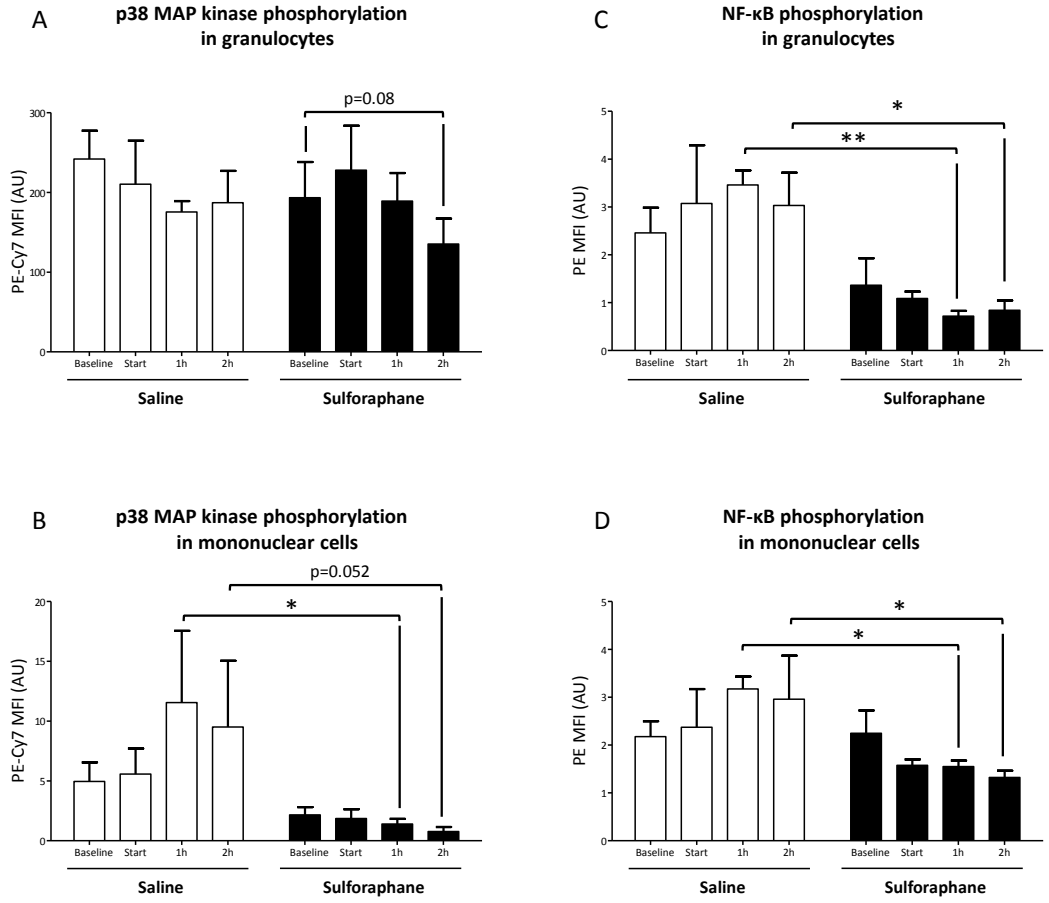

Figure 5.7 p38 MAP kinase and NF-κB activation in leukocytes in response to CPB was suppressed by pre-treatment with sulforaphane

Animals were treated with sulforaphane or with control and were then subjected to CPB for 2h. Peripheral blood samples were collected prior to sulforaphane or control injections (baseline), immediately prior to CPB (cannulation) and at varying times following CPB initiation. Leukocytes were fixed and permeabilised prior to intracellular staining using PE-Cy7-conjugated antibodies that recognise Thr180/Tyr182 phosphorylated p38 MAP kinase or PE-conjugated antibodies that recognise Ser529 phosphorylated RelA or with isotype-matched irrelevant antibodies as a control. Following lysis of red blood cells, fluorescence of granulocytes or mononuclear cells was quantified by flow cytometry (after gating of cells by size and granularity). Mean fluorescence levels were calculated after subtracting values from isotype-control antibodies. Mean values pooled from 5 animals per group are shown with SEM. *p<0.05; **p<0.01 Fisher's least significant difference multi-comparisons test.

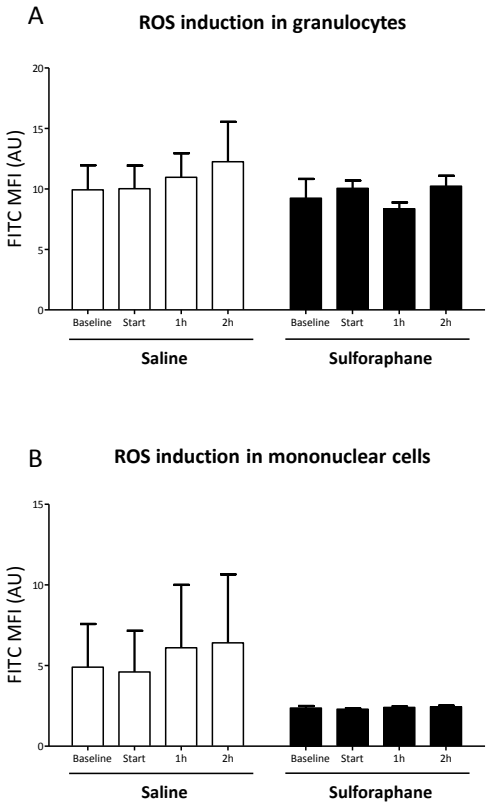

Figure 5.8 Effect of CPB exposure on porcine ROS induction

Animals were treated with sulforaphane or control and were then subjected to CPB for 2h. Peripheral blood samples were collected prior to sulforaphane or control injection (baseline), immediately prior to CPB (cannulation) and at varying times following CPB initiation. Leukocytes were loaded with the APF ROS-sensitive probe. Following lysis of red blood cells, fluorescence of granulocytes or mononuclear cells was quantified by flow cytometry (after gating of cells by size and granularity). Mean fluorescence levels were calculated. Mean values pooled from 5 animals per group are shown with standard error.

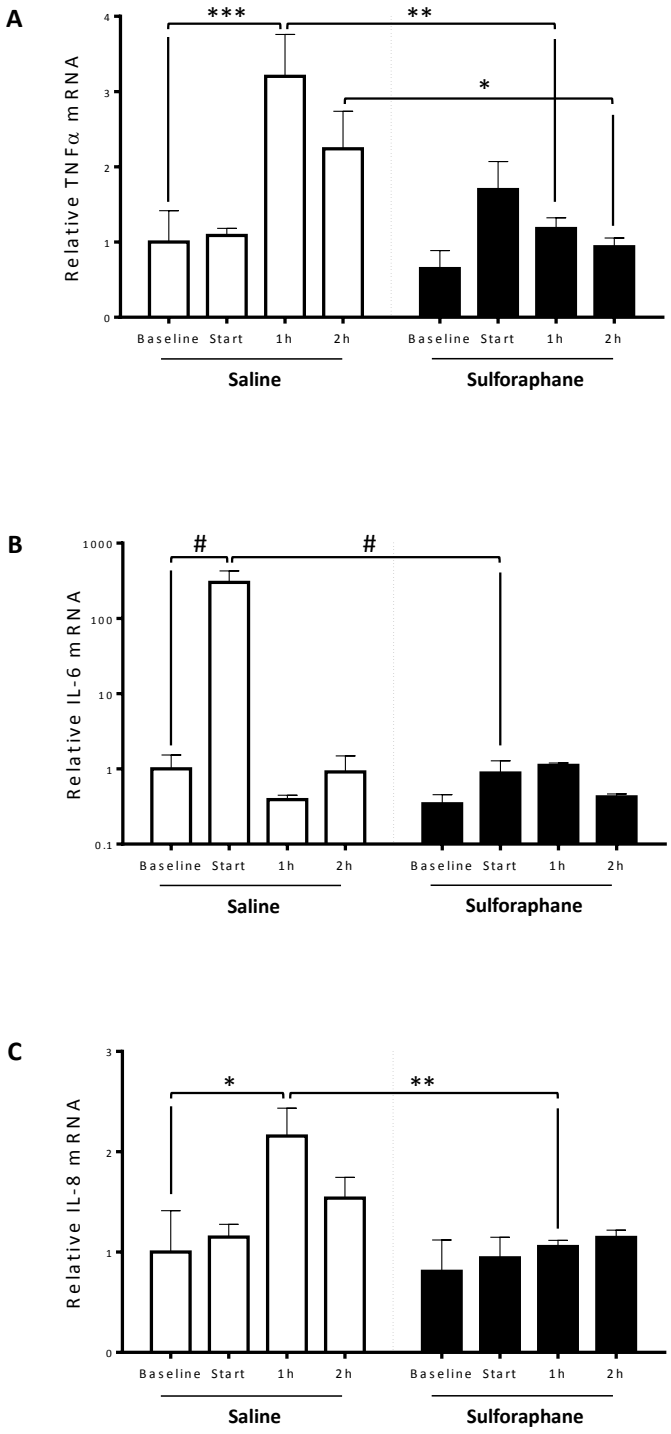

Figure 5.9 Inflammatory cytokine induction in response to CPB was reduced by pre-treatment with sulforaphane

Animals were treated with sulforaphane or with control and were then subjected to CPB for 2h. Peripheral blood samples were collected prior to injections (baseline), immediately prior to CPB (cannulation) and at varying times following CPB initiation. TNFα, IL-8 and IL-6 transcript levels were quantified by real-time PCR. Mean values pooled from 5 animals per group are shown with standard error. *p<0.05; **p<0.01; ***p<0.005; #p<0.001, Bonferroni multi-comparisons test.

5.3.4.2 The effects of Sulforaphane on end-organ inflammation and injury following exposure to cardiopulmonary bypass

Having assessed the intracellular signalling changes and the associated alterations in expression of pro-inflammatory transcripts within leukocytes in the circulation, the next phase of the experiments focused on the biological changes in end-organs and the relative influence of sulforaphane pre-treatment on these tissues. To undertake this assessment, firstly, histological analyses were performed to determine the effects of porcine CPB on renal, lung and myocardial microscopic tissue structure. These were correlated with western blot analyses for protein expression of pro-inflammatory molecules and PCR analysis for the assessment of pro-inflammatory transcripts in tissue compartments. Organs were harvested in a uniform fashion as described in 2.2.16.5 (page 117). Tissues were stored at -80°C prior to thawing and study *en masse* at the completion of the experiments to ensure uniformity of handling and comparability of results.

Histological assessments were performed by a consultant histopathologist blinded to the treatment allocation. There was minor acute tubular necrosis (ATN) in renal samples from 80% (4/5) control pigs undergoing CPB, evidenced by abnormal tubular flattening and debris within the tubular lumina (open arrows in Figure 5.10A, Saline; key features shown at higher magnification in the insets). By contrast, ATN was not observed in kidneys from pigs pre-treated with sulforaphane prior to CPB ($p<0.05$, *Fisher's exact test*)(Figure 5.10A, right panel). This indicates that sulforaphane pre-treatment may have a protective effect on kidneys from damage in response to surgery with CPB. Gross histological changes in heart or lung were not observed suggesting that the architecture of these tissues was resistant to the duration of CPB exposed. In 2/5 myocardial specimens within each group, there were noted to be emigrated neutrophils in the small blood vessel perivascular interstitial spaces (Figure 5.11A). In lung tissues, 9/10 specimens exhibited significant peri-bronchial lymphoid and interstitial hyper-cellularity with increased interstitial lymphoid or myeloid content (Figure 5.12A). Of note, the model did not involve cardioplegia or cross-clamp fibrillation and

therefore the heart was perfused throughout. It is plausible that the absence of oedema in heart or lung relates to the absence of ischemia/reperfusion injury in this porcine model of CPB as we did not wean the animals off of extracorporeal circulatory support, nor did the model feature resumption of ventilation at any point.

The potential influence of sulforaphane on p38 MAP kinase and NF-κB phosphorylation in renal, lung and myocardial tissues was determined by Western blotting. To validate the technique we identified phosphorylated forms of p38 MAP kinase or RelA NF-κB sub-units in cultured porcine aortic endothelial cells stimulated with PMA, which served as a positive control for antibody binding (Figure 5.10B, left panel). Phosphorylated forms of p38 MAP kinase were not detected in renal (Figure 5.10B, right panel) or lung (Figure 5.12B) tissues from pigs exposed to CPB, whereas p38 MAP kinase phosphorylation was detected in the myocardium (Figure 5.11B). Phosphorylated forms of p65 NF-κB were active in all tissues (Figure 5.10B, Figure 5.11B, Figure 5.12B). However, sulforaphane pre-treatment did not influence p38 MAP kinase or NF-κB (RelA) activation by phosphorylation in tissues (Figure 5.10B, Figure 5.11B, Figure 5.12B), indicating that its protective effects are not due to local suppression of either of these signalling pathways. Quantitative RT-PCR was carried out using the internal controls and procedures described above. It demonstrated that sulforaphane reduced expression of IL-6 and TNFα in lung (Figure 5.12C); and reduced IL-6, IL-8 and TNFα in myocardium (Figure 5.11C) but did not alter inflammatory transcripts in renal tissues (Figure 5.10C). Thus we conclude that although sulforaphane can influence cytokine production in tissues, this effect does not account for its ability to reduce the early appearances of ATN in response to surgery with CPB. Moreover, the cytokine expression does not correlate with differences in pro-inflammatory signalling molecular expression, nor gross macroscopic changes.

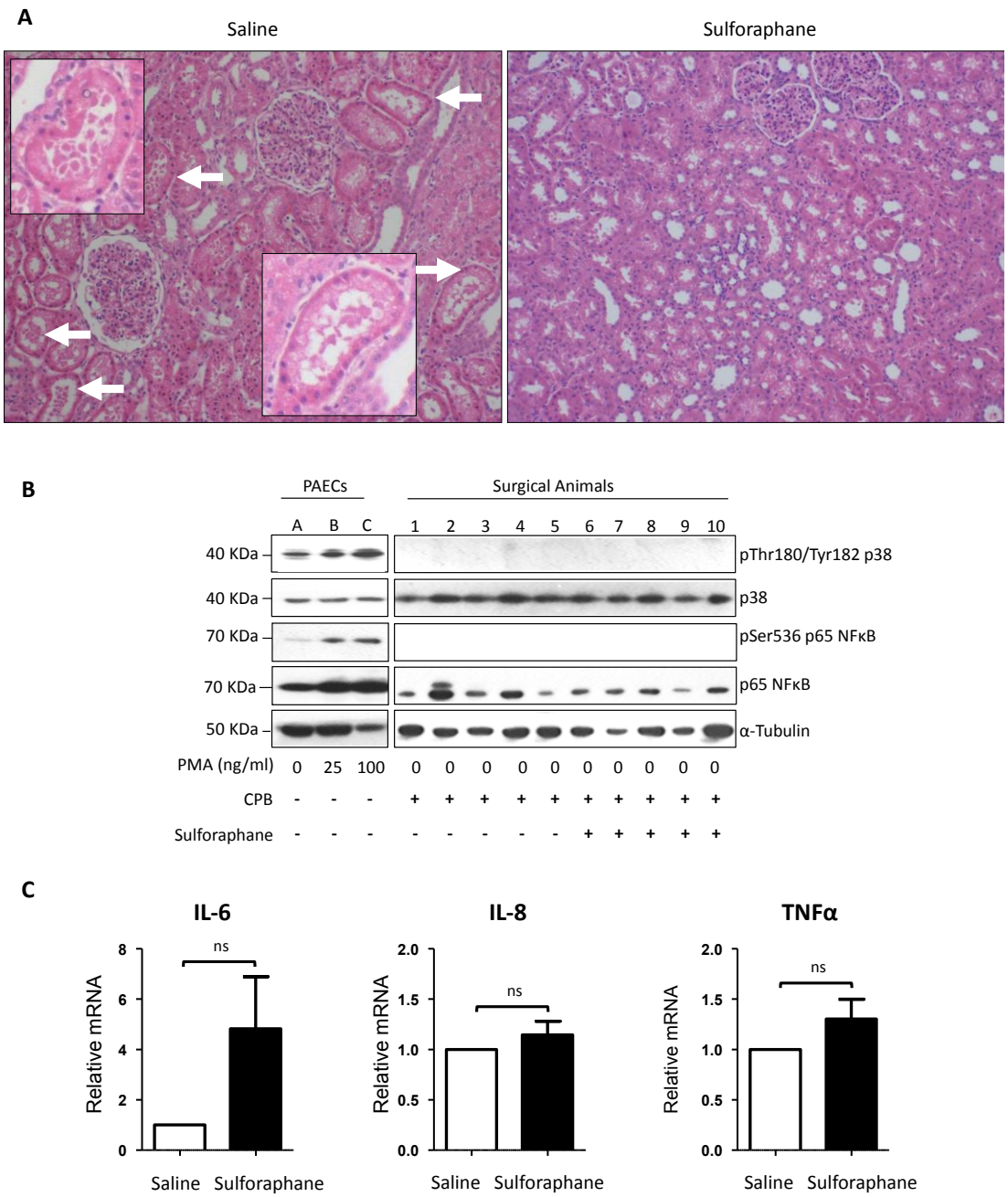

Figure 5.10 Renal effects of sulforaphane post-CPB

Animals were treated with sulforaphane (animals 6-10) or with vehicle alone as a control (animals 1-5) and were then subjected to CPB for 2h. Renal tissues were harvested. Tissue sections were stained with haematoxylin and eosin prior to histological assessment by an experienced pathologist who was blinded to the experimental design (A). Representative images are shown. Arrows indicate abnormal tubular flattening and debris within the tubular lumina. Renal tissue lysates were tested by western blotting using antibodies that recognise Thr180/Tyr182 phosphorylated p38 MAP kinase, total p38 MAP kinase, Ser536 phosphorylated RelA or total RelA, and by using anti-α-tubulin antibodies to assess total protein levels (B). Lysates from phorbol myristyl acetate (PMA)-stimulated PAEC (known to contain phosphorylated p38 MAP kinase and RelA) were tested in parallel and served as a positive control for antibody binding. (C) IL-6, IL-8 and TNFα transcript levels were quantified by real-time PCR. Data were pooled from five animals and mean values ±SEM are shown.

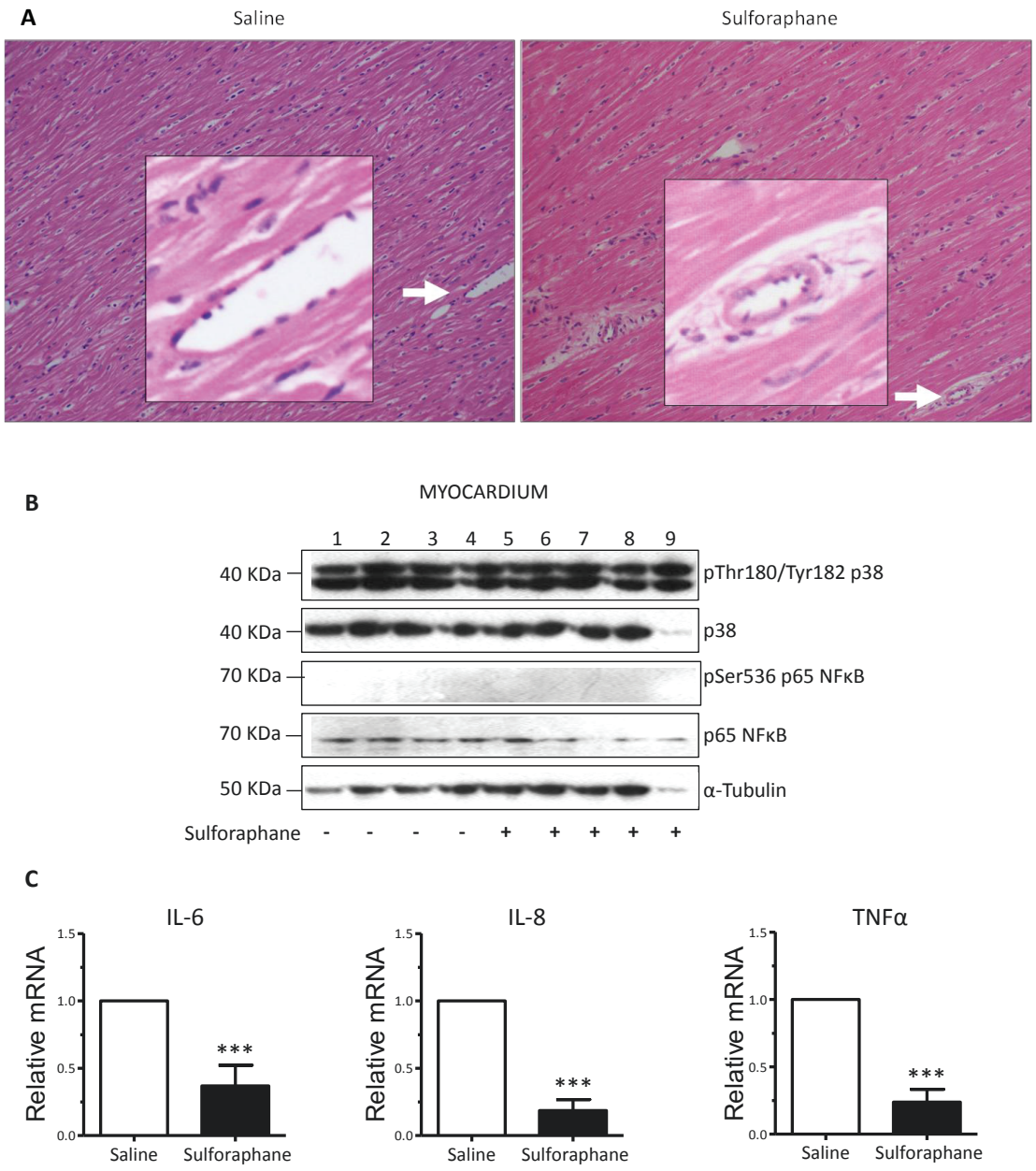

Figure 5.11 Myocardial effects of sulforaphane post-CPB

Animals were treated with sulforaphane (animals 5-9) or with vehicle alone as a control (animals 1-4) and were then subjected to CPB for 2h. Myocardium was harvested. Tissue sections were stained with haematoxylin and eosin prior to histological assessment by an experienced pathologist who was blinded to the experimental design (A). Representative images are shown. Arrows demonstrate neutrophils in perivascular spaces. Myocardial tissue lysates were tested by western blotting using antibodies that recognise Thr180/Tyr182 phosphorylated p38 MAP kinase, total p38 MAP kinase, Ser536 phosphorylated RelA or total RelA, and by using anti-α-tubulin antibodies to assess total protein levels (B). IL-6, IL-8 and TNFα transcript levels were quantified by real-time PCR (C). Data were pooled from five animals and mean values ±SEM are shown. ***p<0.005, Student's t-test.

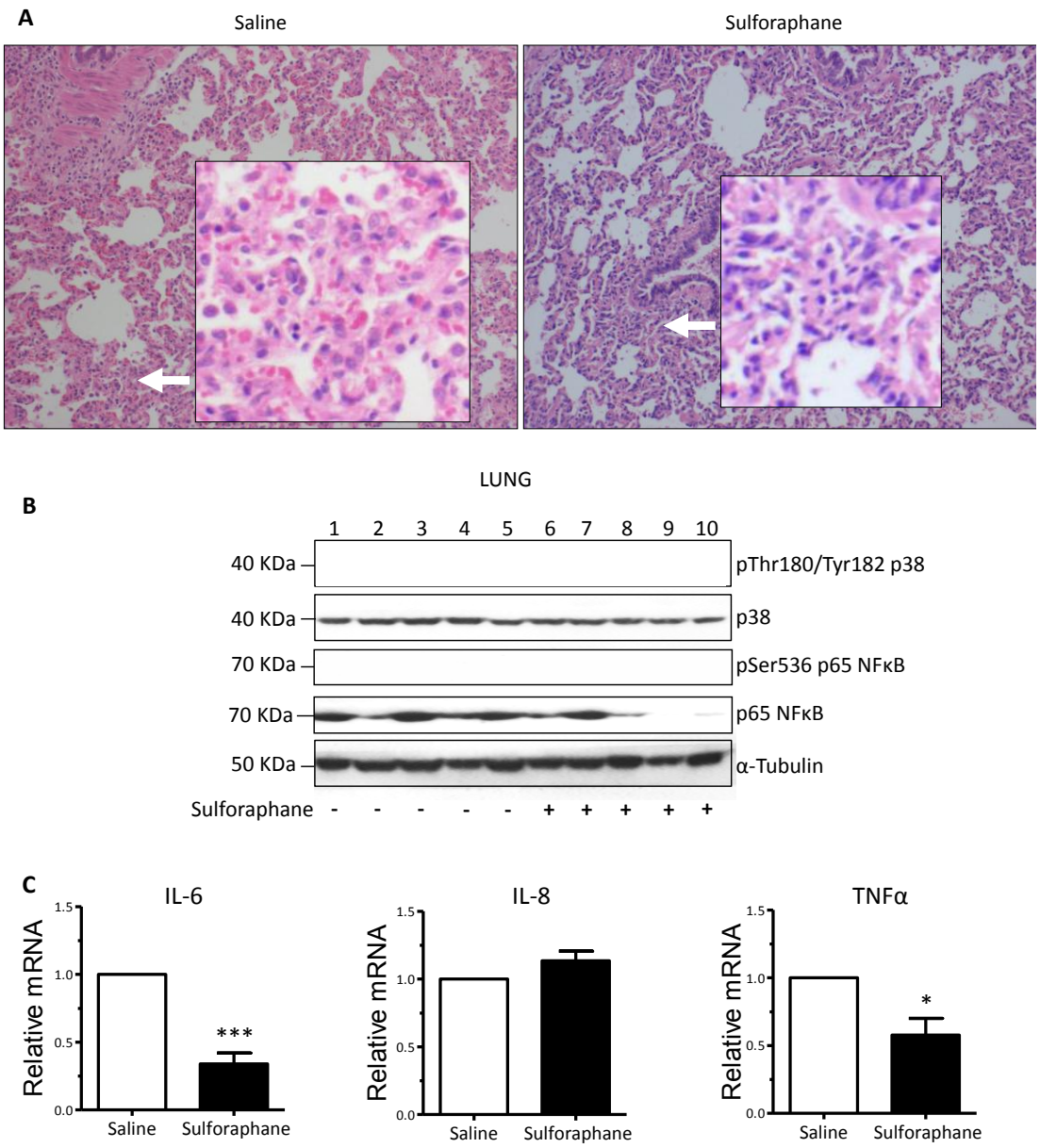

Figure 5.12 Pulmonary effects of sulforaphane post-CPB

Animals were treated with sulforaphane (animals 6-10) or with vehicle alone as a control (animals 1-5) and were then subjected to CPB for 2h. Lung tissue was harvested. Tissue sections were stained with haematoxylin and eosin prior to histological assessment by an experienced pathologist who was blinded to the experimental design (A). Representative images are shown. Arrows demonstrate regions of hypercellularity. Lung tissue lysates were tested by western blotting using antibodies that recognise Thr180/Tyr182 phosphorylated p38 MAP kinase, total p38 MAP kinase, Ser536 phosphorylated RelA or total RelA, and by using anti-α-tubulin antibodies to assess total protein levels (B). IL-6, IL-8 and TNFα transcript levels were quantified by real-time PCR (C). Data were pooled from five animals and mean values ±SEM are shown. *p<0.05; ***p<0.005, Student's t-test.

5.3.5 Effect of homogenate consumption on leukocyte pro-inflammatory activity

Building upon the findings in the earlier portion of this chapter, the final phase of investigation focussed on assessing the effects of a sulforaphane-rich diet in healthy human volunteers. The hypothesis that the consumption of a single dose of a sulforaphane-rich preparation, in the form of a pre-blended homogenate (eliminating the variable of chewing, and action of myrosinase), leads to suppression of inflammatory activation of leukocytes for up to 24 hours was tested.

5.3.5.1 Participants

This study was conducted according to the methods outlined in 2.2.17, page 118. Nine participants were recruited into the study. Three participants withdrew from the study after administration of the first homogenate, all citing the unpalatable nature of the preparations and declined to continue. Data from the remaining 6 participants is presented and broad characteristics are given in Table 5.1.

There were a total of 4 female and 2 male participants with a mean age of 29.5 ± 1.6 years and a BMI 21.7 ± 0.9 kg/m^2, reflecting the 'healthy' young nature of this population. No adverse events were noted from the remaining participants, with specifically no gastro-intestinal upsets nor any adverse clinically apparent immune reaction nor susceptibility to infections, reported in other studies. The most frequent country of origin was the United Kingdom (n=3) with a spread of Northern European, Middle Eastern and Far Eastern ancestry. This cosmopolitan spread of volunteers gives a crude indication of (the absence of) potential genetic polymorphisms, although this was not formally tested in this study.

Participant ID	Sex	Age (years)	BMI (kg/m_2)	Country of Birth	Outcome
1	Male	48	32.5	Republic of Ireland	Completed
	Male			Albania	Withdrew
2	Female	26	16.8	People's Republic of China	Completed
	Female			Italy	Withdrew
	Female			United Kingdom	Withdrew
3	Female	24	20.1	United Kingdom	Completed
4	Female	30	20.3	Iran	Completed
5	Female	27	18.7	Germany	Completed
6	Male	22	21.6	United Kingdom	Completed

Table 5.1 Participant characteristics

5.3.5.2 Consumption of homogenates produces biologically significant levels of sulforaphane in blood

Plasma sulforaphane levels were determined from blood specimens obtained immediately prior to homogenate consumption and then at various time points up until 24 hours following homogenate consumption (Figure 5.13).

Two-way analysis of variance revealed that the effect of time on plasma levels of sulforaphane were significant, $F(3,12) = 78.02$, $p<0.0001$, as was the effect of homogenate consumed, $F(1,4) = 424.7$, $p<0.0001$. Post-hoc evaluation using the *Dunnett* multiple comparisons test showed plasma levels of sulforaphane were significant at 1 hour (mean 30.68 ± 2.88 ng/mL, $p<0.0001$) and also at 6 hours (mean 10.84 ± 0.87 mg/mL, $p<0.0001$), becoming undetectable at 24 hours. Plasma levels of sulforaphane were undetectable in the ASH group at points of measurement.

These data suggest that the BSH preparations can generate biologically active levels of sulforaphane in the plasma, and ASH is a suitable experimental control. The levels measured are approximately $1/10^{th}$ of those found in the porcine model dose delivered by intravenous injection. By visual inspection, the plasma half-life was in the order of approximately 1-2 hours.

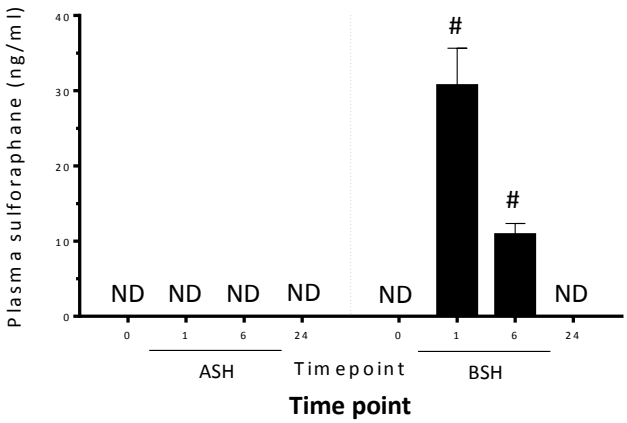

Figure 5.13 Plasma sulforaphane levels following consumption of homogenates
Six healthy volunteers consumed either BSH or ASH alternatively over a 24h period. Blood was sampled at 0 (prior to consumption), 1, 6 and 24 hours after. Plasma sulforaphane levels were detected using Liquid chromatography-Mass spectroscopy methods. Values presented are means ± SEM. ND = not detected, #p<0.0001 by Dunnett's multi-comparison test compared to 0 time point.

5.3.5.3 Consumption of broccoli homogenates was associated with early attenuation of constitutive ROS and p38 MAP kinase levels

Given the cross-over longitudinal design of the trial with multiple measures, a mixed-regression model of statistical inference was conducted with the assistance of Professor Barnaby Reeves, Imperial College trials unit. The data presented in the figures of the following section are based on raw un-adjusted values derived directly from the experiments, and plotted in the graphs. Descriptive statistics (means ± SD) are presented in the text between time points of interest. For comparative analytical purposes, the data distribution was log-transformed (to improve the distribution towards a Gaussian spread) and the log-transformed data was fitted to statistical models, where indicated. Main effects of time; time-plus-homogenate and time plus-homogenate-plus-interactions between-time-and-homogenate consumption were considered in the regression model analysis.

Analysis of whole blood samples revealed considerable variation in ROS levels and p38 MAP kinase and NF-κB phosphorylation in granulocytes and mononuclear cells between individuals that consumed ASH or BSH (Figure 5.14).

Basal constitutive levels of ROS in granulocytes in the ASH group were 25 ± 12.99 FITC MFI units and in the BSH group were 21.04 ± 13.37 FITC MFI units. The final regression model selected for ROS effects included time, intervention and interaction effects to achieve the best fit (*Wald* Chi-square = 8.59 with 2 df, p = 0.014). Within this model, there is a rise in granulocyte ROS at 1 hour that is more pronounced in the control ASH group (48.71 ± 43.22 FITC MFI units) compared to the BSH intervention group (30.29 ± 27.31 FITC MFI units); mean difference 0.4078 log units, 95% CI 0.0645 to 0.7510, p = 0.02 (Figure 5.14A) . There were no statically significant differences between groups at 6 or 24 hours between groups for granulocyte ROS.

Under ex-vivo stress conditions, both ASH and BSH group granulocytes manifest a strong induction of ROS. There appeared to be a rise in PMA-enhanced ROS at 1 hour which appeared to be more pronounced in the ASH group (mean 2936 ± 2441 FITC MFI units) compared to the BSH group (mean 1989 ± 2858 FITC MFI units). However, the regression models for these stressed conditions did not reveal any significant differences between time, intervention nor interaction (*Wald* Chi-square p = 0.37)(Figure 5.14 B).

The constitutive levels of phosphorylated p38 MAP kinase in granulocytes were 79.84 ± 89.36 PE-Cy7 MFI units compared to 98.85 ± 75.62 PE-Cy7 MFI units in the control ASH group. The final regression model selected for p38 MAP kinase effects included time, intervention and interaction to achieve the best fit (*Wald* Chi-square = 8.93 with 2 df, p = 0.012). In this model, there was a greater rise in p38 MAP kinase at 1 hour in the ASH group (113.73 ± 94.256 PE-Cy7 MFI units) compared to the BSH group (67.96 ± 85.03 PE-Cy7 MFI units); mean difference 1.8045 log units, 95% CI (0.5168 – 3.0901), p=0.006 (Figure 5.14C). A difference between groups was not apparent at later time points in the study (Figure 5.14C). Under stress conditions, there was no change between baseline levels of p38 MAP kinase in either BSH and ASH conditions, and the statistical model did not achieve significance (p=0.74)(Figure 5.14D).

The statistical models for constitutive levels of phosphorylated p65 in granulocytes did not reach significance for time or intervention or interaction between ASH or BSH groups (p = 0.26)(Figure 5.14E). However, the models for levels of stress-induced p65 showed a strong time effect (*Wald* chi-square p=0.0001), but no effect from interaction. There was a decline in levels of p65 over time with a strong effect seen at 24 hours compared to baseline for both groups but no statistical interaction, thus implying no differences between homogenates being consumed; but an effect of consumption itself.

Effects in monocytes, lymphocytes and mononuclear cells did not reach significance in statistical modelling of the parameters of interest.

Together, these data show the most proximate measures of pro-inflammatory activation differed at 1 hour between ASH and BSH groups. These effects were for ROS and p38 MAP kinase activation in the granulocyte cell sub-population. This inflammatory modulation was lost at later time points under study. In contrast, homogenate consumption did not alter p65 constitutively but there was strong attenuation of inducible p65 at later timepoints, irrespective of type of homogenate being consumed.

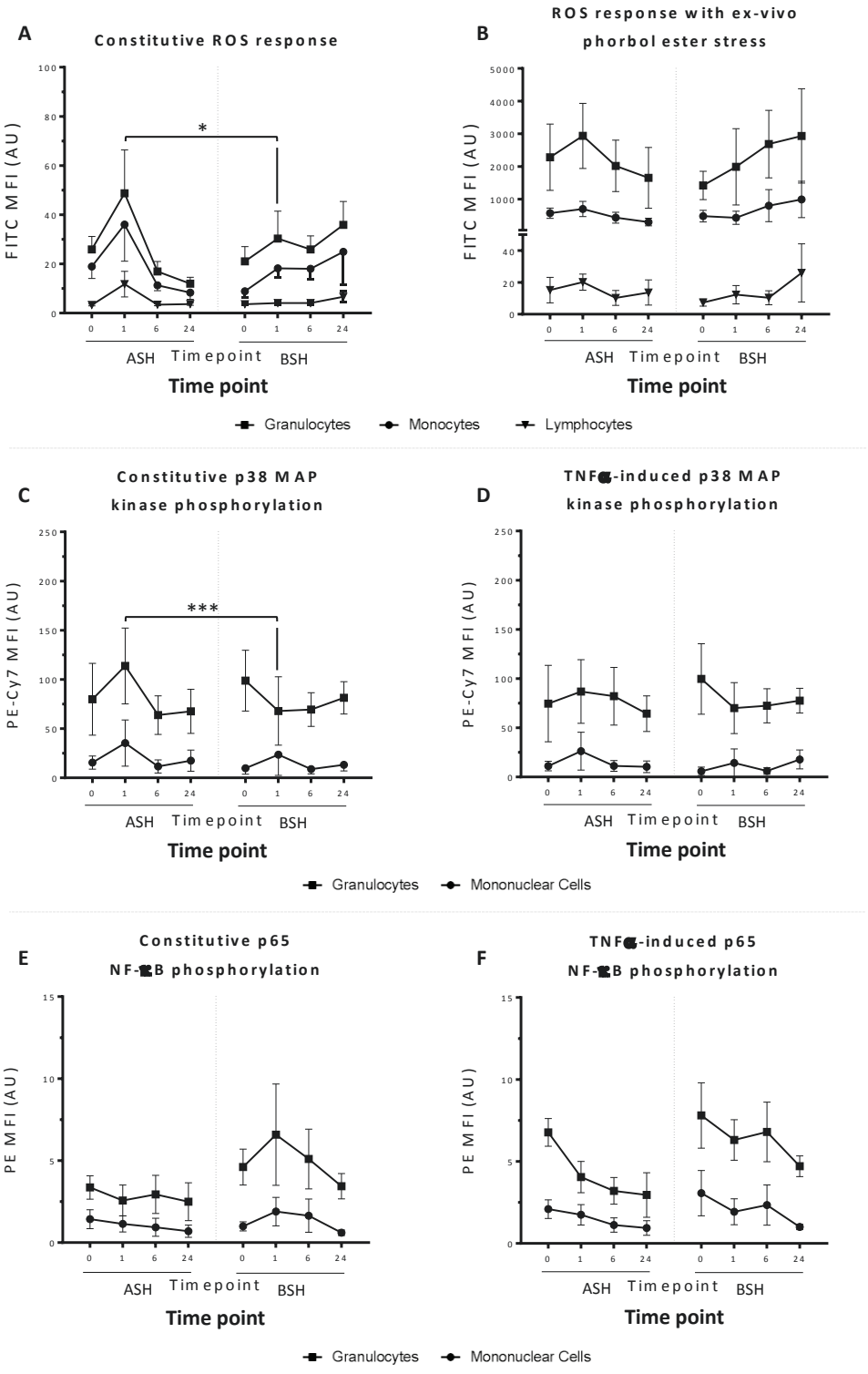

Figure 5.14 Effect of homogenate consumption on pro-inflammatory signalling

Six healthy volunteers consumed either BSH or ASH alternatively over a 24h period. Blood was sampled at 0 (prior to consumption), 1, 6 and 24 hours after. Leukocytes were loaded with the APF ROS-sensitive probe and left as controls (A) or stressed with PMA (B) with analysis by flow cytometry. Alternatively blood was immediately fixed and permeabilised prior to staining with antibodies to phospho-p38 MAP kinase (C) or phospho p65 (E) or subject to TNFα 20ng/ml stress for 30 minutes and then fixed/permeabilised/stained for phosho-p38 (D) or phospho-p65 (F) with subsequent analysis by flow cytometry. Pooled data (n=6) is shown ±SEM. Statistical results from mixed-regression modelling are shown. *p<0.05; ***p<0.005.

5.4 CONCLUSIONS

Investigation of the effects of sulforaphane in this chapter has led to the following summary observations:

- Pre-treatment of human leukocytes with sulforaphane in the micro-molar range for 1 hour's duration can reduce the induction of ROS and NF-κB activation, with a trend towards attenuation of p38 MAP kinase activation, ex-vivo.

- Surgery with CPB in pigs was associated with histological appearances of ATN and this response was suppressed by pre-treatment of animals with sulforaphane intravenous sulforaphane injections. This injection generated micro-molar concentrations of sulforaphane in the plasma throughout the duration of exposure to CPB.

- Surgery with CPB in pigs did not activate ROS, p38 MAP kinase nor NF-κB significantly in circulating leukocytes. Sulforaphane attenuated levels of p38 MAP kinase and NF-κB at 1-2hours

- CPB lead to the induction of IL-6 and IL-8 in circulating leukocytes and these inflammatory responses were reduced by sulforaphane pre-treatment, administered prior to CPB.

- Ingestion of sulforaphane-rich homogenates attenuates constitutive levels of leukocyte ROS and p38 MAP kinase 1 hour post-consumption.

- Ingestion of sulforaphane-rich homogenates generates sulforaphane concentrations in the 0.1μM range in humans.

5.5 DISCUSSION

5.5.1 Context and rationale for studies

When dealing with patients in a clinical setting, there can be considerable variability in their pathophysiology and response to treatment. For example, gender variation, age, degree of coronary disease, medical co-morbidities and variation in concurrent medication use. Operatively, variability arises in the duration of surgery and, inherently, the duration of exposure to CPB depending on the complexity of the operation. These variations in clinical and surgical characteristics may give rise to variable responses to treatment and to discrepant findings in research settings. Because of these factors we studied the influence of surgery and CPB on leukocyte activation in young healthy pigs under well-controlled experimental settings, and also assessed leukocyte responses using isolated cells.

Given the known role of p38 MAP kinase and NF-κB in the transcriptional induction and stability of pro-inflammatory molecules, we reasoned that targeting of these may dampen systemic inflammation in response to CPB. To test this hypothesis we pre-treated cells and experimental animals with sulforaphane and conducted a trial in human volunteers with precursor dietary form. Sulforaphane was selected for study because it is a potent indirect antioxidant that induces numerous endogenous anti-oxidant enzymes (e.g. HO-1, ferritin) via the transcription factor Nrf2. Moreover sulforaphane can suppress arterial inflammation in rodents and can inhibit MAP kinases and NF-κB in cultured vascular cells and leukocytes[322,374,484-486,492-494]. Sulforaphane appears to have relatively fast biological effects within 1-2 hours of treatment including induction of mRNA expression in leukocytes within one hours[501]; suppression of TNFα-induced p38 MAP kinase phosphorylation (but not JNK), reduced mRNA and protein levels of MCP-1 and VCAM-1 and reduction in TNFα-induced NF-κB activity within 1 hour of treatment[493,494] and down-regulation of iNOS and Cox-2 mRNA and protein expression within 2 hours[494]. Together, these observations suggest that Nrf2 is a fast-acting transcription factor and sulforaphane may possess anti-inflammatory effects independent of genes activated via the Nrf2/ARE pathway. The bioactivity of the

metabolites and sulfur components of this molecule also have effects independent of gene transcription. Further studies are required to distinguish between all these possible molecular scenarios.

5.5.2 The benefits of porcine models in cardiovascular research

In view of the complex multicellular nature of the mechanisms involved in systemic inflammation it is recognised that in vivo models are important for studying these processes. In vitro models of inflammation exist and there has been extensive work predominantly using human primary endothelial cells and human primary peripheral blood leukocytes. In vitro studies have generated a body of data, thus allowing focused questions to directed in vivo, so reducing significantly the number of animals required. The pig/large animal model was selected because pigs have a circulation that is anatomically and physiologically similar to humans. These animals possess arteries that develop comparable atherosclerotic lesions[524]. As an omnivore, the pig is also more similar metabolically to the human than rodents. Aside from these considerations, the pig is becoming an increasingly attractive species for vascular biology research, with sequencing of the porcine genome near completion and an expanding reagent base[525-527]. Importantly, the animal is of a suitable size to be connected to a conventional CPB circuit ordinarily used in clinical practice, without any adaptation. In the study presented, adult female landrace pigs were connected to a conventional CPB circuit for a uniform duration of 2 hours. This allowed assessment of the kinetics of leukocyte activation in response to cardiac surgery and CPB under well-controlled experimental conditions in young healthy animals. It also allowed detailed examination of inflammatory genes in various tissue compartments (heart, kidney, lung) not normally procured in human subjects.

A pure reductionist approach was taken with the large animal study in relation to cardiopulmonary bypass. The experimental design focused exclusively on the inflammatory

effects of cardiopulmonary bypass on leukocyte activation and tissue injury. The aim was not to reproduce the clinical scenario in its entirety but to address the important question of what was the isolated direct effect of surgery and cardiopulmonary bypass on pro-inflammatory signalling. A secondary consideration was what was the effect of surgery and bypass on tissues and the relative influence of sulforaphane on this process. There was no assessment of organ function at any point in the study (no echocardiography, no spirometry, and no renal assessment). This approach was taken to isolate alone the effect of CPB, without introducing the variable influence of heparin reversal, weaning off bypass (hypoxia re-oxygenation) and recovery. These are other important considerations for future studies.

5.5.3 Responses to sulforaphane

Sulforaphane administration in human and porcine models exhibited similar and contrasting effects (Table 5.2). NF-κB phosphorylation was reduced by sulforaphane in one or either leukocyte subsets in the isolated leukocytes and the large animal study but not in the BSH study. Sulforaphane inhibited p38 MAP kinase induction in pigs undergoing CPB selectively in mononuclear cells but not in TNFα-activated p38 MAP kinase in human leukocytes. ROS activity was attenuated in human isolated leukocyte and human homogenate studies but not in the porcine model. Several possibilities may afford an explanation for these observations. Firstly, although these are mammalian systems, it is possible that species differences alone can account for the differing reactivity of the individual leukocyte-activation pathways. Another consideration is the selective targeting of sulforaphane on the activated form of p38 MAP kinase, rather than the basal form. If we compare the levels of constitutive p38 MAP kinase in healthy controls (Table 4.7, first column) and to sedated animals in the antibody validation studies (Table 5.2, first column), we see that pigs have approximately double the magnitude of phosphorylated p38 MAP kinase, on the same scale; but possess similar degrees of reactivity to a stressor. This pattern is reversed in the levels of phosphorylated p65 NF-κB; humans have constitutively double the level, on the same scale. The biological relevance of

this is uncertain but may contribute to the varied responses seen between the porcine CPB and mini CPB study. Indeed, in the human CPB studies, p38 MAP kinase was inducible and p65 was to a large degree not inducible by CPB. The reverse pattern was observed in the large animal CPB study; the higher constitutive p38 MAP kinase levels may have approached maximal, thus minimising any enhancement in response to surgery and CPB, whereas lower basal constitutive levels of p65 NF-κB may allow activation. Indeed, the magnitude of the basal p38 MAP kinase response in the large animal CPB study (Table 5.2, third column) is almost twice that of the maximal response in the human mini CPB study (Table 4.7, third column). Perhaps accounting for some of the differences; the humans in the clinical trial were older adults (mean age of 67 years) whereas the large animals were considerably younger pigs (approximately 4-6 months old) without co-morbidity. The animals used in the study were all female, whereas the population in the clinical study was predominantly male (18 out of 26 subjects). The precise effects of sex on inflammation and cardiovascular risk have not yet been precisely defined. However, population studies have shown a reduced cardiovascular risk in women[528] and a potential mechanism for this is the capacity to resist oxidative stress from hormonal influences[529,530]. This may account in part for the observation of relatively little ROS induction in response to exposure to CPB seen in pigs, compared to the clinical study (compare and Figure 5.8). Of course, there may be species differences to explain the divergent findings; a possible explanation is that CPB in pigs was associated with NF-κB activation, by phosphorylation, at Ser529 but in humans, other NF-κB phosphorylation sites may be the key position which we have not been able to detect (e.g. Ser 536) as these are known to respond differently to other upstream DAMP-signalling cascade events[214,531].

The other significant difference between experiments is the physiological dose and distribution of sulforaphane between experiments (Table 4.7, second row). Plasma levels ranged between 0.1 μM - 10μM. However, it is the kinetic of distribution and tissue bioavailability that is important, and not measured. This is an important consideration when

reviewing the differences between leukocyte and lung, kidney and myocardial effects and different mRNA expression kinetics..

Sulforaphane has previously been shown to have a protective effect in reducing inflammation and suppression of p38 MAP kinase and NF-κB in small animal models by our group[374]. This study has also shown for the first time that sulforaphane pre-treatment protects against renal damage and systemic inflammation in response to CPB. This mechanism is associated with inhibition of p38 MAP kinase activation and NF-κB activation in leukocytes and may involve reperfusion injury and contact-activation of blood components[223,532]. Notably, IL-6 induction in leukocytes was evident at the time of cannulation *prior* to CPB, indicating that median sternotomy and/or cannulation of the aorta and right atrium per se was sufficient to activate inflammatory signalling in leukocytes. It is likely that sternotomy and cannulation trigger inflammatory pathways by promoting the release of damage associated molecular patterns into the circulation[181,207], however further studies are required to identify the particular molecular triggers that are responsible. Although treatment with sulforaphane reduced the early appearance of acute tubular necrosis in response to CPB, it did not influence inflammatory signalling or cytokine expression in renal tissues. This was an unexpected histological finding as gross tissue architecture was not disrupted in the lung nor the myocardium. The incidence of acute kidney injury is approximately 30% in patients undergoing cardiac surgery with CPB, the effects manifest in the first few days following surgery, with approximately 1/100 patients needing some form of support therapy[102]. Other groups have reported histological features of tubular injury after 2 hours of CPB exposure[533]. These precede any functional manifestations of kidney injury (oligouria), acidosis, hyperkalaemia as well as biomarker changes; traditionally creatinine but experimentally including neutrophil gelatinase-associated lipocalin. Our experiments were targeted to evaluate the distinct effect of CPB alone, the study was terminated and organs immediately harvested. There was no functional data for the kidney nor other biochemical markers. These may be useful in future studies on the effects of CPB on physiology and influence of

sulforaphane on these processes. Nevertheless, our data suggest that sulforaphane protects the kidney from injury in response to CPB via inactivation of inflammatory signalling pathways in circulating leukocytes. Although the mechanism underlying the differential effects of sulforaphane on leukocyte and non-immune tissues remains uncertain, it is plausible that the bioavailability of this compound is elevated in the circulation and/or that leukocytes are particularly sensitive to endogenous antioxidants.

The clinical trial of homogenate consumption was notably different to investigations in isolated leukocytes and the large animal study. The study was designed to assess whether delivering a precursor form of sulforaphane could generate biologically significant levels in the plasma and whether this in turn would influence pro-inflammatory signalling. In a previous study, consumption of broccoli homogenate, purchased from a local supermarket, generated a peak plasma concentration of 12.15ng/ml achieved[412]. The plasma levels achieved in our human study presented at peak was 30.68 ng/ml (and the context of these in relation to the other studies is set out in Table 5.2, row 2). This is one order of magnitude lower than in the large animal study, but the comparison also needs to take into account the absorption from the jejunum, passage through the enteric circulation; hepatic metabolism and then controlled plasma distribution prior to accumulation in tissues. This, of course is physiologically different to the mode of pure sulforaphane administration intravenously which results in rapid high levels of sulforaphane in the plasma.

Previous studies have shown that 1μM plasma concentrations occur transiently with oral consumption of sulforaphane-rich preparations. In the isolated human leukocyte pre-treatment studies, 1μM concentrations appear to have effects on ROS and p65 activation under the conditions evaluated, and less so on p38 MAP kinase phosphorylation. The effects appear to be most manifest with 5-10μM concentrations used. It is possible that the stimuli utilised (TNFα 20ng/ml and PMA 200ng/ml) could not be overcome by pre-treatment, and future studies should assess the effect of sulforaphane on responses to lower concentrations of

TNFα or PMA. Given the actual dose measured in the plasma (approximately 0.1μM in humans fed broccoli), future experiments may be directed at these levels of concentrations and titrating effects to external stressors.

NF-κB was unaffected and ROS and p38 MAP kinase suppressed in the BSH study. The influence of BSH appeared most prominent 1 hour following ingestion, in keeping with the known pharmacokinetics of sulforaphane[411,412,505]. At later timepoints, there was no effect in leukocytes despite the induction and persistence of anti-inflammatory gene expression reported in the literature[505]. It is difficult to interpret data at later timepoints due to the other interactions and metabolic changes with trial participants and firm conclusions cannot be reached. The constitutive levels that are measured are influenced throughout the day by multiple stimulating events. There were no restrictions on what participants did throughout the duration of the study after the homogenate was consumed. Thus, going for a curry and ingesting curcumin[534] or drinking red wine and ingesting resveratrol[535] could potentially lead to variable responses between individuals. There is a whole host of biologically active nutriceutical research taking place and any one of these factors may influence the results seen. In addition, exercise can enhance NF-κB and ROS-interactions in mammalian systems[536,537]. Thus, the time point which we can be most confident of our data is at 1 hour (before too many confounding factors have taken place). Ex-vivo stress was applied to leukocytes to test their reactivity. Patterns of activation appear to be different but because of the variability of response, it was difficult to draw sound conclusions on the basis of the data.

It is also plausible that other additional compounds in BSH (and ASH) are responsible for some part of these observations, or that individuals exhibit differing pharmacokinetic and pharmacodynamic profiles to the ingestion of this preparation with perhaps an underlying genetic polymorphism. It is also possible that study participants were able to tell the difference between homogenates, and in doing so modify subsequent behaviour. Despite this potential for bias, allocation concealment was found to be adequate; in post-study electronic

questionnaires, 3 out of 6 participants correctly guessed the order in which they had received their homogenates. The appearance, smell and taste of the preparations of the homogenate aliquots was unappealing. This needs to be improved in future studies using homogenate preparations (e.g. with other flavourings), or abrogated using purified forms of this agent. Reassuringly, there were no adverse effects reported, but clearly the study was not powered for untoward events. Further studies are required to examine whether consumption of sulforaphane-containing vegetables prior to surgery with CPB can benefit patients by reducing systemic inflammation.

One final interesting observation arises when considering the levels of pro-inflammatory marker activation in the homogenate study population (Table 5.2, fourth column) and the other healthy population from chapter 3 (Table 4.7, first column). The healthy population in the BSH study is well-defined with stringent inclusion and exclusion criteria, characterised by low BMI and youth and a non-smoking history (defined in 2.2.17.2, page 120). Blood from otherwise 'healthy volunteers' comes from a much broader population (of individuals of apparent good health, willing to donate blood). The clear differences between these two populations are the levels of constitutive ROS as well as the attenuated degree of reactivity to inducible ROS forms. This may represent better long-term redox status and health. Data from the healthy sulforaphane leukocyte pre-treatment population (Table 5.2, second column) are not comparable to other groups due to the inherently different experimental design which accounts for the differences in pro-inflammatory markers, particularly p38 MAP kinase levels – reflecting the effect of DMSO vehicle/sulforaphane treatment and then conventional assay applications.

	antibody optimisation assays (leukocytes from sedated animals)	Sulforaphane pre-treatment (Leukocytes from healthy volunteers)		Sulforaphane in cardiopulmonary bypass (Large animals)		Broccoli homogenate consumption trial (Healthy volunteers)	
Sulforaphane conditions	No sulforaphane	Pre-incubation for 1 hour with varying doses		2mg/kg iv 106 minutes before CPB		Dietary homogenate supplement	
Plasma conc.	N/A	1µM-10µM		1.1µM -1.9µM		0.05µM – 0.16µM	
ROS	N/A	APF Basal G: 53.0 ± 31.5 Mx: 84.3 ± 38.9 L: 4.1 ± 0.3 APF Peak G: 4133 ± 984 (+PMA) Mx: 673 ± 286 (+PMA) L: 17.1 ± 7.5 (+PMA)		APF Basal G: 9.92 ± 4.55 M: 4.90 ± 5.98 APF Peak G:12.25 ± 7.37 (CPB 2h) M:6.41 ± 9.50 (CPB 2h)		APF Basal G: 25.0 ± 12.99 Mx: 18.9 ± 11.8 L: 3.3 ± 0.9 APF Peak G: 2936 ± 2441 (+PMA) Mx: 570 ± 388 (+PMA) L: 15.2 ± 19.7 (+PMA)	
p38 MAP kinase	Basal G: 101.2 ± 25.3 M: 4.1 ± 8.7 Peak G: 172.3 ± 15.0 (TNF) M: 8.7 ± 1.9 (TNF)	Basal G: 13.42 ± 14.52 M: 1.5 ± 1.44 Peak G: 33.38 ± 34.59 (TNF) M: 2.62 ± 2.34 (TNF)		Basal G: 241.9 ± 79.3 M: 5.0 ± 3.6 Peak G: Same as Basal M: 11.55 ± (CPB 1h)		Basal G: 79.84 ± 89.36 M: 15.5 ± 16.2 Peak G: 113.73 ± 94.3 (1h) M: 35.4 ± 57.6	
p65 NF-κB	Basal G: 1.01 ± 0.1 M: 1.22 ± 0.2 Peak G: 5.6 ± 0.6 (TNF) M: 7.0 ± 1.5 (TNF)	Basal G: 5.26 ± 4.24 M: 3.18 ± 1.99 Peak G: 8.53 ± 4.70 (TNF) M: 8.55 ± 5.03 (TNF)		Basal G: 2.46 ± 1.18 M: 2.18 ± 0.72 Peak G: 3.46 ± 0.68 (CPB 1h) M: 3.12 ± 0.58 (CPB 1h)		Basal G: 3.36 ± 1.75 M: 1.43 ± 1.41 Peak G: Same as basal M: Same as basal	
		Cell subpopulation					
	Marker	G	L	G	M	G	L
Effect of Sulforaphane	ROS	↔	↓	↔	↔	↓	↔
	p38 MAP kinase	↔	↔	↔	↓	↓	↔
	p65 NF-κB	↓	↔	↓	↓	↔	↔

Table 5.2 Comparative levels of intracellular pro-inflammatory markers and summary of sulforaphane experiments

Summary data from experiments presented for granulocytes (G), monocytes (Mx), lymphocytes (L) or mononuclear cells (M). Values are given in their respective MFI units.

CHAPTER 6. DISCUSSION

6.1 SUMMARY

6.1.1 Main conclusions of study

- The inflammatory response to cardiac surgery with CPB involves induction of ROS and activation of signalling pathways (e.g. p38 MAP kinase, NF-κB) as early events in leukocyte activation.

- Although molecular changes in response to cardiac surgery with CPB were broadly similar in the porcine model and patients undergoing CABG, there were also notable differences.

- Activation of leukocytes was observed following surgical access but prior to CPB initiation, demonstrating that surgical preparation is sufficient to drive inflammatory signalling.

- Activation of p38 MAP kinase and induction of ROS were lower in patients exposed to mCPB compared to cCPB, suggesting a potential molecular mechanism for the anti-inflammatory effects of mCPB.

- Pre-treatment with sulforaphane reduced NF-κB and p38 MAP kinase activation in leukocytes in response to CPB in the porcine model.

- A small clinical trial suggested that consumption of sulforaphane-rich broccoli sprouts may reduce p38 MAP kinase and ROS activation in humans.

6.1.2 Global context for studies

The thesis presented addresses an important aspect of clinical care, one where there remains many unresolved challenges. The focus of this research endeavour was directed towards reducing the morbidity and mortality associated with the use of extracorporeal circulation in adults. This was conducted by (1) assessing the effects of optimisation of cardiopulmonary bypass technology in the form of miniaturised cardiopulmonary bypass; (2) application of novel ways of measuring the early events in the leukocyte activation cascade and (3) consideration of a pharmacological agent capable of inducing a more favourable cellular and end-organ tissue response following surgery. The pinnacle of cardiac surgery is the ability to restore the optimal function of the heart, without causing neither morbidity nor mortality, in the most elegant way possible. Cardiac surgery has progressed tremendously with constant improvements and technological innovations moving ever-closer towards this apotheosis. There have been many significant developments. Over the last six decades, as surgery on the heart became a reality and a routine aspect of clinical care, there have been refinements in surgical techniques; improvement in peri-operative care management and a more detailed understanding of the molecular mechanisms that drive disease processes. This has made us better clinicians and enhanced the lives of our patients.

Here the novel hypothesis that cardiac surgery promotes systemic inflammation via ROS induction and activation of p38 MAP kinase and NF-κB in leukocytes was tested. This is an important consideration in the recovery and survival of patients undergoing surgery with the use of cardiopulmonary bypass.

6.1.3 The research question and experimental model selection and design

The focus of the research here from the outset was *what is the contribution of cardiopulmonary bypass to pro-inflammatory activation in patients*? The use of cardiopulmonary bypass support technology is only one factor in the complex process of

surgery that contributes to inflammation. There are other factors to consider including the type of surgery (the operative approach), the anticoagulation, cross-clamping, aortic de-clamping, protamine reversal, re-ventilation and recovery from anaesthesia in the immediate peri-operative period. These are important events clinically but have the potential to overshadow the scientific question addressed here (ie. miniaturised vs conventional CPB) as they themselves may influence inflammation and injury. There needs to be a balance between replication and reductionist approaches to scientific interrogation. In many ways the situation can be considered to the analogous set up of cell culture being truly reflective of functional *in vivo* endothelium? Can a large animal model truly represent the human condition? The important point to note is, what is fundamentally the question being asked and the degree of certainty, the power, that is required of the study.

A criticism of the clinical study was that the timing of blood sampling did not correspond with clinical events, and that changes at time points such as at the termination of bypass and cross-clamp release would be of interest. There is no question that these are important transition periods, and a potential rebuttal to these suggestions was that these time points occur variably with the conduct and progression of the surgery and do not reflect a dynamic change in kinetic activity of the effect of CPB. However, if the aim of a study is to understand both dynamic kinetic changes and also the changes at operative transition points then both types of measurements can take place in parallel in future experiments – i.e. (a) in the first run specimens being taken at baseline; post anaesthetic; start of bypass up until 6, 12, 24 hour periods as required and (b) in the parallel run: specimens taken for post-sternotomy, post-aortic cannulation, post initiation of bypass; post cross clamp application; post-cardioplegia; post aortic declamping etc. The approach of parallel blood sampling could yield mechanistic links between intervention and temporal changes observed with the use of cardiopulmonary bypass systems. Of note, in the clinical miniaturised CPB study, the median bypass times were 71-74 minutes in the two groups. This means the CPB exposure was variable, and in fact 5/26 patients were off CPB support at the 1 hour time point. Therefore

the only reliable time point where we are certain the CPB stimulus is ongoing is between the start (0 time point) and 30 minutes. This is a very short time frame to make any inferences regarding the direct influence of CPB. Correspondingly, there is variation in how long CPB has been discontinued for at the 2 hour mark, but may be an observation that correlates with the falls in p38 MAP kinase levels that are induced at the earlier time points in the miniaturised CPB study (Figure 4.3)(Figure 4.7) and to a far less convincing observation in the large animal study (Figure 5.6A). The duration of CPB exposure was considered to be a relatively short period of time that clinically is not usually associated with the induction of SIRS (and we could not ethically justify prolonging the exposure to CPB for research purposes). The alternative consideration of extended bypass times (e.g. 4-6 hours) has the criticism that this is not representative of the actual conduct in practice. Therefore, to achieve balance, in the large animal study presented in chapter 5, a duration 2 hours of CPB was used so that an effectively long period of CPB was ensured and that blood sampling at 'late' time points were taken whilst the stimulus of CPB was ongoing.

For a similar reason a criticism of the large animal cardiopulmonary bypass study was the poor homology and replication with the human clinical scenario. In particular the absence of cardioplegia, cross-clamping, protamine reversal, weaning from bypass and recovery. The approach used in the animal study was centred on the influence of CPB exposure only. Future work could easily replicate these clinical scenarios and address these aspects of the study design to focus on the transition points of interest.

Cardiac surgery is a team exercise and a functional team determines a good functional outcome for patients. The miniaturised cardiopulmonary bypass trial was designed around the practice of one surgeon to minimise variability in practice (and therefore conceptually facilitates tight experimental control). However, the team itself may be variable given the surgical assistants; nursing staff; anaesthetic staff and perfusion staff. We took great care in standardising anaesthesia for all patients in the clinical trial, as well as in the large animal

study. The second aspect of this is that the study has generated surgeon-specific data that may not translate appreciably with the practice of other surgeons. Indeed, for example, the trial surgeon uses a method of cardiac arrest that employs cross-clamp fibrillation. The findings may not be translatable to the scenario of blood cardioplegia that is used more widespread and there are inherent myocardial energetics derangements between these different cardioprotection techniques. Future small studies therefore should be well-controlled in well-defined populations to eliminate noise or expanded to multi-centre large studies to even out the distributions of variability. Indeed, a criticism of the human study miniaturised bypass study was that the patient population was meticulously well-defined, well-controlled and low risk and therefore unlikely to benefit from the (presumably protective) effects of bypass optimisation.

6.1.4 Alternative perspectives on considering the question of CPB and injury

From a technological perspective, the question arises of whether there are further gains to be made in the optimisation of bypass systems or are we approaching a plateau with the technology? This leads to two follow-on considerations (1) can there be any better approach with the application of the technology or (2) do we need to fundamentally do something different?

The first consideration is one around engineering, and the answer is yes there are better versions of bypass available, with caveats. If the starting point is that cardiopulmonary bypass is deleterious because it is not physiological due to flow differences and that biomaterial effects trigger inflammation and injury, then truly physiological bypass is possible in the form of cross-circulation. This was an idea of Lillihei in the 1960s using a larger adult to provide the circulatory support for a smaller child. Lillihei had a successful run of patients and no reported deaths[83]. However, this technique has never since been used given the potential risk of 200% mortality. These approaches were developed at a time when

research was less stringently regulated; when there were no alternatives readily available (like CPB) and when there were no effective cures for some of these heart conditions. The world is now a different place. However, experimentally, this approach affords the opportunity to provide a means of 'extracorporeal' circulation using lungs and heart of 'donor' for a 'recipient'. Such an experimental design could be conducted in inbred animals. This would allow the delineation of the effect of surgery alone and the independent effect of physiological bypass in cloned animals. Of course, the degree of control of physiological and haemodynamic parameters would be difficult in this scenario and it would be difficult (impossible) to identify the source of DAMPs and cytokines from 'donor' or 'recipient' if the circulations are interconnected. However, what this proposed model would be able to distinguish is the effects on end-organ injury with physiological bypass only driven by surgery and presumed DAMPs generation.

The second consideration is about application. Can we apply cardiopulmonary bypass better or what can we do differently? The scenario of off-pump surgery allows for some mechanistic insight into surgery and is often used as a negative control group for comparisons with CPB. The answers that arise from OPCAB studies are not always clear and in agreement with each other. OPCAB can cause SIRS and a multitude of deleterious effects and clearly, is restricted to operations on the surface of the heart, and not open-heart procedures. Miniaturised CPB systems use smaller volumes of prime to reduce blood dilution and are associated with less blood loss and blood transfusion requirements. The inflammatory mechanisms of miniaturised optimised systems was investigated in this thesis. Alternative manipulations in providing pulsatile blood flow (with intra-aortic balloon counter-pulsation) and maintaining the lung as a physiological oxygenator (using the Drew-Anderson bypass technique) have been used independently with reported improvements in inflammatory markers[91,95,170,406-408409,410]. A combination of these approaches may yield a protective synergistic effect (e.g. miniaturised bypass with pulsatile flow and maintained pulmonary circulation/ventilation). Finally, the group of patients who undergo valve implantation

percutaneously may be a group of interest to evaluate the effect of instrumentation/intervention on significant structures in the heart and the associated molecular triggers of inflammation. These are all potential patient groups for consideration in future work.

6.1.5 Detection of in vivo ROS

The role of ROS during cellular signalling is expanding and we have an understanding that sub-lethal changes in ROS events alter signalling cascades and pathways. Fundamentally, these events occur in vivo over short time frames, intracellularly, and therefore present particularly difficult challenges to localise and quantitatively detect. The assays used throughout this thesis has been ex-vivo in nature and in some circumstances evaluated with an additional stressor (Figure 3.5)(Figure 4.1)(Figure 4.2)(Figure 5.5B). These assays therefore are only able to describe the very proximate measure of ex-vivo ROS inducibility. This is the major limitation on the interpretation of the data using this assay. The assays are intrinsically measuring a redox flux event that has already been and gone. The changes that have been measured in the studies, in the presumably constitutive levels of ROS, are - or would appear to be - very subtle next to the magnitudes of the responses seen with stressors, particularly the potent effect of phorbol esters (compare Figure 4.1 and Figure 4.2, with and without stressors]. A criticism of the molecular probes used (particularly DCF) can be inherent instability and auto-fluorescence which presents an unfavourable signal-to-noise ratio. The least auto fluorescent probe (APF) was selected for experimentation and gave excellent results in the presence of a stressor. However, adding a stressor may amplify a ROS-response; but this may be a pathophysiological response and not necessarily simply amplification of the magnitude of a physiological response that was measurable on a smaller scale. Therefore the ex-vivo stressed blood from CPB patients in the ROS pilot studies that are particularly enhanced with APF (Figure 4.2) must be interpreted with caution for this reason, and also the many confounding contributions at this late time point that have been discussed in the summary of

chapter 4. The holy grail of ROS focused research lies in understanding the effectiveness of redox signalling within compartments (i.e. spatial differentiation between cytosolic or mitochondrial in origin) over miniscule time frames with specific live-cell *in vivo* markers that are sensitive to these ROS changes. At present there are no markers in routine experimental use in humans that facilitates quantitative spatial-temporal resolution of ROS. Nanoparticle research is emerging in the literature from animal studies as new forms of *in vivo* probes are developed for molecular interrogation[538]. However, there are questions about reproducibility of data and the toxicity of the nanoparticle approaches that cloud the interpretation of results.

6.1.6 Reliability and validity of pro-inflammatory assays

The assays developed in this series of studies show both sensitivity and specificity for constitutive and inducible levels of ROS (Figure 3.5), p38 MAP kinase (Figure 3.3B, Fig Figure 3.4A) and p65 NF-κB (Figure 3.3C, Figure 3.4B) under well-controlled conditions in isolated leukocytes. However, when applied to different groups of healthy volunteers and patients in clinical scenarios, we see there are of variations between different groups and across species – e.g. higher basal phosphorylated forms of p38 MAP kinase in complex surgical patients compared to health volunteers (Table 4.7, Table 5.2). The potential explanations for these observations have already been covered in more detail in the discussions for Chapter 4 and Chapter 5. The corollary of this is that these absolute values need to be interpreted within context. Flow cytometry is best at describing relative changes and much more work is required to standardise and normalise values between patients and scenarios. It is recognised that these signalling molecules exhibit cross-talk phenomena with interdependent regulation of cascades. As such, p38 MAP kinase and NF-κB signalling events do not occur independently, in isolation, but are instead key nodes within a multi-redundant network regulated by ROS. These markers may be a long way off from being

meaningful clinical markers of active inflammation with power to predict clinically meaningful events.

6.1.7 Identification of leukocytes and assessment of leukocyte activation

Flow cytometry was used as the analytical tool of choice to evaluate leukocyte events throughout this thesis. This approach afforded the opportunity to examine leukocytes on an individual cell basis rapidly in multiple samples. The drawback to this technique is that relative changes are measured intrinsically. Measurements are only directly comparable if performed on the same instrument with the same settings for gates, lasers and thresholds. The data in this thesis are presented as absolute direct values from the instrument. An alternative method of presenting the data from the experiments could be on normalised data and may have been equally appropriate in the analysis of findings. Alternative means of assessing p38 MAP kinase and p65 NF-κB protein expression were considered too slow and required higher volumes of blood starting material (e.g. by Western blotting) – two aspects not compatible with the design of the CPB studies. Pilot experiments with PBMC were conducted but these were not pursued further due to the volumes of blood needed; the time effort required for separation; the limitation of only the mononuclear cell fraction being available (instead of additional assessment of granulocytes) and fundamentally processing and handling the leukocytes altered their intracellular signalling characteristics.

The accumulation of leukocytes in tissue was evaluated using the cantharidin blister assay. This facilitated the limited assessment margination of leukocytes into skin; a composite endpoint of local cantharidin inflammation in addition to the component from systemic inflammation induced by surgery and cardiopulmonary bypass. This demonstrated movement into blisters in response to surgery and CPB in keeping with other studies[195,278]. However, this assay had no discriminating power between the differing types of CPB technology under assessment; it quantifies margination at only two time points (in comparison to multi-point

analysis in blood) in a single organ compartment that has little direct clinical relevance, despite being the largest organ of the body. Indeed, how skin inflammation and lung or heart inflammation are related are not precisely understood. However, the technique did give unique insight into the egression of leukocytes from the vasculature which is a step beyond the mechanistic considerations of other clinical studies of inflammation due to CPB.

Alternatively, radiolabelled white cell scanning can be a useful tool to demonstrate tissue localisation of leukocytes from the systemic circulation in future studies. This is expected to occur the most in the lung and may be used as an index marker of systemic inflammation. PET-CT may be considered as a complementary means for imaging lung inflammation and may be of benefit when included in other future studies. In addition to considering where leukocytes marginate to, the origin of leukocytes and mobilisation (e.g. bone marrow versus circulating) may be of equal importance. Proximate measures may include plasma levels of G-CSF, SDF-1 and distinguishing markers of old and new leukocytes in the circulation such as CXCR4 expression.

6.1.8 Upstream events from pro-inflammatory signalling

As the clinical study progressed in parallel with the animal studies, the observation that ROS (Figure 4.6), p38 MAP kinase (Figure 4.3A, Figure 4.7A) and IL-6 induction (Figure 5.9B) were activated early, in some cases preceding the start of CPB, directed attention away from CPB being the initiating molecular trigger and more upstream events that influence leukocyte behaviour were considered. These were the DAMPs, as discussed in 1.4.4, page 46. Future studies should consider the release of DAMPs into the circulation; receptor expression and receptor distribution for these molecules. A starting group of DAMPs that may be suitable are mtDNA fragments which signal via TLRs. Having identified the kinetics of release of mtDNA, follow up experiments could assess the activation of inflammatory in the dose ranges identified (mimicking the kinetics of release) with readouts such as the ROS; the

general family of MAP kinase markers (such as the ones evaluated here); but also on the presumed negative regulation of apoptosis markers of immune cells and expression of adhesion molecules phenotypically. Furthermore, TLR-receptor antagonism may be assessed using molecular inhibitors or assessment of inflammation in mice where TLR is genetically deleted in specific cell types (using cre/lox technology)[539].

6.1.9 Downstream events from pro-inflammatory signalling

ROS, the MAP kinases and NF-κB have been presented as pro-inflammatory molecules and have a plethora of effects downstream from activation including the expression of adhesion molecules, the promoting of migration and upregulation of inflammatory cytokines. But in addition, along this spectrum of activity are the apoptosis regulatory pathways as well as cytoprotective effects necessary in the resolution of inflammation. In the pig model, pro-inflammatory gene expression was assessed in leukocytes as well as tissue compartments. The genetic networks that are activated following CPB and OPCAB have been mapped linking inflammation-ischaemia-reperfusion as well as cytoprotection[223,224]. These need to be probed and explored further and precisely defined in miniaturised CPB scenarios. A true and complete mechanistic understanding of the activating cascade, the genetic induction, the message transcription, the protein expression and regulation with resultant phenotypical effects on cells and tissues would be very powerful and convincing in future studies. The large animal study reported here made attempts at linking together mechanistic pro-inflammatory signalling events with cytokine gene transcription in leukocytes within the vascular compartment with effects on gene transcripts, protein expression and histological manifestations. In leukocytes, the attenuation of p38 MAP kinase and p65 NF-κB (Figure 5.7) correlated with reduction in mRNA transcripts for IL-8 and TNFα (Figure 5.9). However, the up-regulation of these transcripts in control animals did not correlate with an expected enhancement of p38 MAP kinase nor and expected enhancement of p65 NF-κB. The reasons for these apparent discrepancies may lie in the multi-redundant nature of

inflammatory signalling and other MAP kinases (such as JNK or ERK) or different sites of phosphorylation in NF-κB may drive inflammation in porcine leukocytes preferentially at the points of sampling in the study, and reduction of constitutive p38 MAP kinases and p65 NF-κB are more tightly linked to inflammatory suppression. The interpretation of these interactions can be complex and underlies the results in tissues where there are no phosphorylated forms of p38 MAP kinase or p65 NF-κB, yet changes at a transcriptional level genetically (Figure 5.10-Figure 5.12).

6.2 FUTURE WORK

6.2.1 Evaluate the role and mechanisms of DAMPs in CPB

To define the specific factors that are responsible for ROS and p38 MAP kinase activation in cardiac surgery patients, further studies should be carried out on patients in different surgical and clinical contexts. This should be considered for the off-pump group for coronary revascularisation in a randomised-controlled trial to evaluate the true effect of CPB (or its absence). Additionally, analysis of patients undergoing coronary artery bypass graft surgery via a minimally invasive approach (e.g. through minimal access surgery via anterior thoracotomy, or with a minimalist robotic-thoracoscopic approach) with general anaesthesia would allow the potential response of leukocytes to anaesthetic induction to be assessed independently from median sternotomy. It would be important to correlate the changes in ROS, p38 MAP kinase, NF-κB with biochemical changes in DAMPs such as the release of mitochondrial DNA fragments and their signalling interactions in these proposed scenarios.

Use of electrocautery, with a Bovie device, channels electrical energy through a patient's body and causes controlled diathermy burns at localised points directed by the tip of the device. This is a safe and effective means of achieving dissection and haemostasis during operative procedures. The use of an alternative dissection tool, causing only localised tissue damage, without the necessity for whole body electrical energy conduction, exists in the form of a harmonic scalpel (which dissects using vibration) would facilitate the evaluation of the effects of diathermy on DAMPs and pro-inflammatory signalling.

6.2.2 Evaluate the inflammatory stress profile during prolonged CPB

It is in the scenarios of long CPB exposure that mCPB is hypothesized to be of most benefit and utility, considering the counterpoint position of prolonged conventional-CPB to be deleterious clinically. Prolonged CPB scenarios are expected in complex cardiac procedures (e.g. double valve replacement, re-do valve surgery, aortic root and arch surgery) where the

patient also possesses concurrent, inherent, increased peri-operative risk. These are patient populations to be considered for future evaluations of the effects of conventional versus miniaturised CPB systems. However, when one considers these groups, they represent diverse patient populations (even more so than coronary disease) with multi-systemic complications from their heart disease (e.g. associated pulmonary hypertension and hepatic venous congestion in mitral and tricuspid valvular disease) which may lead to high variation in inflammatory responses and complexities in the interpretation of data.

6.2.3 Delineate the pro-inflammatory changes in aortic valve implantation without the use of cardiopulmonary bypass

A stepping stone between these high-risk, prolonged CPB patients, would be to consider the evaluation of pro-inflammatory signalling in the context of aortic interventions. Aortic valve replacement surgery is the commonest valve procedure performed in the UK and as yet no detailed evaluation of leukocyte signalling has been formally conducted with this procedure. This also affords the opportunity to evaluate a comparable procedure on the aortic valve that does not require the use of CPB, namely Transcatheter Aortic Valve Implantation (TAVI) with aortic valve replacement surgery. The process of TAVI involves implantation of an expandable tissue aortic valve performed percutaneously. This scenario lends well to the evaluation of intracardiac intervention, with anaesthesia, in the absence of cardiopulmonary bypass. Two complicating factors to consider for this are firstly, the current practice of offering TAVI to those patients who are considered *unsuitable* for surgery (i.e. usually having an adverse mortality profile for open heart procedures), and secondly the TAVI valve results do not compare favourably to the characteristics of the valves implanted by open heart procedures. This trial really should only be considered when the technology has reached a standard of non-inferiority, and the procedure can be offered to all patients, rather than selectively, so meaningful inflammatory comparisons can be made in equivalent patient

populations. Pilot data would be illuminating and a TAVI programme exists at the Hammersmith site for a trial of this nature to take place.

6.2.4 Establish a robust multi-faceted model for evaluation and optimisation of CPB technology

There is a need to establish a meaningful way to precisely assess the inflammatory response at multiple levels of the activating cascade. This is of particular importance to CPB and can be applied to other inflammatory systems and conditions. A multi-modality assessment in pigs is possible given their favourable research characteristics. This can build upon the work in this thesis by assessing plasma markers of injury; intracellular assessment of markers of leukocyte activation; multiple cascades of skin blisters to assess leukocyte movement at multiple timepoints; intravital microscopy of porcine peritoneum under anaesthesia; tissue biopsy to assess gene and protein expression (e.g. using RNA sequencing and proteomic technologies to provide an unbiased approach to determine effects on CPB on expression profiles). Furthermore, this can be combined with imaging modalities to provide functional data; echocardiographic assessment of myocardial function; myocardial perfusion imaging to assess ischaemia; PET-CT imaging can determine areas of increased metabolic activity in the lung and combined with haemodynamic monitoring and lung function monitoring whilst anaesthetised and ventilated. The logistics of this is difficult but application of this would yield tremendous mechanistic insights.

6.2.5 Evaluate the combined effect of miniaturised CPB with sulforaphane pre-treatment

The data presented in this thesis has shown that mCPB and sulforaphane can reduce inflammatory activation in response to cardiac surgery with CPB. The molecular basis for the attenuated inflammatory effects of mCPB remains unknown. Nevertheless, it is plausible that these two interventions may have additive or synergistic effects to attenuate pro-inflammatory

activation. This hypothesis could be tested in a porcine model involving 4 groups of animals. Adult pigs would receive cCPB or mCPB with either sulforaphane or a saline injection as control. Similarly, this concept could be tested clinically in future studies in patients about to undergo cardiac surgery.

CHAPTER 7. REFERENCES

1. Weber C, Noels H. Atherosclerosis: current pathogenesis and therapeutic options. *Nat Med.* 2011;17(11):1410-1422.

2. Liu JL, Maniadakis N, Gray A, Rayner M. The economic burden of coronary heart disease in the UK. *Heart.* Dec 2002;88(6):597-603.

3. Leal J, Luengo-Fernandez R, Gray A, Petersen S, Rayner M. Economic burden of cardiovascular diseases in the enlarged European Union. *Eur Heart J.* Jul 2006;27(13):1610-1619.

4. Luengo-Fernandez R, Leal J, Gray A, Petersen S, Rayner M. Cost of cardiovascular diseases in the United Kingdom. *Heart.* Oct 2006;92(10):1384-1389.

5. Weissberg P. Coronary heart disease statistics. *British Heart Foundation Health Promotion Research Group.* 2012.

6. Ludman P. National Audit of Percutaneous Coronary Interventional Procedures Public Report. 2011. http://www.ucl.ac.uk/nicor/audits/adultcardiacintervention.

7. Scarborough P, Bhatnagar P, Wickramasinghe K, Smolina K, Mitchel C, Rayner M. Coronary heart disease statistics. *British Heart Foundation Database.* 2010. http://www.heartstats.org.

8. Moore KJ, Sheedy FJ, Fisher EA. Macrophages in atherosclerosis: a dynamic balance. *Nat Rev Immunol.* Oct 2013;13(10):709-721.

9. Libby P. Inflammation in atherosclerosis. *Nature.* Dec 19-26 2002;420(6917):868-874.

10. Berliner JA, Navab M, Fogelman AM, et al. Atherosclerosis: basic mechanisms. Oxidation, inflammation, and genetics. *Circulation.* May 1 1995;91(9):2488-2496.

11. Libby P. Lipid-lowering therapy stabilizes plaque, reduces events by limiting inflammation. *Am J Manag Care.* Jan 2002;Suppl:1, 4.

12. Gerthoffer WT. Mechanisms of vascular smooth muscle cell migration. *Circ Res.* Mar 16 2007;100(5):607-621.

13. Higuchi ML, Gutierrez PS, Bezerra HG, et al. Comparison between adventitial and intimal inflammation of ruptured and nonruptured atherosclerotic plaques in human coronary arteries. *Arq Bras Cardiol.* Jul 2002;79(1):20-24.

14. Davies MJ. The pathophysiology of acute coronary syndromes. *Heart.* Mar 2000;83(3):361-366.

15. Lee AJ, Fowkes FG, Carson MN, Leng GC, Allan PL. Smoking, atherosclerosis and risk of abdominal aortic aneurysm. *Eur Heart J.* Apr 1997;18(4):671-676.

16. Golledge J, Norman PE. Atherosclerosis and abdominal aortic aneurysm: cause, response, or common risk factors? *Arterioscler Thromb Vasc Biol.* Jun 2010;30(6):1075-1077.

17. Woollard KJ, Geissmann F. Monocytes in atherosclerosis: subsets and functions. *Nat Rev Cardiol.* Feb 2010;7(2):77-86.

18. Stary HC. The sequence of cell and matrix changes in atherosclerotic lesions of coronary arteries in the first forty years of life. *Eur Heart J.* Aug 1990;11 Suppl E:3-19.

19. Thygesen K, Alpert JS, Jaffe AS, Simoons ML, Chaitman BR, White HD. Third universal definition of myocardial infarction. *Nat Rev Cardiol.* Nov 2012;9(11):620-633.

20. Fajadet J, Chieffo A. Current management of left main coronary artery disease. *Eur Heart J.* Jan 2012;33(1):36-50b.

21. Futami C, Tanuma K, Tanuma Y, Saito T. The arterial blood supply of the conducting system in normal human hearts. *Surg Radiol Anat.* Apr 2003;25(1):42-49.

22. Voelkel NF, Quaife RA, Leinwand LA, et al. Right ventricular function and failure: report of a National Heart, Lung, and Blood Institute working group on cellular and molecular mechanisms of right heart failure. *Circulation.* Oct 24 2006;114(17):1883-1891.

23. Pierard LA, Carabello BA. Ischaemic mitral regurgitation: pathophysiology, outcomes and the conundrum of treatment. *Eur Heart J.* Dec 2010;31(24):2996-3005.

24. Abrams DL, Edelist A, Luria MH, Miller AJ. Ventricular Aneurysm. A Reappraisal Based on a Study of Sixty-Five Consecutive Autopsied Cases. *Circulation.* Feb 1963;27:164-169.

25. Sibal AK, Prasad S, Alison P, Nand P, Haydock D. Acute ischaemic ventricular septal defect--a formidable surgical challenge. *Heart Lung Circ.* Feb 2010;19(2):71-74.

26. Little WC, Freeman GL. Pericardial disease. *Circulation.* Mar 28 2006;113(12):1622-1632.

27. Roger VL, Go AS, Lloyd-Jones DM, et al. Heart disease and stroke statistics--2011 update: a report from the American Heart Association. *Circulation.* Feb 1 2011;123(4):e18-e209.

28. Roger VL, Go AS, Lloyd-Jones DM, et al. Heart disease and stroke statistics--2012 update: a report from the American Heart Association. *Circulation.* Jan 3 2012;125(1):e2-e220.

29. Pearson TA, Blair SN, Daniels SR, et al. AHA Guidelines for Primary Prevention of Cardiovascular Disease and Stroke: 2002 Update: Consensus Panel Guide to Comprehensive Risk Reduction for Adult Patients Without Coronary or Other Atherosclerotic Vascular Diseases. American Heart Association Science Advisory and Coordinating Committee. *Circulation.* Jul 16 2002;106(3):388-391.

30. Krauss RM, Eckel RH, Howard B, et al. AHA Dietary Guidelines: revision 2000: A statement for healthcare professionals from the Nutrition Committee of the American Heart Association. *Stroke.* Nov 2000;31(11):2751-2766.

31. Ockene IS, Miller NH. Cigarette smoking, cardiovascular disease, and stroke: a statement for healthcare professionals from the American Heart Association. American Heart Association Task Force on Risk Reduction. *Circulation.* Nov 4 1997;96(9):3243-3247.

32. Thompson PD. Exercise and physical activity in the prevention and treatment of atherosclerotic cardiovascular disease. *Arterioscler Thromb Vasc Biol.* Aug 1 2003;23(8):1319-1321.

33. Stone NJ, Robinson J, Lichtenstein AH, et al. 2013 ACC/AHA Guideline on the Treatment of Blood Cholesterol to Reduce Atherosclerotic Cardiovascular Risk in Adults: A Report of the American College of Cardiology/American Heart Association Task Force on Practice Guidelines. *Circulation.* Nov 12 2013.

34. Levine GN, Bates ER, Blankenship JC, et al. 2011 ACCF/AHA/SCAI Guideline for Percutaneous Coronary Intervention: a report of the American College of Cardiology Foundation/American Heart Association Task Force on Practice Guidelines and the Society for Cardiovascular Angiography and Interventions. *Circulation.* Dec 6 2011;124(23):e574-651.

35. Hillis LD, Smith PK, Anderson JL, et al. 2011 ACCF/AHA Guideline for Coronary Artery Bypass Graft Surgery: a report of the American College of Cardiology Foundation/American Heart Association Task Force on Practice Guidelines. *Circulation.* Dec 6 2011;124(23):e652-735.

36. Montalescot G, Sechtem U, Achenbach S, et al. 2013 ESC guidelines on the management of stable coronary artery disease: the Task Force on the management of stable coronary artery disease of the European Society of Cardiology. *Eur Heart J.* Oct 2013;34(38):2949-3003.

37. Sellke FW, Chu LM, Cohn WE. Current state of surgical myocardial revascularization. *Circ J.* Jun 2010;74(6):1031-1037.

38. Fedakar A, Tasar M, Rabus MB, Alsalehi S, Toker ME, Balkanay M. Hybrid coronary revascularization for the treatment of left main coronary artery disease in high-risk patients. *Heart Surg Forum.* Feb 2012;15(1):E51-55.

39. Repossini A, Tespili M, Saino A, et al. Hybrid revascularization in multivessel coronary artery disease. *Eur J Cardiothorac Surg.* Aug 2013;44(2):288-293; discussion 293-284.

40. Halkos ME, Walker PF, Vassiliades TA, et al. Clinical and Angiographic Results After Hybrid Coronary Revascularization. *Ann Thorac Surg.* Oct 17 2013.

41. Levine GN, Bates ER, Blankenship JC, et al. 2011 ACCF/AHA/SCAI Guideline for Percutaneous Coronary Intervention: executive summary: a report of the American College of Cardiology Foundation/American Heart Association Task Force on Practice Guidelines and the Society for Cardiovascular Angiography and Interventions. *Circulation.* Dec 6 2011;124(23):2574-2609.

42. Bridgewater B, Keogh B, Kinsman R, Walton P. Sixth National Adult Cardiac Surgical Database report. *The Society for Cardiothoracic Surgery in Great Britain & Ireland.* 2008.

43. Deb S, Wijeysundera HC, Ko DT, Tsubota H, Hill S, Fremes SE. Coronary artery bypass graft surgery vs percutaneous interventions in coronary revascularization: a systematic review. *JAMA.* Nov 20 2013;310(19):2086-2095.

44. Lawrie GM. The scientific contributions of Alexis Carrel. *Clin Cardiol.* Jul 1987;10(7):428-430.

45. Cutler EC, Schnitker MT. Total Thyroidectomy for Angina Pectoris. *Ann Surg.* Oct 1934;100(4):578-605.

46. Dobell AR. Arthur Vineberg and the internal mammary artery implantation procedure. *Ann Thorac Surg.* Jan 1992;53(1):167-169.

47. Longmire WP, Jr., Cannon JA, Kattus AA. Direct-vision coronary endarterectomy for angina pectoris. *N Engl J Med.* Nov 20 1958;259(21):993-999.

48. Mueller RL, Rosengart TK, Isom OW. The history of surgery for ischemic heart disease. *Ann Thorac Surg.* Mar 1997;63(3):869-878.

49. Olearchyk AS. Vasilii I. Kolesov. A pioneer of coronary revascularization by internal mammary-coronary artery grafting. *J Thorac Cardiovasc Surg.* Jul 1988;96(1):13-18.

50. Carpentier A, Guermonprez JL, Deloche A, Frechette C, DuBost C. The aorta-to-coronary radial artery bypass graft. A technique avoiding pathological changes in grafts. *Ann Thorac Surg.* Aug 1973;16(2):111-121.

51. Favaloro RG. Landmarks in the development of coronary artery bypass surgery. *Circulation.* Aug 4 1998;98(5):466-478.

52. Loop FD, Lytle BW, Cosgrove DM, et al. Influence of the internal-mammary-artery graft on 10-year survival and other cardiac events. *N Engl J Med.* Jan 2 1986;314(1):1-6.

53. Cameron A, Davis KB, Green G, Schaff HV. Coronary bypass surgery with internal-thoracic-artery grafts--effects on survival over a 15-year period. *N Engl J Med.* Jan 25 1996;334(4):216-219.

54. Pepper J. Controversies in off-pump coronary artery surgery. *Clin Med Res.* Feb 2005;3(1):27-33.

55. Briffa N. Off pump coronary artery bypass: a passing fad or ready for prime time? *Eur Heart J.* Jun 2008;29(11):1346-1349.

56. Nishimura RA. Cardiology patient pages. Aortic valve disease. *Circulation.* Aug 13 2002;106(7):770-772.

57. Vahanian A, Alfieri O, Andreotti F, et al. Guidelines on the management of valvular heart disease (version 2012). *Eur Heart J.* Oct 2012;33(19):2451-2496.

58. Hiratzka LF, Bakris GL, Beckman JA, et al. 2010 ACCF/AHA/AATS/ACR/ASA/SCA/SCAI/SIR/STS/SVM guidelines for the diagnosis and management of patients with Thoracic Aortic Disease: a report of the American College of Cardiology Foundation/American Heart Association Task Force on Practice Guidelines, American Association for Thoracic Surgery, American College of Radiology, American Stroke Association, Society of Cardiovascular Anesthesiologists, Society for Cardiovascular Angiography and Interventions, Society of Interventional Radiology, Society of Thoracic Surgeons, and Society for Vascular Medicine. *Circulation.* Apr 6 2010;121(13):e266-369.

59. Leon MB, Smith CR, Mack M, et al. Transcatheter aortic-valve implantation for aortic stenosis in patients who cannot undergo surgery. *N Engl J Med.* Oct 21 2010;363(17):1597-1607.

60. Faxon DP. Transcatheter aortic valve implantation: coming of age. *Circulation.* Oct 25 2011;124(17):e439-440.

61. Al-Lamee R, Godino C, Colombo A. Transcatheter aortic valve implantation: current principles of patient and technique selection and future perspectives. *Circ Cardiovasc Interv.* Aug 2011;4(4):387-395.

62. Palacios IF. Transcatheter aortic valve implantation: the interventionist vision. *Circulation.* Jun 26 2012;125(25):3233-3236.

63. Turi ZG. Cardiology patient page. Mitral valve disease. *Circulation.* Feb 17 2004;109(6):e38-41.

64. Vahanian A, Iung B. The new ESC/EACTS guidelines on the management of valvular heart disease. *Arch Cardiovasc Dis.* Oct 2012;105(10):465-467.

65. Stoney WS. Evolution of cardiopulmonary bypass. *Circulation.* Jun 2 2009;119(21):2844-2853.

66. Cohn LH. Fifty years of open-heart surgery. *Circulation.* May 6 2003;107(17):2168-2170.

67. Edmunds LH. Cardiopulmonary bypass after 50 years. *N Engl J Med.* Oct 14 2004;351(16):1603-1606.

68. Ghosh S, Falter F, Cook D. *Cardiopulmonary bypass*: Cambridge University Press; 2009.

69. Walpoth BH, Walpoth-Aslan BN, Mattle HP, et al. Outcome of survivors of accidental deep hypothermia and circulatory arrest treated with extracorporeal blood warming. *N Engl J Med.* Nov 20 1997;337(21):1500-1505.

70. Goh MH, Liu XY, Goh YS. Anterior mediastinal masses: an anaesthetic challenge. *Anaesthesia.* Jul 1999;54(7):670-674.

71. Belmont MJ, Wax MK, DeSouza FN. The difficult airway: cardiopulmonary bypass--the ultimate solution. *Head Neck.* May 1998;20(3):266-269.

72. Ohteki H, Norita H, Sakai M, Narita Y. Emergency pulmonary embolectomy with percutaneous cardiopulmonary bypass. *Ann Thorac Surg.* Jun 1997;63(6):1584-1586.

73. Aird WC. Discovery of the cardiovascular system: from Galen to William Harvey. *J Thromb Haemost.* Jul 2011;9 Suppl 1:118-129.

74. Silverman ME. De Motu Cordis: the Lumleian Lecture of 1616: an imagined playlet concerning the discovery of the circulation of the blood by William Harvey. *J R Soc Med.* Apr 2007;100(4):199-204.

75. Pearce JM. Malpighi and the discovery of capillaries. *Eur Neurol.* 2007;58(4):253-255.

76. Stefanadis C, Karamanou M, Androutsos G. Michael Servetus (1511-1553) and the discovery of pulmonary circulation. *Hellenic J Cardiol.* Sep-Oct 2009;50(5):373-378.

77. Azizi MH, Nayernouri T, Azizi F. A brief history of the discovery of the circulation of blood in the human body. *Arch Iran Med.* May 2008;11(3):345-350.

78. Akmal M, Zulkifle M, Ansari A. Ibn nafis - a forgotten genius in the discovery of pulmonary blood circulation. *Heart Views.* Mar 2010;11(1):26-30.

79. Zimmer HG. The heart-lung machine was invented twice--the first time by Max von Frey. *Clin Cardiol.* Sep 2003;26(9):443-445.

80. Konstantinov IE, Alexi-Meskishvili VV. Sergei S. Brukhonenko: the development of the first heart-lung machine for total body perfusion. *Ann Thorac Surg.* Mar 2000;69(3):962-966.

81. Wardrop D, Keeling D. The story of the discovery of heparin and warfarin. *Br J Haematol.* Jun 2008;141(6):757-763.

82. Hunt JG, Kasinsky HE, Elsey RM, et al. Protamines of reptiles. *J Biol Chem.* Sep 20 1996;271(38):23547-23557.

83. Moller JH, Shumway SJ, Gott VL. The first open-heart repairs using extracorporeal circulation by cross-circulation: a 53-year follow-up. *Ann Thorac Surg.* Sep 2009;88(3):1044-1046.

84. Borst HG. Ralph D. Alley lecture. The hammer, the sickle, and the scalpel: a cardiac surgeon's view of Eastern Europe. *Ann Thorac Surg.* Jun 2000;69(6):1655-1662.

85. Karthik S, Grayson AD, Oo AY, Fabri BM. A survey of current myocardial protection practices during coronary artery bypass grafting. *Ann R Coll Surg Engl.* Nov 2004;86(6):413-415.

86. Hogg JC, Doerschuk CM, Wiggs B, Minshall D. Neutrophil retention during a single transit through the pulmonary circulation. *J Appl Physiol (1985).* Oct 1992;73(4):1683-1685.

87. Kochamba GS, Yun KL, Pfeffer TA, Sintek CF, Khonsari S. Pulmonary abnormalities after coronary arterial bypass grafting operation: cardiopulmonary bypass versus mechanical stabilization. *Ann Thorac Surg.* May 2000;69(5):1466-1470.

88. Taggart DP. Respiratory dysfunction after cardiac surgery: effects of avoiding cardiopulmonary bypass and the use of bilateral internal mammary arteries. *Eur J Cardiothorac Surg.* Jul 2000;18(1):31-37.

89. Messent M, Sullivan K, Keogh BF, Morgan CJ, Evans TW. Adult respiratory distress syndrome following cardiopulmonary bypass: incidence and prediction. *Anaesthesia.* Mar 1992;47(3):267-268.

90. Asimakopoulos G, Smith PL, Ratnatunga CP, Taylor KM. Lung injury and acute respiratory distress syndrome after cardiopulmonary bypass. *Ann Thorac Surg.* Sep 1999;68(3):1107-1115.

91. Magnusson L, Wicky S, Tyden H, Hedenstierna G. Repeated vital capacity manoeuvres after cardiopulmonary bypass: effects on lung function in a pig model. *Br J Anaesth.* May 1998;80(5):682-684.

92. Magnusson L, Zemgulis V, Tenling A, et al. Use of a vital capacity maneuver to prevent atelectasis after cardiopulmonary bypass: an experimental study. *Anesthesiology.* Jan 1998;88(1):134-142.

93. McGowan FX, Jr., Ikegami M, del Nido PJ, et al. Cardiopulmonary bypass significantly reduces surfactant activity in children. *J Thorac Cardiovasc Surg.* Dec 1993;106(6):968-977.

94. Schlensak C, Doenst T, Preusser S, Wunderlich M, Kleinschmidt M, Beyersdorf F. Cardiopulmonary bypass reduction of bronchial blood flow: a potential mechanism for lung injury in a neonatal pig model. *J Thorac Cardiovasc Surg.* Jun 2002;123(6):1199-1205.

95. Richter JA, Meisner H, Tassani P, Barankay A, Dietrich W, Braun SL. Drew-Anderson technique attenuates systemic inflammatory response syndrome and improves respiratory function after coronary artery bypass grafting. *Ann Thorac Surg.* Jan 2000;69(1):77-83.

96. Groeneveld AB. Radionuclide assessment of pulmonary microvascular permeability. *Eur J Nucl Med.* Apr 1997;24(4):449-461.

97. Kotani N, Hashimoto H, Sessler DI, et al. Neutrophil number and interleukin-8 and elastase concentrations in bronchoalveolar lavage fluid correlate with decreased arterial oxygenation after cardiopulmonary bypass. *Anesth Analg.* May 2000;90(5):1046-1051.

98. Wasowicz M, Sobczynski P, Biczysko W, Szulc R. Ultrastructural changes in the lung alveoli after cardiac surgical operations with the use of cardiopulmonary bypass (CPB). *Pol J Pathol.* 1999;50(3):189-196.

99. Sole MJ, Drobac M, Schwartz L, Hussain MN, Vaughan-Neil EF. The extraction of circulating catecholamines by the lungs in normal man and in patients with pulmonary hypertension. *Circulation.* Jul 1979;60(1):160-163.

100. Taeger K, Weninger E, Schmelzer F, Adt M, Franke N, Peter K. Pulmonary kinetics of fentanyl and alfentanil in surgical patients. *Br J Anaesth.* Oct 1988;61(4):425-434.

101. Haase M, Bellomo R, Matalanis G, Calzavacca P, Dragun D, Haase-Fielitz A. A comparison of the RIFLE and Acute Kidney Injury Network classifications for cardiac surgery-associated acute kidney injury: a prospective cohort study. *J Thorac Cardiovasc Surg.* Dec 2009;138(6):1370-1376.

102. Rosner MH, Okusa MD. Acute kidney injury associated with cardiac surgery. *Clin J Am Soc Nephrol.* Jan 2006;1(1):19-32.

103. Andersson LG, Bratteby LE, Ekroth R, et al. Renal function during cardiopulmonary bypass: influence of pump flow and systemic blood pressure. *Eur J Cardiothorac Surg.* 1994;8(11):597-602.

104. Sutton TA, Fisher CJ, Molitoris BA. Microvascular endothelial injury and dysfunction during ischemic acute renal failure. *Kidney Int.* Nov 2002;62(5):1539-1549.

105. Adademir T, Ak K, Aljodi M, Elci ME, Arsan S, Isbir S. The effects of pulsatile cardiopulmonary bypass on acute kidney injury. *Int J Artif Organs.* Jul 2012;35(7):511-519.

106. Donnahoo KK, Meldrum DR, Shenkar R, Chung CS, Abraham E, Harken AH. Early renal ischemia, with or without reperfusion, activates NFkappaB and increases TNF-alpha bioactivity in the kidney. *J Urol.* Apr 2000;163(4):1328-1332.

107. Patel NN, Toth T, Jones C, et al. Prevention of post-cardiopulmonary bypass acute kidney injury by endothelin A receptor blockade. *Crit Care Med.* Apr 2011;39(4):793-802.

108. Mishra J, Dent C, Tarabishi R, et al. Neutrophil gelatinase-associated lipocalin (NGAL) as a biomarker for acute renal injury after cardiac surgery. *Lancet.* Apr 2-8 2005;365(9466):1231-1238.

109. Nalysnyk L, Fahrbach K, Reynolds MW, Zhao SZ, Ross S. Adverse events in coronary artery bypass graft (CABG) trials: a systematic review and analysis. *Heart.* Jul 2003;89(7):767-772.

110. Robinson LA, Braimbridge MV, Hearse DJ. Enhanced myocardial protection with high-energy phosphates in St. Thomas' Hospital cardioplegic solution. Synergism of adenosine triphosphate and creatine phosphate. *J Thorac Cardiovasc Surg.* Mar 1987;93(3):415-427.

111. Malik V, Kale SC, Chowdhury UK, Ramakrishnan L, Chauhan S, Kiran U. Myocardial injury in coronary artery bypass grafting: On-pump versus off-pump comparison by measuring heart-type fatty-acid-binding protein release. *Tex Heart Inst J.* 2006;33(3):321-327.

112. Glatz JF, van der Vusse GJ, Simoons ML, Kragten JA, van Dieijen-Visser MP, Hermens WT. Fatty acid-binding protein and the early detection of acute myocardial infarction. *Clin Chim Acta.* Apr 6 1998;272(1):87-92.

113. Ascione R, Caputo M, Angelini GD. Off-pump coronary artery bypass grafting: not a flash in the pan. *Ann Thorac Surg.* Jan 2003;75(1):306-313.

114. Immer FF, Ackermann A, Gygax E, et al. Minimal extracorporeal circulation is a promising technique for coronary artery bypass grafting. *Ann Thorac Surg.* Nov 2007;84(5):1515-1520; discussion 1521.

115. Abdel-Rahman U, Ozaslan F, Risteski PS, et al. Initial experience with a minimized extracorporeal bypass system: is there a clinical benefit? *Ann Thorac Surg.* Jul 2005;80(1):238-243.

116. Skrabal CA, Steinhoff G, Liebold A. Minimizing cardiopulmonary bypass attenuates myocardial damage after cardiac surgery. *ASAIO J.* Jan-Feb 2007;53(1):32-35.

117. Schottler J, Lutter G, Boning A, et al. Is there really a clinical benefit of using minimized extracorporeal circulation for coronary artery bypass grafting? *Thorac Cardiovasc Surg.* Mar 2008;56(2):65-70.

118. Wiesenack C, Liebold A, Philipp A, et al. Four years' experience with a miniaturized extracorporeal circulation system and its influence on clinical outcome. *Artif Organs.* Dec 2004;28(12):1082-1088.

119. Bomberg H, Bierbach B, Flache S, et al. Endothelin and vasopressin influence splanchnic blood flow distribution during and after cardiopulmonary bypass. *J Thorac Cardiovasc Surg.* Feb 2013;145(2):539-547.

120. Ohri SK, Bowles CW, Mathie RT, Lawrence DR, Keogh BE, Taylor KM. Effect of cardiopulmonary bypass perfusion protocols on gut tissue oxygenation and blood flow. *Ann Thorac Surg.* Jul 1997;64(1):163-170.

121. Tao W, Zwischenberger JB, Nguyen TT, et al. Gut mucosal ischemia during normothermic cardiopulmonary bypass results from blood flow redistribution and increased oxygen demand. *J Thorac Cardiovasc Surg.* Sep 1995;110(3):819-828.

122. Braun JP, Buhner S, Kastrup M, et al. Barrier function of the gut and multiple organ dysfunction after cardiac surgery. *J Int Med Res.* Jan-Feb 2007;35(1):72-83.

123. Tsunooka N, Maeyama K, Hamada Y, et al. Bacterial translocation secondary to small intestinal mucosal ischemia during cardiopulmonary bypass. Measurement by diamine oxidase and peptidoglycan. *Eur J Cardiothorac Surg.* Feb 2004;25(2):275-280.

124. Byhahn C, Strouhal U, Martens S, Mierdl S, Kessler P, Westphal K. Incidence of gastrointestinal complications in cardiopulmonary bypass patients. *World J Surg.* Sep 2001;25(9):1140-1144.

125. D'Ancona G, Baillot R, Poirier B, et al. Determinants of gastrointestinal complications in cardiac surgery. *Tex Heart Inst J.* 2003;30(4):280-285.

126. Taylor KM. Brain damage during cardiopulmonary bypass. *Ann Thorac Surg.* Apr 1998;65(4 Suppl):S20-26; discussion S27-28.

127. Brown WR, Moody DM, Challa VR, Stump DA, Hammon JW. Longer duration of cardiopulmonary bypass is associated with greater numbers of cerebral microemboli. *Stroke.* Mar 2000;31(3):707-713.

128. Nussmeier NA, Searles BE. Inflammatory brain injury after cardiopulmonary bypass: is it real? *Anesth Analg.* Feb 1 2010;110(2):288-290.

129. Rivas F. In this Issue: Inflammation. *Cell.* Mar 19 2010;140(6):755,757.

130. Rather LJ. Disturbance of function (functio laesa): the legendary fifth cardinal sign of inflammation, added by Galen to the four cardinal signs of Celsus. *Bull N Y Acad Med.* Mar 1971;47(3):303-322.

131. Heidland A, Klassen A, Rutkowski P, Bahner U. The contribution of Rudolf Virchow to the concept of inflammation: what is still of importance? *J Nephrol.* May-Jun 2006;19 Suppl 10:S102-109.

132. Medzhitov R. Inflammation 2010: new adventures of an old flame. *Cell.* Mar 19 2010;140(6):771-776.

133. Cho JH. The genetics and immunopathogenesis of inflammatory bowel disease. *Nat Rev Immunol.* Jun 2008;8(6):458-466.

134. Abraham C, Cho JH. Inflammatory bowel disease. *N Engl J Med.* Nov 19 2009;361(21):2066-2078.

135. Kaser A, Martinez-Naves E, Blumberg RS. Endoplasmic reticulum stress: implications for inflammatory bowel disease pathogenesis. *Curr Opin Gastroenterol.* Jul 2010;26(4):318-326.

136. McInnes IB, Schett G. Cytokines in the pathogenesis of rheumatoid arthritis. *Nat Rev Immunol.* Jun 2007;7(6):429-442.

137. Hazes JM, Luime JJ. The epidemiology of early inflammatory arthritis. *Nat Rev Rheumatol.* Jul 2011;7(7):381-390.

138. Kessenbrock K, Krumbholz M, Schonermarck U, et al. Netting neutrophils in autoimmune small-vessel vasculitis. *Nat Med.* Jun 2009;15(6):623-625.

139. Coussens LM, Werb Z. Inflammation and cancer. *Nature.* Dec 19-26 2002;420(6917):860-867.

140. Grivennikov SI, Greten FR, Karin M. Immunity, inflammation, and cancer. *Cell.* Mar 19 2010;140(6):883-899.

141. Elinav E, Nowarski R, Thaiss CA, Hu B, Jin C, Flavell RA. Inflammation-induced cancer: crosstalk between tumours, immune cells and microorganisms. *Nat Rev Cancer.* Nov 2013;13(11):759-771.

142. Paparella D, Yau TM, Young E. Cardiopulmonary bypass induced inflammation: pathophysiology and treatment. An update. *Eur J Cardiothorac Surg.* Feb 2002;21(2):232-244.

143. Rubens FD, Mesana T. The inflammatory response to cardiopulmonary bypass: a therapeutic overview. *Perfusion.* 2004;19 Suppl 1:S5-12.

144. Day JR, Taylor KM. The systemic inflammatory response syndrome and cardiopulmonary bypass. *Int J Surg.* 2005;3(2):129-140.

145. Asimakopoulos G. Systemic inflammation and cardiac surgery: an update. *Perfusion.* Sep 2001;16(5):353-360.

146. Taylor KM. SIRS--the systemic inflammatory response syndrome after cardiac operations. *Ann Thorac Surg.* Jun 1996;61(6):1607-1608.

147. Raja SG, Dreyfus GD. Modulation of systemic inflammatory response after cardiac surgery. *Asian Cardiovasc Thorac Ann.* Dec 2005;13(4):382-395.

148. Gu YJ, Boonstra PW, Graaff R, Rijnsburger AA, Mungroop H, van Oeveren W. Pressure drop, shear stress, and activation of leukocytes during cardiopulmonary bypass: a comparison between hollow fiber and flat sheet membrane oxygenators. *Artif Organs.* Jan 2000;24(1):43-48.

149. Kirklin JK, Westaby S, Blackstone EH, Kirklin JW, Chenoweth DE, Pacifico AD. Complement and the damaging effects of cardiopulmonary bypass. *J Thorac Cardiovasc Surg.* Dec 1983;86(6):845-857.

150. Moat NE, Shore DF, Evans TW. Organ dysfunction and cardiopulmonary bypass: the role of complement and complement regulatory proteins. *Eur J Cardiothorac Surg.* 1993;7(11):563-573.

151. Tennenberg SD, Clardy CW, Bailey WW, Solomkin JS. Complement activation and lung permeability during cardiopulmonary bypass. *Ann Thorac Surg.* Oct 1990;50(4):597-601.

152. Bruins P, te Velthuis H, Yazdanbakhsh AP, et al. Activation of the complement system during and after cardiopulmonary bypass surgery: postsurgery activation involves C-reactive protein and is associated with postoperative arrhythmia. *Circulation.* Nov 18 1997;96(10):3542-3548.

153. Pugsley W, Klinger L, Paschalis C, Treasure T, Harrison M, Newman S. The impact of microemboli during cardiopulmonary bypass on neuropsychological functioning. *Stroke.* Jul 1994;25(7):1393-1399.

154. Braekken SK, Russell D, Brucher R, Abdelnoor M, Svennevig JL. Cerebral microembolic signals during cardiopulmonary bypass surgery. Frequency, time of occurrence, and association with patient and surgical characteristics. *Stroke.* Oct 1997;28(10):1988-1992.

155. Levy JH, Tanaka KA. Inflammatory response to cardiopulmonary bypass. *Ann Thorac Surg.* Feb 2003;75(2):S715-720.

156. Asimakopoulos G. Mechanisms of the systemic inflammatory response. *Perfusion.* Jul 1999;14(4):269-277.

157. Taylor RL, Borger MA, Weisel RD, Fedorko L, Feindel CM. Cerebral microemboli during cardiopulmonary bypass: increased emboli during perfusionist interventions. *Ann Thorac Surg.* Jul 1999;68(1):89-93.

158. Liu YH, Wang DX, Li LH, et al. The effects of cardiopulmonary bypass on the number of cerebral microemboli and the incidence of cognitive dysfunction after coronary artery bypass graft surgery. *Anesth Analg.* Oct 2009;109(4):1013-1022.

159. el Habbal MH, Smith LJ, Elliott MJ, Strobel S. Cardiopulmonary bypass tubes and prime solutions stimulate neutrophil adhesion molecules. *Cardiovasc Res.* Jan 1997;33(1):209-215.

160. Moen O, Fosse E, Dregelid E, et al. Centrifugal pump and heparin coating improves cardiopulmonary bypass biocompatibility. *Ann Thorac Surg.* Oct 1996;62(4):1134-1140.

161. Macey MG, McCarthy DA, Trivedi UR, Venn GE, Chambers DJ, Brown KA. Neutrophil adhesion molecule expression during cardiopulmonary bypass: a comparative study of roller and centrifugal pumps. *Perfusion.* Sep 1997;12(5):293-301.

162. Gu YJ, van Oeveren W, Akkerman C, Boonstra PW, Huyzen RJ, Wildevuur CR. Heparin-coated circuits reduce the inflammatory response to cardiopulmonary bypass. *Ann Thorac Surg.* Apr 1993;55(4):917-922.

163. Moen O, Fosse E, Braten J, et al. Differences in blood activation related to roller/centrifugal pumps and heparin-coated/uncoated surfaces in a cardiopulmonary bypass model circuit. *Perfusion.* Mar 1996;11(2):113-123.

164. de Vroege R, van Oeveren W, van Klarenbosch J, et al. The impact of heparin-coated cardiopulmonary bypass circuits on pulmonary function and the release of inflammatory mediators. *Anesth Analg.* Jun 2004;98(6):1586-1594, table of contents.

165. Jakob SM, Stanga Z. Perioperative metabolic changes in patients undergoing cardiac surgery. *Nutrition.* Apr 2010;26(4):349-353.

166. Khabar KS, elBarbary MA, Khouqeer F, Devol E, al-Gain S, al-Halees Z. Circulating endotoxin and cytokines after cardiopulmonary bypass: differential correlation with duration of bypass and systemic inflammatory response/multiple organ dysfunction syndromes. *Clin Immunol Immunopathol.* Oct 1997;85(1):97-103.

167. Vazquez-Jimenez JF, Qing M, Hermanns B, et al. Moderate hypothermia during cardiopulmonary bypass reduces myocardial cell damage and myocardial cell death related to cardiac surgery. *J Am Coll Cardiol.* Oct 2001;38(4):1216-1223.

168. Birdi I, Caputo M, Underwood M, Bryan AJ, Angelini GD. The effects of cardiopulmonary bypass temperature on inflammatory response following cardiopulmonary bypass. *Eur J Cardiothorac Surg.* Nov 1999;16(5):540-545.

169. Diestel A, Roessler J, Berger F, Schmitt KR. Hypothermia downregulates inflammation but enhances IL-6 secretion by stimulated endothelial cells. *Cryobiology.* Dec 2008;57(3):216-222.

170. Suzuki T. Additional lung-protective perfusion techniques during cardiopulmonary bypass. *Ann Thorac Cardiovasc Surg.* Jun 2010;16(3):150-155.

171. Lenz A, Franklin GA, Cheadle WG. Systemic inflammation after trauma. *Injury.* Dec 2007;38(12):1336-1345.

172. Ipaktchi K, Mattar A, Niederbichler AD, et al. Attenuating burn wound inflammatory signaling reduces systemic inflammation and acute lung injury. *J Immunol.* Dec 1 2006;177(11):8065-8071.

173. Zhang Q, Itagaki K, Hauser CJ. Mitochondrial DNA is released by shock and activates neutrophils via p38 map kinase. *Shock.* Jul 2010;34(1):55-59.

174. Tomic V, Russwurm S, Moller E, et al. Transcriptomic and proteomic patterns of systemic inflammation in on-pump and off-pump coronary artery bypass grafting. *Circulation.* Nov 8 2005;112(19):2912-2920.

175. Bhutta AT, Schmitz ML, Swearingen C, et al. Ketamine as a neuroprotective and anti-inflammatory agent in children undergoing surgery on cardiopulmonary bypass: A pilot randomized, double-blind, placebo-controlled trial. *Pediatr Crit Care Med.* Sep 15 2011.

176. Suleiman MS, Zacharowski K, Angelini GD. Inflammatory response and cardioprotection during open-heart surgery: the importance of anaesthetics. *Br J Pharmacol.* Jan 2008;153(1):21-33.

177. Huang Z, Zhong X, Irwin MG, et al. Synergy of isoflurane preconditioning and propofol postconditioning reduces myocardial reperfusion injury in patients. *Clin Sci (Lond).* Jul 2011;121(2):57-69.

178. Cohen AS, Hadjinikolaou L, McColl A, Richmond W, Sapsford RA, Glenville BE. Lipid peroxidation, antioxidant status and troponin-T following cardiopulmonary bypass. A comparison between intermittent crossclamp with fibrillation and crystalloid cardioplegia. *Eur J Cardiothorac Surg.* Aug 1997;12(2):248-253.

179. Osipov RM, Robich MP, Feng J, et al. Effect of hydrogen sulfide on myocardial protection in the setting of cardioplegia and cardiopulmonary bypass. *Interact Cardiovasc Thorac Surg.* Apr 2010;10(4):506-512.

180. Chanani NK, Cowan DB, Takeuchi K, et al. Differential effects of amrinone and milrinone upon myocardial inflammatory signaling. *Circulation.* Sep 24 2002;106(12 Suppl 1):I284-289.

181. Dybdahl B, Wahba A, Lien E, et al. Inflammatory response after open heart surgery: release of heat-shock protein 70 and signaling through toll-like receptor-4. *Circulation.* Feb 12 2002;105(6):685-690.

182. Rinder C. Cellular inflammatory response and clinical outcome in cardiac surgery. *Curr Opin Anaesthesiol.* Feb 2006;19(1):65-68.

183. Clark SC. Lung injury after cardiopulmonary bypass. *Perfusion.* Jul 2006;21(4):225-228.

184. Nathens AB, Marshall JC. Sepsis, SIRS, and MODS: what's in a name? *World J Surg.* May 1996;20(4):386-391.

185. Tsiotou AG, Sakorafas GH, Anagnostopoulos G, Bramis J. Septic shock; current pathogenetic concepts from a clinical perspective. *Med Sci Monit.* Mar 2005;11(3):RA76-85.

186. Asimakopoulos G, Kohn A, Stefanou DC, Haskard DO, Landis RC, Taylor KM. Leukocyte integrin expression in patients undergoing cardiopulmonary bypass. *Ann Thorac Surg.* Apr 2000;69(4):1192-1197.

187. Schapira M, Despland E, Scott CF, Boxer LA, Colman RW. Purified human plasma kallikrein aggregates human blood neutrophils. *J Clin Invest.* May 1982;69(5):1199-1202.

188. Kawahito K, Kawakami M, Fujiwara T, et al. Proinflammatory cytokine levels in patients undergoing cardiopulmonary bypass. Does lung reperfusion influence the release of cytokines? *ASAIO J.* Jul-Sep 1995;41(3):M775-778.

189. Furze RC, Rankin SM. Neutrophil mobilization and clearance in the bone marrow. *Immunology.* Nov 2008;125(3):281-288.

190. Christopher MJ, Link DC. Regulation of neutrophil homeostasis. *Curr Opin Hematol.* Jan 2007;14(1):3-8.

191. Chello M, Mastroroberto P, Quirino A, et al. Inhibition of neutrophil apoptosis after coronary bypass operation with cardiopulmonary bypass. *Ann Thorac Surg.* Jan 2002;73(1):123-129; discussion 129-130.

192. Kalawski R, Bugajski P, Smielecki J, et al. Soluble adhesion molecules in reperfusion during coronary bypass grafting. *Eur J Cardiothorac Surg.* Sep 1998;14(3):290-295.

193. Rinder CS, Bonan JL, Rinder HM, Mathew J, Hines R, Smith BR. Cardiopulmonary bypass induces leukocyte-platelet adhesion. *Blood.* Mar 1 1992;79(5):1201-1205.

194. Stefanou DC, Asimakopoulos G, Yagnik DR, et al. Monocyte Fc gamma receptor expression in patients undergoing coronary artery bypass grafting. *Ann Thorac Surg.* Mar 2004;77(3):951-955.

195. Evans BJ, Haskard DO, Finch JR, Hambleton IR, Landis RC, Taylor KM. The inflammatory effect of cardiopulmonary bypass on leukocyte extravasation in vivo. *J Thorac Cardiovasc Surg.* May 2008;135(5):999-1006.

196. Piccinini AM, Midwood KS. DAMPening inflammation by modulating TLR signalling. *Mediators Inflamm.* 2010;2010.

197. Tang D, Kang R, Coyne CB, Zeh HJ, Lotze MT. PAMPs and DAMPs: signal 0s that spur autophagy and immunity. *Immunol Rev.* Sep 2012;249(1):158-175.

198. Monie TP, Bryant CE, Gay NJ. Activating immunity: lessons from the TLRs and NLRs. *Trends Biochem Sci.* Nov 2009;34(11):553-561.

199. Arslan F, de Kleijn DP, Pasterkamp G. Innate immune signaling in cardiac ischemia. *Nat Rev Cardiol.* Mar 29 2011.

200. Shalhoub J, Falck-Hansen MA, Davies AH, Monaco C. Innate immunity and monocyte-macrophage activation in atherosclerosis. *J Inflamm (Lond).* 2011;8:9.

201. Meylan E, Tschopp J, Karin M. Intracellular pattern recognition receptors in the host response. *Nature.* Jul 6 2006;442(7098):39-44.

202. Dufton N, Perretti M. Therapeutic anti-inflammatory potential of formyl-peptide receptor agonists. *Pharmacol Ther.* Aug 2010;127(2):175-188.

203. Migeotte I, Communi D, Parmentier M. Formyl peptide receptors: a promiscuous subfamily of G protein-coupled receptors controlling immune responses. *Cytokine Growth Factor Rev.* Dec 2006;17(6):501-519.

204. Le Y, Yang Y, Cui Y, et al. Receptors for chemotactic formyl peptides as pharmacological targets. *Int Immunopharmacol.* Jan 2002;2(1):1-13.

205. Gavins FN. Are formyl peptide receptors novel targets for therapeutic intervention in ischaemia-reperfusion injury? *Trends Pharmacol Sci.* Jun 2010;31(6):266-276.

206. Stoecklein VM, Osuka A, Lederer JA. Trauma equals danger--damage control by the immune system. *J Leukoc Biol.* Sep 2012;92(3):539-551.

207. Zhang Q, Raoof M, Chen Y, et al. Circulating mitochondrial DAMPs cause inflammatory responses to injury. *Nature.* Mar 4 2010;464(7285):104-107.

208. Lam NY, Rainer TH, Chan LY, Joynt GM, Lo YM. Time course of early and late changes in plasma DNA in trauma patients. *Clin Chem.* Aug 2003;49(8):1286-1291.

209. Haque A, Kunimoto F, Narahara H, et al. High mobility group box 1 levels in on and off-pump cardiac surgery patients. *Int Heart J.* 2011;52(3):170-174.

210. Leventhal JS, Schroppel B. Toll-like receptors in transplantation: sensing and reacting to injury. *Kidney Int.* Feb 1 2012.

211. Vallejo JG. Role of toll-like receptors in cardiovascular diseases. *Clin Sci (Lond).* Jul 2011;121(1):1-10.

212. Inohara N, Nunez G. NODs: intracellular proteins involved in inflammation and apoptosis. *Nat Rev Immunol.* May 2003;3(5):371-382.

213. Ye Z, Ting JP. NLR, the nucleotide-binding domain leucine-rich repeat containing gene family. *Curr Opin Immunol.* Feb 2008;20(1):3-9.

214. Zhao L, Lee JY, Hwang DH. The phosphatidylinositol 3-kinase/Akt pathway negatively regulates Nod2-mediated NF-kappaB pathway. *Biochem Pharmacol.* Apr 1 2008;75(7):1515-1525.

215. McGhan LJ, Jaroszewski DE. The role of toll-like receptor-4 in the development of multi-organ failure following traumatic haemorrhagic shock and resuscitation. *Injury.* Feb 2012;43(2):129-136.

216. Kaczorowski DJ, Nakao A, McCurry KR, Billiar TR. Toll-like receptors and myocardial ischemia/reperfusion, inflammation, and injury. *Curr Cardiol Rev.* Aug 2009;5(3):196-202.

217. Wang Y, Abarbanell AM, Herrmann JL, et al. Toll-like receptor signaling pathways and the evidence linking toll-like receptor signaling to cardiac ischemia/reperfusion injury. *Shock.* Dec 2010;34(6):548-557.

218. Krejsek J, Kunes P, Kolackova M, et al. Expression of Toll-like receptors 2 and 4 on innate immunity cells modulated by cardiac surgical operation. *Scand J Clin Lab Invest.* 2008;68(8):749-758.

219. Hadley JS, Wang JE, Michaels LC, et al. Alterations in inflammatory capacity and TLR expression on monocytes and neutrophils after cardiopulmonary bypass. *Shock.* May 2007;27(5):466-473.

220. Chalk K, Meisel C, Spies C, et al. Dysfunction of alveolar macrophages after 3 cardiac surgery and postoperative pneumonia? - an 5 observational study. *Crit Care.* Dec 9 2013;17(6):R285.

221. Krejsek J, Kolackova M, Mand'ak J, et al. TLR2 and TLR4 expression on blood monocytes and granulocytes of cardiac surgical patients is not affected by the use of cardiopulmonary bypass. *Acta Medica (Hradec Kralove).* 2013;56(2):57-66.

222. Okubo N, Hatori N, Ochi M, Tanaka S. Comparison of m-RNA expression for inflammatory mediators in leukocytes between on-pump and off-pump coronary artery bypass grafting. *Ann Thorac Cardiovasc Surg.* Feb 2003;9(1):43-49.

223. Liangos O, Domhan S, Schwager C, et al. Whole blood transcriptomics in cardiac surgery identifies a gene regulatory network connecting ischemia reperfusion with systemic inflammation. *PLoS One.* 2010;5(10):e13658.

224. Ghorbel MT, Cherif M, Mokhtari A, Bruno VD, Caputo M, Angelini GD. Off-pump coronary artery bypass surgery is associated with fewer gene expression changes in the human myocardium in comparison with on-pump surgery. *Physiol Genomics.* Jun 2010;42(1):67-75.

225. Chong AJ, Shimamoto A, Hampton CR, et al. Toll-like receptor 4 mediates ischemia/reperfusion injury of the heart. *J Thorac Cardiovasc Surg.* Aug 2004;128(2):170-179.

226. Sun S, Sursal T, Adibnia Y, et al. Mitochondrial DAMPs increase endothelial permeability through neutrophil dependent and independent pathways. *PLoS One.* 2013;8(3):e59989.

227. Lo YM, Rainer TH, Chan LY, Hjelm NM, Cocks RA. Plasma DNA as a prognostic marker in trauma patients. *Clin Chem.* Mar 2000;46(3):319-323.

228. Fournie GJ, Courtin JP, Laval F, et al. Plasma DNA as a marker of cancerous cell death. Investigations in patients suffering from lung cancer and in nude mice bearing human tumours. *Cancer Lett.* May 8 1995;91(2):221-227.

229. Jahr S, Hentze H, Englisch S, et al. DNA fragments in the blood plasma of cancer patients: quantitations and evidence for their origin from apoptotic and necrotic cells. *Cancer Res.* Feb 15 2001;61(4):1659-1665.

230. Stroun M, Lyautey J, Lederrey C, Olson-Sand A, Anker P. About the possible origin and mechanism of circulating DNA apoptosis and active DNA release. *Clin Chim Acta.* Nov 2001;313(1-2):139-142.

231. Lo YM, Zhang J, Leung TN, Lau TK, Chang AM, Hjelm NM. Rapid clearance of fetal DNA from maternal plasma. *Am J Hum Genet.* Jan 1999;64(1):218-224.

232. Elshimali YI, Khaddour H, Sarkissyan M, Wu Y, Vadgama JV. The clinical utilization of circulating cell free DNA (CCFDNA) in blood of cancer patients. *Int J Mol Sci.* 2013;14(9):18925-18958.

233. Kirsch C, Weickmann S, Schmidt B, Fleischhacker M. An improved method for the isolation of free-circulating plasma DNA and cell-free DNA from other body fluids. *Ann N Y Acad Sci.* Aug 2008;1137:135-139.

234. Gu X, Yao Y, Wu G, Lv T, Luo L, Song Y. The plasma mitochondrial DNA is an independent predictor for post-traumatic systemic inflammatory response syndrome. *PLoS One.* 2013;8(8):e72834.

235. Jovic M, Stancic A, Nenadic D, et al. Mitochondrial molecular basis of sevoflurane and propofol cardioprotection in patients undergoing aortic valve replacement with cardiopulmonary bypass. *Cell Physiol Biochem.* 2012;29(1-2):131-142.

236. Cohen MJ, Brohi K, Calfee CS, et al. Early release of high mobility group box nuclear protein 1 after severe trauma in humans: role of injury severity and tissue hypoperfusion. *Crit Care.* 2009;13(6):R174.

237. Park JS, Arcaroli J, Yum HK, et al. Activation of gene expression in human neutrophils by high mobility group box 1 protein. *Am J Physiol Cell Physiol.* Apr 2003;284(4):C870-879.

238. Velegraki M, Papakonstanti E, Mavroudi I, et al. Impaired clearance of apoptotic cells leads to HMGB1 release in the bone marrow of patients with myelodysplastic syndromes and induces TLR4-mediated cytokine production. *Haematologica.* Aug 2013;98(8):1206-1215.

239. Lin CY, Yang TL, Hong GJ, Li CY, Lin FY, Tsai CS. Enhanced intracellular heat shock protein 70 expression of leukocytes and serum interleukins release: comparison of on-pump and off-pump coronary artery surgery. *World J Surg.* Apr 2010;34(4):675-681.

240. Kunes P, Lonsky V, Mand'ak J, et al. The inflammatory response in cardiac surgery. An up-to-date overview with the emphasis on the role of heat shock proteins (HSPs) 60 and 70. *Acta Medica (Hradec Kralove).* 2007;50(2):93-99.

241. Valen G, Hansson GK, Dumitrescu A, Vaage J. Unstable angina activates myocardial heat shock protein 72, endothelial nitric oxide synthase, and transcription factors NFkappaB and AP-1. *Cardiovasc Res.* Jul 2000;47(1):49-56.

242. Foell D, Wittkowski H, Vogl T, Roth J. S100 proteins expressed in phagocytes: a novel group of damage-associated molecular pattern molecules. *J Leukoc Biol.* Jan 2007;81(1):28-37.

243. Hofmann MA, Drury S, Hudson BI, et al. RAGE and arthritis: the G82S polymorphism amplifies the inflammatory response. *Genes Immun.* May 2002;3(3):123-135.

244. Riuzzi F, Sorci G, Donato R. S100B stimulates myoblast proliferation and inhibits myoblast differentiation by independently stimulating ERK1/2 and inhibiting p38 MAPK. *J Cell Physiol.* May 2006;207(2):461-470.

245. Grotterod I, Maelandsmo GM, Boye K. Signal transduction mechanisms involved in S100A4-induced activation of the transcription factor NF-kappaB. *BMC Cancer.* 2010;10:241.

246. Newton RA, Hogg N. The human S100 protein MRP-14 is a novel activator of the beta 2 integrin Mac-1 on neutrophils. *J Immunol.* Feb 1 1998;160(3):1427-1435.

247. Zongo D, Ribereau-Gayon R, Masson F, et al. S100-B protein as a screening tool for the early assessment of minor head injury. *Ann Emerg Med.* Mar 2012;59(3):209-218.

248. Nash DL, Bellolio MF, Stead LG. S100 as a marker of acute brain ischemia: a systematic review. *Neurocrit Care.* 2008;8(2):301-307.

249. Westaby S, Johnsson P, Parry AJ, et al. Serum S100 protein: a potential marker for cerebral events during cardiopulmonary bypass. *Ann Thorac Surg.* Jan 1996;61(1):88-92.

250. Stocker CF, Shekerdemian LS, Visvanathan K, et al. Cardiopulmonary bypass elicits a prominent innate immune response in children with congenital heart disease. *J Thorac Cardiovasc Surg.* May 2004;127(5):1523-1525.

251. Oyama J, Blais C, Jr., Liu X, et al. Reduced myocardial ischemia-reperfusion injury in toll-like receptor 4-deficient mice. *Circulation.* Feb 17 2004;109(6):784-789.

252. Hua F, Ha T, Ma J, et al. Blocking the MyD88-dependent pathway protects the myocardium from ischemia/reperfusion injury in rat hearts. *Biochem Biophys Res Commun.* Dec 16 2005;338(2):1118-1125.

253. Shimamoto A, Chong AJ, Yada M, et al. Inhibition of Toll-like receptor 4 with eritoran attenuates myocardial ischemia-reperfusion injury. *Circulation.* Jul 4 2006;114(1 Suppl):I270-274.

254. Pillay J, den Braber I, Vrisekoop N, et al. In vivo labeling with 2H2O reveals a human neutrophil lifespan of 5.4 days. *Blood.* Jul 29 2010;116(4):625-627.

255. Phillipson M, Kubes P. The neutrophil in vascular inflammation. *Nat Med.* 2011;17(11):1381-1390.

256. Lee WL, Harrison RE, Grinstein S. Phagocytosis by neutrophils. *Microbes Infect.* Nov 2003;5(14):1299-1306.

257. Dahlgren C, Karlsson A. Respiratory burst in human neutrophils. *J Immunol Methods.* Dec 17 1999;232(1-2):3-14.

258. Shi C, Pamer EG. Monocyte recruitment during infection and inflammation. *Nat Rev Immunol.* Nov 2011;11(11):762-774.

259. Semple JW, Italiano JE, Jr., Freedman J. Platelets and the immune continuum. *Nat Rev Immunol.* Apr 2011;11(4):264-274.

260. Semple JW, Freedman J. Platelets and innate immunity. *Cell Mol Life Sci.* Feb 2010;67(4):499-511.

261. Smyth SS, McEver RP, Weyrich AS, et al. Platelet functions beyond hemostasis. *J Thromb Haemost.* Nov 2009;7(11):1759-1766.

262. Clark SR, Ma AC, Tavener SA, et al. Platelet TLR4 activates neutrophil extracellular traps to ensnare bacteria in septic blood. *Nat Med.* Apr 2007;13(4):463-469.

263. Bazzoni G, Dejana E. Endothelial cell-to-cell junctions: molecular organization and role in vascular homeostasis. *Physiol Rev.* Jul 2004;84(3):869-901.

264. Ley K, Laudanna C, Cybulsky MI, Nourshargh S. Getting to the site of inflammation: the leukocyte adhesion cascade updated. *Nat Rev Immunol.* Sep 2007;7(9):678-689.

265. Petri B, Phillipson M, Kubes P. The physiology of leukocyte recruitment: an in vivo perspective. *J Immunol.* May 15 2008;180(10):6439-6446.

266. Luo BH, Carman CV, Springer TA. Structural basis of integrin regulation and signaling. *Annu Rev Immunol.* 2007;25:619-647.

267. Phillipson M, Heit B, Colarusso P, Liu L, Ballantyne CM, Kubes P. Intraluminal crawling of neutrophils to emigration sites: a molecularly distinct process from adhesion in the recruitment cascade. *J Exp Med.* Nov 27 2006;203(12):2569-2575.

268. Bradfield PF, Scheiermann C, Nourshargh S, et al. JAM-C regulates unidirectional monocyte transendothelial migration in inflammation. *Blood.* Oct 1 2007;110(7):2545-2555.

269. Steeber DA, Venturi GM, Tedder TF. A new twist to the leukocyte adhesion cascade: intimate cooperation is key. *Trends Immunol.* Jan 2005;26(1):9-12.

270. Werr J, Johansson J, Eriksson EE, Hedqvist P, Ruoslahti E, Lindbom L. Integrin alpha(2)beta(1) (VLA-2) is a principal receptor used by neutrophils for locomotion in extravascular tissue. *Blood.* Mar 1 2000;95(5):1804-1809.

271. Wang S, Voisin MB, Larbi KY, et al. Venular basement membranes contain specific matrix protein low expression regions that act as exit points for emigrating neutrophils. *J Exp Med.* Jun 12 2006;203(6):1519-1532.

272. Pelletier M, Bouchard A, Girard D. In vivo and in vitro roles of IL-21 in inflammation. *J Immunol.* Dec 15 2004;173(12):7521-7530.

273. Rebuck JW, Crowley JH. A method of studying leukocytic functions in vivo. *Ann N Y Acad Sci.* Mar 24 1955;59(5):757-805.

274. Senn H, Holland JF. Plastic skin chamber technique for comparative studies on localized leukocyte mobilization in man. *Rev Fr Etud Clin Biol.* Apr 1969;14(4):373-377.

275. Senn H, Holland JF, Banerjee T. Kinetic and comparative studies on localized leukocyte mobilization in normal man. *J Lab Clin Med.* Nov 1969;74(5):742-756.

276. Mass MF, Dean PB, Weston WL, Humbert JR. Leukocyte migration in vivo: a new method of study. *J Lab Clin Med.* Dec 1975;86(6):1040-1046.

277. Kiistala U, Mustakallio KK. In-Vivo Separation of Epidermis by Production of Suction Blisters. *Lancet.* Jun 27 1964;1(7348):1444-1445.

278. Day RM, Harbord M, Forbes A, Segal AW. Cantharidin blisters: a technique for investigating leukocyte trafficking and cytokine production at sites of inflammation in humans. *J Immunol Methods.* Nov 1 2001;257(1-2):213-220.

279. Honkanen RE. Cantharidin, another natural toxin that inhibits the activity of serine/threonine protein phosphatases types 1 and 2A. *FEBS Lett.* Sep 20 1993;330(3):283-286.

280. Epstein WL, Kligman AM. Treatment of warts with cantharidin. *AMA Arch Derm.* May 1958;77(5):508-511.

281. Bacelieri R, Johnson SM. Cutaneous warts: an evidence-based approach to therapy. *Am Fam Physician.* Aug 15 2005;72(4):647-652.

282. Adatto MA, Halachmi S, Lapidoth M. Tattoo removal. *Curr Probl Dermatol.* 2011;42:97-110.

283. Tromovitch TA. Cantharadin. *JAMA.* Jan 25 1971;215(4):640.

284. Evans BJ, McDowall A, Taylor PC, Hogg N, Haskard DO, Landis RC. Shedding of lymphocyte function-associated antigen-1 (LFA-1) in a human inflammatory response. *Blood.* May 1 2006;107(9):3593-3599.

285. Philippidis P, Mason JC, Evans BJ, et al. Hemoglobin scavenger receptor CD163 mediates interleukin-10 release and heme oxygenase-1 synthesis: antiinflammatory monocyte-macrophage responses in vitro, in resolving skin blisters in vivo, and after cardiopulmonary bypass surgery. *Circ Res.* Jan 9 2004;94(1):119-126.

286. Bubici C, Papa S, Dean K, Franzoso G. Mutual cross-talk between reactive oxygen species and nuclear factor-kappa B: molecular basis and biological significance. *Oncogene.* Oct 30 2006;25(51):6731-6748.

287. Ray PD, Huang BW, Tsuji Y. Reactive oxygen species (ROS) homeostasis and redox regulation in cellular signaling. *Cell Signal.* May 2012;24(5):981-990.

288. Marchi S, Giorgi C, Suski JM, et al. Mitochondria-ros crosstalk in the control of cell death and aging. *J Signal Transduct.* 2012;2012:329635.

289. Tsutsui H, Kinugawa S, Matsushima S. Oxidative stress and heart failure. *Am J Physiol Heart Circ Physiol.* Dec 2011;301(6):H2181-2190.

290. Penna C, Mancardi D, Rastaldo R, Pagliaro P. Cardioprotection: a radical view Free radicals in pre and postconditioning. *Biochim Biophys Acta.* Jul 2009;1787(7):781-793.

291. Cooke MS, Evans MD, Dizdaroglu M, Lunec J. Oxidative DNA damage: mechanisms, mutation, and disease. *FASEB J.* Jul 2003;17(10):1195-1214.

292. Mittal M, Siddiqui MR, Tran K, Reddy SP, Malik AB. Reactive oxygen species in inflammation and tissue injury. *Antioxid Redox Signal.* Mar 1 2014;20(7):1126-1167.

293. D'Autreaux B, Toledano MB. ROS as signalling molecules: mechanisms that generate specificity in ROS homeostasis. *Nat Rev Mol Cell Biol.* Oct 2007;8(10):813-824.

294. Bienert GP, Moller AL, Kristiansen KA, et al. Specific aquaporins facilitate the diffusion of hydrogen peroxide across membranes. *J Biol Chem.* Jan 12 2007;282(2):1183-1192.

295. Han D, Antunes F, Canali R, Rettori D, Cadenas E. Voltage-dependent anion channels control the release of the superoxide anion from mitochondria to cytosol. *J Biol Chem.* Feb 21 2003;278(8):5557-5563.

296. Hampton MB, Kettle AJ, Winterbourn CC. Inside the neutrophil phagosome: oxidants, myeloperoxidase, and bacterial killing. *Blood.* Nov 1 1998;92(9):3007-3017.

297. Heyworth PG, Cross AR, Curnutte JT. Chronic granulomatous disease. *Curr Opin Immunol.* Oct 2003;15(5):578-584.

298. Li JM, Mullen AM, Yun S, et al. Essential role of the NADPH oxidase subunit p47(phox) in endothelial cell superoxide production in response to phorbol ester and tumor necrosis factor-alpha. *Circ Res.* Feb 8 2002;90(2):143-150.

299. DeLeo FR, Renee J, McCormick S, et al. Neutrophils exposed to bacterial lipopolysaccharide upregulate NADPH oxidase assembly. *J Clin Invest.* Jan 15 1998;101(2):455-463.

300. Dang PM, Stensballe A, Boussetta T, et al. A specific p47phox -serine phosphorylated by convergent MAPKs mediates neutrophil NADPH oxidase priming at inflammatory sites. *J Clin Invest.* Jul 2006;116(7):2033-2043.

301. Patel KD, Zimmerman GA, Prescott SM, McEver RP, McIntyre TM. Oxygen radicals induce human endothelial cells to express GMP-140 and bind neutrophils. *J Cell Biol.* Feb 1991;112(4):749-759.

302. Lo SK, Janakidevi K, Lai L, Malik AB. Hydrogen peroxide-induced increase in endothelial adhesiveness is dependent on ICAM-1 activation. *Am J Physiol.* Apr 1993;264(4 Pt 1):L406-412.

303. Volk AP, Barber BM, Goss KL, et al. Priming of neutrophils and differentiated PLB-985 cells by pathophysiological concentrations of TNF-alpha is partially oxygen dependent. *J Innate Immun.* 2011;3(3):298-314.

304. Kevil CG, Oshima T, Alexander B, Coe LL, Alexander JS. H(2)O(2)-mediated permeability: role of MAPK and occludin. *Am J Physiol Cell Physiol.* Jul 2000;279(1):C21-30.

305. Handy DE, Loscalzo J. Redox regulation of mitochondrial function. *Antioxid Redox Signal.* Jun 1 2012;16(11):1323-1367.

306. Carlsson LM, Jonsson J, Edlund T, Marklund SL. Mice lacking extracellular superoxide dismutase are more sensitive to hyperoxia. *Proc Natl Acad Sci U S A.* Jul 3 1995;92(14):6264-6268.

307. Rahman I, Biswas SK, Kode A. Oxidant and antioxidant balance in the airways and airway diseases. *Eur J Pharmacol.* Mar 8 2006;533(1-3):222-239.

308. Nadeem A, Siddiqui N, Alharbi NO, Alharbi MM, Imam F. Acute glutathione depletion leads to enhancement of airway reactivity and inflammation via p38MAPK-iNOS pathway in allergic mice. *Int Immunopharmacol.* Sep 2014;22(1):222-229.

309. Nadeem A, Siddiqui N, Alharbi NO, Alharbi MM, Imam F, Sayed-Ahmed MM. Glutathione modulation during sensitization as well as challenge phase regulates airway reactivity and inflammation in mouse model of allergic asthma. *Biochimie.* Aug 2014;103:61-70.

310. Ishii T, Warabi E, Yanagawa T. Novel roles of peroxiredoxins in inflammation, cancer and innate immunity. *J Clin Biochem Nutr.* Mar 2012;50(2):91-105.

311. Wang Y, Feinstein SI, Manevich Y, Ho YS, Fisher AB. Lung injury and mortality with hyperoxia are increased in peroxiredoxin 6 gene-targeted mice. *Free Radic Biol Med.* Dec 1 2004;37(11):1736-1743.

312. Wang Y, Manevich Y, Feinstein SI, Fisher AB. Adenovirus-mediated transfer of the 1-cys peroxiredoxin gene to mouse lung protects against hyperoxic injury. *Am J Physiol Lung Cell Mol Physiol.* Jun 2004;286(6):L1188-1193.

313. Lu J, Holmgren A. The thioredoxin antioxidant system. *Free Radic Biol Med.* Jan 2014;66:75-87.

314. Lopert P, Day BJ, Patel M. Thioredoxin reductase deficiency potentiates oxidative stress, mitochondrial dysfunction and cell death in dopaminergic cells. *PLoS One.* 2012;7(11):e50683.

315. Chanas SA, Jiang Q, McMahon M, et al. Loss of the Nrf2 transcription factor causes a marked reduction in constitutive and inducible expression of the glutathione S-transferase Gsta1, Gsta2, Gstm1, Gstm2, Gstm3 and Gstm4 genes in the livers of male and female mice. *Biochem J.* Jul 15 2002;365(Pt 2):405-416.

316. Cho HY, Jedlicka AE, Reddy SP, et al. Role of NRF2 in protection against hyperoxic lung injury in mice. *Am J Respir Cell Mol Biol.* Feb 2002;26(2):175-182.

317. Clarke JD, Hsu A, Williams DE, et al. Metabolism and tissue distribution of sulforaphane in Nrf2 knockout and wild-type mice. *Pharm Res.* Dec 2011;28(12):3171-3179.

318. Hu R, Saw CL, Yu R, Kong AN. Regulation of NF-E2-related factor 2 signaling for cancer chemoprevention: antioxidant coupled with antiinflammatory. *Antioxid Redox Signal.* Dec 1 2010;13(11):1679-1698.

319. Ishii T, Itoh K, Yamamoto M. Roles of Nrf2 in activation of antioxidant enzyme genes via antioxidant responsive elements. *Methods Enzymol.* 2002;348:182-190.

320. Jyrkkanen HK, Kansanen E, Inkala M, et al. Nrf2 regulates antioxidant gene expression evoked by oxidized phospholipids in endothelial cells and murine arteries in vivo. *Circ Res.* Jul 3 2008;103(1):e1-9.

321. Kensler TW, Wakabayashi N, Biswal S. Cell survival responses to environmental stresses via the Keap1-Nrf2-ARE pathway. *Annu Rev Pharmacol Toxicol.* 2007;47:89-116.

322. Thimmulappa RK, Mai KH, Srisuma S, Kensler TW, Yamamoto M, Biswal S. Identification of Nrf2-regulated genes induced by the chemopreventive agent sulforaphane by oligonucleotide microarray. *Cancer Res.* Sep 15 2002;62(18):5196-5203.

323. Yellon DM, Hausenloy DJ. Myocardial reperfusion injury. *N Engl J Med.* Sep 13 2007;357(11):1121-1135.

324. Ambrosio G, Tritto I. Reperfusion injury: experimental evidence and clinical implications. *Am Heart J.* Aug 1999;138(2 Pt 2):S69-75.

325. Elahi MM, Yii M, Matata BM. Significance of oxidants and inflammatory mediators in blood of patients undergoing cardiac surgery. *J Cardiothorac Vasc Anesth.* Jun 2008;22(3):455-467.

326. Goudeau JJ, Clermont G, Guillery O, et al. In high-risk patients, combination of antiinflammatory procedures during cardiopulmonary bypass can reduce incidences of inflammation and oxidative stress. *J Cardiovasc Pharmacol.* Jan 2007;49(1):39-45.

327. Vogt S, Sattler A, Sirat AS, et al. Different profile of antioxidative capacity results in pulmonary dysfunction and amplified inflammatory response After CABG surgery. *J Surg Res.* May 1 2007;139(1):136-142.

328. Davies SW, Duffy JP, Wickens DG, et al. Time-course of free radical activity during coronary artery operations with cardiopulmonary bypass. *J Thorac Cardiovasc Surg.* Jun 1993;105(6):979-987.

329. Bayram H, Erer D, Iriz E, Hakan Zor M, Gulbahar O, Ozdogan ME. Comparison of the effects of pulsatile cardiopulmonary bypass, non-pulsatile cardiopulmonary bypass and off-pump coronary artery bypass grafting on the respiratory system and serum carbonyl. *Perfusion.* Sep 2012;27(5):378-385.

330. Storti S, Cerillo AG, Rizza A, et al. Coronary artery bypass grafting surgery is associated with a marked reduction in serum homocysteine and folate levels in the early postoperative period. *Eur J Cardiothorac Surg.* Oct 2004;26(4):682-686.

331. Tossios P, Bloch W, Huebner A, et al. N-acetylcysteine prevents reactive oxygen species-mediated myocardial stress in patients undergoing cardiac surgery: results of a randomized, double-blind, placebo-controlled clinical trial. *J Thorac Cardiovasc Surg.* Nov 2003;126(5):1513-1520.

332. Fischer UM, Tossios P, Huebner A, Geissler HJ, Bloch W, Mehlhorn U. Myocardial apoptosis prevention by radical scavenging in patients undergoing cardiac surgery. *J Thorac Cardiovasc Surg.* Jul 2004;128(1):103-108.

333. Cuadrado A, Nebreda AR. Mechanisms and functions of p38 MAPK signalling. *Biochem J.* Aug 1 2010;429(3):403-417.

334. Kim JH, Studer RK, Vo NV, Sowa GA, Kang JD. p38 MAPK inhibition selectively mitigates inflammatory mediators and VEGF production in AF cells co-cultured with activated macrophage-like THP-1 cells. *Osteoarthritis Cartilage.* Dec 2009;17(12):1662-1669.

335. Kim EK, Choi EJ. Pathological roles of MAPK signaling pathways in human diseases. *Biochim Biophys Acta.* Apr 2010;1802(4):396-405.

336. Akbarian S, Davis RJ. Keep the 'phospho' on MAPK, be happy. *Nat Med.* Nov 2010;16(11):1187-1188.

337. Rose BA, Force T, Wang Y. Mitogen-activated protein kinase signaling in the heart: angels versus demons in a heart-breaking tale. *Physiol Rev.* Oct 2010;90(4):1507-1546.

338. Khan TA, Bianchi C, Ruel M, Voisine P, Sellke FW. Mitogen-activated protein kinase pathways and cardiac surgery. *J Thorac Cardiovasc Surg.* Mar 2004;127(3):806-811.

339. Diestel A, Roessler J, Pohl-Schickinger A, et al. Specific p38 inhibition in stimulated endothelial cells: a possible new anti-inflammatory strategy after hypothermia and rewarming. *Vascul Pharmacol.* Oct 2009;51(4):246-252.

340. Warny M, Keates AC, Keates S, et al. p38 MAP kinase activation by Clostridium difficile toxin A mediates monocyte necrosis, IL-8 production, and enteritis. *J Clin Invest.* Apr 2000;105(8):1147-1156.

341. Clark AR, Dean JL, Saklatvala J. Post-transcriptional regulation of gene expression by mitogen-activated protein kinase p38. *FEBS Lett.* Jul 3 2003;546(1):37-44.

342. Dong C, Davis RJ, Flavell RA. MAP kinases in the immune response. *Annu Rev Immunol.* 2002;20:55-72.

343. Chase SD, Magnani JL, Simon SI. E-selectin ligands as mechanosensitive receptors on neutrophils in health and disease. *Ann Biomed Eng.* Apr 2012;40(4):849-859.

344. Chi H, Flavell RA. Acetylation of MKP-1 and the control of inflammation. *Sci Signal.* 2008;1(41):pe44.

345. Zhao Q, Wang X, Nelin LD, et al. MAP kinase phosphatase 1 controls innate immune responses and suppresses endotoxic shock. *J Exp Med.* Jan 23 2006;203(1):131-140.

346. Feng L, Zhou X, Liao J, Omary MB. Pervanadate-mediated tyrosine phosphorylation of keratins 8 and 19 via a p38 mitogen-activated protein kinase-dependent pathway. *J Cell Sci.* Jul 1999;112 (Pt 13):2081-2090.

347. Zu YL, Qi J, Gilchrist A, et al. p38 mitogen-activated protein kinase activation is required for human neutrophil function triggered by TNF-alpha or FMLP stimulation. *J Immunol.* Feb 15 1998;160(4):1982-1989.

348. McLeish KR, Knall C, Ward RA, et al. Activation of mitogen-activated protein kinase cascades during priming of human neutrophils by TNF-alpha and GM-CSF. *J Leukoc Biol.* Oct 1998;64(4):537-545.

349. Cain BS, Meldrum DR, Meng X, et al. p38 MAPK inhibition decreases TNF-alpha production and enhances postischemic human myocardial function. *J Surg Res.* May 1 1999;83(1):7-12.

350. Khan TA, Bianchi C, Araujo EG, Ruel M, Voisine P, Sellke FW. Activation of pulmonary mitogen-activated protein kinases during cardiopulmonary bypass. *J Surg Res.* Nov 2003;115(1):56-62.

351. Sakiyama S, Hamilton J, Han B, et al. Activation of mitogen-activated protein kinases during human lung transplantation. *J Heart Lung Transplant.* Dec 2005;24(12):2079-2085.

352. Khan TA, Bianchi C, Ruel M, et al. Mitogen-activated protein kinase inhibition and cardioplegia-cardiopulmonary bypass reduce coronary myogenic tone. *Circulation.* Sep 9 2003;108 Suppl 1:II348-353.

353. Liakopoulos OJ, Schmitto JD, Kazmaier S, et al. Cardiopulmonary and systemic effects of methylprednisolone in patients undergoing cardiac surgery. *Ann Thorac Surg.* Jul 2007;84(1):110-118; discussion 118-119.

354. Trop S, Marshall JC, Mazer CD, et al. Perioperative cardiovascular system failure in South Asians undergoing cardiopulmonary bypass is associated with prolonged inflammation and increased Toll-like receptor signaling in inflammatory monocytes. *J Surg Res.* Oct 7 2013.

355. Rossaint J, Berger C, Van Aken H, et al. Cardiopulmonary bypass during cardiac surgery modulates systemic inflammation by affecting different steps of the leukocyte recruitment cascade. *PLoS One.* 2012;7(9):e45738.

356. Clements RT, Feng J, Cordeiro B, Bianchi C, Sellke FW. p38 MAPK-dependent small HSP27 and alphaB-crystallin phosphorylation in regulation of myocardial function following cardioplegic arrest. *Am J Physiol Heart Circ Physiol.* May 2011;300(5):H1669-1677.

357. Li YP, Huang J, Huang SG, et al. The compromised inflammatory response to bacterial components after pediatric cardiac surgery is associated with cardiopulmonary bypass-suppressed Toll-like receptor signal transduction pathways. *J Crit Care.* Oct 28 2013.

358. Pepe S, Liaw NY, Hepponstall M, et al. Effect of remote ischemic preconditioning on phosphorylated protein signaling in children undergoing tetralogy of fallot repair: a randomized controlled trial. *J Am Heart Assoc.* Jun 2013;2(3):e000095.

359. Van der Heiden K, Cuhlmann S, Luong le A, Zakkar M, Evans PC. Role of nuclear factor kappaB in cardiovascular health and disease. *Clin Sci (Lond).* May 2010;118(10):593-605.

360. Gordon JW, Shaw JA, Kirshenbaum LA. Multiple facets of NF-kappaB in the heart: to be or not to NF-kappaB. *Circ Res.* Apr 29 2011;108(9):1122-1132.

361. Natoli G, Saccani S, Bosisio D, Marazzi I. Interactions of NF-kappaB with chromatin: the art of being at the right place at the right time. *Nat Immunol.* May 2005;6(5):439-445.

362. Dixit V, Mak TW. NF-kappaB signaling. Many roads lead to madrid. *Cell.* Nov 27 2002;111(5):615-619.

363. de Winther MP, Kanters E, Kraal G, Hofker MH. Nuclear factor kappaB signaling in atherogenesis. *Arterioscler Thromb Vasc Biol.* May 2005;25(5):904-914.

364. Hayden MS, Ghosh S. Shared principles in NF-kappaB signaling. *Cell.* Feb 8 2008;132(3):344-362.

365. Takada Y, Mukhopadhyay A, Kundu GC, Mahabeleshwar GH, Singh S, Aggarwal BB. Hydrogen peroxide activates NF-kappa B through tyrosine phosphorylation of I kappa B alpha and serine phosphorylation of p65: evidence for the involvement of I kappa B alpha kinase and Syk protein-tyrosine kinase. *J Biol Chem.* Jun 27 2003;278(26):24233-24241.

366. Gloire G, Legrand-Poels S, Piette J. NF-kappaB activation by reactive oxygen species: fifteen years later. *Biochem Pharmacol.* Nov 30 2006;72(11):1493-1505.

367. Hajra L, Evans AI, Chen M, Hyduk SJ, Collins T, Cybulsky MI. The NF-kappa B signal transduction pathway in aortic endothelial cells is primed for activation in regions predisposed to atherosclerotic lesion formation. *Proc Natl Acad Sci U S A.* Aug 1 2000;97(16):9052-9057.

368. Sun SC. The noncanonical NF-kappaB pathway. *Immunol Rev.* Mar 2012;246(1):125-140.

369. Enesa K, Zakkar M, Chaudhury H, et al. NF-kappaB suppression by the deubiquitinating enzyme Cezanne: a novel negative feedback loop in pro-inflammatory signaling. *J Biol Chem.* Mar 14 2008;283(11):7036-7045.

370. Lawrence T. The nuclear factor NF-kappaB pathway in inflammation. *Cold Spring Harb Perspect Biol.* Dec 2009;1(6):a001651.

371. Manning AM, Bell FP, Rosenbloom CL, et al. NF-kappa B is activated during acute inflammation in vivo in association with elevated endothelial cell adhesion molecule gene expression and leukocyte recruitment. *J Inflamm.* 1995;45(4):283-296.

372. Tak PP, Firestein GS. NF-kappaB: a key role in inflammatory diseases. *J Clin Invest.* Jan 2001;107(1):7-11.

373. Kamata H, Honda S, Maeda S, Chang L, Hirata H, Karin M. Reactive oxygen species promote TNFalpha-induced death and sustained JNK activation by inhibiting MAP kinase phosphatases. *Cell.* Mar 11 2005;120(5):649-661.

374. Zakkar M, Van der Heiden K, Luong le A, et al. Activation of Nrf2 in endothelial cells protects arteries from exhibiting a proinflammatory state. *Arterioscler Thromb Vasc Biol.* Nov 2009;29(11):1851-1857.

375. Enesa K, Ito K, Luong le A, et al. Hydrogen peroxide prolongs nuclear localization of NF-kappaB in activated cells by suppressing negative regulatory mechanisms. *J Biol Chem.* Jul 4 2008;283(27):18582-18590.

376. Langereis JD, Raaijmakers HA, Ulfman LH, Koenderman L. Abrogation of NF-kappaB signaling in human neutrophils induces neutrophil survival through sustained p38-MAPK activation. *J Leukoc Biol.* Oct 2010;88(4):655-664.

377. Zhang YY, Wu JW, Wang ZX. Mitogen-activated protein kinase (MAPK) phosphatase 3-mediated cross-talk between MAPKs ERK2 and p38alpha. *J Biol Chem.* May 6 2011;286(18):16150-16162.

378. Holleyman CR, Larson DF. Apoptosis in the ischemic reperfused myocardium. *Perfusion.* Nov 2001;16(6):491-502.

379. Gill R, Tsung A, Billiar T. Linking oxidative stress to inflammation: Toll-like receptors. *Free Radic Biol Med.* May 1 2010;48(9):1121-1132.

380. Junttila MR, Li SP, Westermarck J. Phosphatase-mediated crosstalk between MAPK signaling pathways in the regulation of cell survival. *FASEB J.* Apr 2008;22(4):954-965.

381. Jijon H, Allard B, Jobin C. NF-kappaB inducing kinase activates NF-kappaB transcriptional activity independently of IkappaB kinase gamma through a p38 MAPK-dependent RelA phosphorylation pathway. *Cell Signal.* Sep 2004;16(9):1023-1032.

382. Bass DA, Olbrantz P, Szejda P, Seeds MC, McCall CE. Subpopulations of neutrophils with increased oxidative product formation in blood of patients with infection. *J Immunol.* Feb 1 1986;136(3):860-866.

383. Drost EM, Kassabian G, Meiselman HJ, Gelmont D, Fisher TC. Increased rigidity and priming of polymorphonuclear leukocytes in sepsis. *Am J Respir Crit Care Med.* Jun 1999;159(6):1696-1702.

384. Chollet-Martin S, Montravers P, Gibert C, et al. Subpopulation of hyperresponsive polymorphonuclear neutrophils in patients with adult respiratory distress syndrome. Role of cytokine production. *Am Rev Respir Dis.* Oct 1992;146(4):990-996.

385. Yuan M, Jordan F, McInnes IB, Harnett MM, Norman JE. Leukocytes are primed in peripheral blood for activation during term and preterm labour. *Mol Hum Reprod.* Nov 2009;15(11):713-724.

386. Pillay J, Hietbrink F, Koenderman L, Leenen LP. The systemic inflammatory response induced by trauma is reflected by multiple phenotypes of blood neutrophils. *Injury.* Dec 2007;38(12):1365-1372.

387. Summers C, Rankin SM, Condliffe AM, Singh N, Peters AM, Chilvers ER. Neutrophil kinetics in health and disease. *Trends Immunol.* Aug 2010;31(8):318-324.

388. Condliffe AM, Kitchen E, Chilvers ER. Neutrophil priming: pathophysiological consequences and underlying mechanisms. *Clin Sci (Lond).* May 1998;94(5):461-471.

389. Moore FA, Moore EE, Read RA. Postinjury multiple organ failure: role of extrathoracic injury and sepsis in adult respiratory distress syndrome. *New Horiz.* Nov 1993;1(4):538-549.

390. Maung AA, Fujimi S, MacConmara MP, et al. Injury enhances resistance to Escherichia coli infection by boosting innate immune system function. *J Immunol.* Feb 15 2008;180(4):2450-2458.

391. Shelley O, Murphy T, Paterson H, Mannick JA, Lederer JA. Interaction between the innate and adaptive immune systems is required to survive sepsis and control inflammation after injury. *Shock.* Aug 2003;20(2):123-129.

392. Elbim C, Chollet-Martin S, Bailly S, Hakim J, Gougerot-Pocidalo MA. Priming of polymorphonuclear neutrophils by tumor necrosis factor alpha in whole blood:

identification of two polymorphonuclear neutrophil subpopulations in response to formyl-peptides. *Blood.* Jul 15 1993;82(2):633-640.

393. Condliffe AM, Chilvers ER, Haslett C, Dransfield I. Priming differentially regulates neutrophil adhesion molecule expression/function. *Immunology.* Sep 1996;89(1):105-111.

394. Kuijper PH, Gallardo Torres HI, van der Linden JA, et al. Neutrophil adhesion to fibrinogen and fibrin under flow conditions is diminished by activation and L-selectin shedding. *Blood.* Mar 15 1997;89(6):2131-2138.

395. Worthen GS, Haslett C, Rees AJ, Gumbay RS, Henson JE, Henson PM. Neutrophil-mediated pulmonary vascular injury. Synergistic effect of trace amounts of lipopolysaccharide and neutrophil stimuli on vascular permeability and neutrophil sequestration in the lung. *Am Rev Respir Dis.* Jul 1987;136(1):19-28.

396. Biffl WL, Moore EE, Zallen G, et al. Neutrophils are primed for cytotoxicity and resist apoptosis in injured patients at risk for multiple organ failure. *Surgery.* Aug 1999;126(2):198-202.

397. Nahum A, Chamberlin W, Sznajder JI. Differential activation of mixed venous and arterial neutrophils in patients with sepsis syndrome and acute lung injury. *Am Rev Respir Dis.* May 1991;143(5 Pt 1):1083-1087.

398. Singh NR, Johnson A, Peters AM, Babar J, Chilvers ER, Summers C. Acute lung injury results from failure of neutrophil de-priming: a new hypothesis. *Eur J Clin Invest.* Dec 2012;42(12):1342-1349.

399. Schwartz JD, Shamamian P, Schwartz DS, et al. Cardiopulmonary bypass primes polymorphonuclear leukocytes. *J Surg Res.* Mar 1998;75(2):177-182.

400. Partrick DA, Moore EE, Fullerton DA, Barnett CC, Jr., Meldrum DR, Silliman CC. Cardiopulmonary bypass renders patients at risk for multiple organ failure via early neutrophil priming and late neutrophil disability. *J Surg Res.* Sep 1999;86(1):42-49.

401. Alevizou A, Dunning J, Park JD. Can a mini-bypass circuit improve perfusion in cardiac surgery compared to conventional cardiopulmonary bypass? *Interact Cardiovasc Thorac Surg.* Apr 2009;8(4):457-466.

402. Ohata T, Mitsuno M, Yamamura M, et al. Minimal cardiopulmonary bypass attenuates neutrophil activation and cytokine release in coronary artery bypass grafting. *J Artif Organs.* 2007;10(2):92-95.

403. Beghi C, Nicolini F, Agostinelli A, et al. Mini-cardiopulmonary bypass system: results of a prospective randomized study. *Ann Thorac Surg.* Apr 2006;81(4):1396-1400.

404. Mulholland JW, Anderson JR, Yarham GJ, Tuladhur S, Saed I, Oliver MD. Miniature cardiopulmonary bypass--the Hammersmith experience. *Perfusion.* May 2007;22(3):161-166.

405. Issitt RW, Mulholland JW, Oliver MD, et al. Aortic surgery using total miniaturized cardiopulmonary bypass. *Ann Thorac Surg.* Aug 2008;86(2):627-631.

406. Ng CS, Arifi AA, Wan S, et al. Ventilation during cardiopulmonary bypass: impact on cytokine response and cardiopulmonary function. *Ann Thorac Surg.* Jan 2008;85(1):154-162.

407. John LC, Ervine IM. A study assessing the potential benefit of continued ventilation during cardiopulmonary bypass. *Interact Cardiovasc Thorac Surg.* Feb 2008;7(1):14-17.

408. Siepe M, Goebel U, Mecklenburg A, et al. Pulsatile pulmonary perfusion during cardiopulmonary bypass reduces the pulmonary inflammatory response. *Ann Thorac Surg.* Jul 2008;86(1):115-122.

409. O'Neil MP, Fleming JC, Badhwar A, Guo LR. Pulsatile versus nonpulsatile flow during cardiopulmonary bypass: microcirculatory and systemic effects. *Ann Thorac Surg.* Dec 2012;94(6):2046-2053.

410. Serraino GF, Marsico R, Musolino G, et al. Pulsatile cardiopulmonary bypass with intra-aortic balloon pump improves organ function and reduces endothelial activation. *Circ J.* 2012;76(5):1121-1129.

411. Ye L, Dinkova-Kostova AT, Wade KL, Zhang Y, Shapiro TA, Talalay P. Quantitative determination of dithiocarbamates in human plasma, serum, erythrocytes and urine: pharmacokinetics of broccoli sprout isothiocyanates in humans. *Clin Chim Acta.* Feb 2002;316(1-2):43-53.

412. Hanlon N, Coldham N, Gielbert A, Sauer MJ, Ioannides C. Repeated intake of broccoli does not lead to higher plasma levels of sulforaphane in human volunteers. *Cancer Lett.* Oct 18 2009;284(1):15-20.

413. D'Acquisto F, Ianaro A. From willow bark to peptides: the ever widening spectrum of NF-kappaB inhibitors. *Curr Opin Pharmacol.* Aug 2006;6(4):387-392.

414. Antoniades C, Bakogiannis C, Tousoulis D, et al. Preoperative atorvastatin treatment in CABG patients rapidly improves vein graft redox state by inhibition of Rac1 and NADPH-oxidase activity. *Circulation.* Sep 14 2010;122(11 Suppl):S66-73.

415. Radaelli A, Loardi C, Cazzaniga M, et al. Inflammatory activation during coronary artery surgery and its dose-dependent modulation by statin/ACE-inhibitor combination. *Arterioscler Thromb Vasc Biol.* Dec 2007;27(12):2750-2755.

416. Sarov-Blat L, Morgan JM, Fernandez P, et al. Inhibition of p38 mitogen-activated protein kinase reduces inflammation after coronary vascular injury in humans. *Arterioscler Thromb Vasc Biol.* Nov 2010;30(11):2256-2263.

417. Lasa M, Abraham SM, Boucheron C, Saklatvala J, Clark AR. Dexamethasone causes sustained expression of mitogen-activated protein kinase (MAPK) phosphatase 1 and phosphatase-mediated inhibition of MAPK p38. *Mol Cell Biol.* Nov 2002;22(22):7802-7811.

418. Clark AR. Anti-inflammatory functions of glucocorticoid-induced genes. *Mol Cell Endocrinol.* Sep 15 2007;275(1-2):79-97.

419. Khan TA, Bianchi C, Araujo E, et al. Aprotinin preserves cellular junctions and reduces myocardial edema after regional ischemia and cardioplegic arrest. *Circulation.* Aug 30 2005;112(9 Suppl):I196-201.

420. Lee DH, Choi HC, Lee KY, Kang YJ. Aprotinin Inhibits Vascular Smooth Muscle Cell Inflammation and Proliferation via Induction of HO-1. *Korean J Physiol Pharmacol.* Apr 2009;13(2):123-129.

421. Hill GE, Springall DR, Robbins RA. Aprotinin is associated with a decrease in nitric oxide production during cardiopulmonary bypass. *Surgery.* Apr 1997;121(4):449-455.

422. Hill GE, Pohorecki R, Alonso A, Rennard SI, Robbins RA. Aprotinin reduces interleukin-8 production and lung neutrophil accumulation after cardiopulmonary bypass. *Anesth Analg.* Oct 1996;83(4):696-700.

423. Force T, Kuida K, Namchuk M, Parang K, Kyriakis JM. Inhibitors of protein kinase signaling pathways: emerging therapies for cardiovascular disease. *Circulation.* Mar 16 2004;109(10):1196-1205.

424. Bain J, Plater L, Elliott M, et al. The selectivity of protein kinase inhibitors: a further update. *Biochem J.* Dec 15 2007;408(3):297-315.

425. Clark JE, Sarafraz N, Marber MS. Potential of p38-MAPK inhibitors in the treatment of ischaemic heart disease. *Pharmacol Ther.* Nov 2007;116(2):192-206.

426. Marber MS, Rose B, Wang Y. The p38 mitogen-activated protein kinase pathway-A potential target for intervention in infarction, hypertrophy, and heart failure. *J Mol Cell Cardiol.* Nov 6 2010.

427. Marber MS, Rose B, Wang Y. The p38 mitogen-activated protein kinase pathway--a potential target for intervention in infarction, hypertrophy, and heart failure. *J Mol Cell Cardiol.* Oct 2011;51(4):485-490.

428. Khan TA, Bianchi C, Ruel M, Feng J, Sellke FW. Differential effects on the mesenteric microcirculatory response to vasopressin and phenylephrine after cardiopulmonary bypass. *J Thorac Cardiovasc Surg.* Mar 2007;133(3):682-688.

429. Thomas CJ, Ng DC, Patsikatheodorou N, et al. Cardioprotection from ischaemia-reperfusion injury by a novel flavonol that reduces activation of p38 MAPK. *Eur J Pharmacol.* May 11 2011;658(2-3):160-167.

430. Yoshimura S, Morishita R, Hayashi K, et al. Inhibition of intimal hyperplasia after balloon injury in rat carotid artery model using cis-element 'decoy' of nuclear factor-kappaB binding site as a novel molecular strategy. *Gene Ther.* Nov 2001;8(21):1635-1642.

431. Laborde F, Abdelmeguid I, Piwnica A. Aortocoronary bypass without extracorporeal circulation: why and when? *Eur J Cardiothorac Surg.* 1989;3(2):152-154; discussion 154-155.

432. Al-Ruzzeh S, George S, Bustami M, et al. Effect of off-pump coronary artery bypass surgery on clinical, angiographic, neurocognitive, and quality of life outcomes: randomised controlled trial. *BMJ.* Jun 10 2006;332(7554):1365.

433. Shroyer AL, Grover FL, Hattler B, et al. On-pump versus off-pump coronary-artery bypass surgery. *N Engl J Med.* Nov 5 2009;361(19):1827-1837.

434. Loeckinger A, Kleinsasser A, Lindner KH, Margreiter J, Keller C, Hoermann C. Continuous positive airway pressure at 10 cm H(2)O during cardiopulmonary bypass improves postoperative gas exchange. *Anesth Analg.* Sep 2000;91(3):522-527.

435. Momin A, Sharabiani M, Mulholland J, et al. Miniaturized cardiopulmonary bypass: the Hammersmith technique. *J Cardiothorac Surg.* 2013;8:143.

436. Momin AU, Sharabiani MT, Kidher E, et al. Feasibility and safety of minimized cardiopulmonary bypass in major aortic surgery. *Interact Cardiovasc Thorac Surg.* Oct 2013;17(4):659-663.

437. Remadi JP, Marticho P, Butoi I, et al. Clinical experience with the mini-extracorporeal circulation system: an evolution or a revolution? *Ann Thorac Surg.* Jun 2004;77(6):2172-2175; discussion 2176.

438. Heyer EJ, Lee KS, Manspeizer HE, et al. Heparin-bonded cardiopulmonary bypass circuits reduce cognitive dysfunction. *J Cardiothorac Vasc Anesth.* Feb 2002;16(1):37-42.

439. Steinberg BM, Grossi EA, Schwartz DS, et al. Heparin bonding of bypass circuits reduces cytokine release during cardiopulmonary bypass. *Ann Thorac Surg.* Sep 1995;60(3):525-529.

440. Aldea GS, Soltow LO, Chandler WL, et al. Limitation of thrombin generation, platelet activation, and inflammation by elimination of cardiotomy suction in patients undergoing coronary artery bypass grafting treated with heparin-bonded circuits. *J Thorac Cardiovasc Surg.* Apr 2002;123(4):742-755.

441. Westerberg M, Bengtsson A, Jeppsson A. Coronary surgery without cardiotomy suction and autotransfusion reduces the postoperative systemic inflammatory response. *Ann Thorac Surg.* Jul 2004;78(1):54-59.

442. Nguyen BA, Suleiman MS, Anderson JR, et al. Metabolic derangement and cardiac injury early after reperfusion following intermittent cross-clamp fibrillation in patients undergoing coronary artery bypass graft surgery using conventional or miniaturized cardiopulmonary bypass. *Mol Cell Biochem.* Oct 2014;395(1-2):167-175.

443. Remadi JP, Rakotoarivelo Z, Marticho P, Benamar A. Prospective randomized study comparing coronary artery bypass grafting with the new mini-extracorporeal circulation Jostra System or with a standard cardiopulmonary bypass. *Am Heart J.* Jan 2006;151(1):198.

444. Fromes Y, Gaillard D, Ponzio O, et al. Reduction of the inflammatory response following coronary bypass grafting with total minimal extracorporeal circulation. *Eur J Cardiothorac Surg.* Oct 2002;22(4):527-533.

445. Huybregts RA, Morariu AM, Rakhorst G, et al. Attenuated renal and intestinal injury after use of a mini-cardiopulmonary bypass system. *Ann Thorac Surg.* May 2007;83(5):1760-1766.

446. Kamiya H, Kofidis T, Haverich A, Klima U. Preliminary experience with the mini-extracorporeal circulation system (Medtronic resting heart system). *Interact Cardiovasc Thorac Surg.* Dec 2006;5(6):680-682.

447. Nollert G, Schwabenland I, Maktav D, et al. Miniaturized cardiopulmonary bypass in coronary artery bypass surgery: marginal impact on inflammation and coagulation but loss of safety margins. *Ann Thorac Surg.* Dec 2005;80(6):2326-2332.

448. Wippermann J, Albes JM, Hartrumpf M, et al. Comparison of minimally invasive closed circuit extracorporeal circulation with conventional cardiopulmonary bypass and with off-pump technique in CABG patients: selected parameters of coagulation and inflammatory system. *Eur J Cardiothorac Surg.* Jul 2005;28(1):127-132.

449. Castiglioni A, Verzini A, Pappalardo F, et al. Minimally invasive closed circuit versus standard extracorporeal circulation for aortic valve replacement. *Ann Thorac Surg.* Feb 2007;83(2):586-591.

450. Remadi JP, Rakotoarivello Z, Marticho P, et al. Aortic valve replacement with the minimal extracorporeal circulation (Jostra MECC System) versus standard cardiopulmonary bypass: a randomized prospective trial. *J Thorac Cardiovasc Surg.* Sep 2004;128(3):436-441.

451. Biancari F, Rimpilainen R. Meta-analysis of randomised trials comparing the effectiveness of miniaturised versus conventional cardiopulmonary bypass in adult cardiac surgery. *Heart.* Jun 2009;95(12):964-969.

452. Perthel M, El-Ayoubi L, Bendisch A, Laas J, Gerigk M. Clinical advantages of using mini-bypass systems in terms of blood product use, postoperative bleeding and air entrainment: an in vivo clinical perspective. *Eur J Cardiothorac Surg.* Jun 2007;31(6):1070-1075; discussion 1075.

453. Rawn JD. Blood transfusion in cardiac surgery: a silent epidemic revisited. *Circulation.* Nov 27 2007;116(22):2523-2524.

454. Vaislic C, Bical O, Farge C, et al. Totally minimized extracorporeal circulation: an important benefit for coronary artery bypass grafting in Jehovah's witnesses. *Heart Surg Forum.* 2003;6(5):307-310.

455. Raman JS, Bellomo R, Hayhoe M, Tsamitros M, Buxton BF. Metabolic changes and myocardial injury during cardioplegia: a pilot study. *Ann Thorac Surg.* Nov 2001;72(5):1566-1571.

456. Buja LM. Myocardial ischemia and reperfusion injury. *Cardiovasc Pathol.* Jul-Aug 2005;14(4):170-175.

457. Liebold A, Khosravi A, Westphal B, et al. Effect of closed minimized cardiopulmonary bypass on cerebral tissue oxygenation and microembolization. *J Thorac Cardiovasc Surg.* Feb 2006;131(2):268-276.

458. Abdel-Rahman U, Martens S, Risteski P, et al. The use of minimized extracorporeal circulation system has a beneficial effect on hemostasis--a randomized clinical study. *Heart Surg Forum.* 2006;9(1):E543-548.

459. Kiaii B, Fox S, Swinamer SA, et al. The early inflammatory response in a mini-cardiopulmonary bypass system: a prospective randomized study. *Innovations (Phila).* Jan-Feb 2012;7(1):23-32.

460. Jacobs S, Holzhey D, Kiaii BB, et al. Limitations for manual and telemanipulator-assisted motion tracking--implications for endoscopic beating-heart surgery. *Ann Thorac Surg.* Dec 2003;76(6):2029-2035; discussion 2035-2026.

461. van Boven WJ, Gerritsen WB, Waanders FG, Haas FJ, Aarts LP. Mini extracorporeal circuit for coronary artery bypass grafting: initial clinical and biochemical results: a comparison with conventional and off-pump coronary artery bypass grafts concerning global oxidative stress and alveolar function. *Perfusion.* Jul 2004;19(4):239-246.

462. Yuruk K, Bezemer R, Euser M, et al. The effects of conventional extracorporeal circulation versus miniaturized extracorporeal circulation on microcirculation during cardiopulmonary bypass-assisted coronary artery bypass graft surgery. *Interact Cardiovasc Thorac Surg.* Sep 2012;15(3):364-370.

463. Mandak J, Brzek V, Svitek V, et al. Peripheral tissue oxygenation during standard CPB and miniaturized CPB (direct oxymetric tissue perfusion monitoring study). *Biomed Pap Med Fac Univ Palacky Olomouc Czech Repub.* Mar 2013;157(1):81-89.

464. Bennett MJ, Rajakaruna C, Bazerbashi S, Webb G, Gomez-Cano M, Lloyd C. Oxygen delivery during cardiopulmonary bypass (and renal outcome) using two systems of extracorporeal circulation: a retrospective review. *Interact Cardiovasc Thorac Surg.* Jun 2013;16(6):760-764.

465. Skrabal CA, Choi YH, Kaminski A, et al. Circulating endothelial cells demonstrate an attenuation of endothelial damage by minimizing the extracorporeal circulation. *J Thorac Cardiovasc Surg.* Aug 2006;132(2):291-296.

466. Willcox BJ, Curb JD, Rodriguez BL. Antioxidants in cardiovascular health and disease: key lessons from epidemiologic studies. *Am J Cardiol.* May 22 2008;101(10A):75D-86D.

467. Katsiki N, Manes C. Is there a role for supplemented antioxidants in the prevention of atherosclerosis? *Clin Nutr.* Feb 2009;28(1):3-9.

468. Jialal I, Devaraj S. Antioxidants and atherosclerosis: don't throw out the baby with the bath water. *Circulation.* Feb 25 2003;107(7):926-928.

469. Dong X, Liu Y, Du M, Wang Q, Yu CT, Fan X. P38 mitogen-activated protein kinase inhibition attenuates pulmonary inflammatory response in a rat cardiopulmonary bypass model. *Eur J Cardiothorac Surg.* Jul 2006;30(1):77-84.

470. Kunitz M, Northrop JH. Isolation from Beef Pancreas of Crystalline Trypsinogen, Trypsin, A Trypsin inhibitor, and an Inhibitor-Trypsin Compound. *The Journal of General Physiology.* 1935;19:991-1007.

471. Mifflin RC, Saada JI, Di Mari JF, Valentich JD, Adegboyega PA, Powell DW. Aspirin-mediated COX-2 transcript stabilization via sustained p38 activation in human intestinal myofibroblasts. *Mol Pharmacol.* Feb 2004;65(2):470-478.

472. Mustonen P, van Willigen G, Lassila R. Epinephrine--via activation of p38-MAPK--abolishes the effect of aspirin on platelet deposition to collagen. *Thromb Res.* Dec 15 2001;104(6):439-449.

473. Senokuchi T, Matsumura T, Sakai M, et al. Statins suppress oxidized low density lipoprotein-induced macrophage proliferation by inactivation of the small G protein-p38 MAPK pathway. *J Biol Chem.* Feb 25 2005;280(8):6627-6633.

474. Schmeisser A, Soehnlein O, Illmer T, et al. ACE inhibition lowers angiotensin II-induced chemokine expression by reduction of NF-kappaB activity and AT1 receptor expression. *Biochem Biophys Res Commun.* Dec 10 2004;325(2):532-540.

475. Isoda K, Young JL, Zirlik A, et al. Metformin inhibits proinflammatory responses and nuclear factor-kappaB in human vascular wall cells. *Arterioscler Thromb Vasc Biol.* Mar 2006;26(3):611-617.

476. Xu JJ, Hendriks BS, Zhao J, de Graaf D. Multiple effects of acetaminophen and p38 inhibitors: towards pathway toxicology. *FEBS Lett.* Apr 9 2008;582(8):1276-1282.

477. Shapiro TA, Fahey JW, Wade KL, Stephenson KK, Talalay P. Human metabolism and excretion of cancer chemoprotective glucosinolates and isothiocyanates of cruciferous vegetables. *Cancer Epidemiol Biomarkers Prev.* Dec 1998;7(12):1091-1100.

478. Taipalensuu J, Falk A, Rask L. A wound- and methyl jasmonate-inducible transcript coding for a myrosinase-associated protein with similarities to an early nodulin. *Plant Physiol.* Feb 1996;110(2):483-491.

479. Petri N, Tannergren C, Holst B, et al. Absorption/metabolism of sulforaphane and quercetin, and regulation of phase II enzymes, in human jejunum in vivo. *Drug Metab Dispos.* Jun 2003;31(6):805-813.

480. Tarozzi A, Angeloni C, Malaguti M, Morroni F, Hrelia S, Hrelia P. Sulforaphane as a potential protective phytochemical against neurodegenerative diseases. *Oxid Med Cell Longev.* 2013;2013:415078.

481. Gao SS, Chen XY, Zhu RZ, Choi BM, Kim BR. Sulforaphane induces glutathione S-transferase isozymes which detoxify aflatoxin B(1)-8,9-epoxide in AML 12 cells. *Biofactors.* Jul-Aug 2010;36(4):289-296.

482. Zhang Y, Callaway EC. High cellular accumulation of sulphoraphane, a dietary anticarcinogen, is followed by rapid transporter-mediated export as a glutathione conjugate. *Biochem J.* May 15 2002;364(Pt 1):301-307.

483. Gross-Steinmeyer K, Stapleton PL, Tracy JH, Bammler TK, Strom SC, Eaton DL. Sulforaphane- and phenethyl isothiocyanate-induced inhibition of aflatoxin B1-mediated genotoxicity in human hepatocytes: role of GSTM1 genotype and CYP3A4 gene expression. *Toxicol Sci.* Aug 2010;116(2):422-432.

484. Itoh K, Chiba T, Takahashi S, et al. An Nrf2/small Maf heterodimer mediates the induction of phase II detoxifying enzyme genes through antioxidant response elements. *Biochem Biophys Res Commun.* Jul 18 1997;236(2):313-322.

485. Xue M, Qian Q, Adaikalakoteswari A, Rabbani N, Babaei-Jadidi R, Thornalley PJ. Activation of NF-E2-related factor-2 reverses biochemical dysfunction of endothelial cells induced by hyperglycemia linked to vascular disease. *Diabetes.* Oct 2008;57(10):2809-2817.

486. Lin W, Wu RT, Wu T, Khor TO, Wang H, Kong AN. Sulforaphane suppressed LPS-induced inflammation in mouse peritoneal macrophages through Nrf2 dependent pathway. *Biochem Pharmacol.* Oct 15 2008;76(8):967-973.

487. Houghton CA, Fassett RG, Coombes JS. Sulforaphane: translational research from laboratory bench to clinic. *Nutr Rev.* Nov 2013;71(11):709-726.

488. Evans PC. The influence of sulforaphane on vascular health and its relevance to nutritional approaches to prevent cardiovascular disease. *EPMA J.* Mar 2011;2(1):9-14.

489. Ishii T, Itoh K, Ruiz E, et al. Role of Nrf2 in the regulation of CD36 and stress protein expression in murine macrophages: activation by oxidatively modified LDL and 4-hydroxynonenal. *Circ Res.* Mar 19 2004;94(5):609-616.

490. Leonard MO, Kieran NE, Howell K, et al. Reoxygenation-specific activation of the antioxidant transcription factor Nrf2 mediates cytoprotective gene expression in ischemia-reperfusion injury. *FASEB J.* Dec 2006;20(14):2624-2626.

491. Ma Q, Battelli L, Hubbs AF. Multiorgan autoimmune inflammation, enhanced lymphoproliferation, and impaired homeostasis of reactive oxygen species in mice lacking the antioxidant-activated transcription factor Nrf2. *Am J Pathol.* Jun 2006;168(6):1960-1974.

492. Kim JY, Park HJ, Um SH, et al. Sulforaphane suppresses vascular adhesion molecule-1 expression in TNF-alpha-stimulated mouse vascular smooth muscle cells: involvement of the MAPK, NF-kappaB and AP-1 signaling pathways. *Vascul Pharmacol.* Mar-Apr 2012;56(3-4):131-141.

493. Chen XL, Dodd G, Kunsch C. Sulforaphane inhibits TNF-alpha-induced activation of p38 MAP kinase and VCAM-1 and MCP-1 expression in endothelial cells. *Inflamm Res.* Aug 2009;58(8):513-521.

494. Heiss E, Herhaus C, Klimo K, Bartsch H, Gerhauser C. Nuclear factor kappa B is a molecular target for sulforaphane-mediated anti-inflammatory mechanisms. *J Biol Chem.* Aug 24 2001;276(34):32008-32015.

495. Kong JS, Yoo SA, Kim HS, et al. Inhibition of synovial hyperplasia, rheumatoid T cell activation, and experimental arthritis in mice by sulforaphane, a naturally occurring isothiocyanate. *Arthritis Rheum.* Jan 2010;62(1):159-170.

496. Guerrero-Beltran CE, Calderon-Oliver M, Tapia E, et al. Sulforaphane protects against cisplatin-induced nephrotoxicity. *Toxicol Lett.* Feb 15 2010;192(3):278-285.

497. Marzec JM, Christie JD, Reddy SP, et al. Functional polymorphisms in the transcription factor NRF2 in humans increase the risk of acute lung injury. *FASEB J.* Jul 2007;21(9):2237-2246.

498. Liu Y, Yin G, Surapisitchat J, Berk BC, Min W. Laminar flow inhibits TNF-induced ASK1 activation by preventing dissociation of ASK1 from its inhibitor 14-3-3. *J Clin Invest.* Apr 2001;107(7):917-923.

499. Gamet-Payrastre L, Li P, Lumeau S, et al. Sulforaphane, a naturally occurring isothiocyanate, induces cell cycle arrest and apoptosis in HT29 human colon cancer cells. *Cancer Res.* Mar 1 2000;60(5):1426-1433.

500. Singh SV, Herman-Antosiewicz A, Singh AV, et al. Sulforaphane-induced G2/M phase cell cycle arrest involves checkpoint kinase 2-mediated phosphorylation of cell division cycle 25C. *J Biol Chem.* Jun 11 2004;279(24):25813-25822.

501. Wang H, Khor TO, Yang Q, et al. Pharmacokinetics and pharmacodynamics of phase II drug metabolizing/antioxidant enzymes gene response by anticancer agent sulforaphane in rat lymphocytes. *Mol Pharm.* Oct 1 2012;9(10):2819-2827.

502. Yochum L, Kushi LH, Meyer K, Folsom AR. Dietary flavonoid intake and risk of cardiovascular disease in postmenopausal women. *Am J Epidemiol.* May 15 1999;149(10):943-949.

503. Genkinger JM, Platz EA, Hoffman SC, Comstock GW, Helzlsouer KJ. Fruit, vegetable, and antioxidant intake and all-cause, cancer, and cardiovascular disease mortality in a community-dwelling population in Washington County, Maryland. *Am J Epidemiol.* Dec 15 2004;160(12):1223-1233.

504. Cornelis MC, El-Sohemy A, Campos H. GSTT1 genotype modifies the association between cruciferous vegetable intake and the risk of myocardial infarction. *Am J Clin Nutr.* Sep 2007;86(3):752-758.

505. Riedl MA, Saxon A, Diaz-Sanchez D. Oral sulforaphane increases Phase II antioxidant enzymes in the human upper airway. *Clin Immunol.* Mar 2009;130(3):244-251.

506. US National Institutes of Health; 2014. http://clinicaltrials.gov/ct2/results?term=Sulforaphane.

507. Setsukinai K, Urano Y, Kakinuma K, Majima HJ, Nagano T. Development of novel fluorescence probes that can reliably detect reactive oxygen species and distinguish specific species. *J Biol Chem.* Jan 31 2003;278(5):3170-3175.

508. Schaff UY, Trott KA, Chase S, et al. Neutrophils exposed to A. phagocytophilum under shear stress fail to fully activate, polarize, and transmigrate across inflamed endothelium. *Am J Physiol Cell Physiol.* Jul 2010;299(1):C87-96.

509. Lee D, Schultz JB, Knauf PA, King MR. Mechanical shedding of L-selectin from the neutrophil surface during rolling on sialyl Lewis x under flow. *J Biol Chem.* Feb 16 2007;282(7):4812-4820.

510. Ghosh S, Galinanes M. Protection of the human heart with ischemic preconditioning during cardiac surgery: role of cardiopulmonary bypass. *J Thorac Cardiovasc Surg.* Jul 2003;126(1):133-142.

511. Vabulas RM, Ahmad-Nejad P, Ghose S, Kirschning CJ, Issels RD, Wagner H. HSP70 as endogenous stimulus of the Toll/interleukin-1 receptor signal pathway. *J Biol Chem.* Apr 26 2002;277(17):15107-15112.

512. Raja SG, Dreyfus GD. Impact of off-pump coronary artery bypass surgery on graft patency: current best available evidence. *J Card Surg.* Mar-Apr 2007;22(2):165-169.

513. Nascimento-Silva V, Arruda MA, Barja-Fidalgo C, Fierro IM. Aspirin-triggered lipoxin A4 blocks reactive oxygen species generation in endothelial cells: a novel antioxidative mechanism. *Thromb Haemost.* Jan 2007;97(1):88-98.

514. Chen B, Zhao J, Zhang S, Wu W, Qi R. Aspirin inhibits the production of reactive oxygen species by downregulating Nox4 and inducible nitric oxide synthase in human endothelial cells exposed to oxidized low-density lipoprotein. *J Cardiovasc Pharmacol.* May 2012;59(5):405-412.

515. Dragomir E, Manduteanu I, Voinea M, Costache G, Manea A, Simionescu M. Aspirin rectifies calcium homeostasis, decreases reactive oxygen species, and increases NO production in high glucose-exposed human endothelial cells. *J Diabetes Complications.* Sep-Oct 2004;18(5):289-299.

516. Violi F, Carnevale R, Pastori D, Pignatelli P. Antioxidant and antiplatelet effects of atorvastatin by Nox2 inhibition. *Trends Cardiovasc Med.* Oct 2 2013.

517. Varin R, Mulder P, Tamion F, et al. Improvement of endothelial function by chronic angiotensin-converting enzyme inhibition in heart failure : role of nitric oxide, prostanoids, oxidant stress, and bradykinin. *Circulation.* Jul 18 2000;102(3):351-356.

518. Gomes A, Costa D, Lima JL, Fernandes E. Antioxidant activity of beta-blockers: an effect mediated by scavenging reactive oxygen and nitrogen species? *Bioorg Med Chem.* Jul 1 2006;14(13):4568-4577.

519. Li JJ, Fang CH, Chen MZ, Chen X, Lee SW. Activation of nuclear factor-kappaB and correlation with elevated plasma c-reactive protein in patients with unstable angina. *Heart Lung Circ.* Jun 2004;13(2):173-178.

520. Liuzzo G, Santamaria M, Biasucci LM, et al. Persistent activation of nuclear factor kappa-B signaling pathway in patients with unstable angina and elevated levels of C-reactive protein evidence for a direct proinflammatory effect of azide and

lipopolysaccharide-free C-reactive protein on human monocytes via nuclear factor kappa-B activation. *J Am Coll Cardiol.* Jan 16 2007;49(2):185-194.

521. Ritchie ME. Nuclear factor-kappaB is selectively and markedly activated in humans with unstable angina pectoris. *Circulation.* Oct 27 1998;98(17):1707-1713.

522. Balistreri CR, Candore G, Accardi G, Colonna-Romano G, Lio D. NF-kappaB pathway activators as potential ageing biomarkers: targets for new therapeutic strategies. *Immun Ageing.* 2013;10(1):24.

523. Mulholland JW, Anderson JR. Preventing the loss of safety margins with miniaturized cardiopulmonary bypass. *Ann Thorac Surg.* Nov 2006;82(5):1952-1953.

524. Gerrity RG, Naito HK, Richardson M, Schwartz CJ. Dietary induced atherogenesis in swine. Morphology of the intima in prelesion stages. *Am J Pathol.* Jun 1979;95(3):775-792.

525. Stocker CJ, Sugars KL, Yarwood H, et al. Cloning of porcine intercellular adhesion molecule-1 and characterization of its induction on endothelial cells by cytokines. *Transplantation.* Aug 27 2000;70(4):579-586.

526. Tsang YT, Stephens PE, Licence ST, Haskard DO, Binns RM, Robinson MK. Porcine E-selectin: cloning and functional characterization. *Immunology.* May 1995;85(1):140-145.

527. Tsang YT, Haskard DO, Robinson MK. Cloning and expression kinetics of porcine vascular cell adhesion molecule. *Biochem Biophys Res Commun.* Jun 15 1994;201(2):805-812.

528. Jousilahti P, Vartiainen E, Tuomilehto J, Puska P. Sex, age, cardiovascular risk factors, and coronary heart disease: a prospective follow-up study of 14 786 middle-aged men and women in Finland. *Circulation.* Mar 9 1999;99(9):1165-1172.

529. Patten RD, Pourati I, Aronovitz MJ, et al. 17beta-estradiol reduces cardiomyocyte apoptosis in vivo and in vitro via activation of phospho-inositide-3 kinase/Akt signaling. *Circ Res.* Oct 1 2004;95(7):692-699.

530. Fujii J, Iuchi Y, Okada F. Fundamental roles of reactive oxygen species and protective mechanisms in the female reproductive system. *Reprod Biol Endocrinol.* 2005;3:43.

531. Kim WI, Ryu HJ, Kim JE, et al. Differential nuclear factor-kappa B phosphorylation induced by lipopolysaccharide in the hippocampus of P2X7 receptor knockout mouse. *Neurol Res.* May 2013;35(4):369-381.

532. Zahler S, Massoudy P, Hartl H, Hahnel C, Meisner H, Becker BF. Acute cardiac inflammatory responses to postischemic reperfusion during cardiopulmonary bypass. *Cardiovasc Res.* Mar 1999;41(3):722-730.

533. Goebel U, Siepe M, Schwer CI, et al. Inhaled carbon monoxide prevents acute kidney injury in pigs after cardiopulmonary bypass by inducing a heat shock response. *Anesth Analg.* Jul 2010;111(1):29-37.

534. Jurenka JS. Anti-inflammatory properties of curcumin, a major constituent of Curcuma longa: a review of preclinical and clinical research. *Altern Med Rev.* Jun 2009;14(2):141-153.

535. Das S, Das DK. Anti-inflammatory responses of resveratrol. *Inflamm Allergy Drug Targets.* Sep 2007;6(3):168-173.

536. Kim SY, Jun TW, Lee YS, Na HK, Surh YJ, Song W. Effects of exercise on cyclooxygenase-2 expression and nuclear factor-kappaB DNA binding in human peripheral blood mononuclear cells. *Ann N Y Acad Sci.* Aug 2009;1171:464-471.

537. Ji LL, Gomez-Cabrera MC, Steinhafel N, Vina J. Acute exercise activates nuclear factor (NF)-kappaB signaling pathway in rat skeletal muscle. *FASEB J.* Oct 2004;18(13):1499-1506.

538. Uusitalo LM, Hempel N. Recent Advances in Intracellular and In Vivo ROS Sensing: Focus on Nanoparticle and Nanotube Applications. *Int J Mol Sci.* 2012;13(9):10660-10679.

539. Polykratis A, van Loo G, Xanthoulea S, Hellmich M, Pasparakis M. Conditional targeting of tumor necrosis factor receptor-associated factor 6 reveals opposing functions of Toll-like receptor signaling in endothelial and myeloid cells in a mouse model of atherosclerosis. *Circulation.* Oct 2 2012;126(14):1739-1751.

CHAPTER 8. APPENDIX

8.1 PUBLISHED MANUSCRIPTS & ABSTRACTS

Metabolic derangement and cardiac injury early after reperfusion following intermittent cross-clamp fibrillation in patients undergoing coronary artery bypass graft surgery using conventional or miniaturised cardiopulmonary bypass

BAV Nguyen, MS Suleiman, J Anderson, P Evans, F Fiorentino, BC Reeves, GD Angelini

Molecular and Cellular Biochemistry 2014 Oct; 395 (1-2):167-75

Sulforaphane pre-treatment prevents systemic inflammation and renal injury in response to cardiopulmonary bypass

Bao Nguyen, Le Luong, Hatam Naase, Mark Vives, Gentjan Jakaj, Jonathan Finch, Joseph Boyle, John Mulholland, Jong-hwan Kwak, Suhkneung Pyo, Amalia de Luca, Thanos Athanasiou, Gianni Angelini, Jon Anderson, Dorian Haskard, Paul Evans

Journal of Thoracic and Cardiovascular Surgery 2014 Aug; 148(2):690-697

Activation of leukocytes during surgery with Cardiopulmonary Bypass is attenuated by sulforaphane in a porcine model

BAV Nguyen, L Luong, G Jakaj, HML Naase, MS Vives, JR Finch, K Dakkak, J Mulholland, JR Anderson, DO Haskard, GD Angelini, PC Evans

European Surgical Research 2013; 50:87

Cardiopulmonary bypass activates multiple pro-inflammatory signalling pathways in peripheral blood leukocytes

BAV Nguyen, JR Anderson, DO Haskard, PC Evans

British Journal of Surgery 2011; 98(S5):58

8.2 POSTER PRESENTATIONS

Activation of leukocytes during surgery with Cardiopulmonary Bypass is attenuated by sulforaphane in a porcine model

Bao Nguyen, Le Luong, G Jakaj, HML Naase, MS Vives, JR Finch, K Dakkak, J Mulholland, JR Anderson, DO Haskard, GD Angelini, PC Evans

European Society of Surgical Research, 2012, Lille, France

Activation of leukocytes during surgery with Cardiopulmonary Bypass is attenuated by sulforaphane in a porcine model: a novel therapeutic strategy

Bao Nguyen, Gentjan Jakaj, Hatem Naase, Le Luong, Jonathan Finch, John Mulholland, Jon Anderson, Dorian Haskard, Gianni Angelini, Paul Evans

Society of Cardiothoracic Surgery, 2012, Manchester, UK

Sulforaphane suppresses inflammatory signalling in leukocytes

BAV Nguyen, GL McDonald, LA Luong, JR Anderson, DO Haskard, PC Evans

Biochemical Society, 2011, London, UK

Characterisation of the inflammatory stress pathways in cardiac surgery

BAV Nguyen, JR Anderson, DO Haskard, PC Evans

GSLSM 5th Annual Meeting, 2011, London, UK

Cardiopulmonary bypass activates multiple pro-inflammatory signalling pathways in peripheral blood leukocytes

BAV Nguyen, JR Anderson, DO Haskard, PC Evans

European Society for Surgical Research, Rheinisch-Westfälische Technische Hochschule, 2011, Aachen, Germany

Coronary artery bypass grafting with cardiopulmonary bypass induces reactive oxygen species and activates p38 and NF-κB signalling pathways in leukocytes

Bao Nguyen, Le Luong, Nicola Ambrose, Jon Anderson., Thanos Athanasiou, Gianni Angelini, Dorian Haskard, Paul Evans

British Heart Foundation Sir John Macmichael Visit, 2010, London, UK

Novel Markers of Inflammatory Stress following Cardiopulmonary Bypass

BAV Nguyen, JR Anderson, GD Angelini, DO Haskard, PC Evans

Graduate School of Life Sciences and Medicine, 2010, London, UK